Highly accurate treatment of dynamical electron correlation through R12 methods and extrapolation techniques

Hoogst nauwkeurige behandeling van dynamische elektronencorrelatie met R12 methoden en extrapolatietechnieken

(met een samenvatting in het Nederlands)

Proefschrift

Ter verkrijging van de graad van doctor aan de Universiteit Utrecht, op gezag van de Rector Magnificus, Prof. Dr. W. H. Gispen, ingevolge het besluit van het College voor Promoties in het openbaar te verdedigen op dinsdag 12 oktober 2004 des ochtends te 10:30 uur

door

Claire Catherine Michèle Samson

geboren op 9 juli 1976 te Aire sur Adour, Frankrijk.

Eerste promotor:

Prof. Dr. F. B. van Duijneveldt
verbonden aan de Faculteit Scheikunde van de Universiteit Utrecht.

Tweede promotor:

Prof. Dr. W. M. Klopper
verbonden aan de Faculteit Scheikunde van de Universiteit Karlsruhe, Duitsland.

The work described in this thesis was financially supported jointly by the Universiteit Utrecht and by the Deutsche Forschungsgemeinschaft through the Center for Functional Nanostructures, Universität Karlsruhe (TH). It was also partially sponsored by Cost Chemistry Action D9.

A mes chers parents,
à Jonas et Sandra.

Beoordelingscommissie:

Prof. Dr. J. P. J. M. van der Eerden (Universiteit Utrecht)
Prof. Dr. H. Rudolph (Universiteit Utrecht)
Prof. Dr. B. M. Weckhuysen (Universiteit Utrecht)

Paranimfen: Dr. F. Barrere
Dr. R. W. A. Havenith

Highly accurate treatment of dynamical electron correlation
through R12 methods and extrapolation techniques
Claire Catherine Michèle Samson
Ph.D. thesis, University of Utrecht, The Netherlands
Met een samenvatting in het Nederlands

Printed by PrintPartners IPSKAMP

ISBN 90-393-3759-4

Contents

1

A short introduction to Quantum Chemistry

1.1 Essence of electron correlation

1.1.1 Time-independent non-relativistic electronic Schrödinger equation

The forces that keep together the atoms in a molecule cannot be described correctly by classical mechanics. The equation introduced by the Austrian physicist Erwin Schrödinger in 1926 [1] dictates the quantum mechanical behavior of molecules at the atomic scale and allows to predict theoretically their physical properties with rigorous accuracy. This thesis aims at the development of improved methods for the approximate solution of the non-relativistic Schrödinger equation in its time-independent form:

$$\hat{H}\Psi \;=\; E\Psi\,. \tag{1.1}$$

Ψ is the total wave function of the considered molecular system. The Hamiltonian $\hat{H}$ is the operator corresponding to the total energy E. It is formulated as:

$$\hat{H} \;=\; \hat{T}_n + \hat{T}_e + \hat{V}_{ee} + \hat{V}_{nn} + \hat{V}_{ne}\,, \tag{1.2}$$

where $\hat{T}_n$ and $\hat{T}_e$ stand for the kinetic energies of nuclei n and electrons e, and $\hat{V}_{ee}$, $\hat{V}_{nn}$ and $\hat{V}_{ne}$ symbolize their potential energies. The Born-Oppenheimer approximation [2] is a central concept for the non-linear solution of this fundamental equation. Based on the fact that nuclei are at least 1800 times heavier than electrons, it consists in uncoupling their motions, treating consequently nuclei as stationary particles for the electronic motion. For the majority of systems, the Born-Oppenheimer approximation introduces very small errors. We can therefore solve the electronic Schrödinger equation parameterically on the nuclear coordinates.

$$\hat{H}_e\Psi_e = E_e\Psi_e \quad \text{and} \quad \hat{H}_e = \hat{T}_e + \hat{V}_{ee} + \hat{V}_{ne}\,. \tag{1.3}$$

The electronic wave function Ψ_e describes a stationary-state of a molecular electronic system and depends concomitantly on the coordinates of each electron in the system. If solutions are generated without any empirical fitting to the experimental data, the corresponding methods are baptized *ab initio*, which originates from the latin expression "from the beginning". Energies calculated from the electronic Schrödinger equation depend on the chosen nuclear coordinates and can be used as the potential for solving the rotational-vibrational problem of a molecule, or to model chemical reactions.

In this context, *ab initio* quantum chemistry serves as a powerful tool to investigate computationally many physical properties of materials such as: geometry of molecules, electron distributions, ionization potentials, electron affinities, multipole moments and vibrational frequencies.

1.1.2 N-electron basis functions

The popular molecular-orbital theory reposes on expressing the total N-electron wave function Ψ_e as product of one-electron functions, the molecular orbitals $\bar{\Phi}_p$. Each molecular orbital is associated with three spatial coordinates and a spin coordinate. The spin space is spanned by two functions α and β corresponding to spin up and spin down, respectively. The occurrence of the spin coordinate originates from the response of electrons in the presence of an external magnetic field. Since electrons are fermions (having a spin angular momentum of 1/2), the electronic wave function should be antisymmetric (change sign) with respect to the interchange of any two electron coordinates (spatial and spin). The Pauli exclusion principle, which states that two electrons cannot be in the same spin orbital, directly results from this antisymmetry principle. Slater determinants SD (Eq. (1.4)) are then convenient mathematical entities to construct suitable N-electron basis functions. If we assume the molecular spin orbitals mutually orthonormal, the normalization factor is the inverse of $\sqrt{N!}$.

$$SD = \frac{1}{\sqrt{N!}} \begin{vmatrix} \bar{\Phi}_1(1) & \bar{\Phi}_2(1) & ... & \bar{\Phi}_N(1) \\ \bar{\Phi}_1(2) & \bar{\Phi}_2(2) & ... & \bar{\Phi}_N(2) \\ ... & ... & ... & ... \\ \bar{\Phi}_1(N) & \bar{\Phi}_2(N) & ... & \bar{\Phi}_N(N) \end{vmatrix} . \tag{1.4}$$

1.1.3 One-electron basis functions

To generate the spatial part Φ_p of of the molecular spin orbitals $\bar{\Phi}_p$, a finite set of analytical functions is required, mostly chosen as atomic basis functions χ_μ.

$$\Phi_p = \sum_\mu c_{\mu p} \chi_\mu \, . \tag{1.5}$$

The index μ is summed over the number M of atomic basis functions and the prefactors $c_{\mu p}$ are called expansion coefficients. This strategy is commonly named linear combination of atomic orbitals (LCAO). Each of these basis functions, which are traditionally centered on the nuclei, is composed of a radial part $R(r)$ and an angular part $Y(\theta, \phi)$, which may be taken as a spherical harmonic function (Figure 1.1). r, θ and ϕ conventionally denote the polar coordinates:

$$\chi_\mu = R(r) * Y(\theta, \phi) \, . \tag{1.6}$$

Two types of atomic basis functions are predominantly used in *ab initio* quantum chemistry, respectively, Slater type orbitals (STOs) and Gaussian type orbitals (GTOs).

$$R_{\text{STO}}(r) = \exp(-\xi r) \quad \text{and} \quad R_{\text{GTO}}(r) = \exp(-\xi r^2) \, . \tag{1.7}$$

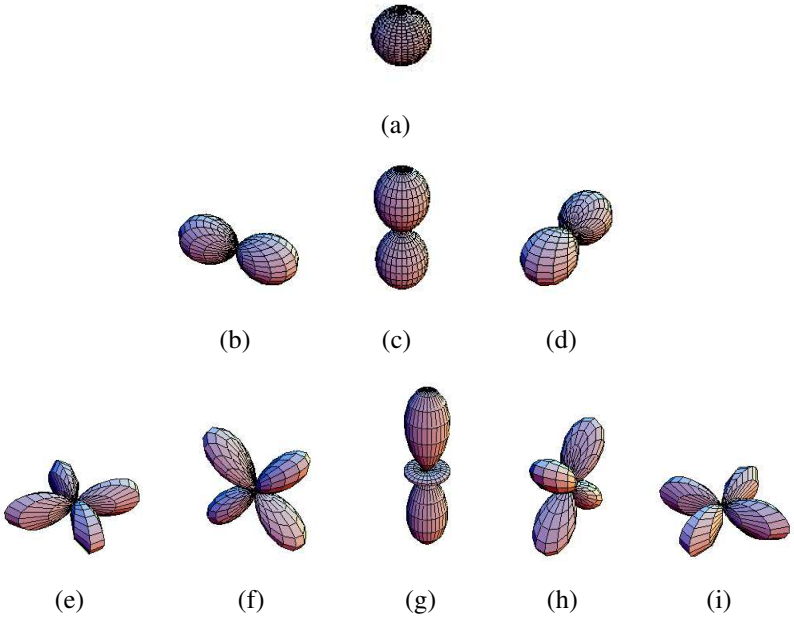

Figure 1.1: The real solid harmonics for angular momenta $\ell \leq 2$ corresponding to (a) s orbital, (b), (c) and (d) respectively p_y, p_z and p_x orbitals, (e), (f), (g), (h) and (i) respectively d_{xy}, d_{yz}, d_{z^2}, d_{zx} and $d_{x^2-y^2}$ orbitals.

For simplification of the integral evaluation, the exponents ξ are constrained to be the same for the $(2\ell+1)$ orbitals of a shell sharing the same angular momentum ℓ. The STO's exponential dependence in r allows the right behavior both close to a nucleus and very far from it but leads to many-center two-electron integrals that cannot be computed analytically. Mainly for this reason, the favored basis-set types are combinations of GTOs, although to reach a given accuracy in the electronic energy one needs a larger number of GTOs than when STOs are used.

1.1.4 Molecular-orbital-based standard models

The Schrödinger equation is a difficult many-body problem that cannot be solved exactly due to the occurrence of the interelectronic repulsion operator $\hat{V}_{ee}$ in the electronic Hamiltonian. Therefore, quantum chemists have developed efficient tools to approximate the solution of this challenging equation, that is to provide a simplified description of the electronic system. The electronic Hamilton operator is kept in its exact form while the approximation is made on the electronic wave function, Ψ_e^{approx}. The corresponding energy E_e^{approx} is the expectation value of the electronic Hamiltonian.

$$E_e^{approx} = \frac{\langle \Psi_e^{approx} | \hat{H}_e | \Psi_e^{approx} \rangle}{\langle \Psi_e^{approx} | \Psi_e^{approx} \rangle} \,. \tag{1.8}$$

This subsection gives an overview of the most common so-called single-reference methods available for the study of closed-shell molecular systems. For such closed-shell molecules, all spatial molecular orbitals that form the reference determinant are doubly occupied by electrons of opposite spins.

Hartree-Fock theory

The starting point of most *ab initio* quantum chemistry methods is the Hartree-Fock theory [3]. The N-electron approximate wave function Ψ_0 is the single determinant that leads to the lowest expectation value of the Hamiltonian.

$$\Psi_e \approx \Psi_0 \,. \tag{1.9}$$

In this framework, each electron experiences the mean electrostatic field set up by the nuclei and the charge distribution of all the remaining electrons which compose the molecule. Since the determination of each optimized molecular spin orbital depends on all the remaining molecular spin orbitals, this method is iterative. Consequently, it is also known as self-consistent field (SCF) procedure. For a basis set of M linearly independent atomic basis functions, one generates $2M$ molecular spin orbitals. The N lowest ones in energy are occupied and form Ψ_0 while the ($2M$-N) remaining ones are denoted virtual spin orbitals. The weak point of this method is that it does not correlate the motion of the electrons, on average they are further apart than described by the Hartree-Fock wave function. Following the Löwdin definition [4], the difference between the exact non-relativistic solution of the electronic Schrödinger equation and the Hartree-Fock (E_{SCF}) energy in a complete one-particle basis set, is denoted correlation energy ($E_{\text{correlation}}$).

Under the assumption that Hartree-Fock provides a reliable approximation of the exact wave function, there exists a range of post-Hartree-Fock methods that account for electron correlation. Below are presented the most conventional schemes widely used nowadays.

Configuration interaction theory

Configuration interaction (CI) theory [5] consists in expanding Ψ_e^{approx} as a linear combination of N-electron basis functions involving other possible determinants formed from the Hartree-Fock reference by excitations of electrons from occupied to virtual molecular spin orbitals. This procedure is referred to as the algebraic approximation. Thus the determinantal basis functions, also called configurations, of the CI wave function are classified as singles (S), doubles (D), triples (T), etc... If $\hat{T}_k$ symbolizes the cluster operator creating the complete set of k-fold excited configurations, implicitly including the expansion coefficients of each configuration in the N-particle space,

then the electronic wave function in its most complete form is written as:

$$\hat{T} \;=\; 1 \;+\; \hat{T}_1 \;+\; ... \;+\; \hat{T}_N \;, \tag{1.10}$$

$$\Psi_e \;\approx\; \hat{T}\,\Psi_0\,. \tag{1.11}$$

The CI wave function is variationally optimized (i.e. by minimizing the energy functional E_e^{approx}) and corresponds to an energy that is an upper-bound to the exact energy of the molecular system. If all the $\binom{2M}{N}$ possible configurations are kept in the expansion (full CI approach, denoted FCI), the resulting energy E_{FCI} is the best possible approximation to the exact solution of the electronic energy in a given basis set. A more restrictive definition of the correlation energy is usually adopted in a given basis set:

$$E^{\text{BASIS}}_{\text{correlation}} = E^{\text{BASIS}}_{\text{FCI}} - E^{\text{BASIS}}_{\text{SCF}}\,. \tag{1.12}$$

Naturally, it is possible to cut off the CI expansion of the wave function at a desired level of excitation. One can so define a hierarchy of truncated CI methods, respectively CISD, CISDT, CISDTQ, etc. For ground-state energies, the importance of an excited contribution decreases with its degree of excitation. Nevertheless, doubly excited configurations are more dominant than singly excited ones since following the Brillouin theorem, the singles do not interact with the Hartree-Fock reference,

$$\langle\Psi_0|\hat{H}_e|\hat{T}_1\Psi_0\rangle = 0\,. \tag{1.13}$$

Møller-Plesset perturbation theory

Many-body perturbation theory (MBPT) [3] is also based on the algebraic approximation but abandons the variational optimization of the wave function. Its basic idea is to partition the Hamilton operator $\hat{H}_e$ into an unperturbed Hamiltonian $\hat{H}_0$ and a perturbation $\hat{V}$ named fluctuation potential and multiplied by a scaling parameter λ which is set equal to one at the end to get the original Hamiltonian.

$$\hat{H}_e = \hat{H}_0 + \lambda\hat{V}\,. \tag{1.14}$$

The most common partitioning, referred to as Møller-Plesset perturbation theory [6], takes the Hartree-Fock effective Hamilton operator as reference and the difference between the electronic Hamiltonian $\hat{H}_e$ and the Hartree-Fock Hamiltonian as fluctuation potential. The wave function as well as the energy are expressed as expansions in a Taylor series in λ:

$$\Psi_e \;\approx\; \lambda^0\,\Psi_0 \;+\; \lambda^1\,\Psi_1 \;+\; \lambda^2\,\Psi_2 \;+\; ...\,, \tag{1.15}$$

$$E_e \;\approx\; \lambda^0\,E_0 \;+\; \lambda^1\,E_1 \;+\; \lambda^2\,E_2 \;+\; ...\,. \tag{1.16}$$

E_n and Ψ_n are the nth-order energy and wave function, respectively and Ψ_0 is the optimized one-determinantal Hartree-Fock reference. The evaluation of the nth-order wave function allows a calculation of the $(2n+1)$th-order energy, according to Wigner's rule. Contrarily to variational CI calculations, there is no guarantee in the framework of perturbation theory that the resulting energy is an upper-bound to the exact energy. Since the Møller-Plesset perturbation theory series might diverge from the third-order on [7, 8], its most successful and popular form is to the second-order (MP2). In this case, the N-particle expansion of the first-order wave function includes only up to doubly excited configurations.

Coupled-cluster theory

Coupled-cluster (CC) theory [9] differs from CI theory by an exponential parameterization of the cluster operator $\hat{T}$:

$$\exp(\hat{T}) \;=\; 1 \;+\; \hat{T} \;+\; \frac{1}{2}\hat{T}^2 \;+\; \frac{1}{6}\hat{T}^3 \;+\; \ldots\,, \tag{1.17}$$

$$\Psi_e \;\approx\; \exp(\hat{T})\,\Psi_0\,. \tag{1.18}$$

The resultant appealing feature is the appearance of configurations in the CC wave function of higher order than for the CI expansion for a chosen cut off of the cluster operator, namely the disconnected clusters. Indeed, for a truncation of the cluster operator after doubles as an example, higher order excitations occur through the products $\hat{T}_1\ \hat{T}_2$, $\hat{T}_2\ \hat{T}_2$ and so on. Physically, a connected cluster operator such as $\hat{T}_4$ corresponds to the simultaneous interaction of four electrons, while a disconnected term $\hat{T}_2\ \hat{T}_2$ corresponds to two non-interacting pairs of interacting electrons. A variational approach for the optimization of the CC wave function is difficult due to its highly non-linear representation. Alternatively a non-variational projection technique and the use of the exact Hausdorff expansion (Eq. (1.19)) are generally used to develop an explicit form for optimizing the CC wave function.

$$\exp(-\hat{T})\hat{H}\exp(\hat{T}) = \hat{H}+[\hat{H},\hat{T}]+\frac{1}{2}[[\hat{H},\hat{T}],\hat{T}]+\frac{1}{3!}[[[\hat{H},\hat{T}],\hat{T}]\hat{T}]+\frac{1}{4!}[[[[\hat{H},\hat{T}],\hat{T}]\hat{T}]\hat{T}]\,. \tag{1.19}$$

Like for CI, one can define a hierarchy of truncated CC methods as CCSD, CCSDT, CCSDTQ, etc. A given CC truncated treatment is not substantially more expensive than its CI counterpart but provides superior results owing to the inclusion of the disconnected clusters. For the same reason as indicated for CISD, CCSD recovers far the largest part of the ground-state correlation energy. Besides, for highly accurate calculations, it is advantageous to introduce the triple correction via a perturbative treatment, denoted CCSD(T), which leads to slightly lower accuracy than CCSDT (with respect to the systematic treatment of the wave function) but for considerable computational savings [10].

Compromise between size-extensivity and variational principle

Size-extensivity reads that the total energy of a set of non-interacting systems is equal to the sum of the energies of each individual system. Truncated CI methods always lack size-extensivity, contrarily to MP2 and truncated CC methods. The variational principle states that the computed energy represents an upper-bound to the true ground-state energy. Truncated CI methods satisfy the variational principle, contrarily to MP2 and truncated CC methods. However, MP2 and CC methods are still recognized to be bounded by a stationary minimum that is the basis-set limit energy (which might be lower than the exact energy). For this reason and since size-extensivity has been proven to be an important requirement for the calculation of relative energies, CI methods are today less popular than MP2 and CC methods.

1.1.5 Considerations on computational cost versus accuracy

Today theoretical chemists have at their disposal tremendous computer facilities (for instance [11]). Partly due to efficient parallelization of computer codes, such machines have remarkably accelerated the development and enlarged the application range of computational chemistry. It is possible nowadays to handle FCI calculations for systems of a few billion determinants [12]. Nevertheless, due to the factorial growth of the number of configurations with the basis-set size, FCI calculations remain hardly tractable even for small molecules when the number of basis functions is large enough to yield accurate results. Thus FCI is not a viable method to compute accurate potential energy surfaces and one should turn towards the direction of more feasible truncated CI, CC, or MBPT methods. From low to high accuracy, the approaches presented in the previous subsection (1.1.4) can be classified as follows: HF, MP2, CISD, CCSD, CCSD(T), CCSDT, etc. Table 1.1 displays the formal scaling of the computational cost of these methods. The term formal is mentioned here since there exist various techniques to reduce conveniently this scaling [13–15]. Practically, the CCSD(T) method is the most reliable *ab initio* molecular-orbital method that is affordable for small to medium-sized molecules. With basis sets close to completeness, it can accomplish very high accuracy. At a lower level, the MP2 model represents a powerful compromise between accuracy and cost. It is widely employed for calculations on weakly bonded systems and on systems which remain out of reach of CC methods.

Table 1.1: Scaling of the computational cost of few molecular-orbital-based conventional methods in terms of the number of atoms K in a given atomic basis.

Method	HF	MP2	CISD, CCSD	CCSD(T)	CCSDT
Scaling	K^4	K^5	K^6	K^7	K^8

Although the correlation energy accounts for only about 1% of the total energy, it is essential to describe it properly in order to reach 'spectroscopic accuracy' (1 μE_h), or even 'chemical accuracy' (1 mE_h). However, some properties like molecular geometries of equilibrium structures are less sensitive to electron correlation, which has led to the practice to perform geometry optimizations and to calculate total electronic energies on different theoretical levels. A further practical procedure consists in neglecting the correlation associated with the innermost electrons, or core electrons by contrast with valence electrons belonging to the outermost shell. This frozen-core approximation is justified by the insensitivity of core charge distributions to external fields and molecular rearrangements.

The electron correlation is roughly partitioned into statical and dynamical correlations. The statical correlation, commonly denoted near-degeneracy correlation, arises from the near-degeneracy of electronic configurations. Indeed, it might happen that the gap between the highest occupied (HOMO) and the lowest unoccupied (LUMO) molecular orbitals is not large enough to guarantee the predominance of a single Slater determinant in the wave function. For such cases, like studies on excited states or dissociation processes, the single-reference based methods fail. There exist few multi-reference methods like multi-configurational self-consistent field (MCSCF), or multiconfigurational perturbation theory (CASPT) [16]. In contrast, the dynamical correlation originates from the Coulomb repulsion between electrons. It can largely be described by the above-mentioned post-Hartree-Fock methods. A sub-partitioning occurs between the long-range dynamical correlation and the short-range dynamical correlation. The long-range correlation is easily described by a relative small number of excited configurations in the wave function expansion while the short-range correlation is mainly responsible for the slow convergence of the wave function with the atomic basis-set size.

It would not be fair to close this section without mentioning density functional theory (DFT), which represents a different way to solve the many-body problem. The leading idea is that the ground-state electronic energy is determined completely by the electron density [17]. The results are rather irregular and not exceedingly accurate but the price-performance ratio of the method can hardly be beaten by molecular-orbital theory. This theory has undeniably given a meaningful impetus to chemistry and it has allowed to solve interesting problems on large molecules out of reach from the standard models [18–20].

In conclusion, the total error, also known as apparent error, induced by an *ab initio* molecular-orbital calculation comes from two sources: first the truncation error in the N-particle configuration space (intrinsic error) and second the error in the one-particle space (basis-set error).

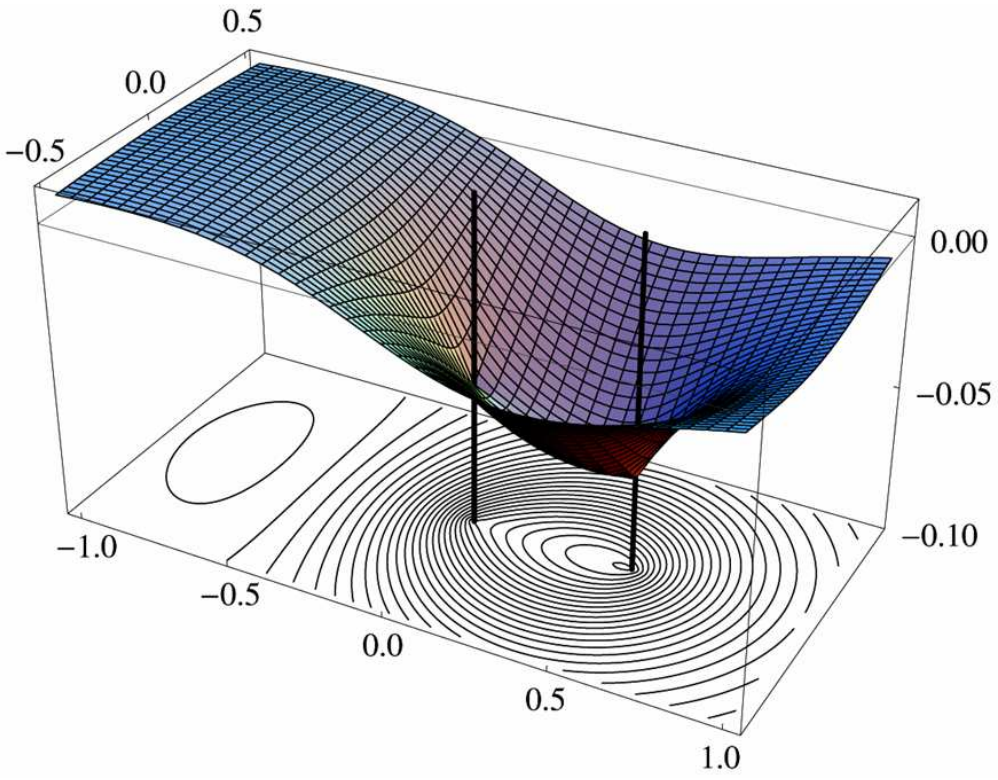

Figure 1.2: Difference $\Delta\Psi_e$ between the exact Ψ_e and Hartree-Fock Ψ_e^{SCF} electronic wave functions, $\Delta\Psi_e = \Psi_e - \Psi_e^{SCF}$, for the ^{1}S ground-state of the helium atom. The nucleus is located at the center of the xy coordinate system (left-most vertical bold stroke), one electron is kept fixed at 0.5 a_0 (x=0.5 a_0 and y = 0 a_0) from the nucleus (right-most vertical bold stroke), and the second electron evolves in the two-dimensional space xy. The electrons have opposite spins.

1.2 Basis-set investigation

1.2.1 Coulomb hole and Coulomb cusp

In the immediate vicinity of one electron, the probability of finding another electron decreases substantially. For instance, considering the helium atom, if one electron is close to the nucleus, the distance of the other electron to the nucleus increases (radial correlation) and it prefers to be on the opposite side (angular correlation) of the nucleus. Besides, considering the H_2 molecule, if one electron is close to one nucleus, it is more likely that the other electron is in the surroundings of the other nucleus (left-right correlation). Such phenomena are referred to as Coulomb correlation and constitute a challenge in the building of the wave function.

Figure 1.2 displays the difference between the exact and the Hartree-Fock wave functions for the ^{1}S helium atom ground-state as a function of the coordinates of one electron. The other electron

is kept fixed at x = 0.5 a_0 and y = 0 a_0. In a plot of the Hartree-Fock wave function itself, the contour lines would consist of concentric circles around the nucleus, undistorted by the fixed electron. The distortion of these contour lines close to the fixed electron clearly indicates that the motion of the free electron depends on the position of the fixed electron. Thus the wave function exhibits a hole around the position of the fixed electron, called Coulomb hole since it is a direct consequence of the Coulomb interaction between two electrons $\frac{1}{r_{12}}$ that becomes singular when $r_{12} = 0$. The minimum of the wave function -0.068 relative to the Hartree-Fock reference is at a distance of 0.49 a_0 from the nucleus, in the proximity of the fixed electron and the maximum 0.012 is on the opposite side of the nucleus, at a distance of 0.79 a_0 from the nucleus and 1.29 a_0 from the fixed electron. At the very position of the fixed electron, the exact wave function presents a cusp, denoted as Coulomb cusp. Kato rigourously demonstrated its existence in 1957 [21]. The Kato's cusp condition states that the spherical average of the first derivative of wave function with respect to the interelectronic distance is equal to half the wave function at this point of coalescence, for two electrons with opposite spins.

$$\lim_{r_{12}\to 0}\Big(\frac{\partial\Psi_e(1,2)}{\partial r_{12}}\Big)_{av} = \frac{\Psi_e(1,2)}{2}\bigg|_{r_{12}=0}. \tag{1.20}$$

1.2.2 Optimization and convergence

Atomic basis-set development is a very difficult task due to the highly non-linear optimization of many parameters: the orbital exponents and contraction coefficients. Two essential requirements should be fulfilled for providing useful series of atomic basis sets in order to approach the basis-set limit solution in a systematic manner. First, the electronic energy should smoothly converge towards the full basis energy as more and more functions are added. Second, the smallest basis should recover the largest part of the total energy. Numerous Gaussian basis sets have been developed for systematic calculations of correlation energies. The most popular of all are the correlation-consistent basis sets, cc-pVXZ (X called cardinal number and X = D, T, Q, 5 and 6), introduced by Dunning in 1989 [22] and widely developed thereafter [23–27]. Table 1.2 lists the number of contracted functions for three types of correlation-consistent bases. The augmented correlation-consistent bases are preferred to describe diffuse electronic charges like in anions or excited states and the polarized core-valence sets allow calculations including the correlation within the core and between the core and the valence electrons.

The basis-set convergence is quicker at the Hartree-Fock level than at the correlated level. This is mainly due to the linear behavior of the wave function at the Coulomb hole which is rather cumbersomely described with post-Hartree-Fock methods employing products of orbitals as N-particle basis functions. Figure 1.3 demonstrates the slow convergence of the FCI expansion of the

wave function for He (^{1}S) with the atomic basis-set size of a consistent series. Using a basis which contains up to g functions still does not describe properly the very short-range electron repulsion. If ℓ represents the highest angular momentum contained in an atomic basis set, the concept of saturation in ℓ of the basis means that the quality of the calculation is not improved by adding any basis function of angular momentum smaller or equal to ℓ. To reach the FCI helium atom ground-state energy within 1 microhartree, the basis set should be saturated up to the angular momentum $\ell = 30$ and for 1 nanohartree accuracy, $\ell = 300$ should be used. Consequently it is very unlikely that such accuracy can be reached with conventional CI-type wave functions.

1.2.3 Extrapolation to the basis-set limit

Correlation-consistent basis sets present the greatest advantage to provide a smooth energy convergence in series towards the basis-set limit. However this convergence is slow due to the difficulties encountered in the description of the short-range electronic interactions. Taking advantage of the smoothness of the convergence, an extrapolation scheme serves as an useful alternative to reach high quality results at lower computational cost. In the series of Dunning atomic basis sets, it has been observed that the basis-set convergence of the (dynamical) correlation energy is approximately proportional to the inverse cube of the cardinal number, that is X^{-3}. Thus, carrying out two distinct energy calculations with consecutive cardinal numbers X-1 (E^{X-1}) and X (E^X), the basis-set limit of the correlation energy $E_\infty^{(X-1)X}$ can be extrapolated with a two-point extrapolation empirical formula (Eq. (1.21)) [28, 29].

$$E_\infty^{(X-1)X} = \frac{X^3 E^X - (X-1)^3 E^{X-1}}{X^3 - (X-1)^3} \,. \tag{1.21}$$

Table 1.2: Dunning-type correlation-consistent basis sets, cc-pVXZ, augmented correlation-consistent basis sets, aug-cc-pVXZ, and correlation-consistent polarized core-valence sets, cc-p CVXZ, for series of second row atoms. X goes from D to 6. The square brackets conventionally mean contracted functions.

Basis type	cc-pVXZ	aug-cc-pVXZ	cc-pCVXZ
D	[3s,2p,1d]	[4s,3p,2d]	[4s,3p,1d]
T	[4s,3p,2d,1f]	[5s,4p,3d,2f]	[6s,5p,3d,1f]
Q	[5s,4p,3d,2f,1g]	[6s,5p,4d,3f,2g]	[8s,7p,5d,3f,1g]
5	[6s,5p,4d,3f,2g,1h]	[7s,6p,5d,4f,3g,2h]	[10s,9p,7d,5f,3g,1h]
6	[7s,6p,5d,4f,3g,2h,1i]	[8s,7p,6d,5f,4g,3h,2i]	[12s,11p,9d,7f,5g,3h,1i]

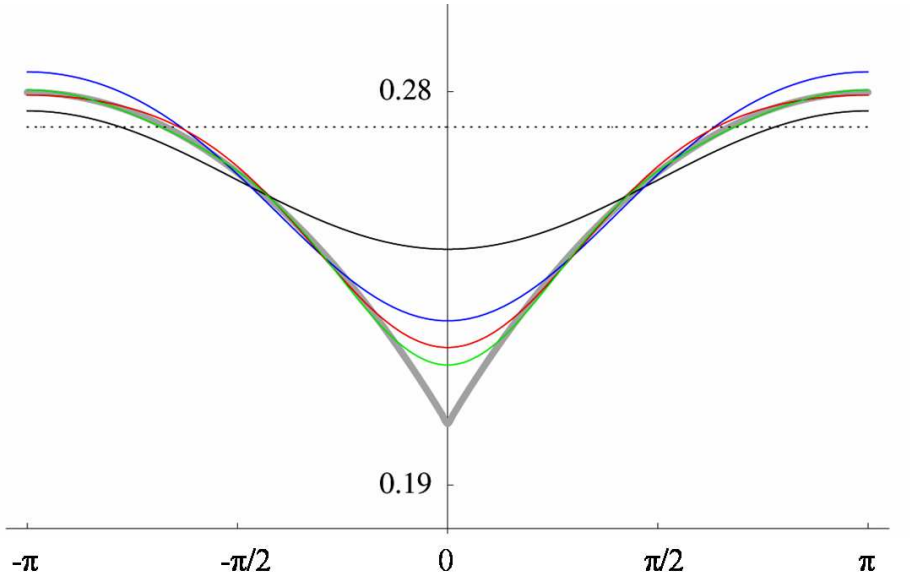

Figure 1.3: Full configuration interaction electronic wave function for the ^{1}S ground-state of the helium atom plotted versus the angle θ formed by the two electrons located on a circle of radius 0.5 a_0 about the nucleus. The dotted line represents the Hartree-Fock wave function in an atomic basis set $1s$ and the thick line is the exact wave function. In decreasing order with respect to the minimum at the intersection with the vertical axis ($\theta = 0$), the FCI wave function corresponds to the following atomic fully optimized basis sets: $2s1p$, $3s2p1d$, $4s3p2d1f$, and $5s4p3d2f1g$.

Since the extrapolation applies to the correlation energy only, one must separate the Hartree-Fock and correlation contributions. Clearly, the agreement of this two-point formula is better with larger cardinal numbers X, that is: $E_\infty^{\{56\}}$ is more accurate than $E_\infty^{\{45\}}$, itself more accurate than $E_\infty^{\{34\}}$, and $E_\infty^{\{34\}}$ is more accurate than $E_\infty^{\{23\}}$.

1.2.4 Basis-set superposition error

A typical problem raised by the incompleteness of the one-electron basis set is referred to as basis-set superposition error (BSSE). This fundamental error arises in the so-called supermolecular model when the interaction energy of a complex AB is defined as the difference between the dimer energy E_{AB} and the energy of the unperturbed monomers at infinite separation, $E_A + E_B$ (Eq. (1.22)).

$$\Delta E_{AB} = E_{AB} - E_A - E_B \,. \tag{1.22}$$

In such calculation, the dimer AB is treated in a larger basis than the monomers (the fragment A in AB can use basis functions of the fragment B, contrarily to the monomer calculation). The most

common strategy to remedy this problem is the counterpoise correction (CP) [30, 31]. It consists in evaluating each monomer energy in the full dimer basis, that is adding the basis functions of B as ghosts in space for the monomer A and vice versa. In this way, the CP correction, which is always positive in variational calculations, is the difference between the corrected E_{AB}^{CP} and the plain E_{AB} interaction energies. If β denotes a one-electron atomic basis set of a given type (e.g. cc-pVXZ), the CP correction reads:

$$\text{CP-correction} = E_{AB}^{CP} - E_{AB} = E_A^{\beta_A} + E_B^{\beta_B} - E_A^{\beta_{AB}} - E_B^{\beta_{AB}} \,. \tag{1.23}$$

It is not perfectly exact to say that the larger the basis, the smaller the BSSE (even though in a complete basis, the BSSE vanishes). In fact, when the size of the basis set increases, each fragment in the dimer calculation gets even more functions that may be used by other fragments to lower their energy. Hence, it is hard to predict the weight of this effect for a given basis set.

1.3 Explicitly correlated wave functions

1.3.1 Basic concept and origins

The weakness of the algebraic approximation manifests itself in the slow convergence of the electronic wave function with the atomic basis-set size, encountered when trying to account properly for the dynamical correlation. The fundamental idea of explicitly correlated wave functions is to create new N-electron basis functions more adapted for describing short-range electron correlation. For a given accuracy, the inclusion of a correlation factor dependent on the interelectronic distance r_{12} in the wave function drastically shortens the length of the expansion. The efficiency of this concept was already demonstrated in the early days of quantum mechanics. In 1929, Hylleraas introduced this model successfully for the helium atom [32] and James and Coolidge extended its use to the hydrogen molecule in 1933 [33]. In the late fifties, Pekeris applied it to ground and excited states of two-electron atoms [34–36] and in 1965, Kolos and Wolniewicz generalized it to describe properly the dissociation process [37]. Unfortunately, since then, the recognition of explicitly correlated wave functions as standard quantum chemistry tool was considerably handicaped by the combined difficulties of the theory and algorithms. First, this approach departs from the algebraic approximation and consequently from the fundamental concepts of 'orbitals' and 'excited configurations', which makes its general understanding more difficult. Furthermore, the implementation of the working equations is rather cumbersome compared to the standard approach. Finally, the occurrence of very expensive "more than two-" electron integrals was for a long time the essential drawback that restricted the application range to two-electron systems. Tardily in the eighties, the idea came up again in the scientific community and a major break-through happened

thanks to the use of approximation techniques for the computation of the difficult integrals. In the following are presented the main schemes which have been developed from then until today.

1.3.2 Linear correlation factor

A first practicable model relies on the use of the bare r_{12} distance between two electrons as correlation factor. Such approach is denoted R12 theory and Kutzelnigg, Klopper and Noga are names that are closely associated with it. It has been widely developed in the framework of MP2 and CC methods, up to CCSD(T) for both open- and closed-shell molecules [38–42]. The conventional N-electron configuration space is combined with a supplementary set of $N(N\text{-}1)/2$ pair functions Ω_{ij} of the form:

$$\Omega_{ij}(1,2,...,N) \;=\; \hat{A}\left(r_{12}\;\bar{\Phi}_i(1)\;\bar{\Phi}_j(2)\;...\;\bar{\Phi}_l(N)\right). \tag{1.24}$$

$\hat{A}$ is an antisymmetrization operator. To prevent eventual complications, the R12 pair functions are additionally projected outside the conventional configuration space. If $\hat{F}_2$ represents the operator that creates the set of the new two-electron dependent terms (including implicitly the corresponding amplitudes), the cluster operator $\hat{T}$ is written as:

$$\hat{T} = \hat{1} + \hat{T}_1 + \hat{T}_2 + \hat{F}_2 + \hat{T}_3 + ... + \hat{T}_N\,. \tag{1.25}$$

Then, the amplitudes corresponding to the extra R12 terms are the only parameters to be determined, simultaneously to the optimization of the conventional expansion coefficients. The achievement of R12 theory resides in the ingenious insertion of the resolution of the identity (i.e. closure relation) to partition the difficult three- and four-electron integrals (and even five-electron integrals for the CC-R12 methods) into products of simple two-electron integrals. Of course, the resolution of the identity requires a basis set close to completeness to be valid but the great advantage is that all integrals can readily be solved analytically.

Concretely, proceeding a R12 calculation consists in treating the correlation energy with a higher quality atomic basis set than the Hartree-Fock energy. Considering the series of Dunning basis sets, a R12 calculation in a basis of cardinal number X roughly allows one to reach the accuracy of the conventional calculation in a basis of cardinal number X+1. Obviously, the closer to completeness the atomic basis set is, the smaller the correction induced by the extra R12 pair functions is. Today R12 methods have been successfully applied to systems of about twenty electrons at the CCSD(T)-R12 level and to molecules containing up to twenty non-hydrogen atoms at the MP2-R12 level. In Table 1.3 are listed a few examples where R12 methods have given valuable chemical answers.

Table 1.3: Review (not exhaustive) of the domain of application of the R12 methods.

Properties	Molecular Systems	References
Binding energy	Benzene-Ar and Benzene-Ne	[43]
	$(HF)_n$ oligomers (n=2-5)	[44]
	CO_2 trimers	[45]
	H_2O dimer, trimer and tetramer	[46, 47]
	H_2O-OH^-	[48]
	benzene dimer	[49]
	H_2 and aromatic systems	[50]
Barrier to linearity	H_2O	[51, 52]
	SiC_2	[53]
Potential energy surface	HF dimer	[54, 55]
	He_2	[56, 57]
	H_2O dimer	[58]
	H_2O-H_2	[59]

1.3.3 Exponential correlation factor

The parallel pioneering works of Boys [60] and Singer [61] have inspired other types of explicitly correlated wave functions that use Gaussian functions as correlation factors.

In coupled-cluster and perturbational schemes

Gaussian geminals (GG) based methods have been developed in the eighties by Szalewicz and co-workers in the fields of MBPT and CC theories [62, 63]. The philosophy of the procedure is identical to R12 theory but the fundamental difference is that Gaussian geminals replace linear r_{12} as correlation factors in the pair functions:

$$\Omega_{ij}(1,2,...,N) \;=\; \hat{A}\,\Big(\exp\big(-\gamma_{ij}\,r_{12}^2\big)\;\bar{\Phi}_i(1)\;\bar{\Phi}_j(2)\;...\;\bar{\Phi}_l(N)\Big)\,. \tag{1.26}$$

There is an extra parameter γ_{ij} to optimize for each GG pair function. However, in the R12 scheme, the correction was given by a supplementary set of N-electron basis functions to the doubly excited configurations, while in the Gaussian Geminal scheme, the doubles are entirely substituted by the explicitly correlated terms. If $\hat{G}_2$ represents the operator that generates all the $N(N\text{-}1)/2$ new

N-electron basis functions (including again implicitly the corresponding amplitudes), the cluster operator $\hat{T}$ is expressed as:

$$\hat{T} = \hat{1} + \hat{T}_1 + \hat{G}_2 + \hat{T}_3 + ... + \hat{T}_N \,. \tag{1.27}$$

As in R12 theory, the GG pair functions are taken orthogonal to the conventional configuration space. Adjustments on the orthogonality condition can lead to new approaches where the difficult many-electron integrals (up to five-electron integrals) are restricted to three electrons. The main applications published up-to-date are at the CCD and MP2 level (Table 1.4).

In variational scheme

Moreover, an exponentially correlated Gaussian functions (ECG) approach has been developed for variational calculations by Cenzek and Rychlewski during the last decade [64, 65]. The building of the approximate wave function goes even further than in the previous methods, in the sense that it completely abandons the molecular-orbital approach. Thus no Hartree-Fock preliminary calculation needs to be done and the wave function is not anymore expanded in terms of Slater determinants but instead in terms of antisymmetrized N-particle functions Ω_k of the form:

$$\Psi_e \approx \sum_k \Omega_k \quad \text{and} \quad \Omega_k(1,2,...,N) = \hat{A}\, \exp\Big(-\sum_i a_i^k r^2_{C_i^k i} - \sum_{ij,i<j} b_{ij}^k r_{ij}^2\Big)\,. \tag{1.28}$$

The indices i and j are summed over the number of electrons N and the index k over the number of terms in the expansion. The operator $\hat{A}$ insures the antisymmetry property. All the functions that span the three-dimensional space are s-type Gaussians and their centers C_i^k are not restricted here to the positions of the nuclei. There are so $N(N$+3)/2 non-linear parameters a_i^k, b_{ij}^k and C_i^k per each N-electron basis function which are variationally optimized. In the case that the number of Ω_k is large enough and that all the parameters are carefully optimized, the calculation with the ECG wave function is identical to a FCI calculation. A typical ECG calculation can contain up to few thousands terms Ω_k in the expansion of the wave function. This variational approach has provided the most accurate calculations for all the small systems studied so far (Table 1.4).

Transcorrelated Hamiltonian

An original alternative to perform explicitly correlated calculations was already suggested in 1969 by Boys and Handy [71] and consists in transforming the electronic Hamiltonian with a correlation function, that is:

$$\hat{H}_e^C = \exp(-\hat{C})\hat{H}\exp(\hat{C}) \quad \text{with} \quad \hat{C} = \sum_{ij,i<j} f(r_{ij})\,, \tag{1.29}$$

Table 1.4: Selected examples of the domains of application of the explicitly correlated Gaussians (ECG) and Gaussian Geminals (GG) methods as well as the methods based on transcorrelated Hamiltonians (TH).

GG		ECG		TH	
Systems	References	Systems	References	Systems	References
He, Be, H_2, LiH	[66]	H_3, He_2^+ and LiH	[64, 65]	Ne, HF, NH_3	
H_2O	[67]	Be and He_2	[68, 69]	and CH_4	[70]

i and j are summed over the number of electrons N. In such form, the similarity-transformed Hamiltonian $\hat{H}_e^C$ is also called transcorrelated Hamiltonian. The correlation function $f(r_{12})$ has so far been exclusively expressed as a linear combination of Gaussian functions and it can be chosen so as to remove the singularities from the Hamiltonian [72]. The electronic wave function Ψ_e can be expressed by a standard CI expansion, but since $\hat{H}_e^C$ has lost its Hermiticity, it has different left and right eigenfunctions, namely $\langle\Psi_e^L|$ and $|\Psi_e^R\rangle$. Due to the Hausdorff expansion (Eq. (1.19)), transcorrelated methods introduce three-electron operators in the Hamiltonian, but no higher rank operators arise, contrarily to all the previously described techniques in this section. For about thirty years, this appealing method was somewhat forgotten but it regained today a vivid interest with the recent progress of Ten-no, who combined the transcorrelated Hamiltonian with a CC treatment of the wave function (Table 1.4) [73, 74].

1.3.4 Advances and challenges

In summary, the slow convergence of the electronic wave function can be overcome if explicitly correlated functions are used to represent cluster functions instead of, or in addition to ordinary molecular-orbital products. Today, these techniques allow one to achieve spectroscopic accuracy in numerous atomic and small- to medium-sized molecular energy calculations. Furthermore, such explicitly correlated wave functions possess several attractive features to enhance the atomic basis-set quality. They are particularly appropriate to improve the deficiency of the atomic basis set in high angular momentum functions. They are as well better adapted to describe the core and core-valence correlation without providing special correlating atomic orbitals. They also reduce significantly the basis-set superposition error. Nevertheless both linear and exponential approaches contain severe drawbacks, which slows down their appliance to large molecular systems.

R12 methods have by far the largest application range among all the enumerated models. For example, Gdanitz has developed a multi-reference configuration interaction (MRCI-R12) approach [75, 76] and current research is oriented on extending their use to excitation energies with the CC2-

R12 Ansatz [77, 78] and on the calculation of first-order molecular properties [79]. However, R12 calculations are not for free and give rise to significant numbers of specific two-electron integrals. Recently, Manby proposed an interesting way to speed up the computation of these special two-electron integrals using density fitting [80, 81]. Finally, R12 methods are restricted by the heavy prerequisite on the resolution of the identity to be properly verified. One then needs large bases which are saturated with functions of angular momenta ℓ up to three times more than the highest occupied orbital one ℓ_{occ} ($\ell = 3\ell_{occ}$).

All the methods employing an exponential correlation factor suffer from a real hindrance due to the expensive optimization of non-linear Gaussian parameters. This has limited their application range so far to ground-state energy calculations on molecules containing less than ten electrons at the CC level and less than four electrons at the variational level. Lately, another alternative to the full optimization has been considered by Persson and Taylor for the Gaussian geminal approach. A predefined set of Gaussian geminals is fixed by fitting the interelectronic distance r_{12} [82]. In the same logic, Ten-no determined the Gaussian exponents for the transcorrelated Hamiltonian by least squares fitting of a short-range weight function [70]. Another stumbling block of these methods remains the expensive calculation of the three-electron integrals in a closed form, that is without the insertion of a closure relation.

It is widely found in the literature that the performance of R12 methods is based on the fact that, in such form, the electronic wave function satisfies the Kato's cusp condition. This statement is right but should be modulated. The fact that exponential correlation factors, without solving the cusp condition, still lead to better electron correlation convergence than the R12 methods (for the H_2 molecule as an example) clearly demonstrates that the most important feature of the explicitly correlated wave functions lies more in their ability to describe the overall shape of the Coulomb hole [83]. Even if, of course, the linear behavior of the wave function at small interelectronic distances is a direct consequence of the Coulomb cusp. To conclude, the explicitly correlated wave functions theory has rapidly evolved during the past two decades and is not anymore solely regarded as an exotic method for benchmark calculations [84].

1.4 Composition of this thesis

This thesis is devoted to the determination of highly accurate ground-state properties for closed-shell molecular systems containing atoms of the first and second rows of the *Periodic Table of Elements*. It essentially focuses on basis-set convergence of the correlation energy inside a given post-Hartree-Fock model. Thus, in the following, it is assumed that the Hartree-Fock reference provides a good approximation for the statical correlation energy and that the chosen molecular-orbital-based model is sufficient for recovering the largest part of the long-range dynamical cor-

relation energy. Since a substantial part of this work concerns further developments on the R12 methods, chapter 2 reviews the leading concepts, fundamental approximations and main working equations of the family of explicitly correlated wave functions that employs a linear correlation factor. More specifically, the review is limited to MP2 and CCSD(T) theories.

Chapters 3 and 4 present two basis-set convergence studies computed via basis-set extrapolation techniques and explicitly correlated wave functions, respectively. First, chapter 3 contains the determination of the equilibrium inversion barrier of ammonia computed at the CCSD(T) level with a new two-point extrapolation scheme. Contrarily to Eq. (1.21) which considers that the basis-set convergence of the total correlation energy scales as X^{-3} (with X the cardinal number of the basis set), the applied scheme is based on the distinction between the convergence of the singlet (X^{-3}) and triplet pair energies (X^{-5}). Second, chapter 4 is a study of the low proton barrier and of the binding energy of the $(H_2O)OH^-$ complex. Data are obtained at the basis-set limit of CCSD(T) by virtue of the R12 correction. The basis-set superposition error is avoided by applying counterpoise correction.

The new developments on the R12 methods aim to extend their application range to larger molecules than the ones computable today. In chapter 5, a new methodology is presented to ease the computation of the R12 correction at the MP2 level. It consists of the introduction of a large (nearly complete) one-electron basis set which adequately solves the resolution of the identity, while the remaining of the calculation can be done with smaller available basis sets. Chapter 6 presents the development in the MP2-R12 framework of a new hybrid correlation factor which is a compromise between the linear correlation factor and the exponential correlation factor, namely $r_{12}\exp(-\gamma r_{12}^2)$, with γ a positive real parameter. The goal of this correlation factor is to provide a vanishing behavior at large interelectronic distances through the Gaussian geminal, while keeping the linear behavior at short electronic distances. This advanced correlation factor has inspired a modified correlation function to speed up the convergence of the standard CI expansion of the wave function via similarity-transformation of the Hamiltonian. The methodology and results for two-electron systems are given in chapter 7. Finally, chapter 8 gives a series of benchmark calculations for MP2-R12 pair energies of both ethylene and ethane, obtained with localized orbitals following the Boys localization criteria. The concluding chapter (chapter 9) presents the possible impact of these developments when combined with local correlation techniques and gives an outlook for eventual future studies in this direction.

Acknowledgments

Figure 1.2 is reproduced from the book *Molecular Electronic-Structure Theory*, written by Trygve Helgaker, Poul Jørgensen, and Jeppe Olsen, with permission of John Wiley & Sons, Ltd.

References

[1] E. Schrödinger, Ann. Physik **79**, 361 (1926).

[2] B. T. Sutcliffe, Adv. Quantum. Chem. **28**, 65 (1997).

[3] A. Szabo and N. S. Ostlund, *Modern Quantum Chemistry, Introduction to Advanced Electronic Structure Theory*, Dover Publications, INC., Mineola, New York, (1982).

[4] P. O. Löwdin, Adv. Chem. Phys. **22**, 207 (1959).

[5] P. E. M. Siegbahn, *Lecture notes in quantum chemistry, European Summerschool in Quantum Chemistry, Vol. 1, pp. 243–284*, B. O. Roos (Ed.), Lund, (2000).

[6] L. Møller and M. S. Plesset, Phys. Rev. **46**, 618 (1934).

[7] J. Olsen, P. Jørgensen, T. Helgaker, and O. Christiansen, J. Chem. Phys. **112**, 9736 (2000).

[8] M. L. Leininger, W. D. Allen, and H. F. Schaefer III, J. Chem. Phys. **112**, 9213 (2000).

[9] R. J. Bartlett, *In: Modern Electronic Structure Theory, pp. 1047–1130*, D. R. Yarkony (Ed.), World Scientific Publishing Co. Ltd., Singapore, (1995).

[10] K. Raghavachari, G. W. Trucks, J. A. Pople, and M. Head-Gordon, Chem. Phys. Lett. **157**, 479 (1989).

[11] SARA Computing and Networking Services, *An advanced center of expertise that supplies a complete package of high-performance computing, high-performance networking and infrastructure services*, www.sara.nl, Amsterdam, the Netherlands.

[12] J. Olsen, P. Jørgensen, H. Koch, A. Balkova, and R. J. Bartlett, J. Chem. Phys. **104**, 8007 (1996).

[13] C. Ochsenfeld, Chem. Phys. Lett. **327**, 216 (2000).

[14] R. A. Kendall and H. A. Früchtl, Theor. Chim. Acta **97**, 158 (1997).

[15] P. J. Knowles, M. Schütz, and H.-J. Werner, *In: Modern Methods and Algorithms of Quantum Chemistry, Vol. 3, pp. 97–179*, J. Grotendorst (Ed.), NIC series, Forschungszentrum Jülich, Germany, (2000).

[16] B. O. Roos, *Lecture notes in quantum chemistry, European Summerschool in Quantum Chemistry, Vol. 2, pp. 285–360*, B. O. Roos (Ed.), Lund, (2000).

[17] P. Hohenberg and W. Kohn, Phys. Rev. **136**, B864 (1964).

[18] F. Furche, R. Ahlrichs, P. Weis, C. Jacob, S. Gilb, T. Bierweiler, and M. M. Kappes, J. Chem. Phys. **117**, 6982 (2002).

[19] P. Nava, M. Sierka, and R. Ahlrichs, Phys. Chem. Chem. Phys. **5**, 3372 (2003).

[20] J. B. Danielsson, J. Uličný, and A. Laaksonen, J. Am. Chem. Soc. **123**, 9817 (2001).

[21] T. Kato, Commun. Pure Appl. Math. **10**, 151 (1957).

[22] T. H. Dunning, Jr., J. Chem. Phys. **90**, 1007 (1989).

[23] R. A. Kendall, T. H. Dunning, Jr., and R. J. Harrison, J. Chem. Phys. **96**, 6796 (1992).

[24] D. E. Woon and T. H. Dunning, Jr., J. Chem. Phys. **98**, 1358 (1993).

[25] D. E. Woon and T. H. Dunning, Jr., J. Chem. Phys. **100**, 2975 (1994).

[26] D. E. Woon and T. H. Dunning, Jr., J. Chem. Phys. **103**, 4572 (1995).

[27] A. K. Wilson, T. van Mourik, and T. H. Dunning, Jr., J. Mol. Struct. (Theochem) **338**, 339 (1996).

[28] T. Helgaker, W. Klopper, H. Koch, and J. Noga, J. Chem. Phys. **106**, 9639 (1997).

[29] A. Halkier, T. Helgaker, P. Jørgensen, W. Klopper, H. Koch, J. Olsen, and A. K. Wilson, Chem. Phys. Lett. **286**, 243 (1998).

[30] S. F. Boys and B. Bernardi, Mol. Phys. **19**, 553 (1970).

[31] F. B. van Duijneveldt, J. G. C. M. van Duijneveldt-van de Rijdt, and J. H. van Lenthe, Chem. Rev. **94**, 1873 (1994).

[32] E. A. Hylleraas, Z. Phys. **54**, 347 (1929).

[33] H. M. James and A. S. Coolidge, J. Chem. Phys. **1**, 825 (1933).

[34] C. L. Pekeris, Phys. Rev. **112**, 1649 (1958).

[35] C. L. Pekeris, Phys. Rev. **115**, 1216 (1959).

[36] C. L. Pekeris, Phys. Rev. **126**, 1470 (1962).

[37] W. Kołos and L. Wolniewicz, J. Chem. Phys. **43**, 2429 (1965).

[38] W. Kutzelnigg, Theor. Chim. Acta **68**, 445 (1985).

[39] W. Klopper and W. Kutzelnigg, Chem. Phys. Lett. **134**, 17 (1987).

[40] W. Klopper, *In: The Encyclopedia of Computational Chemistry, Vol.4, pp. 2351–2375*, P. v. R. Schleyer, N. L. Allinger, T. Clark, J. Gasteiger, P. A. Kollman, H. F. Schaefer III, and P. R. Schreiner (Eds.), John Wiley & Sons, Ltd., Chichester, New York, (1998).

[41] J. Noga, W. Klopper, and W. Kutzelnigg, *In: Recent Advances in Computational Chemistry, Vol. 3, pp. 1–48*, R. J. Bartlett (Ed.), World Scientific Publishing Co. Ltd., Singapore, (1997).

[42] J. Noga and P. Valiron, Chem. Phys. Lett. **324**, 166 (2000).

[43] W. Klopper, H. P. Lüthi, T. Brupbacher, and A. Bauder, J. Chem. Phys. **101**, 9747 (1994).

[44] W. Klopper, M. Quack, and M. A. Suhm, Mol. Phys. **94**, 105 (1998).

[45] S. Tsuzuki, W. Klopper, and H. P. Lüthi, J. Chem. Phys. **111**, 3846 (1999).

[46] W. Klopper and M. Schütz, Ber. Bunsenges. Phys. Chem. **99**, 469 (1995).

[47] W. Klopper, J. G. C. M. van Duijneveldt-van de Rijdt, and F. B. van Duijneveldt, Phys. Chem. Chem. Phys. **2**, 2227 (2000).

[48] C. C. M. Samson and W. Klopper, J. Mol. Struct. (Theochem) **586**, 201 (2002).

[49] M. O. Sinnokrot, E. F. Valeev, and C. D. Sherrill, J. Am. Chem. Soc. **124**, 10887 (2002).

[50] O. Hübner, A. Glöß, M. Fichtner, and W. Klopper, J. Phys. Chem. A **108**, 3019 (2004).

[51] G. Tarczay, A. G. Császár, W. Klopper, V. Szalay, W. D. Allen, and H. F. Schaefer III, J. Chem. Phys. **110**, 11971 (1999).

[52] E. F. Valeev, W. D. Allen, H. F. Schaefer III, and A. G. Császár, J. Chem. Phys. **114**, 2875 (2001).

[53] J. P. Kenny, W. D. Allen, and H. F. Schaefer III, J. Chem. Phys. **118**, 7353 (2003).

[54] W. Klopper, M. Quack, and M. A. Suhm, Chem. Phys. Lett. **261**, 35 (1996).

[55] W. Klopper, M. Quack, and M. A. Suhm, J. Chem. Phys. **108**, 10096 (1998).

[56] W. Klopper and J. Noga, J. Chem. Phys. **103**, 6127 (1995).

[57] M. Jaszuński, W. Klopper, and J. Noga, J. Chem. Phys. **113**, 71 (2000).

[58] G. S. Tschumper, M. L. Leininger, B. C. Hoffman, E. F. Valeev, H. F. Schaefer III, and M. Quack, J. Chem. Phys. **116**, 690 (2002).

[59] P. Valiron, A. Faure, C. Rist, and J. Noga, *High accuracy 5-dimensional H_2O-H_2 interaction potential hypersurface was calculated by combination of 75000 geometries computed at the CCSD(T) level and 1000 geometries at the CCSD(T)-R12 level*, Poster presented at the XIth International Congress of Quantum Chemistry, Bonn, Germany, July 20-26, (2003).

[60] S. F. Boys, Proc. Roy. Soc. (London) **A258**, 402 (1960).

[61] K. Singer, Proc. Roy. Soc. (London) **A258**, 412 (1960).

[62] K. Szalewicz, B. Jeziorski, H. J. Monkhorst, and J. G. Zabolitzky, J. Chem. Phys. **78**, 1420 (1983).

[63] K. Szalewicz, B. Jeziorski, H. J. Monkhorst, and J. G. Zabolitzky, J. Chem. Phys. **79**, 5543 (1983).

[64] W. Cencek and J. Rychlewski, J. Chem. Phys. **98**, 1252 (1993).

[65] W. Cencek and J. Rychlewski, J. Chem. Phys. **102**, 2533 (1995).

[66] B. Jeziorski, H. J. Monkhorst, K. Szalewicz, and J. G. Zabolitzky, J. Chem. Phys. **81**, 368 (1984).

[67] R. Bukowski, B. Jeziorski, S. Rybak, and K. Szalewicz, J. Chem. Phys. **102**, 888 (1995).

[68] J. Komasa, W. Cencek, and J. Rychlewski, Phys. Rev. A **52**, 4500 (1995).

[69] J. Komasa and J. Rychlewski, Chem. Phys. Lett. **249**, 253 (1996).

[70] O. Hino, Y. Tanimura, and S. Ten-no, Chem. Phys. Lett. **353**, 317 (2002).

[71] S. F. Boys and N. C. Handy, Proc. Roy. Soc. (London) **310**, 43 (1969).

[72] J. O. Hirschfelder, J. Chem. Phys. **39**, 3145 (1963).

[73] S. Ten-no, Chem. Phys. Lett. **330**, 169 (2000).

[74] S. Ten-no, Chem. Phys. Lett. **330**, 175 (2000).

[75] R. J. Gdanitz, Chem. Phys. Lett. **210**, 253 (1993).

[76] R. J. Gdanitz and R. Röhse, Int. J. Quantum Chem. **55**, 147 (1996).

[77] C. Hättig and F. Weigend, J. Chem. Phys. **113**, 5154 (2000).

[78] H. Fliegl, C. Hättig, and W. Klopper, *Explicitly-correlated CC2-R12 vertical excitation energies*, Poster presented at the conference entitled: 'Electron Correlation: Ab initio Methods and Density Functional Theory', Bad Herrenalb, Germany, July 16-19, (2003).

[79] A. Glöß, C. Villani, E. Vollmer, and W. Klopper, *Analytical Energy Gradients for the RI-MP2-R12 Method*, Poster presented at the first meeting of the DFG Priority Program 1145, CJD Bonn, Germany, June 1-3, (2003).

[80] F. R. Manby, J. Chem. Phys. **119**, 4607 (2003).

[81] S. Ten-no and F. R. Manby, J. Chem. Phys. **119**, 5358 (2003).

[82] B. J. Persson and P. R. Taylor, J. Chem. Phys. **105**, 5915 (1996).

[83] D. Prendergast, M. Nolan, C. Filippi, S. Fahy, and J. C. Greer, J. Chem. Phys. **115**, 1626 (2001).

[84] E. Bednarz, R. Bukowski, M. Bylicki, W. Cencek, H. Chojnacki, R. Jaquet, B. Jeziorski, J. Karwowski, W. Klopper, J. Komasa, W. Kutzelnigg, J. Noga, G. Pestka, J. Rychlewski, K. Strasburger, and K. Szalewicz, *Explicitly Correlated Wave Functions in Chemistry and Physics: Theory and Applications, Vol. 13*, J. Rychlewski (Ed.), Kluwer Academic Publishers, Dordrecht, (2003).

2

Overview of the R12 theory

2.1 R12 wave function

Extensive reviews on linear explicitly correlated wave functions are available in the literature [1–4]. The modus operandi favored in this chapter is to highlight the most important points of the theory without providing too many technical details.

2.1.1 Notations and definitions

$\bar{\Phi}_i$, $\bar{\Phi}_j$, ... are occupied molecular spin orbitals, $\bar{\Phi}_a$, $\bar{\Phi}_b$, ... are virtual molecular spin orbitals and $\bar{\Phi}_p$, $\bar{\Phi}_q$, ... denote any molecular spin orbitals. The so-called *physicist's* convention (or *bra-ket* notation) is employed in the following to represent integrals over electronic spatial-spin coordinates $\vec{\tau}$. For instance, if $\hat{\omega}_1$ and $\hat{\Omega}_{12}$ are respectively one- and two-electron operators, then:

$$\langle \bar{\Phi}_p(1) | \hat{\omega}_1 | \bar{\Phi}_r(1) \rangle = \int \bar{\Phi}_p^*(1)\, \hat{\omega}_1\, \bar{\Phi}_r(1)\; d\vec{\tau}_1 = \omega_p^r \,. \tag{2.1}$$

$$\langle \bar{\Phi}_p(1)\bar{\Phi}_q(2) | \hat{\Omega}_{12} | \bar{\Phi}_r(1)\bar{\Phi}_s(2) \rangle = \int\int \bar{\Phi}_p^*(1)\bar{\Phi}_q^*(2)\, \hat{\Omega}_{12}\, \bar{\Phi}_r(1)\bar{\Phi}_s(2)\; d\vec{\tau}_1 d\vec{\tau}_2 = \Omega_{pq}^{rs} \,. \tag{2.2}$$

The star * represents the complex conjugate of the corresponding function. A product of two molecular spin orbitals between square brackets symbolizes an antisymmetric two-electron pair function (Eq. (2.3)), as expressed by a Slater two-electron determinant (Eq. (1.4)).

$$\big[\bar{\Phi}_p(1)\bar{\Phi}_q(2)\big] = \frac{1}{\sqrt{2}} \Big(\bar{\Phi}_p(1)\bar{\Phi}_q(2) - \bar{\Phi}_q(1)\bar{\Phi}_p(2) \Big) \,. \tag{2.3}$$

N is the total number of electrons of the considered molecular system and consequently the number of occupied molecular spin orbitals, N_{vir} the number of virtual molecular spin orbitals in the finite space and N_{tot} the total number of molecular spin orbitals in the finite space, $N_{tot} = N + N_{vir}$. N_u denotes the total number of nuclei, and Z the positive nuclear charge. The symbols $\vec{r}$ and $\vec{R}$ correspond respectively to electronic and nuclear positions with respect to an arbitrary spatial coordinate origin and r and R represent respectively electronic and nuclear distances to the origin. r_{12} is the interelectronic distance $|\vec{r}_1 - \vec{r}_2|$ between electrons one and two. The symbol $\sum$ indicates by default a sum starting from integer one and if two indices are specified as subscripts for only one integer as superscript, the two indices sum over the same limiting integer. Atomic units are assumed in the following.

For sake of simplicity, the molecular spin orbitals are designed orthonormal among each other, that is the overlap matrix $\boldsymbol{S}$ between molecular spin orbitals (Eq. (2.4)) is simply the unit matrix.

$$S_p^r = \langle \bar{\Phi}_p(1) | \bar{\Phi}_r(1) \rangle = \delta_p^r \qquad \text{with} \quad \delta_p^r = 1 \quad \text{if} \quad p = r \quad \text{and} \quad \delta_p^r = 0 \quad \text{otherwise} \,. \tag{2.4}$$

The Coulomb and exchange operators, respectively $\hat{j}$ (Eq. (2.5)) and $\hat{k}$ (Eq. (2.6)), correspond to their conventional definitions in the Hartree-Fock theory [5]. Likewise, the one-electron operator

$\hat{h}$ is the sum of the kinetic energy $\hat{t}$ and the interaction between the considered electron with all the nuclei (Eq. (2.7)).

$$\hat{j}_1\,\bar{\Phi}_p(1) = \Big(\sum_i^N \langle\bar{\Phi}_i(2)|\,\frac{1}{r_{12}}\,|\bar{\Phi}_i(2)\rangle\Big)\,\bar{\Phi}_p(1)\,. \tag{2.5}$$

$$\hat{k}_1\,\bar{\Phi}_p(1) = \Big(\sum_i^N \langle\bar{\Phi}_i(2)|\,\frac{1}{r_{12}}\,|\bar{\Phi}_p(2)\rangle\quad\bar{\Phi}_i(1)\Big)\,. \tag{2.6}$$

$$\hat{h}_1\,\bar{\Phi}_p(1) = \Big(-\frac{1}{2}\Delta_1 - \sum_n^{N_u}\frac{Z_n}{|\vec{R}_n-\vec{r}_1|}\Big)\,\bar{\Phi}_p(1)\,. \tag{2.7}$$

$\Delta = \vec{\nabla}\cdot\vec{\nabla}$ is the Laplacian scalar differential operator which is expressed in cartesian coordinates as $\frac{\partial^2}{\partial x^2}+\frac{\partial^2}{\partial y^2}+\frac{\partial^2}{\partial z^2}$ and the differential operator $\vec{\nabla}$ has the following x, y, z coordinates $\{\frac{\partial}{\partial x},\frac{\partial}{\partial y},\frac{\partial}{\partial z}\}$. Then the effective one-electron Fock operator $\hat{f}$ is written as:

$$\hat{f}_1 = \hat{h}_1 + \hat{j}_1 - \hat{k}_1\,. \tag{2.8}$$

The molecular spin orbitals that are eigenfunctions of the Fock operator are named canonical orbitals and their corresponding eigenvalues are the orbital energies. The set of canonical molecular spin orbitals does not uniquely solve the Hartree-Fock equations. It is possible to obtain an infinite number of equivalent sets by unitary transformations of the canonical set. In particular, the Boys [6] and Pipek-Mezey [7] criteria are among the most popular to build the so-called localized molecular spin orbitals. By convention, $\boldsymbol{f}$ is the matrix representation of the Fock operator $\hat{f}$ within the set of molecular spin orbitals (Eq. (2.8)) and the Brillouin condition in its most general form states that the matrix elements f_i^a between the occupied and virtual blocks are zero.

$$f_p^r = \langle\bar{\Phi}_p(1)|\hat{f}_1|\bar{\Phi}_r(1)\rangle \quad\text{and}\quad f_i^a = 0\,. \tag{2.9}$$

The matrices $\boldsymbol{f}_o$ and $\boldsymbol{f}_v$ represent respectively the occupied and virtual blocks of the Fock matrix. $\hat{t}_{12}$ stands for the sum of the kinetic energy operators for electrons one and two and $\hat{f}_{12}$ for the sum of the Fock operators (Eqs. (2.10)).

$$\hat{t}_{12} = \hat{t}_1 + \hat{t}_2 \quad\text{and}\quad \hat{f}_{12} = \hat{f}_1 + \hat{f}_2\,. \tag{2.10}$$

Finally, it is important to define carefully the matrix notation that will be used in this chapter, providing compact and clear working equations. As already pointed out for the overlap or the Fock matrices, a two-index matrix associated with a one-electron operator is simply represented by a bold symbol. If $\boldsymbol{x}$ is the resulting two-index matrix of the matrix product $\boldsymbol{yz}$, then its elements and trace are defined as in Eq. (2.11). Let's define now $\ddot{\boldsymbol{X}}$ as a four-index matrix corresponding to a two-electron operator $\hat{X}_{12}$ (Eq. (2.2)). The adjoint and the trace of such matrix are defined in Eq.

(2.12). If $\ddot{\boldsymbol{Y}}$ and $\ddot{\boldsymbol{Z}}$ are two matrices defined in the same way, then the product $\ddot{\boldsymbol{X}} = \ddot{\boldsymbol{Y}}\,\ddot{\boldsymbol{Z}}$ reads as in Eq. (2.13).

$$x_p^r = \sum_t^{N_{tot}} y_p^t z_t^r \qquad \text{and} \qquad \mathrm{Tr}\,(\boldsymbol{x}) = \sum_t^{N_{tot}} x_t^t \,. \tag{2.11}$$

$$\{\ddot{\boldsymbol{X}}^\dagger\}_{pq}^{rs} = \{X_{rs}^{pq}\}^* \qquad \text{and} \qquad \mathrm{Tr}\,(\ddot{\boldsymbol{X}}) = \sum_{tu}^{N_{tot}} X_{tu}^{tu} \,. \tag{2.12}$$

$$X_{pq}^{rs} = \sum_{tu}^{N_{tot}} Y_{pq}^{tu} Z_{tu}^{rs} \,. \tag{2.13}$$

2.1.2 Hylleraas wave function

The potential of the explicit r_{12} insertion into the wave function was demonstrated by Hylleraas for the ground-state of the helium atom already in 1929 [8]. In terms of $s = r_1 + r_2$, $t = r_1 - r_2$ and $u = r_{12}$ coordinates and given ξ and l_i, m_i and n_i exponents and c_i coefficients variationally optimized for an expansion of length N_t terms, the Hylleraas function reads:

$$\Psi^{\text{Hylleraas}} = \exp(-\xi s) \sum_i^{N_t} c_i s^{l_i} t^{2m_i} u^{n_i} \,. \tag{2.14}$$

The performance of the Hylleraas function is illustrated in Figure 2.1. The optimized energy is plotted as a function of the number of terms generated by truncating the expansion in Eq. (2.14) according to the condition that $l_i + 2m_i + n_i \leq N_{max}$.

2.1.3 Kutzelnigg wave function

The R12 wave function has first been proposed by Kutzelnigg in 1985 [9]. It consists of the insertion of an extra set of contributions into the conventional determinantal expression of the wave function. Inspired by the powerful Hylleraas wave function, such R12 terms are chosen dependent on the interelectronic distance r_{12}. One takes as a convention the notation $\Psi_{ij\ldots}^{ab\cdots}$ for a configuration where a given number of occupied molecular spin orbitals $\bar{\Phi}_i$, $\bar{\Phi}_j$, ... have been replaced in the Hartree-Fock reference wave function Ψ_0 by the same number of virtual molecular spin orbitals $\bar{\Phi}_a$, $\bar{\Phi}_b$, ... For an orthogonal set of molecular spin orbitals, all the configurations are orthogonal among each other. The term $t_{ab\ldots}^{ij\cdots}$ corresponds to the amplitude of such configuration in the expansion of the wave function. To be consistent with this notation, the R12 extra terms are denoted here $\Psi_{ij}^{r_{12}kl}$ (instead of the simplified notation Ω_{ij} introduced in chapter 1, Eq. (1.24)) and c_{kl}^{ij} are their allied amplitudes. In such notation, the CI-type Kutzelnigg wave function is written

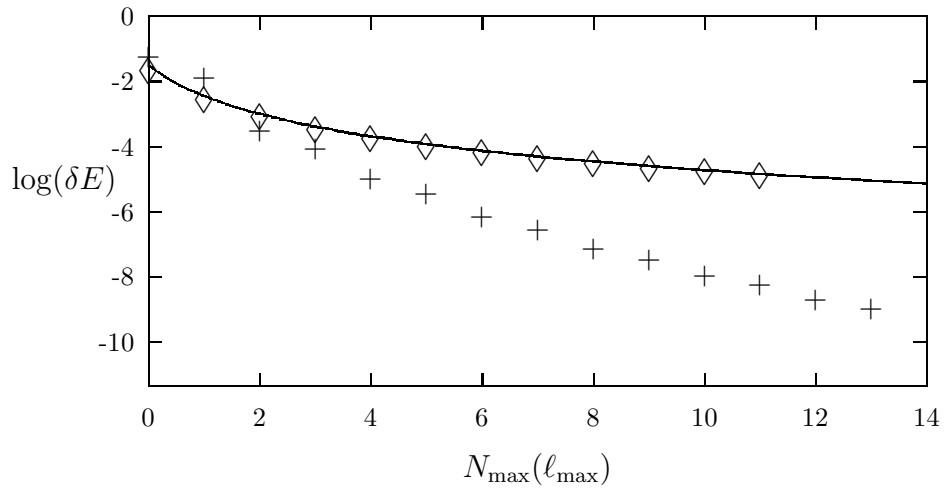

Figure 2.1: Logarithm of the error $\delta E = (E - E_{\text{exact}})/E_{\text{h}}$ of the CI ($\Diamond$) and Hylleraas ($+$) expansions plotted against the maximum angular momentum quantum number $\ell_{\max}$ contained in the CI basis or the maximum $l_i + 2m_i + n_i \leq N_{\max}$ of the Hylleraas-type expansions, respectively. The solid line corresponds to the function: $\log\left\{0.024\,741\,9\,(\ell_{\max}+1)^{-3} + 0.007\,747\,27\,(\ell_{\max}+1)^{-4}\right\}$.

as follows:

$$\Psi_e \approx \Psi_0 + \sum_{i}^{N}\sum_{a}^{N_{vir}} t_a^i \Psi_i^a + \frac{1}{4}\sum_{ij}^{N}\sum_{ab}^{N_{vir}} t_{ab}^{ij}\Psi_{ij}^{ab} + ... + \frac{1}{4}\sum_{ij}^{N}\sum_{kl}^{N} c_{kl}^{ij}\Psi_{ij}^{r_{12}kl}\,. \tag{2.15}$$

This is the modern form of the R12 corrected wave function. Initially the R12 correction was inserted into the conventional CI-type expansion in a slightly different form (Eq. (2.16)) [10].

$$\text{R12-initial} = \frac{1}{2}\sum_{ij}^{N} c_{ij}\Psi_{ij}^{r_{12}ij}\,. \tag{2.16}$$

Each R12 extra term was strictly defined for one unique pair of occupied molecular spin orbitals and completely independent of all the remaining pairs. The modern form of the R12 wave function has been developed because it makes the R12 corrected energy invariant with respect to unitary transformations of the set of molecular spin orbitals [11]. It is thus denoted as "invariant" and the initial form for historical reasons as "non-invariant". Empirically, it has been observed that the non-invariant approach induces errors when the molecular spin orbitals are very delocalized (relative to the Boys localization criteria). Mainly for this reason, the non-invariant approach is not used anymore in practice.

Concretely, the notation $\Psi_{ij}^{r_{12}kl}$ signifies substitution in the Hartree-Fock reference determinant of an occupied pair function $\left[\bar{\Phi}_i(1)\bar{\Phi}_j(2)\right]$ by an explicitly correlated occupied pair function $r_{12}\left[\bar{\Phi}_k(1)\bar{\Phi}_l(2)\right]$. More precisely, one should ensure that the R12 occupied pair functions are strongly orthogonal to the conventional configuration space. If the operator $\hat{Q}$ denotes the required outprojector and $\hat{P}$ designates the one-electron projector onto the finite molecular spin orbital space, then:

$$\hat{P}_1 = \sum_{p}^{N_{tot}} |\bar{\Phi}_p(1)\rangle \langle\bar{\Phi}_p(1)| \quad \text{and} \quad \hat{Q}_1 = \hat{1} - \hat{P}_1 \,. \tag{2.17}$$

$\hat{P}_{12}$ and $\hat{Q}_{12}$ are respectively the products $\hat{P}_1\hat{P}_2$ and $\hat{Q}_1\hat{Q}_2$. The explicitly correlated occupied pair functions are so properly written as:

$$\hat{Q}_{12}r_{12}\left[\bar{\Phi}_k(1)\bar{\Phi}_l(2)\right] \quad \text{or} \quad \left(\hat{1} - \hat{P}_1\right)\left(\hat{1} - \hat{P}_2\right)r_{12}\left[\bar{\Phi}_k(1)\bar{\Phi}_l(2)\right] . \tag{2.18}$$

2.2 MP2-R12 theory

The R12 corrected wave function has been first widely investigated at the MP2 (Møller-Plesset to second-order) level in a series of articles [12–14]. The main reason for such endemic orientation is the relative simplicity to introduce the R12 correction independently into the MP2 correlation energy. Many properties and technicalities have been preliminarly studied at this level, which has inspired the implementation of the R12 correction in an efficient manner for more sophisticated post-Hartree-Fock methods. This section will briefly review the main steps to the MP2-R12 working equations that need to be solved to compute ground-state energies.

2.2.1 Conventional MP2 scheme

As defined in the general introduction (chapter 1), $\hat{H}_e$ is the electronic Hamiltonian, Ψ_0 is the Hartree-Fock reference and Ψ_1 the first-order perturbed wave function which is orthogonal to the Hartree-Fock reference. In the Møller-Plesset partitioning of the Hamitonian, the perturbation $\hat{V}$ is expressed as in Eq. (2.19) and the zeroth-, first- and second-order energies are respectively as in Eq. (2.20).

$$\lambda\hat{V} = \hat{H}_e - \hat{H}_0 \quad \text{with} \quad \hat{H}_0 = \sum_{k}^{N} \hat{f}_k \;\text{ and }\; \lambda = 1 \,. \tag{2.19}$$

$$E_0 = \langle\Psi_0|\hat{H}_0|\Psi_0\rangle \,, \quad E_1 = \langle\Psi_0|\hat{V}|\Psi_0\rangle \,, \quad \text{and} \quad E_2 = \langle\Psi_0|\hat{V}|\Psi_1\rangle \,. \tag{2.20}$$

Consequently, the sum $E_0 + E_1$ is equal to the Hartree-Fock energy and the second-order contribution E_2 is the first level of correction. The latter requires the determination of the first-order wave function (Eq. (2.21)). The factors t_{ab}^{ij} correspond to the amplitudes of the doubly excited configurations Ψ_{ij}^{ab} in the expansion of the first-order wave function, by analogy to the CI-formalism. No single substituted configuration contributes to Ψ_1 consequently to the Brillouin theorem (Eq. (1.13)). By selecting the terms which belong to the first-power of the scaling parameter λ (Eq. (1.14)), one gets Eq. (2.22).

$$\Psi_1 \;=\; \frac{1}{4}\sum_{ij}^{N}\sum_{ab}^{N_{vir}} t_{ab}^{ij}\Psi_{ij}^{ab}\,. \tag{2.21}$$

$$\left(\hat{H}_0 - E_0\right)\Psi_1 = -\left(\hat{V} - E_1\right)\Psi_0\,. \tag{2.22}$$

The matrix $\ddot{\boldsymbol{G}}$ collects the conventional two-electron integrals over the operator r_{12}^{-1} (Eq. (2.23)) and $\ddot{\boldsymbol{T}}_2$ collects the amplitudes t_{ab}^{ij}. The conventional MP2 energy is then given by Eq. (2.24).

$$G_{ij}^{ab} = \langle\left[\bar{\Phi}_i(1)\bar{\Phi}_j(2)\right]|\frac{1}{r_{12}}|\left[\bar{\Phi}_a(1)\bar{\Phi}_b(2)\right]\rangle\,. \tag{2.23}$$

$$E_2^{\text{MP2}} = \frac{1}{4}\,\text{Tr}\left(\ddot{\boldsymbol{G}}\ddot{\boldsymbol{T}}_2\right). \tag{2.24}$$

If the braces notations $\{\ddot{\boldsymbol{T}}_2, \boldsymbol{f}_o\}$ and $\{\boldsymbol{f}_v, \ddot{\boldsymbol{T}}_2\}$ are defined in Eq. (2.25) and projecting Eq. (2.22) on the doubly substituted configurations Ψ_{ij}^{ab}, the conventional MP2 amplitude equations can be written in a concise form (Eq. (2.26)).

$$\{\ddot{\boldsymbol{T}}_2, \boldsymbol{f}_o\}_{ab}^{ij} = \sum_{o}^{N} t_{ab}^{oj} f_o^i + \sum_{o}^{N} t_{ab}^{io} f_o^j \quad \text{and} \quad \{\boldsymbol{f}_v, \ddot{\boldsymbol{T}}_2\}_{ab}^{ij} = \sum_{c}^{N_{vir}} f_a^c t_{cb}^{ij} + \sum_{c}^{N_{vir}} f_b^c t_{ac}^{ij}\,. \tag{2.25}$$

$$\{\boldsymbol{f}_v, \ddot{\boldsymbol{T}}_2\} - \{\ddot{\boldsymbol{T}}_2, \boldsymbol{f}_o\} + \ddot{\boldsymbol{G}}^{\dagger} = \ddot{\boldsymbol{0}}\,. \tag{2.26}$$

2.2.2 Decoupled R12 correction

To stay consistent with the CI-analogy made in the previous subsection (2.2.1), the MP2-R12 first-order wave function is enlarged in its expansion, with an extra set of terms $\Psi_{ij}^{r_{12}kl}$, with corresponding amplitudes c_{kl}^{ij}. Let's call $\ddot{\boldsymbol{C}}$ the matrix that collects the R12 amplitudes c_{kl}^{ij}.

$$\Psi_1 = \frac{1}{4}\sum_{ij}^{N}\sum_{ab}^{N_{vir}} t_{ab}^{ij}\Psi_{ij}^{ab} + \frac{1}{4}\sum_{ij}^{N}\sum_{kl}^{N} c_{kl}^{ij}\Psi_{ij}^{r_{12}kl}\,. \tag{2.27}$$

The matrices $\ddot{\boldsymbol{V}}$, $\ddot{\boldsymbol{X}}$ and $\ddot{\boldsymbol{F}}$, as well as the braces notation $\{\ddot{\boldsymbol{C}}, \boldsymbol{f}_o\}$ are defined beforehand (Eqs. (2.28) to (2.31)) since they are required to derive the R12 amplitudes and correction to the energy.

$$V_{kl}^{ij} = \langle \big[\bar{\Phi}_k(1)\bar{\Phi}_l(2)\big] | r_{12}^{-1} \hat{Q}_{12} r_{12} | \big[\bar{\Phi}_i(1)\bar{\Phi}_j(2)\big] \rangle \,. \tag{2.28}$$

$$X_{kl}^{ij} = \langle \big[\bar{\Phi}_k(1)\bar{\Phi}_l(2)\big] | r_{12} \hat{Q}_{12} r_{12} | \big[\bar{\Phi}_i(1)\bar{\Phi}_j(2)\big] \rangle \,. \tag{2.29}$$

$$F_{kl}^{ij} = \langle \big[\bar{\Phi}_k(1)\bar{\Phi}_l(2)\big] | r_{12} \hat{Q}_{12} \hat{f}_{12} \hat{Q}_{12} r_{12} | \big[\bar{\Phi}_i(1)\bar{\Phi}_j(2)\big] \rangle \,. \tag{2.30}$$

$$\{\ddot{\boldsymbol{C}}, \boldsymbol{f}_o\}_{kl}^{ij} = \sum_o^N C_{kl}^{oj} f_o^i + \sum_o^N C_{kl}^{io} f_o^j \,. \tag{2.31}$$

Using the above-defined matrices and projecting likewise Eq. (2.22) on the extra R12 terms $\Psi_{ij}^{r_{12}kl}$, the R12 amplitude equations are expressed in Eq. (2.32) and the MP2-R12 energy is given by Eq. (2.33).

$$\ddot{\boldsymbol{F}}\ddot{\boldsymbol{C}} - \ddot{\boldsymbol{X}}\{\ddot{\boldsymbol{C}}, \boldsymbol{f}_o\} + \ddot{\boldsymbol{V}}^\dagger = \ddot{\boldsymbol{0}} \,. \tag{2.32}$$

$$E_2^{\text{MP2-R12}} = E_2^{\text{MP2}} + \frac{1}{4} \,\text{Tr}\,(\ddot{\boldsymbol{V}}\ddot{\boldsymbol{C}}) \,. \tag{2.33}$$

It turns out that in the MP2 framework, the determination of the conventional and R12 contributions are fully decoupled. Such theory was first implemented into SORE, a program package entirely dedicated to MP2-R12 calculations [15] but this fortunate simplification has allowed to add recently in a simple manner R12 calculations to already existing computer codes performing MP2 calculations [16, 17].

2.3 CC-R12 theory

The CC frame is the most interesting for doing R12 calculations. Indeed the intrinsic error of the method (e.g. CCSD) is much smaller than for MP2, and it consequently seems more suitable to aim for basis-set limit properties, which can give accurate results comparable to experimental data [18]. Most articles written on the subject use a diagrammatic representation [19] to express the working equations [20, 21]. The goal of this section is to simply outline the principal concepts that lead to these complex working equations and via an ingenious comparison with the MP2-R12 theory, to show that the types of two-electron integrals one needs to compute are not more than those used in the MP2-R12 scheme.

2.3.1 General CCSD(T)-R12 theory

CC theory is characterized by an exponential Ansatz for the wave function (Eqs. (1.17) and (1.18)). The CCSD-R12 cluster operator $\hat{T}$ includes the single and double excitations as well as the operator

$\hat{F}_2$, which applied to the Hartree-Fock determinant Ψ_0 gives the extra set of R12 terms weighted by their amplitudes, namely $\left(c_{kl}^{ij}\Psi_{ij}^{r_{12}kl}\right)$ (Eq. (2.34)). One can transform the electronic Hamiltonian as in Eq. (2.35), which is denoted as similarity-transformed Hamiltonian $\hat{H}_e^T$.

$$\Psi^{\text{CCSD-R12}} = \exp(\hat{T})\Psi_0 \quad \text{with} \quad \hat{T} = \hat{1} + \hat{T}_1 + \hat{T}_2 + \hat{F}_2\,. \tag{2.34}$$

$$\hat{H}_e^T = \exp(-\hat{T})\hat{H}_e\exp(\hat{T}) \quad \text{and} \quad \hat{H}_e^T\Psi_0 = E^{\text{CCSD-R12}}\,\Psi_0\,. \tag{2.35}$$

The conventional way to obtain the CC energy and amplitude equations is to project the Schrödinger equation with the similarity-transformed Hamiltonian on the left onto the successive excited determinants (Eqs. (2.36) to (2.38)). The novelty is the introduction of an extra set of projections on the left with the R12 extensions $\Psi_{ij}^{r_{12}kl}$ (Eq. (2.39)).

$$\langle\Psi_0|\hat{H}_e^T|\Psi_0\rangle = E^{\text{CCSD-R12}}\,. \tag{2.36}$$
$$\langle\Psi_i^a|\hat{H}_e^T|\Psi_0\rangle = 0\,. \tag{2.37}$$
$$\langle\Psi_{ij}^{ab}|\hat{H}_e^T|\Psi_0\rangle = 0\,. \tag{2.38}$$
$$\langle\Psi_{ij}^{r_{12}kl}|\hat{H}_e^T|\Psi_0\rangle = 0\,. \tag{2.39}$$

To express the CCSD-R12 energy in a similar matrix form as the MP2-R12 energy, let's first define another matrix $\ddot{\boldsymbol{T}}'_2$ containing both the connected and disconnected double expansion coefficients (Eq. (2.40)). The CCSD-R12 energy is given in Eq. (2.41). This expression is very similar to the MP2-R12 energy, whith a slight difference through the introduction of singles expansion coefficients in $\ddot{\boldsymbol{T}}'_2$.

$$\{\ddot{\boldsymbol{T}}'_2\}_{ab}^{ij} = t_{ab}^{ij} + t_a^i t_b^j - t_b^i t_a^j \tag{2.40}$$
$$E^{\text{CCSD-R12}} = \frac{1}{4}\,\text{Tr}\,(\ddot{\boldsymbol{G}}\ddot{\boldsymbol{T}}'_2) + \frac{1}{4}\,\text{Tr}\,(\ddot{\boldsymbol{V}}\ddot{\boldsymbol{C}}) \tag{2.41}$$

The post-CCSD-R12 correction due to the triples CCSD(T)-R12 is calculated in exactly the same manner as in the conventional approach CCSD(T).

2.3.2 Link to MP2-R12 working equations

The Hamiltonian is partitioned as in the MP2 theory (Eq. (2.19)), but the fluctuation potential is not anymore taken as a perturbation. Instead, by similarity-transformation of the total electronic Hamiltonian, one gets the relation Eq. (2.42).

$$\hat{H}_e^T = \exp(-\hat{T})\hat{H}_e\exp(\hat{T}) = \hat{H}_0^T + \hat{V}^T\,. \tag{2.42}$$

Since the Brillouin condition states that the Fock matrix elements vanish between the occupied and virtual blocks, the Hausdorff expansion (Eq. (1.19)) of the transformed $\hat{H}_0$ operator stops after the single commutator with the cluster operator $\hat{T}$ (Eq. (2.43)).

$$\hat{H}_0^T = \hat{H}_0 + [\hat{H}_0, \hat{T}_1] + [\hat{H}_0, \hat{T}_2] + [\hat{H}_0, \hat{F}_2]\,. \tag{2.43}$$

Inserting the commutator expression of $\hat{H}_0^T$ (Eq. (2.43)) in Eqs. (2.37) to (2.39) and given that the configurations do not overlap among each other, one obtains (Eqs. (2.44) to (2.46)).

$$\langle \Psi_i^a | [\hat{H}_0, \hat{T}_1] | \Psi_0 \rangle + \langle \Psi_i^a | \hat{V}^T | \Psi_0 \rangle = 0\,. \tag{2.44}$$

$$\langle \Psi_{ij}^{ab} | [\hat{H}_0, \hat{T}_2] | \Psi_0 \rangle + \langle \Psi_{ij}^{ab} | \hat{V}^T | \Psi_0 \rangle = 0\,. \tag{2.45}$$

$$\langle \Psi_{ij}^{r_{12}kl} | [\hat{H}_0, \hat{F}_2] | \Psi_0 \rangle + \langle \Psi_{ij}^{r12kl} | \hat{V}^T | \Psi_0 \rangle = 0\,. \tag{2.46}$$

We can write the MP2-R12 equations in a similar form (Eqs. (2.47) and (2.48)).

$$\langle \Psi_{ij}^{ab} | [\hat{H}_0, \hat{T}_2] | \Psi_0 \rangle + \langle \Psi_{ij}^{ab} | \hat{V} | \Psi_0 \rangle = 0\,. \tag{2.47}$$

$$\langle \Psi_{ij}^{r_{12}kl} | [\hat{H}_0, \hat{F}_2] | \Psi_0 \rangle + \langle \Psi_{ij}^{r12kl} | \hat{V} | \Psi_0 \rangle = 0\,. \tag{2.48}$$

Thus the main difference between CC-R12 and MP2-R12 occurs in the evaluation of the matrix elements over the fluctuation potential $\hat{V}$. In CC-R12 framework, there is a dependence between the conventional amplitude equations and R12 amplitude equations, due to the similarity-transformation of $\hat{V}$ with the cluster operator $\hat{T}$. One requires then to solve simultaneously the CC amplitude equations and the CC-R12 amplitude equations, contrarily to the decoupling in MP2-R12 scheme. Today, there is one single standard implementation of the CCSD(T)-R12 method in the DIRCCR12 program [22].

2.4 Computer implementation

The integral evaluation is a significant part of an R12 calculation altogether in terms of computation time, disk space and memory requirements. This section describes first how the difficult many-electron molecular integrals can be solved, then exposes an efficient way how to solve the corresponding atomic integrals, and finally presents the numerical instability problems one might face.

2.4.1 Standard approximation

So far, the described methods are exact. However, the insertion of the outprojector $\hat{Q}_{12}$ leads to the occurrence of "more than two-" electron integrals. As an example, if $\hat{\Omega}_{12}$, $\hat{\Theta}_{12}$ and $\hat{\Lambda}_{12}$ are

three given two-electron operators related by the relation $\hat{\Omega}_{12} = \hat{\Theta}_{12}\,\hat{Q}_{12}\,\hat{\Lambda}_{12}$ and Ω_{kl}^{ij} denotes a matrix element of $\ddot{\mathbf{\Omega}}$, then Eq. (2.49) illustrates the occurrence of two three-electron integrals. The numbering is changed from electron one to electron three of the orbital $\bar{\Phi}_p$ in the *bra* part of the three-electron integrals, which is justified considering that their coordinates are just integration variables.

$$\begin{aligned}
\Omega_{kl}^{ij} &= \langle\big[\bar{\Phi}_k(1)\bar{\Phi}_l(2)\big]|\hat{\Theta}_{12}(\hat{1}-\hat{P}_1)(\hat{1}-\hat{P}_2)\hat{\Lambda}_{12}|\big[\bar{\Phi}_i(1)\bar{\Phi}_j(2)\big]\rangle \\
&= \langle\big[\bar{\Phi}_k(1)\bar{\Phi}_l(2)\big]|\hat{\Theta}_{12}\hat{\Lambda}_{12}|\big[\bar{\Phi}_i(1)\bar{\Phi}_j(2)\big]\rangle \\
&\quad - \sum_{p}^{N_{tot}}\langle\big[\bar{\Phi}_k(1)\bar{\Phi}_l(2)\big]\bar{\Phi}_p(3)|\hat{\Theta}_{12}\hat{\Lambda}_{23}|\bar{\Phi}_p(1)\big[\bar{\Phi}_i(2)\bar{\Phi}_j(3)\big]\rangle \\
&\quad - \sum_{p}^{N_{tot}}\langle\big[\bar{\Phi}_k(1)\bar{\Phi}_l(2)\big]\bar{\Phi}_p(3)|\hat{\Theta}_{12}\hat{\Lambda}_{13}|\bar{\Phi}_p(2)\big[\bar{\Phi}_i(1)\bar{\Phi}_j(3)\big]\rangle \\
&\quad + \sum_{pq}^{N_{tot}}\langle\big[\bar{\Phi}_k(1)\bar{\Phi}_l(2)\big]|\hat{\Theta}_{12}|\bar{\Phi}_p(1)\bar{\Phi}_q(2)\rangle\ \langle\bar{\Phi}_p(1)\bar{\Phi}_q(2)|\hat{\Lambda}_{12}|\big[\bar{\Phi}_i(1)\bar{\Phi}_j(2)\big]\rangle\,.
\end{aligned} \tag{2.49}$$

Such integrals arise from the evaluation of both matrices $\ddot{\boldsymbol{V}}$ and $\ddot{\boldsymbol{X}}$. Likewise, one could show the appearance of four-electron integrals during the calculation of $\ddot{\boldsymbol{F}}$, due to the exchange operators (Eq. (2.6)), and even up to five-electron integrals in the CC scheme. The key approximation of the R12 theory, called standard approximation, consists in inserting a closure relation, namely the resolution-of-identity RI (Eq. (2.50)) so as to factorize the expensive integrals into simple products of two-electron integrals. Eq. (2.51) gives an example of the RI effect on one of the above three-electron integrals.

$$\sum_{q}^{N_{tot}}|\bar{\Phi}_q(1)\rangle\,\langle\bar{\Phi}_q(1)| \approx \hat{1}\,. \tag{2.50}$$

$$\begin{aligned}
&\langle\big[\bar{\Phi}_k(1)\bar{\Phi}_l(2)\big]\bar{\Phi}_p(3)|\hat{\Theta}_{12}\hat{\Lambda}_{13}|\bar{\Phi}_p(2)\big[\bar{\Phi}_i(1)\bar{\Phi}_j(3)\big]\rangle \approx \\
&\qquad \sum_{q}^{N_{tot}}\langle\big[\bar{\Phi}_k(1)\bar{\Phi}_l(2)\big]|\hat{\Theta}_{12}|\bar{\Phi}_q(1)\bar{\Phi}_p(2)\rangle\,\langle\bar{\Phi}_q(1)\bar{\Phi}_p(2)|\hat{\Lambda}_{12}|\big[\bar{\Phi}_i(1)\bar{\Phi}_j(2)\big]\rangle\,.
\end{aligned} \tag{2.51}$$

Thanks to the RI approximation and through ingenious matrix rearrangements, one is left with the determination of four types of molecular integrals (Eq. (2.52)), in common for MP2-R12 and CCSD-R12 theories. The integrals over the operator r_{12}^2 simplify into products of two one-electron overlap, dipole and quadrupole moment integrals over the operators $\vec{r}_1$ and $\vec{r}_2$. The remaining three types of integrals can be solved by conventional integral evaluation techniques.

$$\Omega_{pq}^{ij} = \langle\bar{\Phi}_p(1)\bar{\Phi}_q(2)|\hat{\Omega}|\bar{\Phi}_i(1)\bar{\Phi}_j(2)\rangle \quad \text{with } \hat{\Omega} = \tfrac{1}{r_{12}},\ r_{12},\ r_{12}^2 \text{ and } [\hat{t}_{12}, r_{12}]\,. \tag{2.52}$$

Of course, the RI inclusion introduces an error since the finite molecular set obtained from a chosen atomic basis set is not complete. Consequently, the closer to completeness the atomic basis set is chosen, the smaller the RI error will be and for well chosen atomic basis sets, the RI error will be negligible compared to the basis-set convergence error. Moreover, two main variants of the standard approximation have been developed on the MP2-R12 level. The following convergences are given for a saturated basis set in ℓ. Variant A solves via RI insertion the matrices which held an energy convergence error proportional to $(\ell+1)^{-5}$ and neglect the others of which the error scales as $(\ell+1)^{-7}$. Variant B is exact in the standard approximation since all matrices are computed with the RI approximation and it is therefore computationally more demanding. It has been empirically observed that MP2-R12/B usually approaches the basis limit from above and MP2-R12/A from below. This result shows that the R12 correction violates the pseudo variational principle inherent to MBPT because the MP2-R12 energy can be below the basis-set limit, but it is not a real drawback for the theory since the resulting energies differ only of few tenths of a mE_h from the limiting value. The CCSD(T)-R12 theory, which has been implemented after the pioneering MP2-R12 studies, is so far available only for the variant B.

2.4.2 Integral evaluation

Hence, four types of two-electron atomic orbital integrals (I_k, $k=1-4$) have to be computed for the developed linear R12 methods (Eqs. (2.53) to (2.56)).

$$I_1 = \langle\chi_a(1)\chi_c(2)|r_{12}^{-1}|\chi_b(1)\chi_d(2)\rangle\,. \tag{2.53}$$

$$I_2 = \langle\chi_a(1)\chi_c(2)|r_{12}|\chi_b(1)\chi_d(2)\rangle\,. \tag{2.54}$$

$$I_3 = \langle\chi_a(1)\chi_c(2)|[\hat{t}_1, r_{12}]|\chi_b(1)\chi_d(2)\rangle\,. \tag{2.55}$$

$$I_4 = \langle\chi_a(1)\chi_c(2)|[\hat{t}_2, r_{12}]|\chi_b(1)\chi_d(2)\rangle\,. \tag{2.56}$$

In nearly all calculations on polyatomic systems, the atomic orbitals χ_a, χ_b, χ_c and χ_d are taken as real primitive Cartesian Gaussians with respective exponents a, b, c and d. An illustration is given for χ_a with electron one (Eq. (2.57)), function centered at nucleus A. N_A is a normalization constant, $x_{1A}=x_1-x_A$, likewise for y_{1A} and z_{1A}, and $i_A+j_A+k_A=\ell_A$, which represents here the total angular momentum quantum number of the orbital.

$$\chi_a(1) = N_A x_{1A}^{i_A}\, y_{1A}^{j_A}\, z_{1A}^{k_A}\, \exp(-a r_{1A}^2)\,, \quad \text{same for } \chi_b(1),\, \chi_c(2) \text{ and } \chi_d(2)\,. \tag{2.57}$$

P and Q represent the centers of charge of the charge distributions of products of spherical Gaussians located on A and B, and on C and D, respectively.

$$\vec{P} = \frac{a\vec{A}+b\vec{B}}{a+b} \quad \text{and} \quad \vec{Q} = \frac{c\vec{C}+d\vec{D}}{c+d}\,. \tag{2.58}$$

The conventional Coulomb interaction integrals I_1 (Eq. (2.53)) are available in any quantum chemistry program that can perform a Hartree-Fock calculation and the integrals over the distance r_{12} (Eq. (2.54)) and over the commutator of the kinetic energy with r_{12} (Eqs. (2.55) and (2.56)) can be obtained from the Coulomb integrals with little computational effort. First, the connection between the Coulomb repulsion integrals and the integrals over r_{12} occurs via second derivative with the center of charge (Eqs. (2.59) and (2.60)).

$$\Delta_1 r_{12} = \frac{2}{r_{12}} . \tag{2.59}$$

$$\Delta_P \langle \chi_a(1)\chi_c(2)|r_{12}|\chi_b(1)\chi_d(2)\rangle = 2\langle \chi_a(1)\chi_c(2)|\frac{1}{r_{12}}|\chi_b(1)\chi_d(2)\rangle . \tag{2.60}$$

Second, it has been shown that the integrals I_3 and I_4 can be computed efficiently from the relationship in Eq. (2.61).

$$\begin{aligned} I_{3,4} = & -N_{3,4}\langle \chi_a(1)\chi_c(2)|\frac{1}{r_{12}}|\chi_b(1)\chi_d(2)\rangle - \hat{\Omega}_{3,4}\langle \chi_a(1)\chi_c(2)|r_{12}|\chi_b(1)\chi_d(2)\rangle , \\ & \text{with } N_3 = \big(\frac{a-b}{a+b}\big), \quad \hat{\Omega}_3 = \vec{\nabla}_P.\vec{\nabla}_R \text{ and } \vec{R} = \vec{A} - \vec{B} \text{ for } I_3 \\ & \text{and } N_4 = \big(\frac{c-d}{c+d}\big), \quad \hat{\Omega}_4 = \vec{\nabla}_Q.\vec{\nabla}_R \text{ and } \vec{R} = \vec{C} - \vec{D} \text{ for } I_4. \end{aligned} \tag{2.61}$$

The standard implementation of these integrals is based on the McMurchie-Davidson scheme that expands Gaussian charge distributions in Hermite functions [23] but more efficient algorithms have been proposed [24]. In such context, none of the non-standard integrals requires much more computational cost than the Coulomb repulsion integrals. An appropriate four-index transformation converts afterwards the atomic orbital integrals into molecular orbital integrals. This step is executed in a direct manner, in order to restrict the memory and disk space requirements [25]. In conclusion, the new integrals required for R12 methods can efficiently be obtained through minor modifications of conventional computer codes, given that the program generates electron repulsion integrals and their first and second derivatives.

2.4.3 Numerical instabilities

Two aspects of the atomic basis-set quality can lead to ill-behaved systems of equations. Either the basis set is chosen extremely near completeness and the R12 correction becomes undetermined, or the basis set is not suitable to resolve properly the identity. The first problem, related to inversion of null matrices, is hardly encountered, and one should use impractical basis sets to reach it. The second problem which destroys the positive definite property of some fundamental matrices, is more common and arduous to overcome. It is more obvious for CC-R12 and local MP2-R12 since in these cases, the working equations have to be solved iteratively and thus the computed quantities

diverge. Neverthless, even for canonical MP2-R12, results obtained with non-positive definite matrices are not trustworthy. Thus it is compulsory to use appropriate atomic basis sets to carry out reliable R12 calculations. In this line, a new theory based on extremal electron pairs has been suggested [26]. Its disadvantage is the many possibilities that exist to select the condition to create these extremal pairs, which makes the theory difficult to implement in a "black-box" perspective. For this reason, it has so far not been widely used. However, basis-set design specially optimized for R12 calculations seems to be the easiest alternative to open up this bottleneck [27, 28].

References

[1] W. Klopper, *In: The Encyclopedia of Computational Chemistry, Vol.4, pp. 2351–2375*, P. v. R. Schleyer, N. L. Allinger, T. Clark, J. Gasteiger, P. A. Kollman, H. F. Schaefer III, and P. R. Schreiner (Eds.), John Wiley & Sons, Ltd., Chichester, New York, (1998).

[2] W. Klopper, *In: Modern Methods and Algorithms of Quantum Chemistry, Vol. 3, pp. 181–229*, J. Grotendorst (Ed.), NIC series, Forschungszentrum Jülich, Germany, (2000).

[3] W. Klopper, *Habil. Thesis*, Swiss Federal Institute of Technology, Zürich, (1996).

[4] W. Klopper and J. Noga, *In: Explicitly Correlated Wave Functions in Chemistry and Physics: Theory and Applications, Vol. 13, pp. 149–183*, J. Rychlewski (Ed.), Kluwer Academic Publishers, Dordrecht, (2003).

[5] A. Szabo and N. S. Ostlund, *Modern Quantum Chemistry, Introduction to Advanced Electronic Structure Theory*, Dover Publications, INC., Mineola, New York, (1982).

[6] S. F. Boys, Rev. Mod. Phys. **32**, 296 (1960).

[7] J. Pipek and P. G. Mezey, Chem. Phys. **90**, 4916 (1989).

[8] E. A. Hylleraas, Z. Phys. **54**, 347 (1929).

[9] W. Kutzelnigg, Theor. Chim. Acta **68**, 445 (1985).

[10] W. Klopper and W. Kutzelnigg, Chem. Phys. Lett. **134**, 17 (1987).

[11] W. Klopper, Chem. Phys. Lett. **186**, 583 (1991).

[12] W. Kutzelnigg and W. Klopper, J. Chem. Phys. **94**, 1985 (1991).

[13] V. Termath, W. Klopper, and W. Kutzelnigg, J. Chem. Phys. **94**, 2002 (1991).

[14] W. Klopper and W. Kutzelnigg, J. Chem. Phys. **94**, 2020 (1991).

[15] W. Klopper, *SORE, a second-order R12 energy program*.

[16] T. Helgaker, H. J. Aa. Jensen, P. Jørgensen, J. Olsen, K. Ruud, H. Ågren, A. A. Auer, K. L. Bak, V. Bakken, O. Christiansen, S. Coriani, P. Dahle, E. K. Dalskov, T. Enevoldsen, B. Fernandez, C. Hättig, K. Hald, A. Halkier, H. Heiberg, H. Hettema, D. Jonsson, S. Kirpekar, R. Kobayashi, H. Koch, K. V. Mikkelsen, P. Norman, M. J. Packer, T. B. Pedersen, T. A. Ruden, A. Sanchez, T. Saue, S. P. A. Sauer, B. Schimmelpfennig, K. O. Sylvester-Hvid, P. R. Taylor, and O. Vahtras, *Dalton, a molecular electronic structure program*, Release 1.2 (2001).

[17] R. Ahlrichs, M. Bär, H-. P. Baron, R. Bauernschmitt, S. Böcker, P. Deglmann, M. Ehrig, K. Eichkorn, S. Elliott, F. Furche, F. Haase, M. Häser, H. Horn, C. Hättig, C. Huber, U. Huniar, M. Kattannek, A. Köhn, C. Kölmel, M. Kollwitz, K. May, C. Ochsenfeld, H. Öhm, A. Schäfer, U. Schneider, M. Sierka, O. Treutler, B. Unterreiner, M. von Arnim, F. Weigend, P. Weis, and H. Weiss, *Turbomole*, Release V5-6 (2003).

[18] W. Klopper and J. Noga, ChemPhysChem **4**, 32 (2003).

[19] F. E. Harris, H. J. Monkhhorst, and D. L. Freeman, *Algebraic and Diagrammatic Methods in Many-Fermion Theory*, Oxford University Press, New York, Oxford, (1992).

[20] J. Noga and W. Kutzelnigg, J. Chem. Phys. **101**, 7738 (1994).

[21] J. Noga, W. Klopper, and W. Kutzelnigg, *In: Recent Advances in Computational Chemistry, Vol. 3, pp. 1–48*, R. J. Bartlett (Ed.), World Scientific Publishing Co. Ltd., Singapore, (1997).

[22] J. Noga and W. Klopper, *DIRCCR12, an integral-direct explicitly correlated coupled-cluster program*.

[23] W. Klopper and R. Röhse, Theor. Chim. Acta **83**, 441 (1992).

[24] E. F. Valeev and H. F. Schaefer III, J. Chem. Phys. **113**, 3990 (2000).

[25] W. Klopper, J. Mol. Struct. (Theochem) **388**, 175 (1996).

[26] W. Klopper, W. Kutzelnigg, H. Müller, J. Noga, and S. Vogtner, *In: Topics in Current Chemistry, Vol. 203, pp. 21–22*, Springer Verlag, Berlin, Heidelberg, (1999).

[27] P. Valiron, S. Kedžuch, and J. Noga, Chem. Phys. Lett. **367**, 723 (2002).

[28] J. Noga and P. Valiron, Collect. Czech. Chem. Commun. **68**, 340 (2003).

3

Equilibrium inversion barrier of NH_3 from extrapolated coupled-cluster pair energies

Abstract

The basis-set convergence of singlet and triplet pair energies of coupled-cluster theory including single and double excitations is accelerated by means of extrapolations based on the distinct convergence behaviors of these pairs. The new extrapolation procedure predicts a nonrelativistic Born–Oppenheimer inversion barrier of 1767$\pm$12 cm^{-1} for NH_3. An effective one-dimensional, vibrationally averaged barrier of 2021$\pm$20 cm^{-1} is obtained when relativistic effects (+20 cm^{-1}), Born–Oppenheimer diagonal corrections (-10 cm^{-1}), and zero-point vibrations (+244 cm^{-1}) are accounted for.

W. Klopper, C. C. M. Samson, G. Tarczay, and A. G. Császár, J. Comput. Chem. **22**, 1306 (2001).

3.1 Introduction

A wealth of empirical and theoretical data is available for the inversion barrier associated with the ν_2 umbrella mode in NH_3[1–21]. Here, it suffices to say that the best empirical procedures predict *effective* one-dimensional, vibrationally averaged barriers in the 2018±10 cm^{-1} range. More problems are encountered in the empirical analyses when attempting to include the effects of zero-point vibrations (ZPV). Due to these difficulties, the inferred bare electronic (i.e., equilibrium) inversion barriers (B_e) scatter between 1794 and 1885 cm^{-1}.

The highest-quality *ab initio* results for the equilibrium inversion barrier of NH_3 have been obtained by Császár, Allen, and Schaefer [21]. Using the focal-point technique [21, 22], these authors determined B_e=1810 cm^{-1} for the barrier at the extrapolated nonrelativistic valence-only level. These focal-point studies indicated that the greatest computational difficulty in assessing the equilibrium inversion barrier of NH_3 lies in the relatively protracted basis-set convergence, a case similar to water [23, 24]. Therefore, we decided to extend the previous investigations with a set of CCSD(T) and CCSD(T)-R12/B calculations that decompose the correlation energy into singlet and triplet pair energies. The new coupled-cluster calculations (a) allow extrapolations based on the pair energies obtained in various correlation-consistent basis sets and thus provide a new and interesting way to arrive at the basis-set limit [25]; and (b) extend the range of directly computed values for the focal-point analysis, and thus can help checking an intrinsic approximation of the focal-point scheme, namely, the neglect of the basis-set dependence of higher-order correlation increments and thus their additivity.

3.2 Computational Methods

3.2.1 Extrapolation of CCSD pair energies

Reference electronic wave functions were determined by the one-determinant restricted Hartree–Fock (RHF) method. Dynamical electron correlation was accounted for by coupled-cluster methods (see, e.g., Refs. [26, 27]), including single and double excitations (CCSD), and in cases also a noniterative perturbative correction for connected triple excitations (e.g., CCSD(T) [28] or CCSD[T] [29]).

The correlation energy of the CCSD model for a closed-shell system can be written as a sum of singlet (s=0) and triplet (s=1) pair energies, both including contributions from single (S) and connected double (D) excitations,

$$E_{\mathrm{CCSD}} = E_{\text{Hartree–Fock}} + E^{\mathrm{S}}_{\mathrm{CCSD}} + E^{\mathrm{D}}_{\mathrm{CCSD}}, \tag{3.1}$$

with

$$E_{\mathrm{CCSD}}^{\mathrm{S}} = \sum_{aibj} t_i^a t_j^b L_{iajb}, \qquad E_{\mathrm{CCSD}}^{\mathrm{D}} = \sum_{aibj} t_{ij}^{ab} L_{iajb}. \tag{3.2}$$

Here, t_i^a and t_{ij}^{ab} are the coupled-cluster amplitudes while $L_{iajb} = 2g_{iajb} - g_{ibja}$ is a linear combination of electronic repulsion integrals [27]. The reason for decomposing the correlation energy into singlet and triplet contributions is that this will enable us to apply extrapolation schemes that take into account the characteristic convergence behaviors of principal expansions of the singlet and triplet energies, which converge as X^{-3} and X^{-5}, respectively, with the cardinal number X of the basis set [30, 31].

The CCSD singlet ($\varepsilon_{ij}^{\mathrm{SD},0}$) and triplet ($\varepsilon_{ij}^{\mathrm{SD},1}$) pair energies are given by

$$\varepsilon_{ij}^{\mathrm{SD},s} = \varepsilon_{ij}^{\mathrm{S},s} + \varepsilon_{ij}^{\mathrm{D},s}, \tag{3.3}$$

with

$$\varepsilon_{ij}^{\mathrm{S},s} = \sum_{ab} t_i^a t_j^b L_{iajb}^s, \qquad \varepsilon_{ij}^{\mathrm{D},s} = \sum_{ab} t_{ij}^{ab} L_{iajb}^s, \tag{3.4}$$

and

$$L_{iajb}^s = \frac{2s+1}{2} \left\{ g_{iajb} + (-1)^s \, g_{ibja} \right\}. \tag{3.5}$$

In our new extrapolation procedure (cf. Ref. [25]), which is a small modification of the two-point extrapolation technique proposed by Helgaker et al. [32–34], the calculated doubles pair energies $\varepsilon_{ij}^{\mathrm{D},s}$ are replaced by the corresponding extrapolated values while the computed singles pair energies $\varepsilon_{ij}^{\mathrm{S},s}$ remain unchanged. When triples contributions are calculated—as in the CCSD(T) model, for example—they also remain unchanged.

The extrapolated doubles pair energies are given by

$$\varepsilon_{ij}^{\mathrm{D},s}(X\text{–}1,X) = \frac{X^{2s+3}\varepsilon_{ij}^{\mathrm{D},s}(X) - (X-1)^{2s+3}\varepsilon_{ij}^{\mathrm{D},s}(X\text{–}1)}{X^{2s+3} - (X-1)^{2s+3}}, \tag{3.6}$$

where $\varepsilon_{ij}^{\mathrm{D},s}(X)$ is the value of the pair energy contribution computed with the cc-pVXZ basis and $\varepsilon_{ij}^{\mathrm{D},s}(X\text{–}1)$ the corresponding value from the cc-pV(X–1)Z basis. At the CCSD/cc-pV(X–1,X)Z extrapolated level, we add the CCSD/cc-pVXZ computed singles contributions to the extrapolated doubles pair energies,

$$\varepsilon_{ij}^{\mathrm{SD},s}(X\text{–}1,\mathrm{X}) = \varepsilon_{ij}^{\mathrm{S},s}(X) + \varepsilon_{ij}^{\mathrm{D},s}(X\text{–}1,X). \tag{3.7}$$

Similarly, we define CCSD(T)/cc-pV(X–1,X)Z energies as the ones obtained by replacing solely the CCSD(T)/cc-pVXZ doubles energy contributions by their CCSD/cc-pV(X–1,X)Z extrapolated counterparts.

The same extrapolation procedure is used for valence-only (frozen-core approximation, FC) and all-electron (FU) correlated calculations as well as for extensions of the correlation-consistent basis sets such as aug-cc-pVXZ or (aug)-cc-pCVXZ.

3.2.2 Geometries, basis sets, and programs

The reference pyramidal (C_{3v}) / planar (D_{3h}) geometries of NH_3 were optimized at the CCSD(T)-(FU)/cc-pCVQZ level of theory to r(N–H) = 101.12 / 99.40 pm and $\angle$(H–N–H) = 106.36 / 120.0 degrees. The decrease in the r(N–H) bond length at the planar geometry is due to the increased s character of the bonding. The following is perhaps the most accurate estimate of the equilibrium geometry of pyramidal NH_3: r_e(N–H) = 101.1 pm and $\angle_e$(H–N–H) = 106.7 degrees [1]. Consequently, just as expected, all-electron correlated *ab initio* equilibrium geometries obtained using a CCSD(T)(FU) wave function with a large basis set are very accurate [27, 35]. The optimized reference geometries were kept fixed throughout the present computational study.

We employed the (aug)-cc-p(C)VXZ correlation-consistent basis sets of Dunning and coworkers [36–38], since these sets approach basis-set completeness in a systematic fashion, thus providing opportunities for extrapolations to the limit of a complete basis.

R12/B computations necessitate the use of basis sets designed differently from the (aug)-cc-p(C)VXZ basis sets [39]. Therefore, a [N/H] = [19s14p8d6f4g3h / 9s6p4d3f] basis set—taken from Ref. [25]—was employed for the R12/B calculations.

The two geometry optimizations were carried out with the program package Gaussian 98 [40], while all (standard) single-point energy calculations were performed with the Dalton program [41]. Nonstandard R12/B calculations were performed with the DIRCCR12-95 program [42].

Calculations of relativistic energies, utilizing the direct perturbation theory (DPT) approach of Kutzelnigg [43, 44] in the framework of the Dirac–Coulomb Hamiltonian, were performed with a modified [45] version of the program package Dalton [41]. Gaunt and Breit energy corrections [46] were determined perturbationally by the MOLFDIR [47, 48] and BERTHA [49, 50] program packages, respectively, using four-component relativistic Dirac–Hartree–Fock wave functions. Uncontracted correlation-consistent basis sets (denoted as u-cc-pCVXZ with X = D and T) were used for the large component and kinetic balance [48, 51] was used to generate the small-component basis functions.

The calculations were performed on SGI Origin 2000 R12000 computers at Utrecht University and at the Academic Computing Services Amsterdam (SARA).

3.3 Results and Discussion

The calculated and extrapolated energies of the C_{3v} and D_{3h} geometries of NH_3 are collected in Tables 3.1–3.5. Table 3.1 contains the R12/B energies while Tables 3.2 and 3.3 display the standard CCSD(FC) pair energies as obtained from calculations and extrapolations in the cc-pVXZ basis sets, in comparision with the R12/B results. The final CCSD(T)(FC) results are shown in Table 3.4, leading to the valence-shell correlation contributions to the inversion barrier shown in Table 3.5.

3.3.1 Hartree–Fock results

Our R12/B results (Table 3.1) include Hartree–Fock energies that are computed with a large basis set comprising 416 basis functions ([N/H] = [19s14p8d6f4g3h/9s6p4d3f]). In this basis, the Hartree–Fock contribution to the inversion barrier amounts to 1613 cm^{-1}. In the largest correlation-consistent basis set of a given family, we obtain $B_{\rm e}^{\rm RHF}$ = 1618 / 1614 cm^{-1} in the cc-pV6Z / aug-cc-pV5Z basis containing 413 / 367 functions.

We have also attempted to extrapolate—to the limit of a complete basis—the Hartree–Fock energies obtained in the correlation-consistent basis sets by fitting the energies from the three largest sets of a given family to the functional form [52–54]

$$E_X = E_\infty + a\exp(-bX). \tag{3.8}$$

From a corresponding fit of the RHF/cc-pVXZ energies for X=4,5,6, we obtain total Hartree–Fock energies of -56.224977 / -56.217625 $E_{\rm h}$ for the C_{3v} / D_{3h} geometries and a barrier of 1613 cm^{-1}.

Table 3.1: R12/B energies (in $E_{\rm h}$) as obtained in the [N/H] = [19s14p8d6f4g3h / 9s6p4d3f] basis with the DIRCCR12-95 program at the CCSD(T)(FU)/cc-pCVQZ optimized geometries of the pyramidal C_{3v} and planar D_{3h} structures of NH_3.

	Valence-shell correlation (FC)		All-electron correlation (FU)	
	C_{3v}	D_{3h}	C_{3v}	D_{3h}
Hartree–Fock	-56.224967	-56.217617	-56.224967	-56.217617
CCSD-R12/B	-56.494225	-56.486043	-56.553677	-56.545796
CCSD(T)-R12/B	-56.503634	-56.495230	-56.563574	-56.555462
CCSD[T]-R12/B[a]	-56.503385	-56.495021	-56.563269	-56.555203

[a] CCSD[T] was originally denoted CCSD+T(CCSD), see Ref. [29].

From the aug-cc-pVXZ family with X=3,4,5, we obtain -56.225148 / -56.217793 E_h, respectively, and a barrier of 1614 cm^{-1}.

Even though similar extrapolations taking into account energies from smaller basis sets (i.e., cc-pVTZ or aug-cc-pVDZ) appear to be not accurate enough, we can safely conclude from our best results that the Hartree–Fock limit for the energy difference between the fixed C_{3v} and D_{3h} geometries of the present study has been determined accurate to within 3 cm^{-1}. We hence adopt a value of $B_\mathrm{e}^\mathrm{RHF}$ = 1613 $\pm$ 3 cm^{-1} for the Hartree–Fock contribution to the inversion barrier.

In earlier work, Császár et al. [21] found $B_\mathrm{e}^\mathrm{RHF}$ = 1628 cm^{-1} for slightly different geometries, but note that the Hartree–Fock contribution is quite sensitive to the geometries used. Our fixed

Table 3.2: Basis-set dependence of the valence-shell CCSD(FC) pair energies (in mE_h) of the C_{3v} structure of NH_3.

Pair	D	T	Q	5	6	(56)[a]	R12/B
				Singlet pairs			
$(2a_1)^2$	-9.89	-11.94	-12.74	-13.00	-13.11	-13.26	-13.25
$1e2a_1$	-29.72	-38.52	-41.37	-42.32	-42.70	-43.23	-43.16
$(1e)^2$	-53.85	-61.13	-63.66	-64.49	-64.82	-65.28	-65.21
$1a_2 2a_1$	-10.51	-14.89	-16.25	-16.70	-16.89	-17.16	-17.14
$1a_2 1e$	-20.62	-25.66	-27.52	-28.18	-28.43	-28.77	-28.72
$(1a_2)^2$	-19.57	-24.19	-25.62	-26.09	-26.29	-26.55	-26.54
Total	-144.15	-176.33	-187.16	-190.77	-192.24	-194.25	-194.02
$\bar{\Delta}_\mathrm{abs}$	4.99	1.77	0.69	0.32	0.18	0.02	
Δ_max	6.97	2.34	0.92	0.45	0.25	0.03	
				Triplet pairs			
$1e2a_1$	-8.83	-11.33	-11.91	-12.08	-12.12	-12.15	-12.16
$(1e)^2$	-13.36	-15.71	-16.16	-16.26	-16.29	-16.32	-16.32
$1a_2 2a_1$	-4.71	-6.62	-7.12	-7.28	-7.32	-7.35	-7.35
$1a_2 1e$	-31.46	-37.64	-38.89	-39.25	-39.35	-39.42	-39.42
Total	-58.35	-71.30	-74.09	-74.87	-75.09	-75.24	-75.24
$\bar{\Delta}_\mathrm{abs}$	2.81	0.66	0.19	0.06	0.02	0.00	
Δ_max	3.98	0.89	0.26	0.08	0.03	0.00	

[a] The notation cc-pV(56)Z denotes extrapolated pair energies that were been obtained by inserting the cc-pV5Z and cc-pV6Z energies into Eqs. (3.6) and (3.7).

geometries correspond to stationary points on the CCSD(T)(FU)/cc-pCVQZ potential energy surface (PES) but *not* to stationary points on the Hartree–Fock PES. The Hartree–Fock contribution thus depends to first order on small changes in the geometries while the total CCSD(T)(FU) barrier depends only to second order on such changes.

3.3.2 Valence-only correlation

The valence-only CCSD(FC) pair energies of the pyramidal and planar structures of NH_3 are displayed in Tables 3.2 and 3.3, respectively, as obtained in the cc-pVXZ basis sets with cardinal numbers ranging from X = 2 to 6. The columns under "(56)" show the pair energies that result from applying our extrapolation scheme—Eqs. (3.6) and (3.7)—to the CCSD(FC)/cc-pV5Z

Table 3.3: Basis-set dependence of the valence-shell CCSD(FC) pair energies (in mE_h) of the D_{3h} structure of NH_3.

Pair	D	T	Q	5	6	(56)[a]	R12/B
				Singlet pairs			
$(2a_1')^2$	-9.48	-11.26	-11.98	-12.22	-12.32	-12.45	-12.45
$1e'2a_1'$	-30.08	-38.81	-41.59	-42.51	-42.89	-43.40	-43.34
$(1e')^2$	-53.34	-60.53	-63.05	-63.87	-64.19	-64.64	-64.58
$1a_2''2a_1'$	-10.66	-16.05	-17.72	-18.31	-18.55	-18.88	-18.84
$1a_2''1e'$	-18.22	-23.54	-25.63	-26.37	-26.66	-27.06	-26.98
$(1a_2'')^2$	-19.93	-24.19	-25.56	-26.01	-26.20	-26.46	-26.44
Total	-141.70	-174.38	-185.53	-189.28	-190.80	-192.90	-192.63
$\bar{\Delta}_\mathrm{abs}$	5.09	1.82	0.71	0.33	0.18	0.03	
Δ_max	8.18	2.79	1.12	0.53	0.29	0.05	
				Triplet pairs			
$1e'2a_1'$	-8.23	-10.47	-10.99	-11.14	-11.18	-11.21	-11.22
$(1e')^2$	-12.85	-14.90	-15.28	-15.38	-15.41	-15.43	-15.43
$1a_2''2a_1'$	-4.74	-6.89	-7.46	-7.64	-7.69	-7.72	-7.72
$1a_2''1e'$	-33.16	-39.54	-40.87	-41.24	-41.36	-41.43	-41.43
Total	-58.98	-71.79	-74.59	-75.40	-75.64	-75.80	-75.80
$\bar{\Delta}_\mathrm{abs}$	2.80	0.67	0.20	0.07	0.03	0.00	
Δ_max	4.14	0.94	0.28	0.09	0.04	0.00	

[a] Cf. Table 3.2.

and CCSD(FC)/cc-pV6Z pair energies. These extrapolated pair energies are compared with the calculated R12/B values.

The mean absolute deviations of the calculated singlet and triplet CCSD(FC)/cc-pVXZ pair energies from the corresponding R12/B reference values are depicted in Figure 3.1 for various cardinal numbers X. This log–log plot reveals the different convergence behaviors of the singlet

Table 3.4: Basis-set dependence of the valence-shell energies (in E_h) of the C_{3v} and D_{3h} reference forms of NH_3.[a]

Method	Basis	X=2	X=3	X=4	X=5	X=6	R12/B
				C_{3v}, calculated			
RHF	cc-pVXZ	-56.19568	-56.21789	-56.22311	-56.22473	-56.22494	-56.22497
	aug-cc-pVXZ	-56.20541	-56.22033	-56.22398	-56.22487		
SD	cc-pVXZ	-0.20250	-0.24764	-0.26124	-0.26565	-0.26733	-0.26926
	aug-cc-pVXZ	-0.21431	-0.25187	-0.26279	-0.26625		
(T)	cc-pVXZ	-0.00379	-0.00763	-0.00870	-0.00907	-0.00920	-0.00916
	aug-cc-pVXZ	-0.00545	-0.00833	-0.00895	-0.00916		
				C_{3v}, extrapolated[b]			
SD	cc-pVXZ		-0.26316	-0.27002	-0.26983	-0.26949	
	aug-cc-pVXZ		-0.26509	-0.26998	-0.26963		
				D_{3h}, calculated			
RHF	cc-pVXZ	-56.18423	-56.20949	-56.21525	-56.21727	-56.21757	-56.21762
	aug-cc-pVXZ	-56.19737	-56.21289	-56.21662	-56.21751		
SD	cc-pVXZ	-0.20068	-0.24617	-0.26013	-0.26469	-0.26645	-0.26843
	aug-cc-pVXZ	-0.21328	-0.25067	-0.26183	-0.26537		
(T)	cc-pVXZ	-0.00340	-0.00733	-0.00844	-0.00886	-0.00900	-0.00898
	aug-cc-pVXZ	-0.00524	-0.00815	-0.00876	-0.00897		
				D_{3h}, extrapolated[b]			
SD	cc-pVXZ		-0.26189	-0.26915	-0.26902	-0.26870	
	aug-cc-pVXZ		-0.26384	-0.26918	-0.26882		

[a] RHF is the restricted Hartree–Fock energy, SD is the CCSD(FC) correlation energy, and (T) denotes the perturbative correction for connected triple excitations at the CCSD(T)(FC) level.

[b] The two values in the column for a given X correspond to the extrapolated cc-pV(X–1,X)Z and aug-cc-pV(X–1,X)Z results.

and triplet pair energies in a very convincing manner—see also Ref. [25].

The convergence to the basis-set limit (or R12/B reference values) is much accelerated by the extrapolation scheme. Whereas the calculated CCSD(FC)/cc-pV6Z singlet pair energies are in error by 0.18 mE_h (ca. 40 cm^{-1}) on average, this error is reduced to 0.02 mE_h (ca. 4 cm^{-1}) by the extrapolation procedure, which thus appears to be capable of reducing the error by one order of magnitude. The extrapolated triplet pair energies are in complete agreement with the R12/B calculation, confirming the X^{-5}-type convergence of these pairs.

Nevertheless, an error of ca. 4 cm^{-1} per singlet pair energy is still significant when considering the inversion barrier of NH_3. It has been demonstrated in earlier studies that X^{-k}-type extrapolations based on sequences of correlation-consistent basis sets yield total electronic energies of small closed-shell molecules accurate to within 1–3 mE_h [25] and their equilibrium atomization energies accurate to within 1–2 kJ/mol [55–57], but it has not yet been investigated whether these extrapolation techniques can be applied successfully to small conformational energy differences such as the barrier in NH_3. We here investigate this aspect of the extrapolation techniques.

If the errors in the extrapolated energies would be strictly statistical, then the statistical error—compared with the R12/B reference value—in the extrapolated barrier would amount to ca. 20 cm^{-1}, as there are 10 valence pairs for both structures (degenerate pairs are counted separately). We observe, in fact, that the CCSD(FC)/cc-pV(56)Z and CCSD(FC)-R12/B correlation contributions to the barrier agree to within 10 cm^{-1} (173 vis-à-vis 183 cm^{-1}, cf. Table 3.5).

Table 3.5: Calculated and extrapolated valence-shell electron-correlation contributions (in cm^{-1}) to the equilibrium inversion barrier of NH_3.[a]

Method	Basis	X=2	X=3	X=4	X=5	X=6	R12/B
				Calculated			
RHF	cc-pVXZ	2513	1843	1726	1637	1618	1613
	aug-cc-pVXZ	1763	1634	1616	1614		
SD	cc-pVXZ	400	321	244	211	194	183
	aug-cc-pVXZ	225	262	210	193		
(T)	cc-pVXZ	87	67	55	46	43	40
	aug-cc-pVXZ	46	40	41	40		
				Extrapolated[b]			
SD	cc-pVXZ		280	191	179	173	
	aug-cc-pVXZ		276	176	177		

[a,b] Cf. Table 3.4.

We shall base our best estimate of the equilibrium inversion barrier on the average value of the extrapolated CCSD(FC)/cc-pV(56)Z, extrapolated CCSD(FC)/aug-cc-pV(Q5)Z, and CCSD(FC)-R12/B pair energies. Hence, we adopt a value of +178 cm^{-1} as our best estimate of the valence-only singles and doubles contribution, with an estimated error bar of 10 cm^{-1}. The corresponding focal-point value is +145 cm^{-1}[21].

The valence-only (T)-triples corrections add 40 cm^{-1} to the barrier at the CCSD(T)-R12/B level (Table 3.5). A two-point X^{-3}-type extrapolation of the triples contributions in the cc-pV5Z (46 cm^{-1}) and cc-pV6Z (43 cm^{-1}) basis sets suggests a limiting value of 39 cm^{-1}. The agreement between this extrapolated value and the R12/B value is remarkable, noting that the convergence behavior of the triples correction has not yet been investigated let alone established mathematically (numerical experiments seem to *indicate* that the leading term is of the order X^{-3}). In any case,

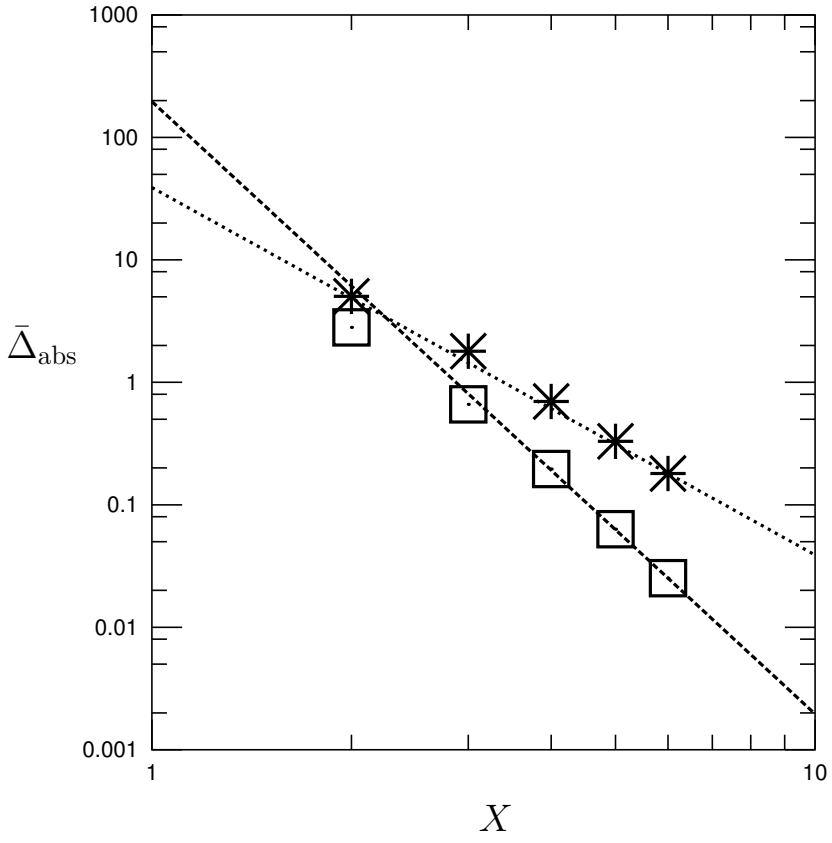

Figure 3.1: Mean absolute deviation ($\bar{\Delta}_{\rm abs}$ in m$E_{\rm h}$) of valence-shell singlet ($*$) and triplet ($\square$) CCSD/cc-pVXZ pair energies of the C_{3v} and D_{3h} structures of NH_3. Shown are the deviations from the CCSD-R12 reference values on a log–log scale as function of the cardinal number X. Also shown are lines with slopes of -3 (dotted) and -5 (dashed) through the CCSD/cc-pV6Z data.

we adopt a value of +40±2 cm^{-1} as our best estimate of the valence-only (T)-triples correction. This value is supported by the corresponding focal-point estimate of +39 cm^{-1}[21].

3.3.3 Core-valence correction

The inclusion of the nitrogen $1s$-core orbital into the CCSD(T)-R12/B correlation treatment decreases the inversion barrier by 64 cm^{-1} (cf. Table 3.1). At the MP2-R12/B level (not reported), the barrier is reduced by 69 cm^{-1}, an amount quite similar to the CCSD(T)-R12/B value. It was observed in Ref. [21] that the MP2 and CCSD(T) core-valence corrections were very similar, and accordingly, the correction obtained at the MP2/cc-pCVQZ level (64 cm^{-1}) was taken as the best estimate of the core-valence correlation effect in that work. This previous best estimate appears to coincide with our present CCSD(T)-R12/B value.

As core-valence correlation effects are usually very efficiently recovered by the R12/B approach, we attach a rather conservative error bar of 4 cm^{-1} to the CCSD(T)-R12/B value and conclude that core-valence correction effects lower the inversion barrier by 64±4 cm^{-1}.

3.3.4 Zero-point vibrational energies

The available *ab initio* works [11, 12, 14, 58] on the vibrational band origins (especially the fundamentals) of one or both reference forms of NH_3 suggest a substantial zero-point vibrational energy (ZPVE) correction to the barrier height. For the pyramidal and the planar forms moderately accurate CISDTQ/DZP harmonic vibrational frequencies [11] are available to us. For the pyramidal form these calculations yield a complementary-mode ZPVE which is only 3.7% larger than the anharmonic result given by a highly accurate [59] CCSD(T)/cc-pVQZ complete quartic force field [14]. Using this same correction for the planar modes as for the pyramidal ones results in a ZPVE correction of 244 cm^{-1}, as reported in Ref. [21]. The recent variational results of Handy, Carter, and Colwell [58], based on an accurate six-dimensional potential energy hypersurface, confirm this ZPVE correction estimate. The value of 244 cm^{-1} is adopted in the present work, with an estimated accuracy of ±15 cm^{-1}.

3.3.5 Relativistic corrections

As has recently been demonstrated for the barrier to linearity of water [21, 61, 62], relativistic effects, arising from consideration of special relativity, make a surprisingly large contribution to the barrier. Although the relativistic contribution to the barrier of NH_3 is only about one–half

Table 3.6: Relativistic first-order energies (in mE_h) obtained at the RHF/cc-pCVXZ and CCSD(T)(FU)/cc-pCVXZ levels.[a]

	Pyramidal (C_{3v})				
cc-pCVXZ	E^{MV}	E^{D1}	E^{D2}	$E^{\Delta\mathrm{DPT}}$	ΔB_e
			RHF		
X=2	-143.341	+114.644	-2.197	+0.015	
X=3	-143.915	+115.162	-2.198	+0.003	
X=4	-146.175	+117.368	-2.199	-0.012	
			CCSD(T)(FU)		
X=2	-143.542	+114.663	-2.064	+0.013	
X=3	-144.255	+115.196	-2.009	+0.035	
X=4	-146.483	+117.374	-1.970	-0.006	
	Planar (D_{3h})				
			RHF		
X=2	-142.939	+114.348	-2.191	+0.014	+0.111
X=3	-143.538	+114.880	-2.193	+0.004	+0.101
X=4	-145.808	+117.093	-2.194	-0.013	+0.096
			CCSD(T)(FU)		
X=2	-143.122	+114.354	-2.059	+0.015	+0.118
X=3	-143.869	+114.909	-2.004	+0.034	+0.103
X=4	-146.116	+117.099	-1.965	-0.006	+0.097

[a] E^{MV} is the mass-velocity term, E^{D1} is the one-electron Darwin term, E^{D2} is the two-electron Darwin term, and $E^{\Delta\mathrm{DPT}}$ is the difference between the first-order energy of DPT and the sum $E^{\mathrm{MV}} + E^{\mathrm{D1}} + E^{\mathrm{D2}}$. ΔB_e is the first-order DPT energy contribution to the barrier height.

of that in water (there is only one lone pair of electrons allowed to rehybridize during the large-amplitude motion versus the two lone pairs of electrons of water), the correction is still substantial. In fact, in a relative sense it is more substantial than in water, because the barrier in NH_3 is only about 1/6 of the barrier in water.

Relativistic results obtained as part of this study are collected into Tables 3.6 and 3.7. The DPT

Table 3.7: Relativistic energy corrections (in mE_h) beyond the Dirac−Coulomb Hamiltonian.[a]

	Pyramidal (C_{3v})			Planar (D_{3h})			
Basis	E^{Gaunt}	$E^{\mathrm{Ret.}}$	E^{Lamb}	E^{Gaunt}	$E^{\mathrm{Ret.}}$	E^{Lamb}	ΔB_e
u-cc-pCVDZ	+4.941	-0.156	+2.562	+4.952	-0.160	+2.555	+0.000
u-cc-pCVTZ	[+4.792]		+2.575	[+4.799]		+2.568	+0.000

[a] All values are obtained at the Hartree–Fock level. Values in brackets are the full Breit energies, $E^{\mathrm{Breit}} = E^{\mathrm{Gaunt}} + E^{\mathrm{Ret}}$. The Lamb-shift values are obtained according to Eq. (3) of Ref. [60].

correction to the barrier decreases with extension of the basis both at the RHF and CCSD(T)(FU) levels. Our final estimate for this first-order relativistic correction is +19 cm^{-1}. Relativistic corrections beyond DPT also influence the barrier. We summarize the results as follows: (a) as expected, the Gaunt energies approximate the total Breit energies to within 5%; (b) while the directly computed Breit energies (Gaunt + Ret., cf. Table 3.7) change slightly upon extension of the basis from u-cc-pCVDZ to u-cc-pCVTZ, the Breit correction to the barrier has a negligible basis set dependency; (c) the Lamb-shift energy correction [60] is comparable to that of the Breit energy correction. The Lamb-shift effect on the barrier is not dependent on the basis and small for both the u-cc-pCVDZ and u-cc-pCVTZ sets. Overall, relativistic effects not considered in the Dirac–Coulomb Hamiltonian seem to have a marginal (+1 cm^{-1}) correction to the equilibrium inversion barrier of ammonia. Therefore, the total relativistic correction to the barrier of NH_3 is +20 cm^{-1} with an estimated error of a few cm^{-1}.

3.4 Summary

At the valence-shell CCSD(T)(FC) level, our best estimate of the barrier amounts to 1613 + 178 + 40 = 1831±11 cm^{-1}. Relativistic effects increase the barrier by 20±2 cm^{-1} while core-valence correlation effects reduce the barrier by 64±4 cm^{-1}. Thus, the total electronic barrier is estimated as 1788±12 cm^{-1} at the Born–Oppenheimer relativistic all-electron CCSD(T)(FU) level. Correlation effects beyond the CCSD(T)(FU) level are presumably very small (a few cm^{-1}) [21] while taking into account the diagonal Born–Oppenheimer correction [21]—of the order of -10 cm^{-1} for the isotope $^{14}NH_3$—yields a final adiabatic equilibrium value of B_e=1777±13 cm^{-1} for $^{14}NH_3$.

To obtain an *effective* barrier for the one-dimensional treatment of the tunneling motion in NH_3, the zero-point vibrational energy of the complementary vibrational modes must be taken into account. This ZPVE amounts to 244±15 cm^{-1} and yields an effective one-dimensional barrier of

2021 ± 20 cm^{-1}.

Acknowledgments

This article is dedicated to professor Paul von Ragué Schleyer on the occasion of his 70th birthday. The authors are grateful to Dr. H. M. Quiney for provision of the BERTHA code. The research of Wim Klopper has been made possible by a fellowship of the Royal Netherlands Academy of Arts and Sciences. The work of Attila G. Császár and György Tarczay has been supported by the Hungarian Ministry of Culture and Education (FKFP 0117/1997) and by the Scientific Research Fund of Hungary (OTKA T024044 and T033074). A grant of computing time from Academic Computing Services Amsterdam (SARA) is gratefully acknowledged.

References

[1] J. L. Duncan and I. M. Mills, Spectrochim. Acta **20**, 523 (1964).

[2] A. Veillard, J. M. Lehn, and B. Munsch, Theor. Chim. Acta **9**, 275 (1968).

[3] M. J. S. Dewar and M. Shanshal, J. Am. Chem. Soc. **91**, 3654 (1969).

[4] A. Pipano, R. R. Gilman, C. F. Bender, and I. Shavitt, Chem. Phys. Lett. **4**, 583 (1970).

[5] A. Rauk, L. C. Allen, and E. Clementi, J. Chem. Phys. **52**, 4133 (1970).

[6] B. Maessen, P. Bopp, D. R. McLaughlin, and M. Wolfsberg, Z. Naturforsch. A **39**, 1005 (1984).

[7] P. R. Bunker, W. P. Kraemer, and V. Špirko, Can. J. Phys. **62**, 1801 (1984).

[8] W. Foerner, J. Čížek, P. Otto, J. Ladik, and E. O. Steinborn, Chem. Phys. **97**, 235 (1985).

[9] P. Botschwina, J. Chem. Phys. **87**, 1453 (1987).

[10] G. E. Scuseria, A. E. Scheiner, J. E. Rice, T. J. Lee, and H. F. Schaefer III, Int. J. Quantum Chem. Symp. **21**, 495 (1987).

[11] T. J. Lee, R. B. Remington, Y. Yamaguchi, and H. F. Schaefer III, J. Chem. Phys. **89**, 408 (1988).

[12] V. Špirko and W. P. Kraemer, J. Mol. Spectr. **133**, 331 (1989).

[13] G. Campoy, A. Palma, and L. Sandoval, Int. J. Quantum Chem. Symp. **23**, 355 (1989).

[14] J. M. L. Martin, T. J. Lee, and P. R. Taylor, J. Chem. Phys. **97**, 8361 (1992).

[15] H. U. Suter and T.-K. Ha, J. Mol. Struct. (Theochem) **283**, 151 (1993).

[16] A. L. L. East and L. Radom, J. Mol. Struct. **376**, 437 (1996).

[17] F. Jensen, Chem. Phys. Lett. **261**, 633 (1996).

[18] R. J. Bartlett, J. E. Del Bene, S. A. Perera, and R. P. Mattie, J. Mol. Struct. (Theochem) **400**, 157 (1997).

[19] J. S. Lee, J. Phys. Chem. A **101**, 8762 (1997).

[20] H. Müller, W. Kutzelnigg, and J. Noga, Mol. Phys. **93**, 535 (1997).

[21] A. G. Császár, W. D. Allen, and H. F. Schaefer III, J. Chem. Phys. **108**, 9751 (1998).

[22] W. D. Allen, A. L. L. East, and A. G. Császár, *In: Structures and Conformations of Non-Rigid Molecules*, J. Laane, M. Dakkouri, B. van der Veken, and H. Oberhammer (Eds.), NATO ARW Series C, Kluwer Academic Publishers, Dordrecht, (1993).

[23] G. Tarczay, A. G. Császár, W. Klopper, V. Szalay, W. D. Allen, and H. F. Schaefer III, J. Chem. Phys. **110**, 11971 (1999).

[24] E. F. Valeev, W. D. Allen, H. F. Schaefer III, and A. G. Császár, J. Chem. Phys. **114**, 2875 (2001).

[25] W. Klopper, Mol. Phys. **99**, 481 (2001).

[26] R. J. Bartlett, *In: Modern Electronic Structure Theory, pp. 1047–1130*, D. R. Yarkony (Ed.), World Scientific Publishing Co. Ltd., Singapore, (1995).

[27] T. Helgaker, P. Jørgensen, and J. Olsen, *Molecular Electronic-Structure Theory*, John Wiley & Sons, Ltd., Chichester, New York, (2000).

[28] K. Raghavachari, G. W. Trucks, J. A. Pople, and M. Head-Gordon, Chem. Phys. Lett. **157**, 479 (1989).

[29] M. Urban, J. Noga, S. J. Cole, and R. J. Bartlett, J. Chem. Phys. **83**, 404 (1985).

[30] W. Kutzelnigg and J. D. Morgan III, J. Chem. Phys. **96**, 4484 (1992).

[31] J. W. Ochterski, G. A. Petersson, and J. A. Montgomery, Jr., J. Chem. Phys. **104**, 2598 (1996).

[32] T. Helgaker, W. Klopper, H. Koch, and J. Noga, J. Chem. Phys. **106**, 9639 (1997).

[33] A. Halkier, T. Helgaker, P. Jørgensen, W. Klopper, H. Koch, J. Olsen, and A. K. Wilson, Chem. Phys. Lett. **286**, 243 (1998).

[34] A. Halkier, T. Helgaker, W. Klopper, P. Jørgensen, and A. G. Császár, Chem. Phys. Lett. **310**, 385 (1999).

[35] A. G. Császár and W. D. Allen, J. Chem. Phys. **104**, 2746 (1996).

[36] T. H. Dunning, Jr., J. Chem. Phys. **90**, 1007 (1989).

[37] R. A. Kendall, T. H. Dunning, Jr., and R. J. Harrison, J. Chem. Phys. **96**, 6796 (1992).

[38] A. K. Wilson, T. van Mourik, and T. H. Dunning, Jr., J. Mol. Struct. (Theochem) **338**, 339 (1996).

[39] W. Klopper, *In: The Encyclopedia of Computational Chemistry, Vol.4, pp. 2351–2375*, P. v. R. Schleyer, N. L. Allinger, T. Clark, J. Gasteiger, P. A. Kollman, H. F. Schaefer III, and P. R. Schreiner (Eds.), John Wiley & Sons, Ltd., Chichester, New York, (1998).

[40] M. J. Frisch, G. W. Trucks, H. B. Schlegel, G. E. Scuseria, M. A. Robb, J. R. Cheeseman, V. G. Zakrzewski, J. A. Montgomery, Jr., R. E. Stratmann, J. C. Burant, S. Dapprich, J. M. Millam, A. D. Daniels, K. N. Kudin, M. C. Strain, O. Farkas, J. Tomasi, V. Barone, M. Cossi, R. Cammi, B. Mennucci, C. Pomelli, C. Adamo, S. Clifford, J. Ochterski, G. A. Petersson, P. Y. Ayala, Q. Cui, K. Morokuma, D. K. Malick, A. D. Rabuck, K. Raghavachari, J. B. Foresman, J. Cioslowski, J. V. Ortiz, A. G. Baboul, B. B. Stefanov, G. Liu, A. Liashenko, P. Piskorz, I. Komaromi, R. Gomperts, R. L. Martin, D. J. Fox, T. Keith, M. A. Al-Laham, C. Y. Peng, A. Nanayakkara, M. Challacombe, P. M. W. Gill, B. Johnson, W. Chen, M. W. Wong, J. L. Andres, C. Gonzalez, M. Head-Gordon, E. S. Replogle, and J. A. Pople, *Gaussian, Inc., Pittsburgh PA*, Gaussian 98, Revision A.7 (1998).

[41] T. Helgaker, H. J. Aa. Jensen, P. Jørgensen, J. Olsen, K. Ruud, H. Ågren, T. Andersen, K. L. Bak, V. Bakken, O. Christiansen, E. K. Dalskov, T. Enevoldsen, B. Fernandez, H. Heiberg, H. Hettema, D. Jonsson, S. Kirpekar, R. Kobayashi, H. Koch, K. V. Mikkelsen, P. Norman, M. J. Packer, T. Saue, S. P. A. Sauer, P. R. Taylor, and O. Vahtras, *Dalton, a molecular electronic structure program*, Release 1.1.

[42] J. Noga and W. Klopper, *DIRCCR12, an integral-direct explicitly correlated coupled-cluster program*.

[43] W. Kutzelnigg, Z. Phys. D **11**, 15 (1989).

[44] W. Kutzelnigg, Phys. Rev. A **54**, 1183 (1996).

[45] W. Klopper, J. Comput. Chem. **18**, 20 (1997).

[46] W. Kutzelnigg, Physica Scripta **36**, 416 (1987).

[47] P. J. C. Aerts, O. Visser, L. Visscher, H. Merenga, W. A. de Jong, and W. C. Nieuwpoort, *MOLFDIR*, University of Groningen, The Netherlands.

[48] L. Visscher, O. Visser, P. J. C. Aerts, H. Merenga, and W. C. Nieuwpoort, Comput. Phys. Commun. **81**, 120 (1994).

[49] H. M. Quiney, H. Skaane, and I. P. Grant, Adv. Quantum. Chem. **32**, 1 (1998).

[50] I. P. Grant and H. M. Quiney, Int. J. Quantum Chem. **80**, 283 (2000).

[51] I. P. Grant and H. M. Quiney, Adv. At. Mol. Phys. **23**, 37 (1988).

[52] D. Feller, J. Chem. Phys. **96**, 6104 (1992).

[53] A. Halkier, T. Helgaker, P. Jørgensen, W. Klopper, and J. Olsen, Chem. Phys. Lett. **302**, 437 (1999).

[54] F. Jensen, J. Chem. Phys. **110**, 6601 (1999).

[55] J. M. L. Martin and G. de Oliveira, J. Chem. Phys. **111**, 1843 (1999).

[56] K. L. Bak, P. Jørgensen, J. Olsen, T. Helgaker, and W. Klopper, J. Chem. Phys. **112**, 9229 (2000).

[57] T. Helgaker, W. Klopper, A. Halkier, K. L. Bak, P. Jørgensen, and J. Olsen, *In: Understanding Chemical Reactivity, Vol. 22, pp. 1–30*, J. Cioslowski (Ed.), Kluwer Academic Publishers, Dordrecht, (2001).

[58] N. C. Handy, S. Carter, and S. M. Colwell, Mol. Phys. **96**, 477 (1999).

[59] A. G. Császár, *In: The Encyclopedia of Computational Chemistry*, P. v. R. Schleyer, N. L. Allinger, T. Clark, J. Gasteiger, P. A. Kollman, H. F. Schaefer III, and P. R. Schreiner (Eds.), John Wiley & Sons, Ltd., Chichester, New York, (1998).

[60] P. Pyykkö, K. G. Dyall, A. G. Császár, G. Tarczay, O. L. Polyansky, and J. Tennyson, Phys. Rev. A **63**, 024502 (2001).

[61] A. G. Császár, G. Tarczay, M. L. Leininger, O. L. Polyansky, J. Tennyson, and W. D. Allen, *In: Spectroscopy from Space*, J. Demaison and K. Sarka (Eds.), NATO ARW Series C, Kluwer Academic Publishers, Dordrecht, (2000).

[62] H. M. Quiney, H. Skaane, and I. P. Grant, Chem. Phys. Lett. **290**, 473 (1998).

4

Ab initio calculation of proton barrier and binding energy of the $(H_2O)OH^-$ complex

Abstract

The very low barrier (of the order of 1 kJ mol^{-1}) to proton transfer in the $(H_2O)OH^-$ complex is accurately computed by the coupled-cluster method including single and double excitations plus perturbative corrections for triple excitations [CCSD(T)]. By virtue of the coupled-cluster R12 method [CCSD(T)-R12], which employs explicitly correlated wave functions, results are obtained close to the limit of a complete basis set of atomic orbitals (AOs). The basis-set superposition error is avoided by applying the full function counterpoise approach to the three fragments OH^-, H^+, and OH^-. The most accurate computed value for the proton barrier amounts to $\delta = 0.9 \pm 0.3$ kJ mol^{-1}, which is 4–5 times this value below the lowest vibrational energy level. The three lowest vibrational energy levels are calculated from a one-dimensional potential energy curve describing the position of the bonding proton between the two OH^- fragments. The electronic binding energy with respect to dissociation into H_2O and OH^- is estimated to $D_e = 109 \pm 10$ kJ mol^{-1} at the level of explicitly correlated CCSD(T)-R12 theory.

C. C. M. Samson and W. Klopper, J. Mol. Struct. (Theochem) **586**, 201 (2002).

4.1 Introduction

In the charged and hydrogen-bonded $(H_2O)OH^-$ complex, two equivalent equilibrium structures of C_1 symmetry are interconnected through a transition structure $[HOHOH^-]‡$ of C_2 symmetry that consitutes a barrier to proton transfer between two OH^- fragments (Figures 4.1 and 4.2).

Numerous *ab initio* studies have been concerned with this proton transfer and the nature of the hydrogen bonding in $(H_2O)OH^-$ during the last decade [1–16]. Both wave function based quantum chemical methods—such as second-order Møller-Plesset perturbation theory (MP2)—and Kohn-Sham density-functional theory (DFT) methods have been applied, but neither the wave function based, nor the DFT calculations have proven fully satisfactory as the results were strongly dependent on the basis set or on the functionals used. For example, barriers in the range from 0.1 to 2.0 kJ mol^{-1} are reported in Ref. [12].

To date, the most accurate results seem to have been obtained in recent work by Deyerl et al. [13]. These authors have computed a barrier height of δ = 1.3 kJ mol^{-1} and an electronic binding energy of D_e = 116.9 kJ mol^{-1} at the QCISD(T)(fc)/6-311++G(3df,2p) // QCISD(fc)/6-311++G(d,p) level. A correction of -6.3 kJ mol^{-1} for zero-point vibrational energy (ZPVE), computed from QCISD(fc)/6-311++G(d,p) harmonic frequencies, has yielded D_0 = 110.6 kJ mol^{-1}[13]. Møller-Plesset perturbation theory calculations yield similar results for the electronic binding energy—D_e = 115.7 kJ mol^{-1} at the MP2(fu)/aug-cc-pVTZ level [5]—but the barrier seems to amount to only δ = 0.35 kJ mol^{-1} at the MP2(fc)/aug-cc-pVTZ level [16]. In view of the discrepancies between previous results, a more accurate and conclusive computational determination of the very low barrier to proton transfer seems desirable.

For this relatively small molecular system with two non-hydrogen atoms, three hydrogen atoms, and 20 electrons, it has recently become possible to carry out highly accurate coupled-cluster calculations using explicitly correlated wave functions that depend explicitly on the inter-electronic coordinates. At the level of coupled-cluster theory including single and double excita-

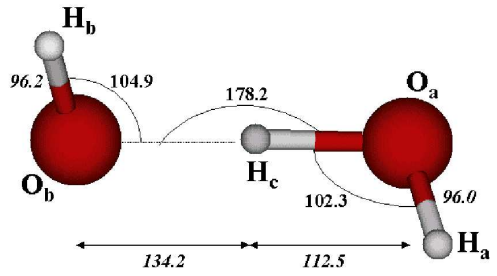

Figure 4.1: Optimized geometry of the equilibrium structure of $(H_2O)OH^-$. Lengths are given in pm and angles in degrees (cf. Table 4.3).

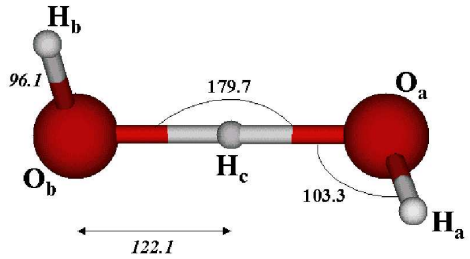

Figure 4.2: Optimized geometry of the [HOHOH$^-$]‡ transition structure. Lengths are given in pm and angles in degrees (cf. Table 4.3).

tions plus perturbative triple excitations, such an explicitly correlated approach has been termed the CCSD(T)-R12 method [17–19].

Moreover, the $(H_2O)OH^-$ complex represents a challenging case study for the recently proposed MP2-limit correction [20]. In this approximation, finite-basis CCSD(T) energies are improved by substituting the MP2 portion of that energy by the corresponding infinite-basis MP2 estimate that is obtained from the MP2-R12/A method.

4.2 Computational details

Standard aug-cc-pVDZ and aug-cc-pVTZ Gaussian basis sets have been used as well as two non-standard Gaussian basis sets denoted QTZ and "R12 basis". The QTZ basis is given in Ref. [21] and comprises 233 contracted Gaussians. This basis reads $8s5p4d3f2g$ for O and $4s3p2d$ for H. Its quality compares with aug-cc-pVQZ for O and aug-cc-pVTZ for H. The R12 basis is taken from Ref. [20] and comprises 389 uncontracted Gaussians. It reads $15s9p7d5f$ for O and $9s7p5d$ for H.

A three-fragment counterpoise approach (CP) has been applied, in which counterpoise corrected electronic energies of the complex $(H_2O)OH^-$ are obtained by subtracting the electronic energies of the H^+ fragment and the two distinct OH^- fragments in the basis of $(H_2O)OH^-$, and adding instead the electronic energies of these fragments in the same nuclear configuration but in their own basis. The same procedure has been applied to the electronic energy of the [HOHOH$^-$]‡ transition structure. Of course, the electronic energy of H^+ is always zero. Energies that have not been corrected are labeled "no-CP".

We have used the quantum chemistry program `Gaussian 98` [22] for the MP2(fc)/QTZ geometry optimizations as well as for coupled-cluster single-point energy calculations with the aug-cc-pVDZ, aug-cc-pVTZ, and QTZ basis sets, and the programs `SORE` [23] and `DIRCCR12` [24] for the explicitly correlated R12 calculations. Core orbitals ($1s$ orbital on O) were excluded from the correlation treatments and only the spherical components of the basis sets were used. The

calculations were performed on SGI Origin 2000 R12000 computers at Utrecht University and SARA Computing and Networking Services (Amsterdam).

4.3 Results

4.3.1 Electric molecular properties

An accurate theoretical description of the bonding in the $(H_2O)OH^-$ complex can only be achieved when the employed computational methods and AO basis sets are able to yield accurate numerical values for the electric molecular properties of the fragments. The electric dipole and quadrupole moments (Table 4.1) as well as static electric dipole polarizabilities (Table 4.2) of H_2O and OH^- have therefore been investigated by computing these properties numerically by means of finite-field perturbation theory (from a fifth-order polynomial fit to nine equidistant field strengths in the range $[-0.004, +0.004]$ atomic units). The results in Tables 4.1 and 4.2 are compared with previous high-level electron-correlation calculations by Maroulis [25] and Chong and Langhoff [26] and show that the electric molecular properties are indeed well recovered by the methods and basis sets employed in the present work. Only the results for the polarizability of the negative OH^- ion might seem somewhat inadequate, but this property if very difficult to compute. Its value changes strongly with the level of electron-correlation treatment or the order of perturbation theory [26].

4.3.2 Optimized geometries

The MP2(fc)/QTZ optimized geometries are shown in Figures 4.1 and 4.2 and the parameters are given in Table 4.3.

For the equilibrium structure of $(H_2O)OH^-$, the main difference from a water molecule and OH^- ion at infinite distance is the position of the central proton between the two O atoms. The two OH distances to this proton are 134.2 and 112.5 pm, respectively, and can be described as an $O\cdots H$ intermolecular hydrogen bond and stretched intramolecular OH bond. The OH distance in water under the same conditions is only 96.0 pm. The free OH bonds of the complex (96.0 and 96.2 pm) are not much influenced by the complexation. The two HOH angles are 102.3 and 104.9° and are close to the HOH angle in the water molecule (104.4°). The $O\cdots H$–O hydrogen bond is almost linear (178.2°).

For the $[HOHOH^-]^\ddagger$ transition structure, the two equal free OH bonds are 96.1 pm long and the two equal HOH angles amount to 103.3°. Furthermore, the $O\cdots H\cdots O$ angle is even closer to linearity than in the equilibrium structure (179.7°).

The optimized geometries are very similar to the MP2(fc)/aug-cc-pVTZ geometries obtained in Ref. [16]. This applies in particular to the [HOHOH$^-$]‡ transition structure, whereas the present equilibrium geometry is somewhat less asymmetric than the MP2(fc)/aug-cc-pVTZ geometry [16]. Interestingly, at the QCISD(fc)/6-311++G(d,p) level, the equilibrium geometry is significantly more asymmetric, showing OH distances to the central proton of 144.0 and 106.1 pm [13].

Table 4.1: Electric dipole (μ) and electric quadrupole (Θ) moments (in atomic units) of OH^- and H_2O at their CCSD(T)(fu)/cc-pCVQZ geometries.[a] For OH^-, the z-axis is chosen along the OH bond and for H_2O the z-axis is the C_2 axis while the y-axis is perpendicular to the molecular plane. The calculations were performed in the R12 basis with 167 and 222 contracted Gaussians for OH^- and H_2O, respectively.[b]

Molecule	Method	μ/ea_0	Θ_{xx}/ea_0^2	Θ_{yy}/ea_0^2	Θ_{zz}/ea_0^2
H_2O	Hartree–Fock	0.781	1.885	-1.794	-0.091
	MP2(fc)	0.731	1.933	-1.835	-0.097
	MP2-R12/A(fc)	0.736	1.939	-1.841	-0.098
	MP2-R12/B(fc)	0.735	1.940	-1.844	-0.095
	CCSD-R12/B(fc)	0.739	1.894	-1.800	-0.094
	CCSD[T]-R12/B(fc)	0.729	1.899	-1.802	-0.096
	CCSD(T)-R12/B(fc)	0.730	1.898	-1.802	-0.096
	Reference values[c]	0.724	1.912	-1.804	-0.108
OH^-	Hartree–Fock	0.495			1.812
	MP2(fc)	0.427			2.153
	MP2-R12/A(fc)	0.423			2.050
	MP2-R12/B(fc)	0.403			1.870
	CCSD-R12/B(fc)	0.435			1.885
	CCSD[T]-R12/B(fc)	0.415			1.991
	CCSD(T)-R12/B(fc)	0.420			1.951
	Reference value[d]	0.405			

[a] OH^-: R_{OH} = 96.331 pm; H_2O: R_{OH} = 95.712 pm and $\angle_{HOH}$ = 104.225°.

[b] The origin is at the molecule's center of mass; $\Theta_{xx} = \sum_i q_i \left\{\langle x_i^2\rangle - \frac{1}{2}\langle y_i^2\rangle - \frac{1}{2}\langle z_i^2\rangle\right\}$, where the sum runs over electrons and nuclei; similar for Θ_{yy} and Θ_{zz}.

[c] Ref. [25].

[d] Ref. [26].

With 246.7 and 244.2 pm, the OO distances are not very different in the equilibrium and transition structures, respectively, and in view of the similarity between the equilibrium and transition structures, it seems reasonable to consider the proton exchange in $(H_2O)OH^-$ in terms of a one-dimensional Schrödinger equation for a particle moving back and forth between the O atoms in a one-dimensional potential.

Table 4.2: Static dipole polarizability (α, in atomic units) of OH^- and H_2O at their CCSD(T)(fu)/cc-pCVQZ geometries.[a] For OH^-, the z-axis is chosen along the OH bond and for H_2O the z-axis is the C_2 axis while the y-axis is perpendicular to the molecular plane. The calculations were performed in the R12 basis with 167 and 222 contracted Gaussians for OH^- and H_2O, respectively.

Molecule	Method	$\alpha_{xx}/4\pi\epsilon_0 a_0^3$	$\alpha_{yy}/4\pi\epsilon_0 a_0^3$	$\alpha_{zz}/4\pi\epsilon_0 a_0^3$
H_2O	Hartree–Fock	9.16	7.86	8.50
	MP2(fc)	9.94	9.43	9.66
	MP2-R12/A(fc)	9.87	9.32	9.58
	MP2-R12/B(fc)	9.84	9.27	9.52
	CCSD-R12/B(fc)	9.66	8.85	9.23
	CCSD[T]-R12/B(fc)	9.85	9.17	9.48
	CCSD(T)-R12/B(fc)	9.82	9.11	9.44
	Reference values[b]	9.93	9.34	9.59
OH^-	Hartree–Fock		19.9	17.2
	MP2(fc)		31.4	22.3
	MP2-R12/A(fc)		29.4	21.4
	MP2-R12/B(fc)		25.3	20.3
	CCSD-R12/B(fc)		26.1	19.6
	CCSD[T]-R12/B(fc)		32.8	21.0
	CCSD(T)-R12/B(fc)		29.8	21.2
	Reference values[c]		51.8	26.8

[a] See Table 4.1.

[b] Ref. [25].

[c] Ref. [26].

4.3.3 Electronic binding energy

The electronic binding energy (D_e) has been computed at the CP corrected CCSD(T)-R12/B(fc)/ /MP2(fc)/QTZ level (Table 4.4). At the optimized equilibrium structure, the interaction energy (ΔE) between the H_2O and OH^- fragments amounts to about -160 kJ mol^{-1}, but a deformation energy of about 50 kJ mol^{-1} must be added to obtain D_e. This deformation energy occurs mainly in the H_2O fragment, where one intramolecular OH bond is stretched by as much as 16.5 pm.

Table 4.3: Geometrical parameters (cf. Figures 4.1 and 4.2).[a]

Species	Parameter	Here[b]	Ref. [13][c]	Ref. [5][d]	Ref. [12][e]	Ref. [10][f]	Ref. [16][g]
OH^-	O–H	96.6	96.5	96.4			
H_2O	O–H	96.0	95.9	95.9			
	H–O–H	104.4	103.6	104.3			
(H_2O)OH^-	O_a–H_a	96.0	95.8	95.9	96.1	97.5	96.1
(C_1)	O_b–H_b	96.2	96.1	96.1	96.3	97.6	96.4
	O_a–H_c	112.5	106.1	110.7	111.7	116.2	111.2
	O_b–H_c	134.2	144.0	136.4	136.2	133.8	136.5
	H_a–O_a–H_c	102.3	100.6	102.0		102.5	
	H_b–O_b–H_c	104.9	108.1	105.0	106.1	104.2	
	O_a–H_c–O_b	178.2	174.7	177.9		178.7	177.9
	H_a–O_a–O_b–H_b	101.7	92.8	101.3	109.1	100.5	101.5
	O_b–H_c–O_a–H_a	337.4	336.9	334.0		341.0	
[$HOHOH^-$]‡	O_a–H_a	96.1	95.9				96.2
(C_2)	O_a–H_c	122.1	121.0				122.1
	O_a–H_c–O_b	179.7	178.0				179.8
	H_a–O_a–H_c	103.3	102.7				
	H_a–O_a–O_b–H_b	101.6					101.2

[a] Bond lengths in pm and angles in degrees.

[b] MP2(fc)/QTZ.

[c] QCISD(fc)/6-311++G(d,p).

[d] MP2(fu)/aug-cc-pVTZ.

[e] B3LYP/6-311++G(d,p).

[f] BLYP/aug-cc-pVDZ.

[g] MP2(fc)/aug-cc-pVTZ.

At the CCSD(T)-R12/B(fc) level, the CP correction amounts to ca. 5 kJ mol^{-1}. Furthermore, the differences between the MP2, CCSD, CCSD(T), and CCSD[T] levels are rather small (1–2 kJ mol^{-1}), and we adopt the CCSD(T)-R12/B(fc) value of D_e = 109.0 kJ mol^{-1} as our best estimate of the electronic binding energy of $(H_2O)OH^-$. The result obtained by Deyerl et al. [13] is ca. 8 kJ mol^{-1} larger than our best estimate. This is presumably due to the neglect of basis-set superposition error (BSSE) in Ref. [13].

In view of the earlier mentioned energy differences, it seems reasonable to attach an error bar of $\pm$10 kJ mol^{-1} to our best estimate to account for further geometry relaxation, high-order correlation, and basis-set effects.

4.3.4 Barrier to proton exchange

Table 4.4 shows counterpoise corrected (CP) and uncorrected (no-CP) computed values for the barrier (δ) to proton exchange, as obtained in the R12 basis for the MP2(fc)/QTZ geometries of the equilibrium and transition structures given in Table 4.3.

At the CCSD(T)-R12/B(fc) level, the BSSE is very small (0.03 kJ mol^{-1}), but high-order correlation effects are substantial. From MP2-R12/B(fc) to CCSD-R12/B(fc), the barrier increases from 0.44 to 1.11 kJ mol^{-1} while it is reduced again to 0.82 kJ mol^{-1} at the CCSD(T)-R12/B(fc)

Table 4.4: Proton barrier (δ) of $(H_2O)OH^-$, interaction energy (ΔE) between the fragments OH^- and H_2O in the complex, and electronic binding energy (D_e) with respect to dissociation into OH^- and H_2O at their MP2(fc)/QTZ optimized equilibrium geometries (cf. Table 4.3). All calculations were performed in the R12 basis with 389 contracted Gaussians and either do include (CP) or do not include (no-CP) the three-fragment counterpoise correction mentioned in the text.

	δ/kJ mol^{-1}		ΔE/kJ mol^{-1}		D_e/kJ mol^{-1}	
Method	no-CP	CP	no-CP	CP	no-CP	CP
Hartree–Fock	2.89	2.89	-155.8	-155.6	89.8	89.6
MP2(fc)	0.57	0.63	-160.8	-152.3	110.9	102.5
MP2-R12/A(fc)	0.45	0.45	-162.6	-159.7	113.5	110.6
MP2-R12/B(fc)	0.40	0.44	-166.4	-156.9	117.1	107.6
CCSD-R12/B(fc)	1.08	1.11	-162.3	-157.9	111.2	106.8
CCSD[T]-R12/B(fc)	0.84	0.87	-161.7	-156.6	113.1	108.0
CCSD(T)-R12/B(fc)	0.79	0.82	-162.9	-157.8	114.1	109.0

level. In view of this oscillatory behavior, it seems not impossible that the barrier would again increase a little (presumably of the order of 0.1 kJ mol^{-1}) at the full CCSDT level.

Furthermore, the barrier would of course look slightly different when the geometries had been optimized at a level of correlation higher than MP2 (e.g., at the CCSD(T) level), but it is difficult to substantiate such effects. From the potential energy curves derived in Section 4.3.6, it follows that the barrier changes by $V(1.7\ \mathrm{pm})^2(24.3\ \mathrm{pm})^2 \approx$0.1 kJ mol^{-1} when the central proton moves 1.7 pm away from the CCSD(T)(fc)/QTZ minimum (at x_e = 13.00 pm) to the MP2(fc)/QTZ minimum (at x_e = 11.30 pm) along the O$\cdots$H$\cdots$O bond. Deyerl et al. [13] have obtained a QCISD geometry for [HOHOH$^-$]‡ that is very similar to our MP2 structure, but a QCISD geometry for $(H_2O)OH^-$ at equilibrium that is very different in terms of the position of the central proton. Thus, geometry effects beyond the MP2 level could be noticeable and could very well lower the equilibrium structure somewhat more than the transition structure and hence increase the barrier height.

In view of the above considerations, we adopt the value δ = 0.9$\pm$0.3 kJ mol^{-1} as our best estimate of the barrier to proton exchange in $(H_2O)OH^-$.

4.3.5 MP2-limit correction

In the preceeding sections, the electronic binding energy and the barrier to proton exchange of the hydrogen bonded $(H_2O)OH^-$ complex were determined computationally at the CCSD(T)-R12/B(fc)//MP2(fc)/QTZ level, and best estimates were presented on the basis of these calculations.

As the barrier is only of the order of 1 kJ mol^{-1}, we anticipate that it will be well below the lowest vibrational energy level of the complex. Note that an energy of 1 kJ mol^{-1} corresponds to the ground-state energy of a proton in a one-dimensional box as large as 140 pm. In a first approximation, an estimate of the lowest vibrational energy level can be obtained by computing a

Table 4.5: Proton barrier (δ in kJ mol^{-1}) of $(H_2O)OH^-$.

	MP2(fc)		CCSD(T)(fc)		MP2-limit corrected CCSD(T)(fc)	
Basis	no-CP	CP	no-CP	CP	no-CP	CP
aug-cc-pVDZ	0.795	0.845	1.157	1.234	0.807	0.835
aug-cc-pVTZ	0.330	0.446	0.673	0.796	0.789	0.796
QTZ	0.200	0.451	0.553	0.781	0.799	0.776

potential energy curve for the central proton moving in one dimension between the OH^- fragments.

However, as CCSD(T)-R12 calculations—with the `DIRCCR12` program—of this potential energy curve would be too time-consuming, we decided to apply the MP2-limit correction approach from Ref. [20]. Applied to CCSD(T)(fc)/QTZ results, this correction consists of subtracting the corresponding MP2(fc)/QTZ energies and adding instead its MP2-R12/A(fc) counterparts. By doing so, the MP2(fc) portion of the CCSD(T)(fc)/QTZ energy is replaced by its infinite-basis value.

Table 4.5 shows the results of MP2-limit corrected CCSD(T)(fc) calculations in the aug-cc-pVTZ, aug-cc-pVQZ, and QTZ basis sets (at the fixed geometries of Table 4.3). In these basis sets, the uncorrected (no-CP) CCSD(T)(fc) barriers amount to 1.16, 0.67, and 0.55 kJ mol^{-1}, respectively, and from these monotonically decreasing values, one might be tempted to extrapolate a value of about 0.46 kJ mol^{-1} for the limit in an infinite basis. This extrapolation is incorrect, however, as the underlying values were contaminated by the BSSE. The three-fragment CP correction yields barriers of 1.23, 0.80, and 0.78 kJ mol^{-1} for the three basis sets. When the MP2-limit correction is applied, the range of results is brought down to 0.78–0.84 kJ mol^{-1}. Interestingly, it makes little different whether the CCSD(T)(fc) energies had been CP corrected or not. The MP2-limit correction accounts for BSSE at the MP2 level and this appears to be sufficient.

The most important conclusion from Table 4.5 is that all the MP2-limit corrected results (0.78–0.84 kJ mol^{-1}) are in good agreement with the calculated CCSD(T)-R12/B(fc) result of Table 4.4 (0.82 kJ mol^{-1}). We have hence applied the MP2-limit correction approach for the construction of a potential energy curve.

Table 4.6: Total electronic energies (in E_h) of [HOHOH$^-$]‡ as a function of the position (x) of the proton relative to the midpoint of the O$\cdots$H$\cdots$O bond.

x/pm	MP2-R12/A(fc)	MP2(fc)/QTZ	CCSD(T)(fc)/QTZ	MP2-limit corrected CCSD(T)(fc)/QTZ
0.000	-152.153284	-152.102247	-152.120840	-152.171877
5.425	-152.153380	-152.102330	-152.120974	-152.172024
10.850	-152.153519	-152.102428	-152.121215	-152.172307
16.275	-152.153231	-152.102071	-152.121069	-152.172229
21.700	-152.151679	-152.100418	-152.119663	-152.170924
27.125	-152.147572	-152.096170	-152.115669	-152.167071
32.550	-152.139036	-152.087444	-152.107186	-152.158778

4.3.6 Potential energy curve

For the computation of a one-dimensional potential energy curve for proton exchange, the OO distance was kept fixed at the equilibrium value of 246.7 pm, and the dihedral angle H_a–O_a–O_b–H_b was kept fixed at the equilibrium value of 101.7°. For the intramolecular OH bonds and HOH angles, the averaged values of 96.1 pm and 103.4° were chosen, respectively. The O···H···O hydrogen bond was kept linear, and the position of the proton was described by a coordinate x relative to the midpoint of this bond. Calculations were performed at seven equidistant points in the range $0 \leq x \leq 32.55$ pm. For x = 32.55 pm, the proton is at a distance of 90.80 pm from the O atom, where the potential is sufficiently repulsive (ca. 35 kJ mol^{-1} above the minimum). By symmetry, 13 grid points were obtained, which were fitted to the function $V(x) = V\{(x + x_e)(x - x_e)\}^2$. The one-dimensional Schrödinger equation was solved numerically using the Numerov–Cooley method.

The computed energies and the results from the corresponding fits are collected in Tables 4.6 and 4.7, respectively. All QTZ energies were corrected for BSSE by the three-fragment CP approach.

At the three-fragment CP corrected MP2(fc)/QTZ level, the minimum of $V(x)$ is located at x_e = 11.3 pm. This point corresponds to the position $r(O_a$–$H_c)$ = 112.05 pm and $r(O_b$–$H_c)$ = 134.65 pm, which is in good agreement (to within 0.5 pm) with the MP2(fc)/QTZ optimized equilibrium structure (Table 4.3). Since the minimum at x_e = 11.3 pm is indeed close to the fully optimized equilibrium structure, we may conclude that the geometry optimization in the QTZ basis is only little affected by the BSSE. The barrier on the CP corrected MP2(fc)/QTZ potential energy curve amounts to 0.74 kJ mol^{-1}, which is almost 0.2 kJ mol^{-1} above the corresponding barrier of 0.45 kJ mol^{-1} given in Table 4.5, which refers to the fully optimized equilibrium and transition struc-

Table 4.7: Potential parameters and vibrational levels. All QTZ results include the three-fragment counterpoise correction mentioned in the text.

				MP2-limit corrected
	MP2-R12/A(fc)	MP2(fc)/QTZ	CCSD(T)(fc)/QTZ	CCSD(T)(fc)/QTZ
δ/kJ mol^{-1}	0.90	0.74	1.33	1.54
V/kJ mol^{-1}pm^{-4}	4.51×10^{-5}	4.53×10^{-5}	4.66×10^{-5}	4.64×10^{-5}
x_e/pm	11.87	11.30	13.00	13.50
$E_{v=0}$/cm^{-1}	428	430	433	434
$E_{v=1}$/cm^{-1}	1513	1537	1483	1462
$E_{v=2}$/cm^{-1}	3116	3154	3079	3045

tures. The present value is higher than its counterpart in Table 4.5, since the transition structure is discriminated against the equilibrium structure by the fixed OO distance of 246.7 pm.

At the CP corrected CCSD(T)(fc)/QTZ level, the proton barrier on this analytical potential energy curve $V(x)$ amounts to 1.33 kJ mol^{-1}, and the MP2-limit correction increases the barrier further to 1.54 kJ mol^{-1} (Table 4.7). At the MP2-limit (and CP corrected) CCSD(T)(fc)/QTZ level, the minimum is located at x_e = 13.5 pm, corresponding to the position $r(\mathrm{O}_a\text{–}\mathrm{H}_c)$ = 109.85 pm and $r(\mathrm{O}_b\text{–}\mathrm{H}_c)$ = 136.85 pm.

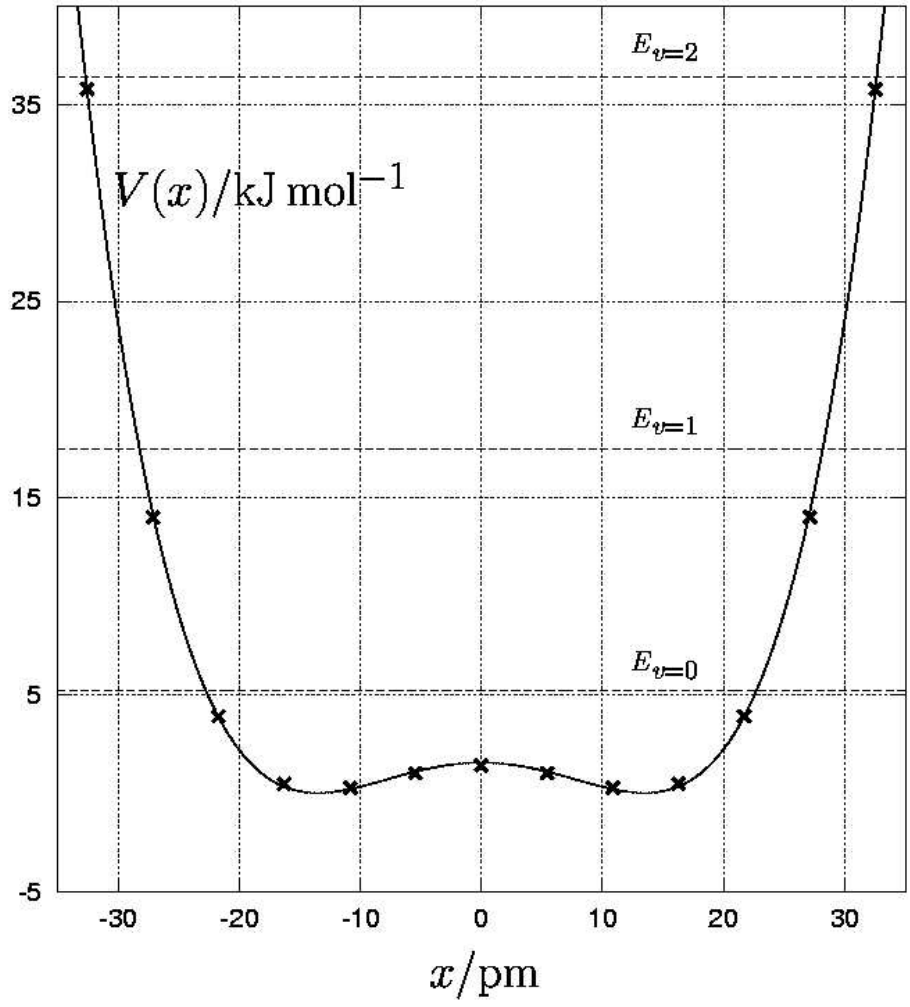

Figure 4.3: Double-well potential $V(x) = V\{(x + x_e)(x - x_e)\}^2$ including the 13 grid points that were computed at the MP2-limit corrected CCSD(T)(fc)/QTZ level (V = 4.64×10^{-5} kJ mol^{-1}pm^{-4} and x_e = 13.5 pm). The three lowest vibrational levels are also shown.

The first vibrational energy level at 5.2 kJ mol^{-1} is roughly four times higher than the proton barrier, and the ground-state probability distribution of the proton position has its maximum at x=0.

4.4 Conclusion

It appears that the lowest vibrational energy level (5.2 kJ mol^{-1}) in a one-dimensional double-well potential for $(H_2O)OH^-$ is 5–6 times higher than the barrier (0.9$\pm$0.3 kJ mol^{-1}) on that potential (cf. Figure 4.3). Hence, the barrier has little effect on the probability distribution of the hydrogen-bonding proton. The electronic binding energy with respect to dissociation into H_2O and OH^- is estimated to D_e= 109$\pm$10 kJ mol^{-1}.

Acknowledgments

The research of W.K. has been made possible by a fellowship of the Royal Netherlands Academy of Arts and Sciences. The authors thank Dr. J. G. C. M. van Duijneveldt-van de Rijdt and Professor F. B. van Duijneveldt for many helpful discussions. We gratefully acknowledge partial support from COST Chemistry Action D9 (Working Group 13/98) and a generous grant of computing time from National Computing Facilities (NCF) Foundation.

References

[1] K. Luth and S. Scheiner, J. Chem. Phys. **97**, 7507 (1992).

[2] K. Luth and S. Scheiner, J. Chem. Phys. **97**, 7519 (1992).

[3] S. Gronert, J. Am. Chem. Soc. **115**, 10258 (1993).

[4] J. E. Del Bene and I. Shavitt, J. Mol. Struct. (Theochem) **307**, 27 (1994).

[5] S. S. Xantheas, J. Am. Chem. Soc. **117**, 10373 (1995).

[6] A. T. Pudzianowski, J. Phys. Chem. **100**, 4781 (1996).

[7] S. Scheiner and M. Čuma, J. Am. Chem. Soc. **118**, 1511 (1996).

[8] J. A. Platts and K. E. Laidig, J. Phys. Chem. **100**, 13455 (1996).

[9] M. E. Tuckerman, D. Marx, M. L. Klein, and M. Parrinello, Science **275**, 817 (1997).

[10] C. Perez del Valle and J. J. Novoa, Chem. Phys. Lett. **269**, 401 (1997).

[11] L. R. Corrales, J. Chem. Phys. **110**, 9071 (1999).

[12] D. Wei, E. I. Proynov, A. Milet, and D. R. Salahub, J. Phys. Chem. A **104**, 2384 (2000).

[13] H.-J. Deyerl, A. K. Luong, T. G. Clements, and R. E. Continetti, Faraday Discuss. **115**, 147 (2000).

[14] J. R. Pliego, Jr. and J. M. Riveros, J. Chem. Phys. **112**, 4045 (2000).

[15] M. Kowal, S. Roszak, and J. Leszczynski, J. Chem. Phys. **114**, 8251 (2001).

[16] D. H. Barich, J. B. Nicholas, and J. F. Haw, J. Phys. Chem. A **105**, 4708 (2001).

[17] J. Noga, W. Kutzelnigg, and W. Klopper, Chem. Phys. Lett. **199**, 497 (1992).

[18] J. Noga and W. Kutzelnigg, J. Chem. Phys. **101**, 7738 (1994).

[19] J. Noga, W. Klopper, and W. Kutzelnigg, *In: Recent Advances in Computational Chemistry, Vol. 3, pp. 1–48*, R. J. Bartlett (Ed.), World Scientific Publishing Co. Ltd., Singapore, (1997).

[20] W. Klopper and H. P. Lüthi, Mol. Phys. **96**, 559 (1999).

[21] W. Klopper, J. G. C. M. van Duijneveldt-van de Rijdt, and F. B. van Duijneveldt, Phys. Chem. Chem. Phys. **2**, 2227 (2000).

[22] M. J. Frisch, G. W. Trucks, H. B. Schlegel, G. E. Scuseria, M. A. Robb, J. R. Cheeseman, V. G. Zakrzewski, J. A. Montgomery, Jr., R. E. Stratmann, J. C. Burant, S. Dapprich, J. M. Millam, A. D. Daniels, K. N. Kudin, M. C. Strain, O. Farkas, J. Tomasi, V. Barone, M. Cossi, R. Cammi, B. Mennucci, C. Pomelli, C. Adamo, S. Clifford, J. Ochterski, G. A. Petersson, P. Y. Ayala, Q. Cui, K. Morokuma, D. K. Malick, A. D. Rabuck, K. Raghavachari, J. B. Foresman, J. Cioslowski, J. V. Ortiz, A. G. Baboul, B. B. Stefanov, G. Liu, A. Liashenko, P. Piskorz, I. Komaromi, R. Gomperts, R. L. Martin, D. J. Fox, T. Keith, M. A. Al-Laham, C. Y. Peng, A. Nanayakkara, M. Challacombe, P. M. W. Gill, B. Johnson, W. Chen, M. W. Wong, J. L. Andres, C. Gonzalez, M. Head-Gordon, E. S. Replogle, and J. A. Pople, *Gaussian, Inc., Pittsburgh PA*, Gaussian 98, Revision A.7 (1998).

[23] W. Klopper, *SORE, a second-order R12 energy program.*

[24] J. Noga and W. Klopper, *DIRCCR12, an integral-direct explicitly correlated coupled-cluster program.*

[25] G. Maroulis, Chem. Phys. Lett. **289**, 403 (1998).

[26] D. P. Chong and S. R. Langhoff, J. Chem. Phys. **570**, 93 (1990).

5

Explicitly correlated second-order Møller-Plesset methods with auxiliary basis sets

Abstract

In explicitly correlated Møller-Plesset (MP2-R12) methods, the first-order wave function is expanded not only in terms of products of one-electron functions—that is, orbitals—but also in terms of two-electron functions that depend linearly on the interelectronic coordinates r_{ij}. With these functions, three- and four-electron integrals occur, but these integrals can be avoided by inserting a resolution of the identity (RI) in terms of the one-electron basis. In previous work, only one single basis was used for both the electronic wave function and the RI approximation. In the present work, a new computational approach is developed that uses an auxiliary basis set to represent the RI. This auxiliary basis makes it possible to employ standard basis sets in explicitly correlated MP2-R12 calculations.

W. Klopper and C. C. M. Samson, J. Chem. Phys. **116**, 6397 (2002).

5.1 Introduction

Beyond the Hartree–Fock level, basis-set truncation errors greatly frustrate efforts to compute highly accurate molecular electronic energies and properties [1–5]. Such errors occur when insufficiently large basis sets of products of one-electron functions (atomic orbitals, AOs) are employed to expand the many-electron wave function. Moreover, due to the drastic increase of computation time with the size of the AO basis, it often happens that this basis cannot be increased to the size that would be required to achieve the prescribed high accuracy. Experience has shown, for example, that the computation time of a correlated electronic-structure calculation in a correlation-consistent cc-pVXZ basis grows as $\propto X^{12}$ with its cardinal number X while basis-set truncation errors only disappear as $\propto X^{-3}$ [6].

The importance of the basis-set truncation error and the slow convergence with the size of the AO basis have been recognized for a long time, and various techniques have been developed to overcome the basis-set convergence problems. Among these, we find extrapolation and scaling techniques as well as empirical additive corrections [6–18]. Widely used methods include the complete-basis-set (CBS) approach [9, 10] and the G3 model chemistry [13, 14].

The basis-set truncation errors and slow convergence problems can be addressed more directly by adding two-electron basis functions to the expansion in orbital products. When such two-electron functions depend explicitly on the interelectronic distances $r_{ij} = |\vec{r}_i - \vec{r}_j|$, the convergence to the limit of a complete basis is significantly accelerated [19–23]. Since 1985, various methods have been developed that employ two-electron functions that depend linearly on r_{ij}. Today, these methods are known as R12 methods [24–28]. A key issue in these methods is that multicenter three- and four-electron integrals (and even five-electron integrals in coupled-cluster theory) are avoided by introducing the resolution of the identity (RI) represented in the AO basis. As these many-electron integrals are avoided by virtue of the RI approximation, R12 calculations can be performed on fairly large molecules (e.g., ferrocene [29]) and molecular complexes (e.g., benzene–neon [30], water trimer and tetramer [31, 32]), but very large AO basis sets must be employed to ensure that the RI approximation is a good one that does not introduce other types of unwanted basis-set errors.

In this article, we present a new formulation of R12 theory that utilizes an auxiliary basis set for the RI approximation. This auxiliary basis can then be chosen such that the basis-set errors due to the RI approximation become arbitrarily small (i.e., negligible in comparison with other errors). Most importantly, there will no longer be constraints on the size of the AO basis that is used to expand the molecular electronic wave function.

In Section 5.2, we present the matrix elements that contribute to the MP2-R12 energy and show how they can be evaluated by introducing an auxiliary basis set. As the R12 functions can be

chosen strongly orthogonal to either the full molecular orbital space (Ansatz **1**) or to the occupied molecular orbital space (Ansatz **2**), we derive the working equations for both cases. The computer implementations of both Ansätze are given in Section 5.3. The newly developed methods are summarized in Section 5.4 and numerical results are shown in Sections 5.5 and 5.6, respectively, for the Ne atom and for calculations in correlation-consistent basis sets on the systems CH_2 ($^1A_1$), H_2O, NH_3, HF, N_2, CO, Ne, and F_2.

5.2 Methodology

5.2.1 The R12 Ansatz

In closed-shell explicitly correlated MP2-R12 theory, the first-order wave function is expanded not only in a basis of double excitations containing the orbital product $\varphi_a(1)\varphi_b(2)$ (as in standard MP2 theory), but also in a basis of two-electron basis functions

$$\chi_{mn}(1,2) = \hat{w}_{12}|\varphi_m(1)\varphi_n(2)\rangle, \tag{5.1}$$

where $\hat{w}_{12}$ is an appropriate correlation factor (see, e.g., Ref. [23]). In this article, we shall investigate two possible Ansätze for the explicitly correlated function $\chi_{mn}(1,2)$. In Ansatz **1**, the correlation factor is chosen as

$$\hat{w}_{12} = (1-\hat{P}_1)(1-\hat{P}_2)r_{12}, \tag{5.2}$$

whereas in Ansatz **2**, it is chosen as

$$\hat{w}_{12} = (1-\hat{O}_1)(1-\hat{O}_2)r_{12}. \tag{5.3}$$

Note that the correlation factor contains projection operators, which can be chosen in different manners (cf. Ref. [33]). $\hat{P}_1$ is the one-electron projector onto the space of orthonormal spatial orbitals $\varphi_p(1)$ that is spanned by the finite basis set of N atomic orbitals (AO basis),

$$\hat{P}_1 = \sum_p |\varphi_p(1)\rangle\langle\varphi_p(1)|. \tag{5.4}$$

A number of n orbitals are occupied (with $2n$ electrons) in the reference Hartree–Fock function and $N-n$ orbitals are empty—or virtual. The projector $\hat{O}_1$ onto the occupied orbital space is given by

$$\hat{O}_1 = \sum_i |\varphi_i(1)\rangle\langle\varphi_i(1)|. \tag{5.5}$$

As usual, we denote occupied orbitals by the indices i, j, k, ... , virtual orbitals by a, b, c, ... , and arbitrary (i.e., either occupied or virtual) orbitals by p, q, r, ... We denote the one-electron basis $\{\varphi_p(1)\}_{p=1,\ldots,N}$ as *orbital basis* and also introduce an orthonormal *auxiliary basis* $\{\varphi_{p'}(1)\}_{p'=1,\ldots,N'}$ with corresponding projector

$$\hat{P}'_1 = \sum_{p'} |\varphi_{p'}(1)\rangle\langle\varphi_{p'}(1)|. \tag{5.6}$$

In previous MP2-R12 work, no distinction was made between the Ansätze **1** and **2**, because—after insertion of the resolution of the identity in the framework of the standard approximation—they both led to the same working equations and hence to the same numerical results. This is no longer true when the three- and four-electron integrals are computed exactly [34, 35] or when an auxiliary basis set is used. Then, the two Ansätze indeed yield different results, as we shall see below. Furthermore, it is important to realize that the Ansätze **1** and **2** are not approximations but refer to different wave function expansions.

5.2.2 Second-order pair energies

We can write the MP2-R12 correlation energy in terms of singlet ($s = 0$) and triplet ($s = 1$) pair energies,

$$E^{(2)} = \sum_{s=0,1} (2s+1) \sum_{i \le j} \left(d_{ij}^s + e_{ij}^s \right), \tag{5.7}$$

where e_{ij}^s is the conventional MP2 pair energy and d_{ij}^s the pair energy contribution from the explicitly correlated functions. In Eq. (5.7) it is understood that intraorbital triplet pair energies vanish, that is, $e_{ii}^1 = d_{ii}^1 = 0$.

Let us define spin-adapted vectors $\bar{\mathbf{V}}^{(ij,s)}$ and matrices $\bar{\mathbf{B}}^{(ij,s)}$ as follows:

$$\bar{V}_{kl}^{(ij,s)} = \left(1+\delta_i^j\right)^{-1/2} \left(1+\delta_k^l\right)^{-1/2} \left(\tilde{V}_{kl}^{(ij)} + (1-2s)\tilde{V}_{lk}^{(ij)} \right), \tag{5.8}$$

$$\bar{B}_{kl,mn}^{(ij,s)} = \left(1+\delta_k^l\right)^{-1/2} \left(1+\delta_m^n\right)^{-1/2} \left(\tilde{B}_{kl,mn}^{(ij)} + (1-2s)\tilde{B}_{lk,mn}^{(ij)} \right), \tag{5.9}$$

where δ_i^j is Kronecker's delta and $i \le j$, $k \le l$, and $m \le n$ for $s = 0$ and $i < j$, $k < l$, and $m < n$ for $s = 1$. The R12 pair contributions are then given by the expression

$$d_{ij}^s = -\left\{\bar{\mathbf{V}}^{(ij,s)}\right\}^{\mathrm{T}} \left\{\bar{\mathbf{B}}^{(ij,s)}\right\}^{-1} \bar{\mathbf{V}}^{(ij,s)}. \tag{5.10}$$

This equation has been derived in Ref. [36] and is equivalent to Eq. (15) of that paper. See also Ref. [37]

5.2.3 Matrix elements

In the MP2-R12 method, the following vector components and matrix elements must be computed:

$$\tilde{V}_{kl}^{(ij)} = V_{kl}^{(ij)} - \sum_{ab} \frac{C_{kl,ab}^{(ij)}}{\varepsilon_a + \varepsilon_b - \varepsilon_i - \varepsilon_j} \langle \varphi_a(1)\varphi_b(2)|g_{12}|\varphi_i(1)\varphi_j(2)\rangle, \tag{5.11}$$

$$\tilde{B}_{kl,mn}^{(ij)} = B_{kl,mn}^{(ij)} - \sum_{ab} \frac{C_{kl,ab}^{(ij)}}{\varepsilon_a + \varepsilon_b - \varepsilon_i - \varepsilon_j} C_{ab,mn}^{(ij)}, \tag{5.12}$$

where

$$\begin{aligned} V_{kl}^{(ij)} &= \langle \chi_{kl}(1,2)|g_{12}|\varphi_i(1)\varphi_j(2)\rangle \\ &= \langle \varphi_k(1)\varphi_l(2)|\hat{w}_{12}^{\dagger} g_{12}|\varphi_i(1)\varphi_j(2)\rangle, \end{aligned} \tag{5.13}$$

$$\begin{aligned} B_{kl,mn}^{(ij)} &= \langle \chi_{kl}(1,2)|\hat{f}_{12} - \varepsilon_i - \varepsilon_j|\chi_{mn}(1,2)\rangle, \\ &= \langle \varphi_k(1)\varphi_l(2)|\hat{w}_{12}^{\dagger}(\hat{f}_{12} - \varepsilon_i - \varepsilon_j)\hat{w}_{12}|\varphi_m(1)\varphi_n(2)\rangle, \end{aligned} \tag{5.14}$$

$$\begin{aligned} C_{kl,ab}^{(ij)} &= \langle \chi_{kl}(1,2)|\hat{f}_{12} - \varepsilon_i - \varepsilon_j|\varphi_a(1)\varphi_b(2)\rangle \\ &= \langle \varphi_k(1)\varphi_l(2)|\hat{w}_{12}^{\dagger}(\hat{f}_{12} - \varepsilon_i - \varepsilon_j)|\varphi_a(1)\varphi_b(2)\rangle, \end{aligned} \tag{5.15}$$

and

$$g_{12} = r_{12}^{-1}, \qquad \hat{f}_{12} = \hat{F}_1 + \hat{F}_2. \tag{5.16}$$

$\hat{F}_1$ is the one-electron Fock operator and ε_i is the orbital energy of the occupied molecular orbital $\varphi_i(1)$. The explicitly correlated functions in Ansatz **1** are strongly orthogonal to all pairs of the orbital basis. As a consequence, all matrix elements $C_{kl,ab}^{(ij)}$ vanish for this Ansatz. These matrix elements describe the coupling between the doubly substituted determinants of conventional MP2 theory with the explicitly correlated functions. These matrix elements do *not vanish* for Ansatz **2**, where the explicitly correlated functions are strongly orthogonal only to pairs of occupied orbitals. For this reason, we have defined vectors $\tilde{\mathbf{V}}^{(ij)}$ and matrices $\tilde{\mathbf{B}}^{(ij)}$ that include the coupling (zero or not) with the doubly substituted determinants.

Finally, it is useful to define the matrix

$$X_{kl,mn} = \langle \varphi_k(1)\varphi_l(2)|\hat{w}_{12}^{\dagger}\hat{w}_{12}|\varphi_m(1)\varphi_n(2)\rangle, \tag{5.17}$$

which is an intermediate quantity that is used when the $\tilde{\mathbf{B}}^{(ij)}$ matrices are computed.

5.2.4 Working equations for Ansatz 1

Let us first investigate the two-electron operator product

$$\begin{aligned} \hat{w}_{12}^{\dagger} g_{12} &= r_{12}(1-\hat{P}_1)(1-\hat{P}_2)r_{12}^{-1} \\ &= r_{12}(1-\hat{P}_1-\hat{P}_2+\hat{P}_1\hat{P}_2)r_{12}^{-1}. \end{aligned} \tag{5.18}$$

It contains four terms. The first term is trivial, the fourth term factorizes into a product of two-electron integrals, but the second and third terms, where the operators $\hat{P}_1$ and $\hat{P}_2$ occur alone, lead to three-electron integrals. Consider, for example,

$$\langle\varphi_k(1)\varphi_l(2)|r_{12}\hat{P}_1 g_{12}|\varphi_i(1)\varphi_j(2)\rangle = \sum_p \langle\varphi_k(1)\varphi_l(2)\varphi_p(3)|r_{12}g_{23}|\varphi_p(1)\varphi_j(2)\varphi_i(3)\rangle. \tag{5.19}$$

It has been common practice in the R12 methods to avoid these three-electron integrals by inserting the resolution of the identity ($\hat{P}_2$) into the integrals with a single projector,

$$\hat{P}_1 \rightarrow \hat{P}_1\hat{P}_2, \tag{5.20}$$

and similarly by inserting $\hat{P}_1$,

$$\hat{P}_2 \rightarrow \hat{P}_1\hat{P}_2. \tag{5.21}$$

This computational strategy has been termed "standard approximation" (SA) in previous work (the SA actually also involves a few more approximations). In the new method that we propose here, we employ an auxiliary basis $\{\varphi_{p'}(1)\}_{p'=1,\ldots,N'}$ and make the substitutions

$$\hat{P}_1 \rightarrow \hat{P}_1\hat{P}'_2, \qquad \hat{P}_2 \rightarrow \hat{P}'_1\hat{P}_2. \tag{5.22}$$

We will denote our new approach as "auxiliary basis set" (ABS) approximation. Thus, for the product $g_{12}\hat{w}_{12}$ in the standard and ABS approximations, we find

$$\hat{w}_{12}^{\dagger} g_{12} \overset{SA}{\approx} 1 - r_{12}\hat{P}_1\hat{P}_2 g_{12} \tag{5.23}$$

and

$$\hat{w}_{12}^{\dagger} g_{12} \overset{ABS}{\approx} 1 - r_{12}\hat{P}_1\hat{P}'_2 g_{12} - r_{12}\hat{P}'_1\hat{P}_2 g_{12} + r_{12}\hat{P}_1\hat{P}_2 g_{12}, \tag{5.24}$$

respectively. Obviously, the matrix elements of Eq. (5.17) can be computed in the same manner,

$$\hat{w}_{12}^{\dagger}\hat{w}_{12} = \hat{w}_{12}^{\dagger} r_{12} \overset{ABS}{\approx} r_{12}^2 - r_{12}\hat{P}_1\hat{P}'_2 r_{12} - r_{12}\hat{P}'_1\hat{P}_2 r_{12} + r_{12}\hat{P}_1\hat{P}_2 r_{12}. \tag{5.25}$$

Let us now turn to the matrix elements of Eq. (5.14). To evaluate these elements, we rewrite the corresponding two-electron operator as

$$\begin{aligned}\hat{w}_{12}^{\dagger}(\hat{f}_{12}-\varepsilon_i-\varepsilon_j)\hat{w}_{12} &= \tfrac{1}{2}\hat{w}_{12}^{\dagger}[\hat{f}_{12},\hat{w}_{12}]+\tfrac{1}{2}[\hat{w}_{12}^{\dagger},\hat{f}_{12}]\hat{w}_{12} \\ &+ \tfrac{1}{2}\hat{w}_{12}^{\dagger}\hat{w}_{12}(\hat{f}_{12}-\varepsilon_i-\varepsilon_j)+\tfrac{1}{2}(\hat{f}_{12}-\varepsilon_i-\varepsilon_j)\hat{w}_{12}^{\dagger}\hat{w}_{12}. \end{aligned} \tag{5.26}$$

The last two terms of Eq. (5.26) are easily computed when we assume that the occupied orbitals are eigenfunctions of the Fock operator in the sense of the *generalized* Brillouin condition (GBC) [26]. We then obtain

$$\langle\varphi_k(1)\varphi_l(2)|\hat{w}_{12}^{\dagger}\hat{w}_{12}(\hat{f}_{12}-\varepsilon_i-\varepsilon_j)|\varphi_m(1)\varphi_n(2)\rangle \overset{GBC}{\approx} (\varepsilon_m+\varepsilon_n-\varepsilon_i-\varepsilon_j)X_{kl,mn}. \tag{5.27}$$

Concerning Ansatz **1**, we furthermore assume that the *extended* Brillouin condition (EBC) [26] is satisfied, that is, we assume that the orbital space is closed under the Fock operator. Then,

$$[\hat{f}_{12},(1-\hat{P}_1)(1-\hat{P}_2)] \overset{EBC}{\approx} 0, \tag{5.28}$$

and we obtain

$$\hat{w}_{12}^{\dagger}[\hat{f}_{12},\hat{w}_{12}] \overset{EBC}{\approx} \hat{w}_{12}^{\dagger}[\hat{f}_{12},r_{12}] = \hat{w}_{12}^{\dagger}[\hat{T}_1+\hat{T}_2,r_{12}]-\hat{w}_{12}^{\dagger}[\hat{K}_1+\hat{K}_2,r_{12}], \tag{5.29}$$

where $\hat{T}_1$ and $\hat{K}_1$ are the one-electron kinetic energy and exchange operators, respectively.

The ABS approximation can now be applied to the matrix elements over the commutator of r_{12} with the kinetic energy operator,

$$\begin{aligned}\hat{w}_{12}^{\dagger}[\hat{T}_1+\hat{T}_2,r_{12}] &\overset{ABS}{\approx} r_{12}[\hat{T}_1+\hat{T}_2,r_{12}]-r_{12}\hat{P}_1\hat{P}_2'\,[\hat{T}_1+\hat{T}_2,r_{12}] \\ &- r_{12}\hat{P}_1'\hat{P}_2\,[\hat{T}_1+\hat{T}_2,r_{12}]+r_{12}\hat{P}_1\hat{P}_2\,[\hat{T}_1+\hat{T}_2,r_{12}]. \end{aligned} \tag{5.30}$$

No further approximations are required, and the computation of the corresponding two-electron Gaussian integrals over $r_{12}[\hat{T}_1+\hat{T}_2,r_{12}]$ and $[\hat{T}_1+\hat{T}_2,r_{12}]$ is straightforward [38] when it is noted that

$$\tfrac{1}{2}r_{12}[\hat{T}_1+\hat{T}_2,r_{12}]+\tfrac{1}{2}[r_{12},\hat{T}_1+\hat{T}_2]r_{12} = \tfrac{1}{2}[r_{12},[\hat{T}_1+\hat{T}_2,r_{12}]] = 1. \tag{5.31}$$

The matrix elements over the commutator of r_{12} with the exchange operator are more difficult, however. In the present work, we suggest to approximate these integrals by first inserting the ABS approximation into $\hat{w}_{12}^{\dagger}$,

$$\begin{aligned}\hat{w}_{12}^{\dagger}[\hat{K}_1+\hat{K}_2,r_{12}] &\overset{ABS}{\approx} r_{12}[\hat{K}_1+\hat{K}_2,r_{12}]-r_{12}\hat{P}_1\hat{P}_2'\,[\hat{K}_1+\hat{K}_2,r_{12}] \\ &- r_{12}\hat{P}_1'\hat{P}_2\,[\hat{K}_1+\hat{K}_2,r_{12}]+r_{12}\hat{P}_1\hat{P}_2\,[\hat{K}_1+\hat{K}_2,r_{12}], \end{aligned} \tag{5.32}$$

and subsequently, by inserting the ABS approximation into the two-electron integrals over the operators $r_{12}[\hat{K}_1 + \hat{K}_2, r_{12}]$ and $[\hat{K}_1 + \hat{K}_2, r_{12}]$, where needed. This yields

$$\begin{aligned}\langle\varphi_k(1)\varphi_l(2)|\hat{w}_{12}^\dagger\,\hat{K}_1\,r_{12}|\varphi_m(1)\varphi_n(2)\rangle \;&\overset{ABS}{\approx}\; \sum_{p'q'r'} r_{kl}^{p'q'}\,K_{p'}^{r'}\,r_{r'q'}^{mn} - \sum_{pq'r'} r_{kl}^{pq'}\,K_{p}^{r'}\,r_{r'q'}^{mn} \\ &-\; \sum_{p'qr'} r_{kl}^{p'q}\,K_{p'}^{r'}\,r_{r'q}^{mn} + \sum_{pqr'} r_{kl}^{pq}\,K_{p}^{r'}\,r_{r'q}^{mn} \end{aligned} \tag{5.33}$$

and

$$\langle\varphi_k(1)\varphi_l(2)|\hat{w}_{12}^\dagger\,r_{12}\,\hat{K}_1|\varphi_m(1)\varphi_n(2)\rangle \overset{ABS}{\approx} \sum_{r'} X_{kl,r'n}K_{r'}^m, \tag{5.34}$$

where

$$K_p^q = \langle\varphi_p(1)|\hat{K}_1|\varphi_q(1)\rangle, \qquad r_{pq}^{rs} = \langle\varphi_p(1)\varphi_q(2)|r_{12}|\varphi_r(1)\varphi_s(2)\rangle. \tag{5.35}$$

5.2.5 Working equations for Ansatz 2

The working equations for Ansatz **2** are very similar to those for Ansatz **1**. In an obvious manner, the ABS approximation yields

$$\hat{w}_{12}^\dagger g_{12} \;\overset{ABS}{\approx}\; 1 - r_{12}\hat{O}_1\hat{P}_2' g_{12} - r_{12}\hat{P}_1'\hat{O}_2 g_{12} + r_{12}\hat{O}_1\hat{O}_2 g_{12}, \tag{5.36}$$

$$\hat{w}_{12}^\dagger \hat{w}_{12} \;\overset{ABS}{\approx}\; r_{12}^2 - r_{12}\hat{O}_1\hat{P}_2' r_{12} - r_{12}\hat{P}_1'\hat{O}_2 r_{12} + r_{12}\hat{O}_1\hat{O}_2 r_{12}, \tag{5.37}$$

for the operator products $\hat{w}_{12}^\dagger g_{12}$ and $\hat{w}_{12}^\dagger \hat{w}_{12}$, respectively.

We again employ Eqs. (5.26) and (5.27) for the computation of the elements of the matrices $\mathbf{B}^{(ij)}$. In contrast to Ansatz **1**, however, we need not to satisfy the EBC to arrive at Eq. (5.29). Rather, it is sufficient to satisfy the GBC. Since, by virtue of the GBC,

$$[\hat{f}_{12}, (1-\hat{O}_1)(1-\hat{O}_2)] \overset{GBC}{\approx} 0, \tag{5.38}$$

we obtain

$$\hat{w}_{12}^\dagger[\hat{f}_{12}, \hat{w}_{12}] \overset{GBC}{\approx} \hat{w}_{12}^\dagger[\hat{f}_{12}, r_{12}] = \hat{w}_{12}^\dagger[\hat{T}_1 + \hat{T}_2, r_{12}] - \hat{w}_{12}^\dagger[\hat{K}_1 + \hat{K}_2, r_{12}]. \tag{5.39}$$

In the framework of the ABS approximation, the matrix elements involving the kinetic energy and exchange operators are computed according to

$$\begin{aligned}\hat{w}_{12}^\dagger[\hat{T}_1 + \hat{T}_2, r_{12}] \;&\overset{ABS}{\approx}\; r_{12}[\hat{T}_1 + \hat{T}_2, r_{12}] - r_{12}\hat{O}_1\hat{P}_2'\,[\hat{T}_1 + \hat{T}_2, r_{12}] \\ &-\; r_{12}\hat{P}_1'\hat{O}_2\,[\hat{T}_1 + \hat{T}_2, r_{12}] + r_{12}\hat{O}_1\hat{O}_2\,[\hat{T}_1 + \hat{T}_2, r_{12}], \end{aligned} \tag{5.40}$$

$$\begin{aligned}\langle\varphi_k(1)\varphi_l(2)|\hat{w}_{12}^{\dagger}\,\hat{K}_1\,r_{12}|\varphi_m(1)\varphi_n(2)\rangle \quad &\overset{ABS}{\approx} \quad \sum_{p'q'r'} r_{kl}^{p'q'}\,K_{p'}^{r'}\,r_{r'q'}^{mn} - \sum_{iq'r'} r_{kl}^{iq'}\,K_{i}^{r'}\,r_{r'q'}^{mn} \\ &- \quad \sum_{p'jr'} r_{kl}^{p'j}\,K_{p'}^{r'}\,r_{r'j}^{mn} + \sum_{ijr'} r_{kl}^{ij}\,K_{i}^{r'}\,r_{r'j}^{mn}, \end{aligned} \tag{5.41}$$

and

$$\langle\varphi_k(1)\varphi_l(2)|\hat{w}_{12}^{\dagger}\,r_{12}\,\hat{K}_1|\varphi_m(1)\varphi_n(2)\rangle \overset{ABS}{\approx} \sum_{r'} X_{kl,r'n}K_{r'}^{m}. \tag{5.42}$$

Eq. (5.42) differs from Eq. (5.34) only by the matrix $\mathbf{X}$, which contains integrals over the operator of Eq. (5.25) in Ansatz **1** but over the operator of Eq. (5.37) in Ansatz **2**.

In Ansatz **2**, also matrix elements $C_{kl,ab}^{(ij)}$ occur [Eq. (5.15)]. By virtue of the GBC, we obtain

$$\begin{aligned} C_{kl,ab}^{(ij)} \quad &\overset{GBC}{\approx} \quad \langle\varphi_k(1)\varphi_l(2)|[r_{12},\hat{f}_{12}]|\varphi_a(1)\varphi_b(2)\rangle + (\varepsilon_k+\varepsilon_l-\varepsilon_i-\varepsilon_j)r_{kl}^{ab} \\ &\overset{ABS}{\approx} \quad \langle\varphi_k(1)\varphi_l(2)|[r_{12},\hat{T}_1+\hat{T}_2]|\varphi_a(1)\varphi_b(2)\rangle + (\varepsilon_k+\varepsilon_l-\varepsilon_i-\varepsilon_j)r_{kl}^{ab} \\ &+ \quad \sum_{p'}(K_k^{p'}\,r_{p'l}^{ab} - r_{kl}^{p'b}K_{p'}^{a}) + \sum_{q'}(K_l^{q'}\,r_{kq'}^{ab} - r_{kl}^{aq'}\,K_{q'}^{b}). \end{aligned} \tag{5.43}$$

Although not necessary, one could at this point go one step further and assume that the EBC holds, that is, that the virtual orbitals are eigenfunctions of the Fock operator. Then, the $C_{kl,ab}^{(ij)}$ coupling elements simplify to

$$C_{kl,ab}^{(ij)} \overset{EBC}{\approx} (\varepsilon_a+\varepsilon_b-\varepsilon_i-\varepsilon_j)r_{kl}^{ab}. \tag{5.44}$$

Following Ref. [35], we shall attach an asterisk to the method's acronym when we utilize Eq. (5.44). Approach **2*** thus differs from approach **2** by using Eq. (5.44) instead of Eq. (5.43). We obtain for approach **2***

$$\tilde{V}_{kl}^{(ij)}(\mathbf{2^*}) \quad \overset{EBC}{\approx} \quad V_{kl}^{(ij)} - \sum_{ab} r_{kl}^{ab}\langle\varphi_a(1)\varphi_b(2)|g_{12}|\varphi_i(1)\varphi_j(2)\rangle, \tag{5.45}$$

$$\tilde{B}_{kl,mn}^{(ij)}(\mathbf{2^*}) \quad \overset{EBC}{\approx} \quad B_{kl,mn}^{(ij)} - \tfrac{1}{2}\sum_{ab} r_{kl}^{ab}C_{ab,mn}^{(ij)} - \tfrac{1}{2}\sum_{ab} r_{mn}^{ab}C_{ab,kl}^{(ij)}. \tag{5.46}$$

Concerning Eq. (5.12), we emphasize that only the matrix elements $C_{kl,ab}^{(ij)}$ are approximated according to Eq. (5.44), whereas the elements $C_{ab,mn}^{(ij)}$ are not, and care must be taken to symmetrize the matrices $\tilde{\mathbf{B}}^{(ij)}$ (this symmetrization is carried out by adding the corresponding two terms with weights of $1/2$ each). This seems a somewhat inconsistent approach. The only reason for proceeding in this manner, however, is that we wish to define such ABS-based A and B methods that reduce to the previous approximations A and B of the original MP2-R12 work when the orbital basis $\{\varphi_p(1)\}_{p=1,\ldots,N}$ is employed as auxiliary basis. Also Ansatz **1** reduces to the original MP2-R12 work when the orbital and auxiliary basis sets are identical.

One could speak of a **2**** approach when also the $C^{(ij)}_{ab,mn}$ matrix elements in Eq. (5.46) were approximated according to Eq. (5.44), but this **2**** approach is not considered in the present article. Since the **2*** simplification is already unnecessary from a computational point of view (the approach is only briefly mentioned in the present work), we have chosen not to pursue the hypothetical **2**** form at all.

5.3 Computer implementation

The new MP2-R12 methods **1**, **2**, and **2*** have been implemented into a local version of the DALTON program [39], partly by modifying and extending the code developed by Koch and co-workers for the integral-direct transformation of two-electron integrals from the AO basis into the basis of molecular orbitals [40–42].

When discussing the computer implementation, we shall introduce the approximations A, A′, and B. In approximation B, all matrix elements are evaluated as indicated in Sections 5.2.4 and 5.2.5. Hence, approximation B includes no other approximations than the resolution-of-identity in terms of the auxiliary basis set. The approximations A and A′ have been described in some detail in Ref. [43] and include additional approximations concerned with the neglect of certain integrals. In approximation A′, all terms are neglected that involve the exchange operator. Thus, Eqs. (5.33) and (5.34) are neglected for Ansatz **1**, and similarly, Eqs. (5.41) and (5.42) for Ansatz **2**. In addition to the terms that are neglected in approximation A′, also Eq. (5.27) is neglected in approximation A. This term is usually much smaller than the first two terms on the right-hand side of Eq. (5.26).

5.3.1 Implementation of Ansatz 1

All variants of MP2-R12 theory start with the computation of the following six types of integrals:

$$g_{ij}^{pq}, \qquad g_{ij}^{pq'}, \qquad r_{ij}^{pq}, \qquad r_{ij}^{pq'}, \qquad t_{ij}^{pq}, \qquad t_{ij}^{pq'}, \tag{5.47}$$

where r_{pq}^{rs} is given by Eq. (5.35), and

$$g_{pq}^{rs} = \langle\varphi_p(1)\varphi_q(2)|r_{12}^{-1}|\varphi_r(1)\varphi_s(2)\rangle, \tag{5.48}$$

$$t_{pq}^{rs} = \langle\varphi_p(1)\varphi_q(2)|[\hat{T}_1+\hat{T}_2, r_{12}]|\varphi_r(1)\varphi_s(2)\rangle. \tag{5.49}$$

It is important to note that only integrals with *one* auxiliary function at the most occur in Eq. (5.47). The computational effort of a calculation with n occupied orbitals, N orbital basis functions and N' auxiliary functions scales as nN^4 for the g_{ij}^{pq} integrals (as in conventional MP2 theory) and as $nN'N^3$ for the $g_{ij}^{pq'}$ integrals, and the computation time required for the six integrals of Eq. (5.47)

thus scales as $n(N+N')N^3$. With these six two-electron integrals available, as well as with the integrals

$$s_{pq}^{rs} = \langle\varphi_p(1)\varphi_q(2)|r_{12}^2|\varphi_r(1)\varphi_s(2)\rangle, \tag{5.50}$$

which factorize into products of one-electron integrals, we can construct all the matrices that are needed for the approximations A and A′ of R12 theory. For these approximations, the matrices $\mathbf{B}^{(ij)}$ are defined as [36, 43]

$$\begin{aligned} B_{kl,mn}^{(ij)}(\mathrm{A}) &= \tfrac{1}{2}(T_{kl,mn}+T_{mn,kl}), & (5.51)\\ B_{kl,mn}^{(ij)}(\mathrm{A}') &= B_{kl,mn}^{(ij)}(\mathrm{A}) + \tfrac{1}{2}(\varepsilon_k+\varepsilon_l+\varepsilon_m+\varepsilon_n-2\varepsilon_i-2\varepsilon_j)X_{kl,mn}. & (5.52)\end{aligned}$$

Note that the matrices $\mathbf{B}^{(ij)}(\mathrm{A})$ and $\mathbf{B}^{(ij)}(\mathrm{A}')$ differ only by form of Eq. (5.27) (in symmetrized form), which is neglected in approximation A. The vectors $\mathbf{V}^{(ij)}$ and intermediates $\mathbf{X}$ and $\mathbf{T}$ are computed as

$$\begin{aligned} V_{kl}^{(ij)} &= \delta_k^i\delta_l^j - \sum_{pq'}(r_{kl}^{pq'}g_{pq'}^{ij} + r_{lk}^{pq'}g_{pq'}^{ji}) + \sum_{pq} r_{kl}^{pq}g_{pq}^{ij}, & (5.53)\\ X_{kl,mn} &= s_{kl}^{mn} - \sum_{pq'}(r_{kl}^{pq'}r_{pq'}^{mn} + r_{lk}^{pq'}r_{pq'}^{nm}) + \sum_{pq} r_{kl}^{pq}r_{pq}^{mn}, & (5.54)\\ T_{kl,mn} &= \delta_k^m\delta_l^n - \sum_{pq'}(r_{kl}^{pq'}t_{pq'}^{mn} + r_{lk}^{pq'}t_{pq'}^{nm}) + \sum_{pq} r_{kl}^{pq}t_{pq}^{mn}. & (5.55)\end{aligned}$$

For approximation B, we also need two-electron integrals that involve *two* orbitals of the auxiliary basis. Namely, in this approximation, we must compute the $\mathbf{B}^{(ij)}$ matrices according to

$$B_{kl,mn}^{(ij)}(\mathrm{B}) = B_{kl,mn}^{(ij)}(\mathrm{A}') + \tfrac{1}{2}(Q_{kl,mn}+Q_{mn,kl}) - \tfrac{1}{2}(P_{kl,mn}+P_{mn,kl}). \tag{5.56}$$

The matrix elements $Q_{kl,mn}$ represent the integrals that also occur in the original MP2-R12/B work, while the matrix elements $P_{kl,mn}$ only occur in the ABS-based approach. When the orbital and auxiliary sets are identical, the matrix elements $P_{kl,mn}$ all vanish. The elements $Q_{kl,mn}$ follow from Eq. (5.34) while the elements $P_{kl,mn}$ follow from Eq. (5.33).

The matrix elements $Q_{kl,mn}$ are most efficiently computed by introducing intermediate orbitals $\varphi_{m^*}(1)$ that are defined as

$$\varphi_{m^*}(1) = \sum_{r'}\varphi_{r'}(1)\,K_{r'}^m. \tag{5.57}$$

In terms of these orbitals, the matrix elements $Q_{kl,mn}$ are given by

$$\begin{aligned} Q_{kl,mn} &= s_{kl}^{m^*n} - \sum_{pq'}(r_{kl}^{pq'}r_{pq'}^{m^*n} + r_{lk}^{pq'}r_{pq'}^{nm^*}) + \sum_{pq} r_{kl}^{pq}r_{pq}^{m^*n}\\ &+ s_{kl}^{mn^*} - \sum_{pq'}(r_{kl}^{pq'}r_{pq'}^{mn^*} + r_{lk}^{pq'}r_{pq'}^{n^*m}) + \sum_{pq} r_{kl}^{pq}r_{pq}^{mn^*} = X_{kl,m^*n} + X_{kl,mn^*}. \end{aligned} \tag{5.58}$$

Relative to approximations A and A′, the essential extra work required for approximation B consists of the computation of the two-electron integrals $r^{pq'}_{m^*n}$, $r^{pq'}_{mn^*}$, $r^{pq}_{m^*n}$, and $r^{pq}_{mn^*}$. The computation time for this step of the calculation scales as $n(N+N')N'N^2$.

As already mentioned, the ABS approximation enables the evaluation of the integrals of Eq. (5.33). In our current implementation, these integrals are computed by choosing the orthonormal auxiliary basis such that the exchange matrix becomes diagonal in that space,

$$K^{q'}_{p'} = \delta^{q'}_{p'}\lambda_{p'}. \tag{5.59}$$

Then, the following four intermediates are computed:

$$p^{mn}_{p'q'} = (\lambda_{p'} + \lambda_{q'})r^{mn}_{p'q'}, \tag{5.60}$$

$$p^{mn}_{p'q} = \lambda_{p'}r^{mn}_{p'q} + \sum_{r'} K^{r'}_{q} r^{mn}_{p'r'}, \tag{5.61}$$

$$p^{mn}_{pq'} = \lambda_{q'}r^{mn}_{pq'} + \sum_{r'} K^{r'}_{p} r^{mn}_{r'q'}, \tag{5.62}$$

$$p^{mn}_{pq} = \sum_{r'} (K^{r'}_{p} r^{mn}_{r'q} + K^{r'}_{q} r^{mn}_{pr'}), \tag{5.63}$$

from which the matrix elements $P_{kl,mn}$ are obtained as

$$P_{kl,mn} = \sum_{p'q'} r^{p'q'}_{kl} p^{mn}_{p'q'} - \sum_{pq'} r^{pq'}_{kl} p^{mn}_{pq'} - \sum_{p'q} r^{p'q}_{kl} p^{mn}_{p'q} + \sum_{pq} r^{pq}_{kl} p^{mn}_{pq}. \tag{5.64}$$

Two-electron integrals must be computed that involve *two* functions of the auxiliary basis, both for the matrix representation of the exchange operator in the auxiliary basis ($K^{q'}_{p'}$) and for the $r^{p'q'}_{kl}$ integrals. The corresponding computation times scale as $(N')^2N^2$ and $n(N')^2N^2$, respectively.

5.3.2 Implementation of Ansatz 2

Assuming that the integrals of Eq. (5.47) are available, we can compute

$$V^{(ij)}_{kl} = \delta^i_k\delta^j_l - \sum_{mq'} (r^{mq'}_{kl} g^{ij}_{mq'} + r^{mq'}_{lk} g^{ji}_{mq'}) + \sum_{mn} r^{mn}_{kl} g^{ij}_{mn}, \tag{5.65}$$

$$X_{kl,mn} = s^{mn}_{kl} - \sum_{iq'} (r^{iq'}_{kl} r^{mn}_{iq'} + r^{iq'}_{lk} r^{nm}_{iq'}) + \sum_{ij} r^{ij}_{kl} r^{mn}_{ij}, \tag{5.66}$$

$$T_{kl,mn} = \delta^m_k\delta^n_l - \sum_{iq'} (r^{iq'}_{kl} t^{mn}_{iq'} + r^{iq'}_{lk} t^{nm}_{iq'}) + \sum_{ij} r^{ij}_{kl} t^{mn}_{ij}, \tag{5.67}$$

as well as

$$C^{(ij)}_{kl,ab}(\mathrm{A}) = = -t^{ab}_{kl}, \tag{5.68}$$

$$C^{(ij)}_{kl,ab}(\mathrm{A}') = C^{(ij)}_{kl,ab}(\mathrm{A}) + (\varepsilon_k + \varepsilon_l - \varepsilon_i - \varepsilon_j) r^{ab}_{kl}. \tag{5.69}$$

We also need integrals of the type $r^{ab}_{kl^*}$ to compute

$$C^{(ij)}_{kl,ab}(\mathrm{B}) = C^{(ij)}_{kl,ab}(\mathrm{A}') + r^{ab}_{k^*l} + r^{ab}_{kl^*} - \sum_{r'}(r^{r'b}_{kl}K^a_{r'} + r^{ar'}_{kl}K^b_{r'}). \tag{5.70}$$

Hence, for the above quantities, we need two-electron integrals with only *one* auxiliary function, and no more integrals are needed for the approximations A and A′. For the more elaborate B approximation, however, we must compute two-electron integrals with *two* auxiliary functions. Namely, we need to evaluate the quantities

$$Q_{kl,mn} = X_{kl,m^*n} + X_{kl,mn^*} \tag{5.71}$$

$$P_{kl,mn} = \sum_{p'q'} r^{p'q'}_{kl}p^{mn}_{p'q'} - \sum_{iq'} r^{iq'}_{kl}p^{mn}_{iq'} - \sum_{p'j} r^{p'j}_{kl}p^{mn}_{p'j} + \sum_{ij} r^{ij}_{kl}p^{mn}_{ij}, \tag{5.72}$$

which contribute to the matrix $\mathbf{B}^{(ij)}(\mathrm{B})$,

$$B^{(ij)}_{kl,mn}(\mathrm{A}) = \tfrac{1}{2}(T_{kl,mn} + T_{mn,kl}), \tag{5.73}$$

$$B^{(ij)}_{kl,mn}(\mathrm{A}') = B^{(ij)}_{kl,mn}(\mathrm{A}) + \tfrac{1}{2}(\varepsilon_k + \varepsilon_l + \varepsilon_m + \varepsilon_n - 2\varepsilon_i - 2\varepsilon_j)X_{kl,mn}, \tag{5.74}$$

$$B^{(ij)}_{kl,mn}(\mathrm{B}) = B^{(ij)}_{kl,mn}(\mathrm{A}') + \tfrac{1}{2}(Q_{kl,mn} + Q_{mn,kl}) - \tfrac{1}{2}(P_{kl,mn} + P_{mn,kl}). \tag{5.75}$$

Finally, for approximation $\xi = \mathrm{A}$, A′, or B, the vectors $\tilde{\mathbf{V}}^{(ij)}(\xi)$ and matrices $\tilde{\mathbf{B}}^{(ij)}(\xi)$ are computed as

$$\tilde{V}^{(ij)}_{kl}(\xi) = V^{(ij)}_{kl} - \sum_{ab}\frac{C^{(ij)}_{kl,ab}(\mathrm{B})}{\varepsilon_a + \varepsilon_b - \varepsilon_i - \varepsilon_j}g^{ij}_{ab}, \tag{5.76}$$

$$\tilde{B}^{(ij)}_{kl,mn}(\xi) = B^{(ij)}_{kl,mn}(\xi) - \tfrac{1}{2}\sum_{ab}\frac{C^{(ij)}_{kl,ab}(\mathrm{B})C^{(ij)}_{ab,mn}(\xi) + C^{(ij)}_{mn,ab}(\mathrm{B})C^{(ij)}_{ab,kl}(\xi)}{\varepsilon_a + \varepsilon_b - \varepsilon_i - \varepsilon_j}. \tag{5.77}$$

Note that the full coupling matrix of approach B, that is, $\mathbf{C}^{(ij)}(\mathrm{B})$, occurs in Eqs. (5.76) and (5.77), not only in approach B itself, but also in the approximations A and A′. Computationally, almost nothing is gained by neglecting certain terms in $\mathbf{C}^{(ij)}$. They are nonetheless neglected in the $\mathbf{C}^{(ij)}(\xi)$ matrix of Eq. (5.77) in an effort to remain consistent with previous R12 work. This becomes clear when we consider the **2*** approach. In this approach, the $C^{(ij)}_{kl,ab}(\mathrm{B})$ are replaced by the integrals r^{ab}_{kl},

$$\tilde{V}^{(ij)}_{kl}(\xi\text{*}) = V^{(ij)}_{kl} - \sum_{ab} r^{ab}_{kl}g^{ij}_{ab}, \tag{5.78}$$

$$\tilde{B}^{(ij)}_{kl,mn}(\xi\text{*}) = B^{(ij)}_{kl,mn}(\xi) - \tfrac{1}{2}\sum_{ab} r^{ab}_{kl}C^{(ij)}_{ab,mn}(\xi) - \tfrac{1}{2}\sum_{ab} r^{ab}_{mn}C^{(ij)}_{ab,kl}(\xi). \tag{5.79}$$

Due to the A and A′ approximations in the matrix elements $C^{(ij)}_{ab,mn}(\xi)$, the approach **2*** corresponds exactly to the original MP2-R12/A and MP2-R12/A′ methods when the orbital and auxiliary basis sets are identical.

5.4 Overview of MP2-R12 approaches

An overview of the new MP2-R12 approaches is presented in Table 5.1.

It is assumed in all methods that the *generalized* Brillouin condition (GBC) holds. This condition is basically satisfied in an AO basis of near Hartree–Fock-limit quality. The *extended* Brillouin condition (EBC), which is much more difficult to satisfy than the GBC, needs only to be satisfied for Ansatz **1**. The EBC is not needed at all for Ansatz **2** and the approach transforms into the **2*** method when the EBC is nonetheless assumed to hold.

Approximation A (including A′) is characterized by the neglect of the commutator between the

Table 5.1: Overview of MP2-R12 approaches.

Approach		GBC used?[a]	EBC used?[b]	$[\hat{K}_1 + \hat{K}_2, r_{12}]$ neglected?[c]	$L'_{\max}$[d]	Computing time[e]	Without ABS[f]
1	A	Yes	Yes	Yes	$L_{\max} + 2L_{\mathrm{occ}}$	$n(N+N')N^3$	A
	A′	Yes	Yes	Yes	$L_{\max} + 2L_{\mathrm{occ}}$	$n(N+N')N^3$	A′
	B	Yes	Yes	No	∞	$n(N+N')^2N^2$	B
2	A	Yes	No	Yes	$\max(L_{\max}, 3L_{\mathrm{occ}})$	$n(N+N')N^3$	None[g]
	A′	Yes	No	Yes	$\max(L_{\max}, 3L_{\mathrm{occ}})$	$n(N+N')N^3$	None[g]
	B	Yes	No	No	∞	$n(N+N')^2N^2$	None[g]
2*	A	Yes	Yes	Yes	$3L_{\mathrm{occ}}$	$n(N+N')N^3$	A
	A′	Yes	Yes	Yes	$3L_{\mathrm{occ}}$	$n(N+N')N^3$	A′
	B	Yes	Yes	No	∞	$n(N+N')^2N^2$	B

[a] Is the generalized Brillouin condition assumed to be satisfied?

[b] Is the extended Brillouin condition assumed to be satisfied?

[c] Are the $[\hat{K}_1 + \hat{K}_2, r_{12}]$ matrix elements neglected?

[d] $L'_{\max}$ is the angular momentum quantum number after which the auxiliary basis can be truncated in an atomic calculation where L_{occ} is the highest occupied angular momentum and $L_{\max}$ is the highest angular momentum of the orbital basis.

[e] n is the number of occupied Hartree–Fock orbitals, N is the number of orbital basis functions, and N' is the number of auxiliary basis functions.

[f] Previous MP2-R12 method to which the new approach reduces when no auxiliary basis set is used.

[g] There is no previous MP2-R12 method that corresponds to this variant.

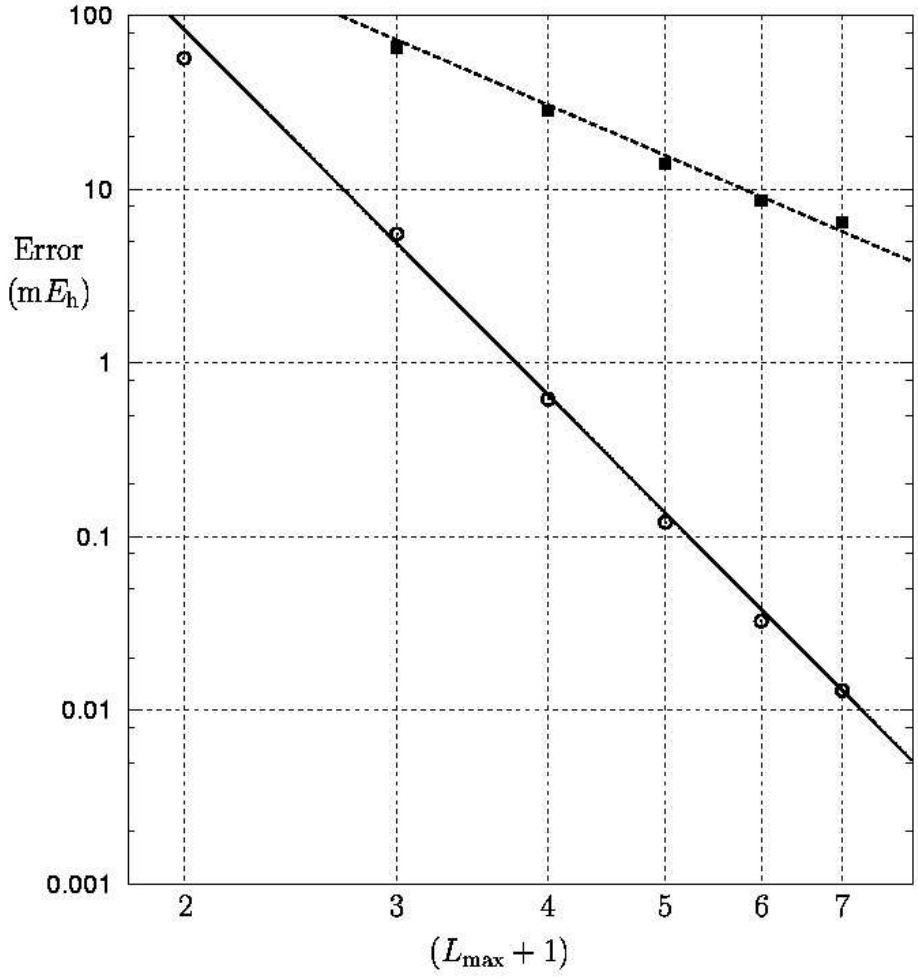

Figure 5.1: Error in the all-electron second-order Møller-Plesset correlation energy of Ne as computed in subsets of the $20s14p11d9f7g5h3i$ basis. Comparison between the conventional MP2 (■) and the new MP2-R12/**2**B approach (○). The dashed and solid lines show $(L_{\max}+1)^{-3}$ and $(L_{\max}+1)^{-7}$ behavior, respectively.

exchange operators and the linear r_{12} term [43].

Furthermore, it is worthwhile to consider the maximum angular momentum quantum number $L'_{\max}$ of auxiliary basis functions that contribute to the matrix elements in an atomic calculation. Auxiliary basis functions with angular momentum greater than $L'_{\max}$ do not contribute. It is seen from Table 5.1 that the auxiliary basis sets do not truncate in approximation B. This is due to the matrices $\mathbf{P}$ in Eqs. (5.64) and (5.72). Numerically, these matrices contribute little to the final energies and their contributions converge quickly with the extension of the (auxiliary) basis set. If the $\mathbf{P}$ matrices were omitted, the maximum angular momentum value $L'_{\max}$ at which the RI can be

truncated would be the same for approximations B and A (or A′).

For the **2*** approach, it is found that $L'_{\max} = 3L_{\rm occ}$. In the **2** approach itself, auxiliary functions up to $L_{\max}$ (the highest angular momentum of the orbital basis) also contribute. This is due to the matrix elements $C^{(ij)}_{kl,ab}(\mathrm{B})$ in Eqs. (5.76) and (5.77), which are computed according to Eq. (5.70). Auxiliary functions up to $L_{\max}$ contribute to the last term (i.e., the sum over r') in that equation. For Ansatz **1**, the maximum angular momentum value of the auxiliary basis is $L'_{\max} = L_{\max} + 2L_{\rm occ}$ rather than $3L_{\rm occ}$ as the R12 functions are chosen strongly orthogonal to orbital pairs of the full orbital basis and not only to the occupied space.

Concerning the computational effort of the new MP2-R12 calculations, it is important to realize that calculations carried out in approximation A (including A′) scale only linear with the number N' of auxiliary functions. When approximation B is used, however, the computation time grows quadratically with N'. The MP2-R12/B methods are thus significantly more time-consuming than the MP2-R12/A and MP2-R12/A′ methods when $N' >> N$. If, on the other hand, the orbital and auxiliary basis sets are identical (as in the original MP2-R12 work) or similar in size with $N' \approx N$, then the MP2-R12/B method is only ca. 30% more expensive than MP2-R12/A or MP2-R12/A′.

Finally, Table 5.1 also indicates that Ansatz **1** transforms into the original MP2-R12 approach when the orbital basis set is used for the RI approximation. Ansatz **2** does not transform into any previous method, but its **2*** variant has been chosen such that it, too, transforms into the original MP2-R12 approach.

Table 5.2: All-electron Møller-Plesset second-order energies ($E^{(2)}$ in m$E_{\rm h}$) of the Ne atom.

		Original method		New Ansatz **1**		New Ansatz **2**	
Basis[a]	MP2[b]	R12/A′	R12/B	R12/A′	R12/B	R12/A′	R12/B
sp	-191.99	-688.49	-506.95	-361.84	-330.37	-362.45	-331.33
spd	-322.27	-408.78	-395.11	-361.97	-358.19	-390.71	-382.59
$spdf$	-359.84	-389.71	-387.19	-376.20	-375.30	-389.76	-387.49
$spdfg$	-374.12	-388.62	-387.89	-383.27	-382.95	-388.67	-387.99
$spdfgh$	-379.46	-388.29	-388.01	-386.13	-385.97	-388.35	-388.07
$spdfghi$	-381.65	-388.19	-388.04	-387.69	-387.56	-388.24	-388.09

[a] Subsets of the $20s14p11d9f7g5h3i$ basis. The $32s24p18d15f12g9h6i$ basis was applied as auxiliary basis in all calculations.

[b] Conventional all-electron MP2 energy.

5.5 Numerical results: The Ne atom

Calculations have been performed in subsets of a Gaussian basis set of the type $20s14p11d9f7g5h$-$3i$. Its $20s14p11d9f7g5h$ subset is given in full detail in Ref. [35], and three sets of i-type Gaussians with exponents 6.454503, 3.202905, and 1.567200 have been added to form the $20s14p11d$-$9f7g5h3i$ basis. In conjunction with this basis, an auxiliary basis of the form $32s24p18d15f12g$-$9h6i$ has been employed. Its $32s$ ($n_0 = 32$) and $24p$ ($n_1 = 24$) sets are even-tempered sets of the form $0.005 \times 3^{(k-1)/2}$ for $k = 1, \ldots, n_\ell$ while the exponents of the d- ($\ell = 2$) through i-sets ($\ell = 6$) are given by the expression $(0.002\ell + 0.003) \times 3^{(k+\ell-1)/2}$ for $k = 1, \ldots, n_\ell$.

Table 5.2 shows the all-electron second-order correlation energies of Ne that are obtained in the subsets $20s14p$, $20s14p11d$, $20s14p11d9f$, and so on, by means of conventional MP2 calculations, the original MP2-R12 method, and by means of the new Ansätze **1** and **2**. In the sp subset, the original MP2-R12 energies are clearly not variational. In approximations A′ and B, energies of -688.5 mE_h and -506.95 mE_h are obtained, respectively, which are much too low. This behavior is the result of using the $20s14p$ orbital basis for the RI approximation in these original MP2-R12 calculations, and is not observed when the large auxiliary basis set is employed.

Table 5.3: Møller-Plesset second-order pair energies ($E^{(2)}$ in mE_h) of the Ne atom as computed by Ansatz **2**, in approximation B, in subsets of the $20s14p11d9f7g5h3i$ basis (using the auxiliary basis $32s24p18d15f12g9h6i$).

Pair	sp	spd	$spdf$	$spdfg$	$spdfgh$	$spdfghi$	Ref. [35]
$1s^2$ (^1S)	-40.140	-40.243	-40.252	-40.252	-40.252	-40.252	-40.252
$1s2s$ (^1S)	-3.831	-3.956	-3.971	-3.973	-3.974	-3.974	-3.974
$1s2s$ (^3S)	-1.534	-1.578	-1.582	-1.582	-1.582	-1.582	-1.582
$2s^2$ (^1S)	-11.906	-12.023	-12.036	-12.038	-12.039	-12.039	-12.038
$1s2p$ (^1P)	-3.631	-7.750	-8.132	-8.171	-8.176	-8.177	-8.176
$1s2p$ (^3P)	-10.636	-13.777	-13.901	-13.909	-13.910	-13.910	-13.911
$2s2p$ (^1P)	-46.566	-59.526	-60.341	-60.453	-60.476	-60.482	-60.472
$2s2p$ (^3P)	-21.732	-26.557	-26.694	-26.706	-26.708	-26.708	-26.708
$2p^2$ (^1S)	-45.286	-45.503	-45.550	-45.566	-45.571	-45.573	-45.565
$2p^2$ (^3P)	-82.192	-87.108	-87.317	-87.337	-87.340	-87.340	-87.341
$2p^2$ (^1D)	-63.874	-84.570	-87.714	-87.999	-88.047	-88.057	-88.042
Total	-331.33	-382.59	-387.49	-387.99	-388.07	-388.09	-388.06

Table 5.4: Møller-Plesset second-order energies ($E^{(2)}$ in mE_h) of the Ne atom.

Pair	Ref. [44]	Ref. [45]	Ref. [46]	Ref. [47]		Ref. [35]	This work
	Extrap.[a]	Extrap.[b]	Extrap.[c]	Calc.[d]	Extrap.[e]	Calc.[f]	Calc.[g]
$1s^2$	-40.24	-40.22	-40.25	-40.229	-40.255	-40.252	-40.252
$1s2s$	-5.55	-5.56	-5.55	-5.555	-5.557	-5.556	-5.556
$2s^2$	-12.05	-12.02	-12.02	-12.003	-12.037	-12.038	-12.039
$1s2p$	-22.16	-22.17	-22.06	-22.078	-22.094	-22.087	-22.087
$2s2p$	-87.30	-87.15	-87.10	-86.982	-87.188	-87.180	-87.190
$2p^2$	-221.01	-220.80	-220.81	-220.686	-220.973	-220.948	-220.970
Total	-388.3	-387.9	-387.8	-387.53	-388.11	-388.06	-388.09

[a] With extrapolation for $\ell > 6$.

[b] With extrapolation for $\ell > 9$.

[c] Recommended values from R12 calculations and extrapolations.

[d] Calculated with $\ell \leq 12$.

[e] With extrapolation for $\ell > 12$.

[f] Calculated in the $20s14p11d9f7g5h$ basis.

[g] Calculated by the new MP2-R12/**2**B method in the $20s14p11d9f7g5h3i$ orbital basis in conjunction with the $32s24p18d15f12g9h6i$ auxiliary basis.

Table 5.5: Exponents of Gaussian basis functions.

	C	N	O	F	Ne
d	126.0	194.0	230.0	292.0	369.0
	55.0	83.8	100.0	127.0	161.0
f	24.1	37.2	61.6	88.9	123.0
	11.5	17.4	27.4	39.1	53.9
g	12.9	19.8	29.5	39.4	49.8
	5.84	8.74	12.4	16.3	20.4
h	4.84	7.06	10.0	13.4	17.4

Furthermore, Ansatz **2** appears to be clearly superior to Ansatz **1**.

In approximation **2**A′, there is a tendency to overshoot the magnitude of the correlation energy due to the neglect of exchange terms, and the results appear to converge from below towards the basis-set limit. The MP2-R12/**2**B energies converge from above, and the convergence is rapid in both cases. Figure 5.1, which depicts the error of the computed MP2 energy with respect to an estimated basis-set limit energy of -388.107 mE_h, compares the convergence of the MP2-R12/**2**B approach with conventional MP2 calculations. It seems that the MP2-R12/**2**B results can be well described in terms of an $(L_\mathrm{max}+1)^{-7}$ dependence, which is a much faster convergence than the conventional $(L_\mathrm{max}+1)^{-3}$ behavior [48].

Table 5.3 displays the individual singlet and triplet pair energies of the MP2-R12/**2**B calculations shown in Table 5.2, in comparison with the results of Ref. [35]. In the work of Wind et al. [35], the same $20s14p11d9f7g5h$ was used as in the present work, three-electron integrals were evaluated exactly (i.e., without RI approximation), but the wave function Ansatz was slightly different from the present work (i.e., not orbital-invariant [36]). Nevertheless, the agreement between the results of Ref. [35] and the column under $spdfgh$ is striking—the maximum deviation is only 6 μE_h. In view of this excellent agreement, we are confident that our MP2-R12/**2**B pair energies in the $20s14p11d9f7g5h3i$ basis are the most accurate, directly computed Ne pair energies to date.

A comparison between our present calculations and selected literature data [44–47] is presented in Table 5.4. Our results agree closely (to within 7 μE_h) with the accurate but extrapolated pair energies of Flores [47]. It is remarkable that a calculation in terms of a partial-wave expansion with partial waves up to $\ell = 12$ is in error by ca. 0.6 mE_h and that an extrapolation for $\ell > 12$ is needed to improve the accuracy to the microhartree level [47, 49]. The new MP2-R12/**2**B approach yields this level of accuracy without the need for extrapolations.

5.6 Numerical results: Molecules

5.6.1 Geometries and basis sets

All molecular structures were kept fixed throughout the present study. These fixed structures correspond to equilibrium geometries that were optimized at the CCSD(T)(FULL)/cc-pCVQZ level (FULL means that all electrons were correlated). They were taken from Ref. [50] and are identical to the structures used in Refs. [51, 52].

The (augmented) polarized valence correlation-consistent basis sets (aug-)cc-pVXZ are used as orbital basis [53–59] when only the valence shell is correlated, in conjunction with the auxiliary basis $19s14p8d6f4g3h2i$ for C, N, O, F, and Ne and $9s6p4d3f2g$ for H. The latter sets for C, N, O, F, and Ne were obtained by adding the two i-type sets of the aug-cc-pV6Z basis to the basis

sets of Ref. [51]. For H, the two g-type sets of the aug-cc-pV5Z basis were added to the basis set of Ref. [51].

The (augmented) polarized core–valence correlation-consistent basis sets (aug-)cc-pCVXZ are used as orbital basis [57, 59] when all orbitals are correlated, in conjunction with the auxiliary basis $19s14p10d8f6g4h2i$ for C, N, O, F, and Ne and $9s6p4d3f2g$ for H. These auxiliary basis sets for all-electron correlated calculations were obtained from the above-mentioned auxiliary basis sets for valence shell correlated calculations by adding d-, f-, g-, and h-type Gaussians. The exponents of these Gaussians are given in Table 5.5.

5.6.2 Results

The results of the calculations on small molecules are collected in Table 5.6 (valence-shell correlation in cc-pVXZ basis sets), Table 5.7 (valence-shell correlation in aug-cc-pVXZ basis sets), Table 5.8 (all-electron correlation in cc-pCVXZ basis sets), and Table 5.9 (all-electron correlation in aug-cc-pCVXZ basis sets). For the NH_3 molecule, the calculations in the cc-pV6Z, aug-cc-pV6Z, and aug-cc-pCV5Z basis were not feasible on the computer hardware currently available to us.

Again, we observe that Ansatz **2** is superior to Ansatz **1**, except for the largest basis sets (aug-)cc-pV6Z and (aug-)cc-pCV5Z. For these set, however, the differences are small.

As usual, the energies of approximation A$'$ are more negative than those of approximation B. Since the MP2-R12/A$'$ calculations in the correlation-consistent basis sets do not overshoot the magnitude of the second-order energy—as happened before in Section 5.5 for the Ne atom—the MP2-R12/A$'$ energies are found closer to the estimated basis-set limits than the MP2-R12/B results. Note, however, that this better agreement is to some extent fortuitous. It is based on a cancellation of errors, as certain matrix elements are neglected in approximations A and A$'$. No matrix elements are neglected in approximation B.

Table 5.10 summarizes the results of Tables 5.6 through 5.9 by reporting the percentage of the second-order Møller-Plesset correlation energy that is recovered by the various methods. See also Figures 5.2 and 5.3. Even in the largest basis sets, the conventional MP2 approach does not succeed in recovering more than 98% of the basis-set limit second-order energy, and it is clear from Figures 5.2 and 5.3 that it seems rather difficult to recover the remaining 2%.

With the MP2-R12 methods, this level of accuracy (98 %) is already reached in basis sets with cardinal number X=4 (valence-shell correlation) or X=3 (all-electron correlation). Concerning this comparison, it is noted that the computation time for these MP2-R12 calculations is significantly shorter than for the conventional MP2 calculations in the (aug-)cc-pV6Z and (aug-)cc-pCV5Z basis sets.

Table 5.6: Valence-shell Møller-Plesset second-order correlation energies ($E^{(2)}$ in mE_h) of the Ne atom and some small molecules as computed by the new MP2-R12 method in the correlation-consistent basis sets cc-pVXZ with $2 \leq X \leq 6$ (using the auxiliary basis $19s14p8d6f4g3h2i$ for C, N, O, F, and Ne and $9s6p4d3f2g$ for H).

Method	System[a]	X=2	X=3	X=4	X=5	X=6	Limit[b]
1A′	CH_2 ($^1A_1$)	-132.85	-147.82	-152.81	-154.72	-156.03	-155.9
	H_2O	-244.32	-279.10	-291.65	-297.33	-300.10	-300.5
	NH_3	-221.50	-249.21	-258.49	-262.39	n.a.[c]	-264.5
	HF	-254.09	-293.23	-308.33	-315.51	-318.80	-319.7
	N_2	-355.86	-395.27	-410.18	-416.71	-419.86	-421.0
	CO	-339.30	-377.99	-393.03	-399.61	-402.80	-403.9
	Ne	-249.16	-289.83	-306.54	-314.92	-318.70	-320.1
	F_2	-488.24	-561.95	-589.77	-603.23	-609.32	-611.7
2A′	CH_2 ($^1A_1$)	-145.24	-150.37	-153.83	-154.90	-155.43	-155.9
	H_2O	-272.08	-287.80	-295.38	-298.27	-299.49	-300.5
	NH_3	-242.80	-255.36	-261.11	-263.11	n.a.[c]	-264.5
	HF	-286.74	-303.57	-312.69	-316.50	-318.17	-319.7
	N_2	-390.28	-405.62	-415.38	-418.50	-419.96	-421.0
	CO	-374.40	-389.19	-398.58	-401.69	-402.98	-403.9
	Ne	-283.08	-300.51	-310.86	-315.66	-317.92	-320.1
	F_2	-553.51	-581.53	-598.70	-605.72	-608.92	-611.7
1B	CH_2 ($^1A_1$)	-128.79	-146.80	-152.37	-154.52	-155.89	-155.9
	H_2O	-236.85	-277.39	-290.66	-296.88	-299.88	-300.5
	NH_3	-215.72	-247.92	-257.82	-262.06	n.a.[c]	-264.5
	HF	-244.21	-290.98	-306.94	-314.96	-318.57	-319.7
	N_2	-347.43	-392.99	-408.76	-416.24	-419.60	-421.0
	CO	-330.65	-375.79	-391.80	-399.17	-402.55	-403.9
	Ne	-236.16	-287.00	-304.80	-314.30	-318.44	-320.1
	F_2	-469.28	-557.71	-587.15	-602.42	-608.88	-611.7
2B	CH_2 ($^1A_1$)	-135.69	-147.84	-152.81	-154.42	-155.17	-155.9
	H_2O	-256.02	-283.13	-293.44	-297.39	-299.05	-300.5
	NH_3	-229.11	-251.53	-259.60	-262.43	n.a.[c]	-264.5
	HF	-268.44	-297.95	-310.26	-315.39	-317.59	-319.7
	N_2	-372.17	-400.25	-412.97	-417.46	-419.44	-421.0
	CO	-355.50	-383.64	-396.24	-400.70	-402.49	-403.9
	Ne	-263.47	-294.35	-308.13	-314.41	-317.24	-320.1
	F_2	-518.79	-571.05	-594.05	-603.68	-607.88	-611.7

[a] Fixed geometries and reference energies were taken from Refs. [51, 52].

[b] Average of MP2-R12/A and MP2-R12/B energies from Refs. [51, 52].

[c] Not available.

Table 5.7: Valence-shell Møller-Plesset second-order correlation energies ($E^{(2)}$ in mE_h) of the Ne atom and some small molecules as computed by the new MP2-R12 method in the *augmented* correlation-consistent basis sets aug-cc-pVXZ with $2 \leq X \leq 6$ (same auxiliary basis as in Table 5.6).

Method	System[a]	X=2	X=3	X=4	X=5	X=6	Limit[b]
1A′	CH_2 ($^1A_1$)	-135.63	-149.23	-153.42	-155.07	-156.32	-155.9
	H_2O	-256.61	-283.92	-293.88	-298.29	-300.62	-300.5
	NH_3	-230.09	-252.70	-260.08	-263.11	n.a.[c]	-264.5
	HF	-267.54	-298.70	-310.79	-316.60	-319.52	-319.7
	N_2	-362.16	-398.94	-411.92	-417.68	-420.57	-421.0
	CO	-346.39	-381.21	-394.50	-400.47	-403.47	-403.9
	Ne	-260.48	-294.90	-308.59	-316.00	-319.46	-320.1
	F_2	-509.94	-570.97	-593.49	-605.19	-610.71	-611.7
2A′	CH_2 ($^1A_1$)	-147.25	-152.42	-154.74	-155.48	-155.75	-155.9
	H_2O	-278.56	-292.91	-297.90	-299.56	-300.09	-300.5
	NH_3	-248.15	-258.91	-262.76	-263.90	n.a.[c]	-264.5
	HF	-292.94	-310.47	-316.36	-318.49	-319.20	-319.7
	N_2	-392.43	-409.77	-417.16	-419.54	-420.40	-421.0
	CO	-376.37	-392.58	-399.97	-402.40	-403.28	-403.9
	Ne	-288.49	-309.31	-315.85	-318.59	-319.48	-320.1
	F_2	-560.14	-593.34	-604.64	-609.05	-610.55	-611.7
1B	CH_2 ($^1A_1$)	-132.61	-148.43	-153.08	-154.93	-156.21	-155.9
	H_2O	-251.04	-282.54	-293.16	-297.92	-300.40	-300.5
	NH_3	-225.75	-251.66	-259.63	-262.89	n.a.[c]	-264.5
	HF	-260.61	-296.96	-309.77	-316.17	-319.31	-319.7
	N_2	-355.28	-397.11	-410.72	-417.29	-420.34	-421.0
	CO	-339.63	-379.46	-393.53	-400.12	-403.25	-403.9
	Ne	-252.63	-292.94	-307.29	-315.52	-319.24	-320.1
	F_2	-497.19	-567.86	-591.47	-600.23	-610.29	-611.7
2B	CH_2 ($^1A_1$)	-141.03	-151.01	-154.25	-155.30	-155.66	-155.9
	H_2O	-269.05	-290.36	-296.89	-299.14	-299.89	-300.5
	NH_3	-239.87	-256.88	-262.06	-263.62	n.a.[c]	-264.5
	HF	-282.06	-307.39	-315.01	-317.98	-319.00	-319.7
	N_2	-379.44	-406.22	-415.60	-419.01	-420.18	-421.0
	CO	-363.50	-389.09	-398.52	-401.89	-403.05	-403.9
	Ne	-276.65	-305.76	-314.16	-318.00	-319.25	-320.1
	F_2	-539.93	-587.74	-601.79	-608.09	-610.15	-611.7

[a,b,c] As for Table 5.6.

Table 5.8: All-electron Møller-Plesset second-order correlation energies ($E^{(2)}$ in mE_h) of the Ne atom and some small molecules as computed by the new MP2-R12 method in the *core-valence* correlation-consistent basis sets cc-pCVXZ with $2 \leq X \leq 5$ (using the auxiliary basis $19s14p10d8f6g4h2i$ for C, N, O, F, and Ne and $9s6p4d3f2g$ for H).

Method	System[a]	X=2	X=3	X=4	X=5	Limit[b]
1A′	CH_2 ($^1A_1$)	-182.72	-199.54	-206.34	-209.01	-209.9
	H_2O	-295.51	-338.97	-352.99	-359.04	-362.1
	NH_3	-270.83	-305.45	-316.32	-320.91	-322.9
	HF	-306.66	-356.96	-373.43	-380.54	-384.6
	N_2	-455.48	-506.91	-525.24	-532.91	-536.9
	CO	-438.48	-490.02	-508.55	-515.88	-519.7
	Ne	-302.89	-357.46	-375.21	-380.30	-388.1
	F_2	-593.47	-690.09	-718.74	-732.61	-740.6
2A′	CH_2 ($^1A_1$)	-198.69	-205.50	-208.96	-209.31	-209.9
	H_2O	-337.74	-353.83	-358.49	-360.53	-362.1
	NH_3	-303.28	-316.43	-320.32	-321.93	-322.9
	HF	-358.77	-374.27	-379.35	-381.65	-384.6
	N_2	-509.90	-527.57	-533.64	-536.06	-536.9
	CO	-491.97	-510.78	-517.03	-519.04	-519.7
	Ne	-233.73	-368.48	-381.17	-386.37	-388.1
	F_2	-692.40	-722.36	-731.48	-736.90	-740.6
1B	CH_2 ($^1A_1$)	-175.04	-198.54	-205.80	-208.75	-209.9
	H_2O	-286.26	-337.17	-351.87	-358.50	-362.1
	NH_3	-264.39	-303.93	-315.87	-320.52	-322.9
	HF	-295.15	-355.15	-371.93	-379.90	-384.6
	N_2	-445.56	-504.91	-522.52	-532.55	-536.9
	CO	-427.77	-487.90	-506.78	-515.36	-519.7
	Ne	-288.45	-355.56	-373.26	-382.57	-388.1
	F_2	-571.54	-685.68	-716.62	-731.57	-740.6
2B	CH_2 ($^1A_1$)	-186.34	-202.00	-207.17	-208.66	-209.9
	H_2O	-318.09	-348.09	-356.62	-360.12	-362.1
	NH_3	-286.76	-311.75	-319.08	-321.05	-322.9
	HF	-335.14	-367.53	-375.76	-381.79	-384.6
	N_2	-484.91	-518.92	-530.15	-534.81	-536.9
	CO	-467.19	-503.39	-513.69	-517.79	-519.7
	Ne	-343.67	-374.48	-377.23	-384.14	-388.1
	F_2	-649.88	-709.27	-725.05	-735.14	-740.6

[a,b] As for Table 5.6.

Table 5.9: All-electron Møller-Plesset second-order correlation energies ($E^{(2)}$ in mE_h) of the Ne atom and some small molecules as computed by the new MP2-R12 method in the *augmented core-valence* correlation-consistent basis sets aug-cc-pCVXZ with $2 \leq X \leq 5$ (same auxiliary basis as in Table 5.8).

Method	System[a]	X=2	X=3	X=4	X=5	Limit[b]
1A′	CH_2 ($^1A_1$)	-184.44	-200.84	-206.92	-209.35	-209.9
	H_2O	-307.31	-343.58	-355.12	-359.98	-362.1
	NH_3	-279.14	-309.24	-317.87	n.a.[c]	-322.9
	HF	-319.07	-362.21	-375.75	-381.61	-384.6
	N_2	-462.61	-510.77	-526.94	-534.05	-536.9
	CO	-445.71	-492.00	-509.70	-516.73	-519.7
	Ne	-312.28	-362.35	-377.35	-384.46	-388.1
	F_2	-612.01	-697.65	-722.36	-734.58	-740.6
2A′	CH_2 ($^1A_1$)	-201.21	-207.52	-209.48	-209.87	-209.9
	H_2O	-363.30	-359.64	-361.72	-362.15	-362.1
	NH_3	-309.59	-320.11	-322.55	n.a.[c]	-322.9
	HF	-360.00	-380.58	-383.94	-384.67	-384.6
	N_2	-514.07	-531.80	-536.01	-537.83	-536.9
	CO	-496.35	-514.46	-518.93	-519.84	-519.7
	Ne	-367.65	-383.94	-386.87	-388.44	-388.1
	F_2	-705.67	-734.93	-739.08	-740.78	-740.6
1B	CH_2 ($^1A_1$)	-179.19	-199.41	-206.51	-209.17	-209.9
	H_2O	-300.08	-341.67	-354.34	-359.53	-362.1
	NH_3	-274.46	-307.44	-317.93	n.a.[c]	-322.9
	HF	-310.49	-360.10	-375.08	-381.09	-384.6
	N_2	-453.30	-508.65	-525.56	-533.55	-536.9
	CO	-436.84	-490.99	-508.46	-516.31	-519.7
	Ne	-302.91	-360.07	-375.88	-383.92	-388.1
	F_2	-597.25	-693.62	-721.87	-733.60	-740.6
2B	CH_2 ($^1A_1$)	-192.61	-205.38	-208.81	-209.61	-209.9
	H_2O	-332.51	-355.84	-360.17	-361.37	-362.1
	NH_3	-297.91	-317.31	-321.49	n.a.[c]	-322.9
	HF	-358.09	-378.22	-381.77	-383.57	-384.6
	N_2	-494.01	-526.73	-533.46	-536.19	-536.9
	CO	-477.58	-509.52	-516.22	-519.16	-519.7
	Ne	-342.47	-378.00	-386.16	-387.25	-388.1
	F_2	-676.34	-726.93	-734.72	-739.44	-740.6

[a,b] As for Table 5.8.

[c] Not available.

Table 5.10: Average percentage of the valence-shell (cc-pVXZ and aug-cc-pVXZ results) and all-electron (cc-pCVXZ and aug-cc-pCVXZ results) second-order Møller-Plesset correlation energy that is recovered by the various approaches.

Basis	X	MP2	**1**A′	**2**A′	**1**B	**2**B
cc-pVXZ	2	67.2	82.0	91.2	79.3	85.8
	3	86.8	92.9	95.7	92.3	94.1
	4	93.9	97.0	98.2	96.7	97.6
	5	96.8	98.9	99.2	98.7	98.9
	6	98.0	99.7	99.6	99.7	99.5
aug-cc-pVXZ	2	72.0	84.9	92.6	83.0	89.2
	3	88.8	94.2	97.3	93.7	96.4
	4	94.8	97.6	99.0	97.3	98.7
	5	97.3	99.2	99.6	99.0	99.5
	6	98.3	100.0	99.8	99.9	99.8
cc-pCVXZ	2	66.7	82.5	89.8	79.7	88.6
	3	87.6	93.8	97.5	93.3	96.3
	4	94.5	97.5	99.0	97.2	98.3
	5	97.2	99.1	99.6	99.0	99.4
aug-cc-pCVXZ	2	70.7	84.6	95.9	82.6	91.6
	3	89.1	94.7	99.1	94.2	98.1
	4	95.3	98.0	99.8	97.8	99.4
	5	97.5	99.4	100.0	99.2	99.8

5.7 Conclusion

By using an auxiliary basis set for the RI approximation in R12 theory, we have developed new MP2-R12 methods that can be employed for calculations in standard basis sets. In the present work, we have chosen to keep this auxiliary basis large and constant for all calculations in the correlation-consistent basis sets, and the auxiliary basis was thus chosen notably larger than the

largest correlation-consistent basis. For calculations in small standard basis sets, aiming at describing ca. 95% of the correlation energy, for example, such large auxiliary basis sets are probably not needed, and it seems worthwhile to investigate the effect of the auxiliary basis on the computed energies in more detail and to optimize suitable auxiliary basis sets for use in conjunction with selected correlation-consistent or other standard Gaussian basis sets. Work along these lines is in progress.

It also seems worthwhile to investigate the convergence of the R12 calculations in correlation-consistent basis sets in more detail. In conventional calculations, this convergence goes as X^{-3}

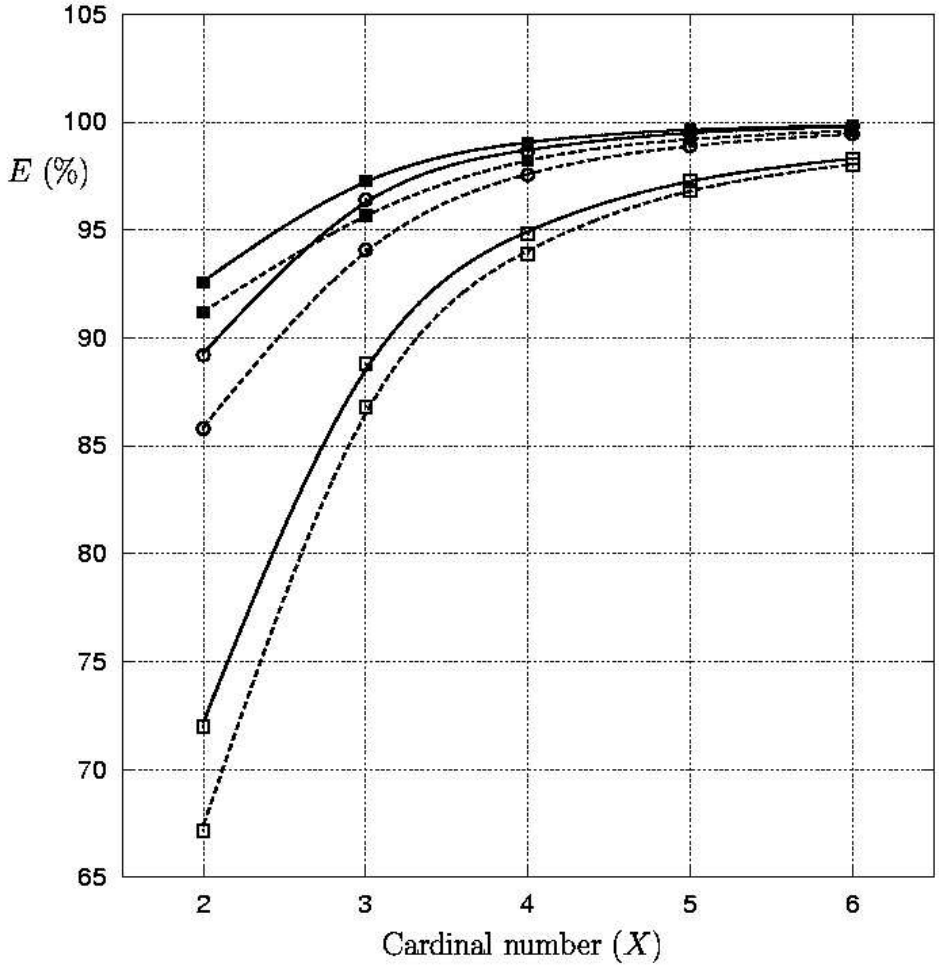

Figure 5.2: Average percentage of the valence-shell second-order Møller-Plesset correlation energy that is recovered by the standard MP2 (□) and new MP2-R12/**2**A′ (■) and MP2-R12/**2**B (○) methods in the cc-pVXZ (dashed lines) and aug-cc-pVXZ (solid lines) basis sets.

[1]. For R12 calculations, a convergence close to X^{-7} [26] should be achievable for the principal expansion, that is, for basis sets with correlation-consistent composition. The calculations on the Ne atom, for instance, showed a convergence of the form $(L_{\max}+1)^{-7}$ (Figure 5.1). To obtain this convergence rate, however, the exponents of the Gaussian functions must be reoptimized for use in R12 theory. Today, their exponents are optimized for calculations without R12 terms.

When an auxiliary basis set is used, two different Ansätze can be distinguished in R12 theory: **1** versus **2**. In general, Ansatz **2** outperforms **1**, and Ansatz **2** is recommended for future work with the new ABS-based MP2-R12 method.

When all matrix elements are computed (approximation B), the computation times of the new

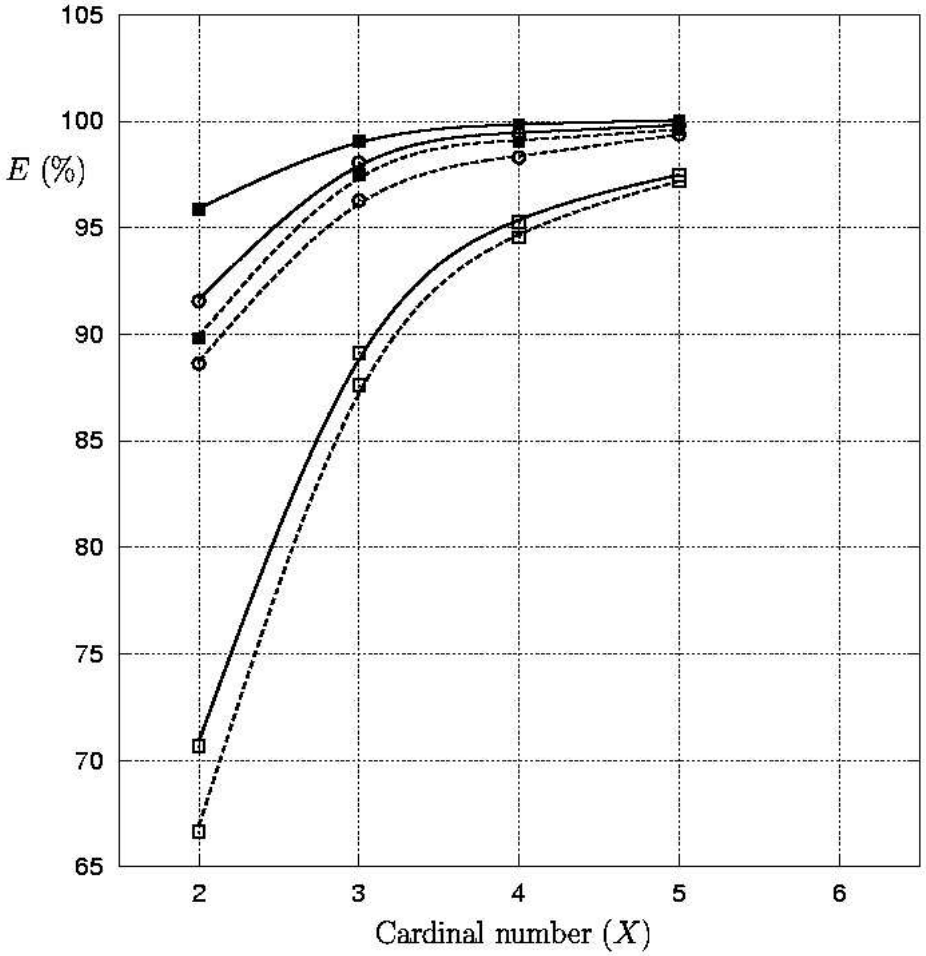

Figure 5.3: Average percentage of the all-electron second-order Møller-Plesset correlation energy that is recovered by the standard MP2 (□) and new MP2-R12/**2**A′ (■) and MP2-R12/**2**B (○) methods in the cc-pCVXZ (dashed lines) and aug-cc-pCVXZ (solid lines) basis sets.

approaches grow quadratically with the number of auxiliary basis functions. When certain exchange terms are neglected, however, the scaling becomes only linear (approximations A and A$'$). This is an important advantage of the approximations A and A$'$.

Work is in progress to implement computational methods that utilize auxiliary basis sets in explicitly correlated coupled-cluster theory (CC-R12).

Acknowledgments

The research of W.K. has been made possible by a fellowship of the Royal Netherlands Academy of Arts and Sciences. The calculations were performed on SGI Origin 2000 R12000 computers at Utrecht University and at Academic Computing Services Amsterdam (SARA). We gratefully acknowledge partial support from COST Chemistry Action D9 (Working Group 13/98) and a generous grant of computing time from National Computing Facilities (NCF) Foundation.

References

[1] T. Helgaker, P. Jørgensen, and J. Olsen, *Molecular Electronic-Structure Theory*, John Wiley & Sons, Ltd., Chichester, New York, (2000).

[2] K. L. Bak, P. Jørgensen, J. Olsen, T. Helgaker, and W. Klopper, J. Chem. Phys. **112**, 9229 (2000).

[3] T. H. Dunning, Jr., J. Phys. Chem. A **104**, 9062 (2000).

[4] T. Helgaker, W. Klopper, A. Halkier, K. L. Bak, P. Jørgensen, and J. Olsen, *In: Understanding Chemical Reactivity, Vol. 22, pp. 1–30*, J. Cioslowski (Ed.), Kluwer Academic Publishers, Dordrecht, (2001).

[5] K. L. Bak, A. Halkier, P. Jørgensen, J. Olsen, T. Helgaker, and W. Klopper, J. Mol. Struct. **567–568**, 375 (2001).

[6] T. Helgaker, W. Klopper, H. Koch, and J. Noga, J. Chem. Phys. **106**, 9639 (1997).

[7] D. Feller and K. A. Peterson, J. Chem. Phys. **108**, 154 (1998).

[8] D. Feller and K. A. Peterson, J. Chem. Phys. **110**, 8384 (1999).

[9] J. W. Ochterski, G. A. Petersson, and J. A. Montgomery, Jr., J. Chem. Phys. **104**, 2598 (1996).

[10] G. A. Petersson and M. J. Frisch, J. Phys. Chem. A **104**, 2183 (2000).

[11] P. L. Fast, M. L. Sánchez, and D. G. Truhlar, J. Chem. Phys. **111**, 2921 (1999).

[12] J. M. Rodgers, P. L. Fast, and D. G. Truhlar, J. Chem. Phys. **112**, 3141 (2000).

[13] L. A. Curtiss, K. Raghavachari, P. C. Redfern, V. Rassolov, and J. A. Pople, J. Chem. Phys. **109**, 7764 (1998).

[14] L. A. Curtiss, P. C. Redfern, K. Raghavachari, and J. A. Pople, J. Chem. Phys. **114**, 108 (2001).

[15] J. M. L. Martin and G. de Oliveira, J. Chem. Phys. **111**, 1843 (1999).

[16] S. Parthiban and J. M. L. Martin, J. Chem. Phys. **114**, 6014 (2001).

[17] A. G. Császár, W. D. Allen, and H. F. Schaefer III, J. Chem. Phys. **108**, 9751 (1998).

[18] A. G. Császár and M. L. Leininger, J. Chem. Phys. **114**, 5491 (2001).

[19] W. Cencek and J. Rychlewski, J. Chem. Phys. **102**, 2533 (1995).

[20] B. J. Persson and P. R. Taylor, J. Chem. Phys. **105**, 5915 (1996).

[21] R. J. Gdanitz, J. Chem. Phys. **110**, 706 (1999).

[22] R. Bukowski, B. Jeziorski, and K. Szalewicz, J. Chem. Phys. **110**, 4165 (1999).

[23] W. Klopper, *In: The Encyclopedia of Computational Chemistry, Vol.4, pp. 2351–2375*, P. v. R. Schleyer, N. L. Allinger, T. Clark, J. Gasteiger, P. A. Kollman, H. F. Schaefer III, and P. R. Schreiner (Eds.), John Wiley & Sons, Ltd., Chichester, New York, (1998).

[24] W. Kutzelnigg, Theor. Chim. Acta **68**, 445 (1985).

[25] W. Klopper and W. Kutzelnigg, Chem. Phys. Lett. **134**, 17 (1987).

[26] W. Kutzelnigg and W. Klopper, J. Chem. Phys. **94**, 1985 (1991).

[27] J. Noga and W. Kutzelnigg, J. Chem. Phys. **101**, 7738 (1994).

[28] J. Noga, W. Klopper, and W. Kutzelnigg, *In: Recent Advances in Computational Chemistry, Vol. 3, pp. 1–48*, R. J. Bartlett (Ed.), World Scientific Publishing Co. Ltd., Singapore, (1997).

[29] W. Klopper and H. P. Lüthi, Chem. Phys. Lett. **262**, 546 (1996).

[30] W. Klopper, H. P. Lüthi, T. Brupbacher, and A. Bauder, J. Chem. Phys. **101**, 9747 (1994).

[31] W. Klopper, M. Schütz, H. P. Lüthi, and S. Leutwyler, J. Chem. Phys. **103**, 1085 (1995).

[32] M. Schütz, W. Klopper, H. P. Lüthi, and S. Leutwyler, J. Chem. Phys. **103**, 6114 (1995).

[33] R. J. Gdanitz and R. Röhse, Int. J. Quantum Chem. **55**, 147 (1996).

[34] P. Wind, T. Helgaker, and W. Klopper, Theor. Chim. Acta **106**, 280 (2001).

[35] P. Wind, W. Klopper, and T. Helgaker, Theor. Chim. Acta **107**, 173 (2002).

[36] W. Klopper, Chem. Phys. Lett. **186**, 583 (1991).

[37] W. Klopper and J. Almlöf, J. Chem. Phys. **99**, 5167 (1993).

[38] W. Klopper and R. Röhse, Theor. Chim. Acta **83**, 441 (1992).

[39] T. Helgaker, H. J. Aa. Jensen, P. Jørgensen, J. Olsen, K. Ruud, H. Ågren, A. A. Auer, K. L. Bak, V. Bakken, O. Christiansen, S. Coriani, P. Dahle, E. K. Dalskov, T. Enevoldsen, B. Fernandez, C. Hättig, K. Hald, A. Halkier, H. Heiberg, H. Hettema, D. Jonsson, S. Kirpekar, R. Kobayashi, H. Koch, K. V. Mikkelsen, P. Norman, M. J. Packer, T. B. Pedersen, T. A. Ruden, A. Sanchez, T. Saue, S. P. A. Sauer, B. Schimmelpfennig, K. O. Sylvester-Hvid, P. R. Taylor, and O. Vahtras, *Dalton, a molecular electronic structure program*, Release 1.2 (2001).

[40] H. Koch, O. Christiansen, R. Kobayashi, P. Jørgensen, and T. Helgaker, Chem. Phys. Lett. **233**, 94 (1994).

[41] H. Koch, A. Sánches de Merás, T. Helgaker, and O. Christiansen, J. Chem. Phys. **104**, 4157 (1996).

[42] H. Koch, P. Jørgensen, and T. Helgaker, J. Chem. Phys. **104**, 9528 (1996).

[43] W. Klopper, W. Kutzelnigg, H. Müller, J. Noga, and S. Vogtner, Top. Curr. Chem. **203**, 21 (1999).

[44] I. Lindgren and S. Salomonson, Phys. Scripta **21**, 335 (1980).

[45] K. Jankowski and P. Malinowksi, Phys. Rev. A **21**, 45 (1980).

[46] V. Termath, W. Klopper, and W. Kutzelnigg, J. Chem. Phys. **94**, 2002 (1991).

[47] J. R. Flores, Phys. Rev. A **46**, 6063 (1992).

[48] W. Kutzelnigg and J. D. Morgan III, J. Chem. Phys. **96**, 4484 (1992).

[49] J. R. Flores and D. Kolb, J. Phys. B **32**, 779 (1999).

[50] K. L. Bak, J. Gauss, P. Jørgensen, J. Olsen, T. Helgaker, and J. F. Stanton, J. Chem. Phys. **114**, 6548 (2001).

[51] W. Klopper, Mol. Phys. **99**, 481 (2001).

[52] W. Klopper, C. C. M. Samson, G. Tarczay, and A. G. Császár, J. Comput. Chem. **22**, 1306 (2001).

[53] T. H. Dunning, Jr., J. Chem. Phys. **90**, 1007 (1989).

[54] R. A. Kendall, T. H. Dunning, Jr., and R. J. Harrison, J. Chem. Phys. **96**, 6796 (1992).

[55] D. E. Woon and T. H. Dunning, Jr., J. Chem. Phys. **98**, 1358 (1993).

[56] D. E. Woon and T. H. Dunning, Jr., J. Chem. Phys. **100**, 2975 (1994).

[57] D. E. Woon and T. H. Dunning, Jr., J. Chem. Phys. **103**, 4572 (1995).

[58] A. K. Wilson, T. van Mourik, and T. H. Dunning, Jr., J. Mol. Struct. (Theochem) **338**, 339 (1996).

[59] The basis-set parameters were obtained from the Extensible Computational Chemistry Environment Basis Set Database, Version 10/12/01, as developed and distributed by the Molecular Science Computing Facility, Environmental and Molecular Sciences Laboratory which is part of the Pacific Northwest Laboratory, P.O. Box 999, Richland, Washington 99352, USA, and funded by the U.S. Department of Energy. The Pacific Northwest Laboratory is a multi-program laboratory operated by Battelle Memorial Institute for the U.S., Department of Energy under contract DE-AC06-76RLO 1830.

6

Computation of two-electron Gaussian integrals for wave functions including the correlation factor $r_{12}\exp(-\gamma r_{12}^2)$

Abstract

Explicitly correlated molecular electronic-structure calculations with the damped correlation factor $r_{12}\exp(-\gamma r_{12}^2)$ require two-electron integrals that are different from the already implemented R12 integrals. The aim of such a correlation factor, which combines the interelectronic distance with a Gaussian-type function, is to avoid integrals with large interelectronic distances, thus making it possible to use R12 methods for large molecular systems. In particular, an important perspective of the new correlation factor is to be able to utilize *local-correlation techniques* for explicitly correlated wave functions, such that computation times will asymptotically scale linearly with the size of the molecule. For the development of such techniques, the correlation factor must be restricted to the (physically meaningful) short range of the correlation cusp of the Coulomb hole. In the present paper, the evaluation of all two-electron integrals needed for damped-R12 theory is described, as implemented in a local version of the Dalton program.

C. C. M. Samson, W. Klopper, and T. Helgaker, Comp. Phys. Commun. **149**, 1 (2002).

6.1 Introduction

Most *ab initio* methods represent the electronic wave function by a linear combination of products of one-electron functions, which do not describe accurately the Coulomb hole and which cannot represent the electron-correlation cusp [1–5]. The R12 method improves this description by using two-electron basis functions of the form $f_{12}\,\psi_i(\vec{r}_1)\,\psi_j(\vec{r}_2)$, where $\psi_i(\vec{r}_1)$ and $\psi_j(\vec{r}_2)$ are molecular spin-orbitals and f_{12} a correlation factor.

So far, the only correlation factor explored in R12 theory is the interelectronic distance $f_{12} = r_{12} = |\vec{r}_1 - \vec{r}_2|$. In combination with several types of approximations designed to remove the three- and four-electron integrals involved [6–8], this factor has given very accurate results for a variety of small and medium-sized molecules. Nevertheless, use of the linear r_{12} factor, which does not vanish for large electronic separations, becomes awkward for large molecules. For such systems, therefore, we wish to investigate the correlation factor $f_{12} = r_{12}\,\exp(-\gamma r_{12}^2)$, which vanishes for large separations between the electrons—see Figure 6.1. Rather than expanding the correlation factor in a basis of Gaussian geminals alone [9–11], which also vanish for large r_{12}, we wish to investigate products of the linear r_{12} factor with such Gaussians.

Clearly, with the introduction of a new correlation factor, we must develop a scheme for the calculation of two-electron integrals involving this factor. The scheme presented in this paper is based on the McMurchie–Davidson method for the evaluation of one- and two-electron integrals over Gaussian atomic orbitals [12]. As demonstrated here, none of the five nonstandard two-electron integrals that arise from the use of the damped r_{12} factors require much more effort than do the usual two-electron integrals over Gaussian functions, indicating that the damped-R12 method will be practicable for large systems. Indeed, the particular damping function chosen for our correlation factor—that is, the Gaussian factor $\exp(-\gamma r_{12}^2)$—was selected with computational ease in mind. Other damping factors such as the complementary error function $\mathrm{erfc}(\gamma r_{12})$ are possible but lead to a more complicated integral evaluation.

6.2 Integral evaluation

We begin our discussion of two-electron integral evaluation by examining the overall structure of the integrals in Subsection 6.2.1. Next, in Subsection 6.2.2, we introduce the McMurchie–Davidson expansion of overlap distributions in Hermite functions followed by the expansion of Cartesian integrals in Hermite integrals in Subsection 6.2.3. Finally, the recursive evaluation of the spherical and nonspherical Hermite integrals is treated in Subsections 6.2.4 and 6.2.5.

6.2.1 Structure of the Cartesian two-electron damped-R12 integrals

Within the standard approximations of R12 theory, there are six different two-electron integrals to be evaluated. The integrals I_1 and I_2 originate from the Coulomb repulsion:

$$\begin{aligned} I_1 &= (ab|r_{12}^{-1}|cd) \\ &= \iint \psi_a^*(\vec{r}_1)\psi_c^*(\vec{r}_2)\, r_{12}^{-1}\, \psi_b(\vec{r}_1)\psi_d(\vec{r}_2)\,\mathrm{d}\vec{r}_1\,\mathrm{d}\vec{r}_2, \qquad (6.1) \\ I_2 &= (ab|r_{12}^{-1} f_{12}|cd) = (ab|\exp(-\gamma\, r_{12}^2)|cd) \\ &= \iint \psi_a^*(\vec{r}_1)\psi_c^*(\vec{r}_2)\, \exp(-\gamma\, r_{12}^2)\, \psi_b(\vec{r}_1)\psi_d(\vec{r}_2)\,\mathrm{d}\vec{r}_1\,\mathrm{d}\vec{r}_2; \qquad (6.2) \end{aligned}$$

the integrals I_3 and I_4 are overlap integrals:

$$\begin{aligned} I_3 &= (ab|f_{12}|cd) = (ab|r_{12}\exp(-\gamma\, r_{12}^2)|cd) \\ &= \iint \psi_a^*(\vec{r}_1)\psi_c^*(\vec{r}_2)\, r_{12}\exp(-\gamma\, r_{12}^2)\, \psi_b(\vec{r}_1)\psi_d(\vec{r}_2)\,\mathrm{d}\vec{r}_1\,\mathrm{d}\vec{r}_2, \qquad (6.3) \\ I_4 &= (ab|f_{12}f'_{12}|cd) = (ab|r_{12}^2\exp(-(\gamma+\gamma')\, r_{12}^2)|cd) \\ &= \iint \psi_a^*(\vec{r}_1)\psi_c^*(\vec{r}_2)\, r_{12}^2\exp(-(\gamma+\gamma')\, r_{12}^2)\, \psi_b(\vec{r}_1)\psi_d(\vec{r}_2)\,\mathrm{d}\vec{r}_1\,\mathrm{d}\vec{r}_2; \qquad (6.4) \end{aligned}$$

and the integrals I_5 and I_6 involve commutators with the kinetic-energy operator $\hat{T}$:

$$\begin{aligned} I_5 &= (ab|[f_{12},\hat{T}_1]|cd) = (ab|[r_{12}\exp(-\gamma\, r_{12}^2),\hat{T}_1]|cd) \\ &= \iint \psi_a^*(\vec{r}_1)\psi_c^*(\vec{r}_2)\, [r_{12}\exp(-\gamma\, r_{12}^2),\hat{T}_1]\, \psi_b(\vec{r}_1)\psi_d(\vec{r}_2)\,\mathrm{d}\vec{r}_1\,\mathrm{d}\vec{r}_2, \qquad (6.5) \\ I_6 &= (ab|[[f_{12},\hat{T}_1],f'_{12}]|cd) = (ab|[[r_{12}\exp(-\gamma\, r_{12}^2),\hat{T}_1], r_{12}\exp(-\gamma'\, r_{12}^2)]|cd) \\ &= \iint \psi_a^*(\vec{r}_1)\psi_c^*(\vec{r}_2)[[r_{12}\exp(-\gamma\, r_{12}^2),\hat{T}_1], r_{12}\exp(-\gamma'\, r_{12}^2)]\psi_b(\vec{r}_1)\psi_d(\vec{r}_2)\mathrm{d}\vec{r}_1\mathrm{d}\vec{r}_2. \qquad (6.6) \end{aligned}$$

For flexibility in the choice of the correlation factor, two different exponents γ and γ' and thus two different correlation factors $f_{12} = r_{12}\,\exp(-\gamma r_{12}^2)$ and $f'_{12} = r_{12}\,\exp(-\gamma'\, r_{12}^2)$ have been introduced in I_4 and I_6.

Before we begin our discussion of the evaluation of the damped-R12 integrals, a few general remarks on their structure are in order. In the following, we assume that the integration is over real, primitive Cartesian orbitals with exponents a, b, c, and d centered on $\mathbf{A}$, $\mathbf{B}$, $\mathbf{C}$, and $\mathbf{D}$, respectively:

$$\begin{aligned} \psi_a(\vec{r}_1,a,\mathbf{A}) &= x_{1A}^i y_{1A}^k z_{1A}^m \exp\left(-a r_{1A}^2\right), \qquad (6.7) \\ \psi_b(\vec{r}_1,b,\mathbf{B}) &= x_{1B}^j y_{1B}^l z_{1B}^n \exp\left(-b r_{1B}^2\right), \qquad (6.8) \\ \psi_c(\vec{r}_2,c,\mathbf{C}) &= x_{2C}^{i'} y_{2C}^{k'} z_{2C}^{m'} \exp\left(-c r_{2C}^2\right), \qquad (6.9) \\ \psi_d(\vec{r}_2,d,\mathbf{D}) &= x_{2D}^{j'} y_{2D}^{l'} z_{2D}^{n'} \exp\left(-d r_{2D}^2\right). \qquad (6.10) \end{aligned}$$

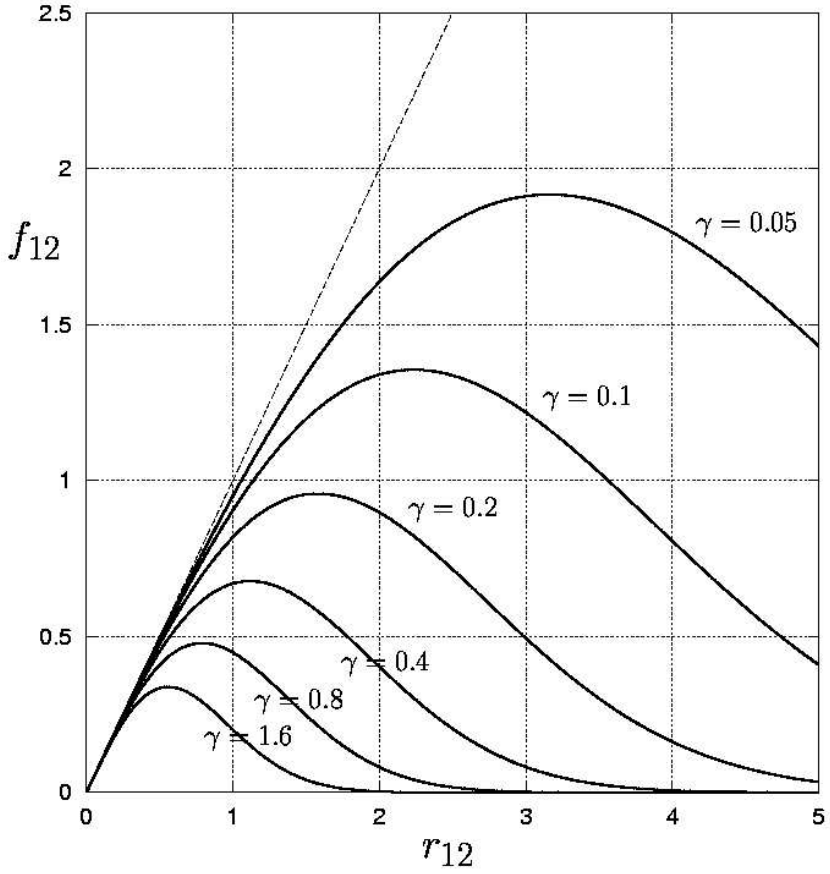

Figure 6.1: *Correlation factor* $f_{12} = r_{12}\,\exp(-\gamma r_{12}^2)$ *for various values of* γ.

The transformation of integrals to a symmetrized, contracted spherical-harmonic basis may be carried out in the same manner as for the usual two-electron integrals I_1 and is not discussed further here.

Next, we observe that the integrals involving the kinetic-energy operator can be expressed in the following manner [13]:

$$\begin{aligned} I_5 &= \frac{1}{2}\left(ab\left|\nabla_1^2 r_{12}\exp\left(-\gamma r_{12}^2\right) - r_{12}\exp\left(-\gamma r_{12}^2\right)\nabla_1^2\right|cd\right) \\ &= \frac{1}{2}\left(\left(\nabla_1^2 a\right)b - a\left(\nabla_1^2 b\right)\left|r_{12}\exp\left(-\gamma r_{12}^2\right)\right|cd\right) \\ &= \frac{1}{2}\left(\nabla_A^2 - \nabla_B^2\right) I_3, \end{aligned} \tag{6.11}$$

$$\begin{aligned} I_6 &= \left(ab\left|\left(\vec{\nabla}_1 f_{12}\right)\cdot\left(\vec{\nabla}_1 f'_{12}\right)\right|cd\right) \\ &= \left(ab\left|\left(1-2\gamma r_{12}^2\right)\left(1-2\gamma' r_{12}^2\right)\,\exp\left[-\left(\gamma+\gamma'\right)\,r_{12}^2\right]\right|cd\right), \end{aligned} \tag{6.12}$$

where $\vec{\nabla}_1$ is the gradient operator with respect to the coordinates of the first electron and whereas

$\vec{\nabla}_A$ and $\vec{\nabla}_B$ denote gradients with respect to $\mathbf{A}$ and $\mathbf{B}$, respectively. Comparing these expressions for I_5 and I_6 with those for I_2 – I_4 in Eqs. (6.2)–(6.4), we conclude that all two-electron integrals needed in damped-R12 theory can be computed from integrals over the operators $r_{12}^k \exp(-\beta\, r_{12}^2)$ with k = 0, 1, 2, 4 and $\beta = \gamma$ or $\beta = \gamma + \gamma'$. We note, however, that the I_5 integrals are obtained as second derivatives of the integrals I_3; as we shall see, the evaluation of I_5 according to Eq. (6.11) can be carried out in an efficient manner, requiring not much more effort than the evaluation of the other damped-R12 integrals.

In the standard R12 approach, the correlation factor f_{12} is chosen to be equal to r_{12}. In this special case, the integral I_2 need not to be evaluated since the operator in I_2 reduces to $r_{12}^{-1}\, r_{12} = 1$. Also, the integral I_4 over r_{12}^2 factorizes into products of one-electron integrals and the operator I_6 reduces to $[[r_{12}, \hat{T}_1], r_{12}] = 1$. With the use of the new, damped correlation factor, these simplifications do not occur.

6.2.2 Expansion of Cartesian overlap distributions in Hermite functions

In our evaluation of two-electron integrals, we adopt the McMurchie–Davidson scheme [12], expanding the Cartesian overlap distributions in Hermite integrals. In this approach, we write the overlap distribution $\psi_a(\vec{r}_1, a, \mathbf{A})\psi_b(\vec{r}_1, b, \mathbf{B})$ as a linear combination of Hermite functions

$$\Lambda_{tuv}(\vec{r}_1, p, \mathbf{P}) = \frac{\mathrm{d}^t}{\mathrm{d}P_x^t}\frac{\mathrm{d}^u}{\mathrm{d}P_y^u}\frac{\mathrm{d}^v}{\mathrm{d}P_z^v}\exp\left(-p r_{1P}^2\right), \tag{6.13}$$

with exponent p and centered at $\mathbf{P}$,

$$p = a + b, \tag{6.14}$$

$$\mathbf{P} = \frac{a\mathbf{A} + b\mathbf{B}}{p}, \tag{6.15}$$

in the following manner [12]:

$$\begin{aligned}\psi_a(\vec{r}_1, a, \mathbf{A})\psi_b(\vec{r}_1, b, \mathbf{B}) &= \sum_{t=0}^{i+j} E_t^{ij} \sum_{u=0}^{k+l} E_u^{kl} \sum_{v=0}^{m+n} E_v^{mn} \Lambda_{tuv}(\vec{r}_1, p, \mathbf{P}) \\ &= \sum_{tuv} E_{tuv}^{ab} \Lambda_{tuv}(\vec{r}_1, p, \mathbf{P}).\end{aligned} \tag{6.16}$$

As demonstrated in Ref. [14], the expansion coefficients E_t^{ij} of the first electron may be evaluated from the following two-term recurrence relations

$$E_0^{00} = \exp\left(-\frac{ab}{a+b}X_{AB}^2\right), \tag{6.17}$$

$$E_0^{i+1,j} = -\frac{b}{p}X_{AB}E_0^{ij} + E_1^{ij}, \tag{6.18}$$

$$E_0^{i,j+1} = \frac{a}{p}X_{AB}E_0^{ij} + E_1^{ij}, \tag{6.19}$$

$$E_t^{ij} = \frac{1}{2pt}\left(iE_{t-1}^{i-1,j} + jE_{t-1}^{i,j-1}\right), \tag{6.20}$$

and likewise for E_u^{kl} and E_v^{mn}. Similar relations may be used for the second electron. In the original McMurchie–Davidson method, three-term recurrence relations are used for these coefficients [12]. Similarly, we may expand the overlap distribution of the second electron as

$$\psi_c(\vec{r}_2, c, \mathbf{C})\psi_d(\vec{r}_2, d, \mathbf{D}) = \sum_{\tau\upsilon\phi} E_{\tau\upsilon\phi}^{cd}\Lambda_{\tau\upsilon\phi}(\vec{r}_2, q, \mathbf{Q}) \tag{6.21}$$

where $q = c + d$ and $\mathbf{Q} = (c\mathbf{C} + d\mathbf{D})/q$, and where the coefficients $E_{\tau\upsilon\phi}^{cd}$ of the second electron are different from the coefficients E_{tuv}^{ab} of the first electron.

6.2.3 Expansion of Cartesian integrals in Hermite integrals

We now introduce the following basic two-electron integrals over spherical Gaussian functions with centers at $\mathbf{P}$ and $\mathbf{Q}$:

$$D_k(\beta) = \iint \exp(-pr_{1P}^2)\exp(-qr_{2Q}^2)r_{12}^k\exp(-\beta r_{12}^2)\,\mathrm{d}\vec{r}_1\,\mathrm{d}\vec{r}_2. \tag{6.22}$$

Inserting the Hermite expansions of the overlap distributions Eqs. (6.16) and (6.21) in the integrals Eqs. (6.1)–(6.4) and Eq. (6.6), we obtain

$$I_k = \sum_{tuv} E_{tuv}^{ab}\sum_{\tau\upsilon\phi}(-1)^{\tau+\upsilon+\phi}\,E_{\tau\upsilon\phi}^{cd}\,R_k^{t+\tau,u+\upsilon,v+\phi}, \qquad k = 1, 2, 3, 4, 6; \tag{6.23}$$

with

$$R_1^{tuv} = \frac{\mathrm{d}^t}{\mathrm{d}P_x^t}\frac{\mathrm{d}^u}{\mathrm{d}P_y^u}\frac{\mathrm{d}^v}{\mathrm{d}P_z^v} D_{-1}(0), \tag{6.24}$$

$$R_2^{tuv} = \frac{\mathrm{d}^t}{\mathrm{d}P_x^t}\frac{\mathrm{d}^u}{\mathrm{d}P_y^u}\frac{\mathrm{d}^v}{\mathrm{d}P_z^v} D_0(\gamma), \tag{6.25}$$

$$R_3^{tuv} = \frac{\mathrm{d}^t}{\mathrm{d}P_x^t}\frac{\mathrm{d}^u}{\mathrm{d}P_y^u}\frac{\mathrm{d}^v}{\mathrm{d}P_z^v} D_1(\gamma), \tag{6.26}$$

$$R_4^{tuv} = \frac{\mathrm{d}^t}{\mathrm{d}P_x^t}\frac{\mathrm{d}^u}{\mathrm{d}P_y^u}\frac{\mathrm{d}^v}{\mathrm{d}P_z^v} D_2(\gamma+\gamma'), \tag{6.27}$$

$$R_6^{tuv} = \frac{\mathrm{d}^t}{\mathrm{d}P_x^t}\frac{\mathrm{d}^u}{\mathrm{d}P_y^u}\frac{\mathrm{d}^v}{\mathrm{d}P_z^v} \left[D_0(\gamma+\gamma') - 2(\gamma+\gamma')D_2(\gamma+\gamma') + 4\gamma\gamma' D_4(\gamma+\gamma')\right]. \tag{6.28}$$

To obtain these expressions, we have taken the differentation operators with respect to the components of $\mathbf{P}$ and $\mathbf{Q}$ outside the integration and invoked the translational invariance of the integrals to replace derivatives with respect to $\mathbf{Q}$ by derivatives with respect to $-\mathbf{P}$.

The integrals I_5 in Eq. (6.11) require special attention. By substituting Eq. (6.23) in Eq. (6.11), we obtain:

$$I_5 = \frac{1}{2}\left(\nabla_A^2 - \nabla_B^2\right) \sum_{tuv} E_{tuv}^{ab} \sum_{\tau\upsilon\phi} (-1)^{\tau+\upsilon+\phi}\, E_{\tau\upsilon\phi}^{cd}\, R_3^{t+\tau,u+\upsilon,v+\phi}. \tag{6.29}$$

Since the coefficients E_{tuv}^{ab} depend only on $\mathbf{A}-\mathbf{B}$ and the integrals R_3^{tuv} only on $\mathbf{P}$, it is advantageous to express I_5 in terms of derivatives with respect to these coordinates rather than with respect to $\mathbf{A}$ and $\mathbf{B}$ [15]. From the relations

$$\frac{\mathrm{d}}{\mathrm{d}A_x} = \frac{a}{p}\frac{\mathrm{d}}{\mathrm{d}P_x} + \frac{\mathrm{d}}{\mathrm{d}X_{AB}}, \tag{6.30}$$

$$\frac{\mathrm{d}}{\mathrm{d}B_x} = \frac{b}{p}\frac{\mathrm{d}}{\mathrm{d}P_x} - \frac{\mathrm{d}}{\mathrm{d}X_{AB}}, \tag{6.31}$$

where X_{AB} is the x component of $\mathbf{A}-\mathbf{B}$, we then obtain [13]:

$$\begin{aligned} I_5 &= \frac{a-b}{2p}\sum_{tuv} E_{tuv}^{ab} \sum_{\tau\upsilon\phi} (-1)^{\tau+\upsilon+\phi}\, E_{\tau\upsilon\phi}^{cd}\, \nabla_P^2 R_3^{t+\tau,u+\upsilon,v+\phi} \\ &+ \sum_{tuv} \vec{\nabla}_X E_{tuv}^{ab} \cdot \sum_{\tau\upsilon\phi} (-1)^{\tau+\upsilon+\phi}\, E_{\tau\upsilon\phi}^{cd}\, \vec{\nabla}_P R_3^{t+\tau,u+\upsilon,v+\phi}. \end{aligned} \tag{6.32}$$

The derivatives of the Hermite integrals Eq. (6.26) are given by

$$\vec{\nabla}_P R_3^{tuv} = \left[\, R_3^{t+1,u,v},\ R_3^{t,u+1,v},\ R_3^{t,u,v+1}\,\right]^{\mathrm{T}}, \tag{6.33}$$

$$\nabla_P^2 R_3^{tuv} = R_3^{t+2,u,v} + R_3^{t,u+2,v} + R_3^{t,u,v+2}, \tag{6.34}$$

while the elements of $\vec{\nabla}_X E_t^{ij}$ are obtained from recurrence relations obtained by differentiating Eqs. (6.17)–(6.20). For the x component, for example, we obtain for the coefficients

$$F_t^{ij} = \frac{\mathrm{d}E_t^{ij}}{\mathrm{d}X_{AB}} \tag{6.35}$$

the recurrence relations

$$F_0^{00} = -\frac{2ab}{p} X_{AB} E_0^{00}, \tag{6.36}$$

$$F_0^{i+1,j} = -\frac{b}{p} X_{AB} F_0^{ij} + F_1^{ij} - \frac{b}{p} E_0^{i+1,j}, \tag{6.37}$$

$$F_0^{i,j+1} = \frac{a}{p} X_{AB} F_0^{ij} + F_1^{ij} + \frac{a}{p} E_0^{i,j+1}, \tag{6.38}$$

$$F_t^{ij} = \frac{1}{2pt} \left(i F_{t-1}^{i-1,j} + j F_{t-1}^{i,j-1} \right), \tag{6.39}$$

and similarly for the y and z components.

6.2.4 Evaluation of the spherical Hermite integrals

In the present section, we consider the evaluation of the spherical Hermite integrals $D_k(\beta)$ of Eq. (6.22). We begin by noting the following relations among these integrals:

$$D_{k+1}(\beta) = -D'_{k-1}(\beta), \tag{6.40}$$

$$D_{2k-1}(\beta) = \frac{2}{\sqrt{\pi}} \int_0^\infty D_{2k}(\beta + t^2)\, \mathrm{d}t. \tag{6.41}$$

The first relation is obtained straightforwardly by differentation of Eq. (6.22); the second relation follows by introducing in Eq. (6.22) the integral transform

$$\frac{1}{r_{12}} = \frac{2}{\sqrt{\pi}} \int_0^\infty \exp(-t^2\, r_{12}^2)\, \mathrm{d}t, \tag{6.42}$$

as pioneered by Boys for the two-electron repulsion integrals [16]. We may therefore generate the necessary integrals $D_k(\beta)$ by explicit integration for $D_0(\beta)$, followed by application of Eqs. (6.40) and (6.41) to yield the remaining integrals.

The overlap integral $D_0(\beta)$ is easily evaluated as it contains only Gaussian functions. By integrating over the x, y, and z coordinates separately,

$$\begin{aligned} D_0(\beta) &= \int_{-\infty}^{\infty}\int_{-\infty}^{\infty} \exp\left[-p(x_1 - P_x)^2 - q(x_2 - Q_x)^2 - \beta(x_1 - x_2)^2\right] \mathrm{d}x_1\, \mathrm{d}x_2 \\ &\times \int_{-\infty}^{\infty}\int_{-\infty}^{\infty} \exp\left[-p(y_1 - P_y)^2 - q(y_2 - Q_y)^2 - \beta(y_1 - y_2)^2\right] \mathrm{d}y_1\, \mathrm{d}y_2 \\ &\times \int_{-\infty}^{\infty}\int_{-\infty}^{\infty} \exp\left[-p(z_1 - P_z)^2 - q(z_2 - Q_z)^2 - \beta(z_1 - z_2)^2\right] \mathrm{d}z_1\, \mathrm{d}z_2, \end{aligned} \tag{6.43}$$

and introducing the reduced exponent

$$\alpha = \frac{pq}{p+q}, \tag{6.44}$$

we obtain

$$D_0(\beta) = \left(\frac{\pi^2}{pq}\right)^{\frac{3}{2}} \left(\frac{\alpha}{\alpha+\beta}\right)^{\frac{3}{2}} \exp\left(-\frac{\alpha\beta}{\alpha+\beta} R_{PQ}^2\right), \tag{6.45}$$

$$D_2(\beta) = \left(\frac{3}{2} + \frac{\alpha^2}{\alpha+\beta} R_{PQ}^2\right) \frac{D_0(\beta)}{\alpha+\beta}, \tag{6.46}$$

$$D_4(\beta) = \left[\frac{15}{4} + \frac{5\alpha^2}{\alpha+\beta} R_{PQ}^2 + \frac{\alpha^4}{(\alpha+\beta)^2} R_{PQ}^4\right] \frac{D_0(\beta)}{(\alpha+\beta)^2}, \tag{6.47}$$

where we have applied Eq. (6.40) to yield $D_2(\beta)$ and $D_4(\beta)$. The even-order integrals $D_{2n}(\beta)$ are thus easily evaluated in closed form.

To calculate the odd-order spherical integrals $D_{2n-1}(\beta)$, we begin by deriving an expression for $D_{-1}(\beta)$, from which we next generate $D_1(\beta)$ by differentiation according to Eq. (6.40). From Eqs. (6.41) and (6.45), we obtain

$$D_{-1}(\beta) = \frac{2}{\sqrt{\pi}} \left(\frac{\pi^2}{pq}\right)^{\frac{3}{2}} \int_0^\infty \left(\frac{\alpha}{\alpha+\beta+t^2}\right)^{\frac{3}{2}} \exp\left(-\alpha\, R_{PQ}^2 \frac{\beta+t^2}{\alpha+\beta+t^2}\right) \mathrm{d}t. \tag{6.48}$$

The variable substitution

$$u^2 = \frac{t^2}{\alpha+\beta+t^2} \tag{6.49}$$

gives

$$\mathrm{d}t = (\alpha+\beta)^{-1} (\alpha+\beta+t^2)^{\frac{3}{2}}\, \mathrm{d}u, \tag{6.50}$$

with integration limits 0 and 1 for u. Integral Eq. (6.48) then becomes

$$D_{-1}(\beta) = 2\sqrt{\frac{\alpha+\beta}{\pi}} F_0\left(\frac{\alpha^2}{\alpha+\beta} R_{PQ}^2\right) D_0(\beta), \tag{6.51}$$

where we have introduced the Boys function of order n:

$$F_n(x) = \int_0^1 \exp(-xt^2) t^{2n}\, \mathrm{d}t. \tag{6.52}$$

Finally, differentiation of D_{-1} with respect to β according to Eq. (6.40) and use of the relations

$$F_n'(x) = -F_{n+1}(x), \tag{6.53}$$

$$F_n'(x) = \frac{\exp(-x) - (2n+1)F_n(x)}{2x}, \tag{6.54}$$

yields:

$$D_1(\beta) = \left[\exp\left(-\frac{\alpha^2}{\alpha+\beta}R_{PQ}^2\right) + \left(1 + \frac{2\alpha^2}{\alpha+\beta}R_{PQ}^2\right) F_0\left(\frac{\alpha^2}{\alpha+\beta}R_{PQ}^2\right)\right] \frac{D_0(\beta)}{\sqrt{\pi(\alpha+\beta)}}. \quad (6.55)$$

For a more compact representation of the integrals, we introduce

$$\bar{R}_{PQ}^2 = \frac{\alpha}{\alpha+\beta}R_{PQ}^2, \quad (6.56)$$

and obtain for the damped integrals:

$$\begin{aligned}
D_0(\beta) &= \left(\frac{\pi^2}{pq}\right)^{\frac{3}{2}} \left(\frac{\alpha}{\alpha+\beta}\right)^{\frac{3}{2}} \exp\left(-\beta\bar{R}_{PQ}^2\right), & (6.57)\\
D_2(\beta) &= \left(\frac{\pi^2}{pq}\right)^{\frac{3}{2}} \left(\bar{R}_{PQ}^2 + \frac{3}{2\alpha}\right) \left(\frac{\alpha}{\alpha+\beta}\right)^{\frac{5}{2}} \exp\left(-\beta\bar{R}_{PQ}^2\right), & (6.58)\\
D_4(\beta) &= \left(\frac{\pi^2}{pq}\right)^{\frac{3}{2}} \left(\bar{R}_{PQ}^4 + \frac{5}{\alpha}\bar{R}_{PQ}^2 + \frac{15}{4\alpha^2}\right) \left(\frac{\alpha}{\alpha+\beta}\right)^{\frac{7}{2}} \exp\left(-\beta\bar{R}_{PQ}^2\right), & (6.59)\\
D_{-1}(\beta) &= \left(\frac{\pi^2}{pq}\right)^{\frac{3}{2}} \sqrt{\frac{4\alpha}{\pi}}\, F_0\left(\alpha\bar{R}_{PQ}^2\right) \left(\frac{\alpha}{\alpha+\beta}\right) \exp\left(-\beta\bar{R}_{PQ}^2\right), & (6.60)\\
D_1(\beta) &= \left(\frac{\pi^2}{pq}\right)^{\frac{3}{2}} \sqrt{\frac{4\alpha}{\pi}} \left[\left(\bar{R}_{PQ}^2 + \frac{1}{2\alpha}\right) F_0\left(\alpha\bar{R}_{PQ}^2\right) + \frac{1}{2\alpha}\exp\left(-\alpha\bar{R}_{PQ}^2\right)\right] \\
&\times \left(\frac{\alpha}{\alpha+\beta}\right)^2 \exp\left(-\beta\bar{R}_{PQ}^2\right). & (6.61)
\end{aligned}$$

In the special case when $\beta = 0$ (no damping), $\bar{R}_{PQ}^2$ becomes R_{PQ}^2 and the two last factors in each integral become equal to one.

6.2.5 Evaluation of nonspherical Hermite integrals

To evaluate the nonspherical Hermite integrals Eqs. (6.24)–(6.28) from the spherical integrals discussed in Section 6.2.5, we first introduce the auxiliary integrals

$$H_{tuv}^{mn}(\mu,\nu) = \frac{\mathrm{d}^t}{\mathrm{d}P_x^t}\frac{\mathrm{d}^u}{\mathrm{d}P_y^u}\frac{\mathrm{d}^v}{\mathrm{d}P_z^v}\frac{\mathrm{d}^m}{\mathrm{d}\mu^m} \exp\left(-\mu R_{PQ}^2\right) F_n\left(\nu R_{PQ}^2\right) \quad (6.62)$$

which correspond to the Boys function Eq. (6.52) damped by a Gaussian. Inserting the expressions Eqs. (6.57)–(6.61) in Eqs. (6.24)–(6.28), we obtain:

$$R_1^{tuv} = \left(\frac{\pi^2}{pq}\right)^{\frac{3}{2}} \sqrt{\frac{4\alpha}{\pi}}\; H_{tuv}^{00}(0,\alpha), \tag{6.63}$$

$$R_2^{tuv} = \left(\frac{\pi^2}{pq}\right)^{\frac{3}{2}} \left(\frac{\alpha}{\alpha+\gamma}\right)^{\frac{3}{2}} H_{tuv}^{00}\left(\frac{\alpha\gamma}{\alpha+\gamma},0\right), \tag{6.64}$$

$$\begin{aligned} R_3^{tuv} &= \left(\frac{\pi^2}{pq}\right)^{\frac{3}{2}} \sqrt{\frac{4\alpha}{\pi}} \left(\frac{\alpha}{\alpha+\gamma}\right)^2 \\ &\times \left[\frac{1}{2\alpha} H_{tuv}^{00}(\alpha,0) + \frac{1}{2\alpha} H_{tuv}^{00}\left(\frac{\alpha\gamma}{\alpha+\gamma},\frac{\alpha^2}{\alpha+\gamma}\right) - \frac{\alpha}{\alpha+\gamma} H_{tuv}^{10}\left(\frac{\alpha\gamma}{\alpha+\gamma},\frac{\alpha^2}{\alpha+\gamma}\right)\right], \end{aligned} \tag{6.65}$$

$$\begin{aligned} R_4^{tuv} &= \left(\frac{\pi^2}{pq}\right)^{\frac{3}{2}} \left(\frac{\alpha}{\alpha+\gamma+\gamma'}\right)^{\frac{5}{2}} \\ &\times \left[\frac{3}{2\alpha} H_{tuv}^{00}\left(\frac{\alpha\gamma+\alpha\gamma'}{\alpha+\gamma+\gamma'},0\right) - \frac{\alpha}{\alpha+\gamma+\gamma'} H_{tuv}^{10}\left(\frac{\alpha\gamma+\alpha\gamma'}{\alpha+\gamma+\gamma'},0\right)\right], \end{aligned} \tag{6.66}$$

$$\begin{aligned} R_6^{tuv} &= \left(\frac{\pi^2}{pq}\right)^{\frac{3}{2}} \left(\frac{\alpha}{\alpha+\gamma+\gamma'}\right)^{\frac{3}{2}} \left\{\left[1 - \frac{3(\gamma+\gamma')}{\alpha+\gamma+\gamma'} + \frac{15\gamma\gamma'}{(\alpha+\gamma+\gamma')^2}\right] H_{tuv}^{00}\left(\frac{\alpha\gamma+\alpha\gamma'}{\alpha+\gamma+\gamma'},0\right)\right. \\ &+ 2\left[\gamma+\gamma' - \frac{10\gamma\gamma'}{\alpha+\gamma+\gamma'}\right] \left(\frac{\alpha}{\alpha+\gamma+\gamma'}\right)^2 H_{tuv}^{10}\left(\frac{\alpha\gamma+\alpha\gamma'}{\alpha+\gamma+\gamma'},0\right) \\ &+ \left.4\gamma\gamma' \left(\frac{\alpha}{\alpha+\gamma+\gamma'}\right)^4 H_{tuv}^{20}\left(\frac{\alpha\gamma+\alpha\gamma'}{\alpha+\gamma+\gamma'},0\right)\right\}. \end{aligned} \tag{6.67}$$

Clearly, the integrals R_k^{tuv} needed for the evaluation of the damped-R12 integrals are simple linear combinations of the damped Hermite integrals Eq. (6.62), whose recursive evaluation is now considered.

To determine recurrence relations for the damped Hermite integrals, we proceed as follows:

$$\begin{aligned} H_{t+1,u,v}^{mn} &= \frac{\mathrm{d}^t}{\mathrm{d}P_x^t}\frac{\mathrm{d}^u}{\mathrm{d}P_y^u}\frac{\mathrm{d}^v}{\mathrm{d}P_z^v}\frac{\mathrm{d}^m}{\mathrm{d}\mu^m}\frac{\mathrm{d}}{\mathrm{d}P_x} \exp\left(-\mu R_{PQ}^2\right) F_n\left(\nu R_{PQ}^2\right) && (6.68)\\ &= -2\frac{\mathrm{d}^t}{\mathrm{d}P_x^t}\frac{\mathrm{d}^m}{\mathrm{d}\mu^m}\mu X_{PQ} H_{0uv}^{0n} - 2\nu\frac{\mathrm{d}^t}{\mathrm{d}P_x^t} X_{PQ} H_{0uv}^{m,n+1}. && (6.69) \end{aligned}$$

By making use of the relations

$$\frac{\mathrm{d}^t}{\mathrm{d}P_x^t} X_{PQ} = t\frac{\mathrm{d}^{t-1}}{\mathrm{d}P_x^{t-1}} + X_{PQ}\frac{\mathrm{d}^t}{\mathrm{d}P_x^t}, \tag{6.70}$$

$$\frac{\mathrm{d}^m}{\mathrm{d}\mu^m}\mu = m\frac{\mathrm{d}^{m-1}}{\mathrm{d}\mu^{m-1}} + \mu\frac{\mathrm{d}^m}{\mathrm{d}\mu^m}, \tag{6.71}$$

we obtain:

$$\begin{aligned} H^{mn}_{t+1,u,v} &= -2\left(t\frac{\mathrm{d}^{t-1}}{\mathrm{d}P_x^{t-1}} + X_{PQ}\frac{\mathrm{d}^{t}}{\mathrm{d}P_x^{t}}\right)\left(m\frac{\mathrm{d}^{m-1}}{\mathrm{d}\mu^{m-1}} + \mu\frac{\mathrm{d}^{m}}{\mathrm{d}\mu^{m}}\right) H^{0n}_{0uv} \\ &\quad -2\nu\left(t\frac{\mathrm{d}^{t-1}}{\mathrm{d}P_x^{t-1}} + X_{PQ}\frac{\mathrm{d}^{t}}{\mathrm{d}P_x^{t}}\right) H^{m,n+1}_{0uv} \\ &= -2tmH^{m-1,n}_{t-1,u,v} - 2t\mu H^{mn}_{t-1,u,v} - 2X_{PQ}mH^{m-1,n}_{tuv} - 2X_{PQ}\mu H^{mn}_{tuv} \\ &\quad -2\nu t H^{m,n+1}_{t-1,u,v} - 2\nu X_{PQ} H^{m,n+1}_{tuv}. \end{aligned} \tag{6.72}$$

Similar relations may be established for increments in u and v, giving the following three sets of six-term recurrence relations:

$$\begin{aligned} H^{mn}_{t+1,u,v}(\mu,\nu) &= -2\mu\left[tH^{mn}_{t-1,u,v}(\mu,\nu) + X_{PQ}H^{mn}_{tuv}(\mu,\nu)\right] \\ &\quad - 2m\left[tH^{m-1,n}_{t-1,u,v}(\mu,\nu) + X_{PQ}H^{m-1,n}_{tuv}(\mu,\nu)\right] \\ &\quad - 2\nu\left[tH^{m,n+1}_{t-1,u,v}(\mu,\nu) + X_{PQ}H^{m,n+1}_{tuv}(\mu,\nu)\right], \end{aligned} \tag{6.73}$$

$$\begin{aligned} H^{mn}_{t,u+1,v}(\mu,\nu) &= -2\mu\left[uH^{mn}_{t,u-1,v}(\mu,\nu) + Y_{PQ}H^{mn}_{tuv}(\mu,\nu)\right] \\ &\quad - 2m\left[uH^{m-1,n}_{t,u-1,v}(\mu,\nu) + Y_{PQ}H^{m-1,n}_{tuv}(\mu,\nu)\right] \\ &\quad - 2\nu\left[uH^{m,n+1}_{t,u-1,v}(\mu,\nu) + Y_{PQ}H^{m,n+1}_{tuv}(\mu,\nu)\right], \end{aligned} \tag{6.74}$$

$$\begin{aligned} H^{mn}_{t,u,v+1}(\mu,\nu) &= -2\mu\left[vH^{mn}_{t,u,v-1}(\mu,\nu) + Z_{PQ}H^{mn}_{tuv}(\mu,\nu)\right] \\ &\quad - 2m\left[vH^{m-1,n}_{t,u,v-1}(\mu,\nu) + Z_{PQ}H^{m-1,n}_{tuv}(\mu,\nu)\right] \\ &\quad - 2\nu\left[vH^{m,n+1}_{t,u,v-1}(\mu,\nu) + Z_{PQ}H^{m,n+1}_{tuv}(\mu,\nu)\right]. \end{aligned} \tag{6.75}$$

Using these recurrence relations, we may generate all the necessary integrals H^{mn}_{tuv}, starting from the source integrals

$$H^{mn}_{000}(\mu,\nu) = (-1)^m R^{2m}_{PQ}\exp\left(-\mu R^2_{PQ}\right)F_n\left(\nu R^2_{PQ}\right). \tag{6.76}$$

The evaluation of the Boys function $F_n\left(\nu R^2_{PQ}\right)$ may be carried out as discussed in Ref. [14].

Although the recurrence relations Eqs. (6.73)–(6.75) look rather complicated, some simplifications occur in important special cases. For example, whenever one of the two arguments μ or ν to $H^{mn}_{tuv}(\mu,\nu)$ is zero—as happens in many cases in Eqs. (6.63)–(6.67)—the six-term recurrence relations reduce to four-term recurrences. We also note that, in the evaluation of the Hermite integrals Eqs. (6.63)–(6.67), only integrals of the type $H^{m0}_{tuv}(\mu,\nu)$ are needed. The integrals $H^{mn}_{tuv}(\mu,\nu)$ with $n > 0$ were introduced only because they arise upon differentation of $H^{m0}_{tuv}(\mu,\nu)$, playing the role of intermediates in the recurrence relations Eqs. (6.73)–(6.75). Finally, it should be realized that, in the application of the recurrence relations Eqs. (6.73)–(6.75), all integrals $H^{k,n}_{tuv}$ with $k < m$ and all integrals $H^{m,k}_{tuv}$ with $k > n$ must be evaluated before the integrals H^{mn}_{tuv} are attempted.

6.3 Conclusion

All integrals discussed in this paper have been implemented in a local version of the Dalton [17] program and will be used to investigate explicitly correlated methods for large molecular systems. For small systems, some preliminary calculations on systems such as H_2O, CO and F_2 have shown that the computation time does not differ significantly from previous R12 methods. For large systems, however, the new correlation factor is expected to reduce dramatically the number of significant integrals, thereby making the calculations more efficient.

Acknowledgments

The authors thank Pål Dahle for calculations with his Gaussians Geminals code which allowed the verification of $(ab|\exp(-\gamma\, r_{12}^2)|cd)$ integrals. The research of W.K. has been made possible by a fellowship of the Royal Netherlands Academy of Arts and Sciences. We gratefully acknowledge partial support from COST Chemistry Action D9.

References

[1] C. Schwartz, Phys. Rev. **126**, 1015 (1962).

[2] R. N. Hill, J. Chem. Phys. **83**, 1173 (1985).

[3] W. Kutzelnigg, Theor. Chim. Acta **68**, 445 (1985).

[4] W. Klopper and W. Kutzelnigg, Chem. Phys. Lett. **134**, 17 (1987).

[5] W. Kutzelnigg and J. D. Morgan III, J. Chem. Phys. **96**, 4484 (1992).

[6] P. Wind, T. Helgaker, and W. Klopper, Theor. Chim. Acta **106**, 280 (2001).

[7] P. Wind, W. Klopper, and T. Helgaker, Theor. Chim. Acta **107**, 173 (2002).

[8] W. Klopper and C. C. M. Samson, J. Chem. Phys. **116**, 6397 (2002).

[9] B. J. Persson and P. R. Taylor, J. Chem. Phys. **105**, 5915 (1996).

[10] B. J. Persson and P. R. Taylor, Theor. Chim. Acta **97**, 240 (1997).

[11] P. Dahle and P. R. Taylor, Theor. Chim. Acta **105**, 401 (2001).

[12] L. E. McMurchie and E. R. Davidson, J. Comput. Phys. **26**, 218 (1978).

[13] W. Klopper and R. Röhse, Theor. Chim. Acta **83**, 441 (1992).

[14] T. Helgaker, P. Jørgensen, and J. Olsen, *Molecular Electronic-Structure Theory*, John Wiley & Sons, Ltd., Chichester, New York, (2000).

[15] T. Helgaker and P. R. Taylor, Theor. Chim. Acta **83**, 177 (1992).

[16] S. F. Boys, Proc. Roy. Soc. (London) **A200**, 542 (1950).

[17] T. Helgaker, H. J. Aa. Jensen, P. Jørgensen, J. Olsen, K. Ruud, H. Ågren, A. A. Auer, K. L. Bak, V. Bakken, O. Christiansen, S. Coriani, P. Dahle, E. K. Dalskov, T. Enevoldsen, B. Fernandez, C. Hättig, K. Hald, A. Halkier, H. Heiberg, H. Hettema, D. Jonsson, S. Kirpekar, R. Kobayashi, H. Koch, K. V. Mikkelsen, P. Norman, M. J. Packer, T. B. Pedersen, T. A. Ruden, A. Sanchez, T. Saue, S. P. A. Sauer, B. Schimmelpfennig, K. O. Sylvester-Hvid, P. R. Taylor, and O. Vahtras, *Dalton, a molecular electronic structure program*, Release 1.2 (2001).

7

Similarity-transformed Hamiltonians by means of Gaussian-damped interelectronic distances

Abstract

A method is presented to improve the description of electron correlation in configuration interaction (CI) calculations. In this method, the standard CI expansion ψ is multiplied by a correlation function $\phi = \exp F$ with

$$F = \sum_{m=1}^{M} c_m \sum_{i<j} r_{ij} \exp(-\gamma_m r_{ij}^2).$$

With this correlation function, the total wave function $\Psi = \phi\psi$ exhibits the right behavior when two electrons coalesce while F vanishes for large interelectronic distances. The correlation function is implemented using the methodology of similarity-transformed Hamiltonians (STH) and is applied to two-electron systems. A generalization to many-electron systems is indicated. The new method yields more accurate results than standard CI calculations of the energy and interelectronic distance of the He atom. The H_2 molecule was chosen to study the long-range behavior of the correlation function.

H. J. A. Zweistra, C. C. M. Samson, and W. Klopper, Collect. Czech. Chem. Commun. **68**, 374 (2003).

7.1 Introduction

In nonrelativistic quantum chemistry, much effort has been put forth to compute approximate solutions of the time-independent Schrödinger equation $\hat{H}\Psi = E\Psi$. The convergence of the calculation of accurate approximate solutions of the Hamiltonian is often hampered by electron correlation, a phenomenon related to the instantaneous repulsions among the electrons. Electron correlation cannot be taken into account by independent-particle models (*e.g.*, Hartree–Fock) where instantaneous repulsions are neglected. Although such models may yield acceptable results on many occasions, correlation effects need to be taken into account for various purposes, for example for the description of bond dissociation and dispersion forces. In the present study, an attempt is undertaken to enhance the description of electron correlation in order to improve the convergence and accuracy of configuration interaction (CI) calculations.

The exact nonrelativistic wave function satisfies Kato's correlation cusp condition[1]

$$\lim_{r_{ij}\to 0}\left(\frac{\partial\Psi}{\partial r_{ij}}\right)_{\text{av}} = \frac{1}{2}\Psi_{(r_{ij}=0)}, \tag{7.1}$$

where "av" stands for spherical averaging. The description of the correlation cusp and the amount of electron correlation in CI calculations can be significantly enhanced if we add a correlation function to the wave function, that is, if we write the wave function as $\Psi = \phi\psi$, where ψ is a standard CI-type expansion (*i.e.*, a linear combination of orbital products) and ϕ is a correlation function [2–4]. Since $\partial\psi/\partial r_{ij} = 0$, it follows that ϕ should satisfy the cusp condition. This fact can be exploited to design appropriate correlation functions. Furthermore, ϕ should remain finite when r_{ij} approaches infinity in order not to corrupt the standard CI-type expansion ψ. In the present study, therefore, we have decided to investigate the correlation function $\phi = \exp F$ with

$$F = \sum_{m=1}^{M} c_m \sum_{i<j} G_{ij}^m \tag{7.2}$$

and

$$G_{ij}^m = r_{ij}\exp(-\gamma_m r_{ij}^2). \tag{7.3}$$

Note that ϕ satisfies the cusp condition when

$$\sum_{m=1}^{M} c_m = 1/2, \tag{7.4}$$

irrespective of ψ. Moreover, the correlation function approaches unity when r_{ij} becomes large.

In this paper, we shall present a method to implement the above-described correlation function using the transcorrelated method previously developed by Boys and Handy [5–12] and reviewed

by one of us [13, 14] as well as by Nooijen and Bartlett [15]. All of the formulae for the implementation are derived for any number of electrons but the method has thus far been applied only to two-electron systems.

Our present work is closely related to the very recent work by Ten-no and co-workers [16–20]. However, their method differs from ours since they use correlation functions with

$$\tilde{G}_{ij}^{m} = \exp(-\gamma_m r_{ij}^2), \tag{7.5}$$

that is, *without* the linear r_{ij} term. The Gaussian functions (Eq. 7.5) do not satisfy the correlation cusp. Rather, they are used to fit the Coulomb hole. One motivation for the present work was to supplement the method of Ten-no and co-workers by linear r_{ij} terms.

Calculations on the He atom were performed in large basis sets of Gaussian atomic orbitals (AOs) to assess the quality of the description of short-range correlation by the new wave functions. The H_2 molecule (with different internuclear distances) was used as a model system to investigate the long-range behavior of the correlation function and to optimize the parameter γ, which determines the range of correlations. We furthermore indicate how to calculate expectation values using the new wave functions and, finally, we investigate the convergence behavior of the new method in comparison with traditional CI.

7.2 Theory

7.2.1 Similarity-transformed Hamiltonians

In atomic units, the molecular electronic Hamiltonian is written as

$$\hat{H} = V_{\mathrm{nuc}} + \sum_i \hat{h}_i + \sum_{i<j} \frac{1}{r_{ij}}, \tag{7.6}$$

where V_{nuc} is the nuclear repulsion energy

$$V_{\mathrm{nuc}} = \sum_{K<L} \frac{Z_K Z_L}{r_{KL}}, \tag{7.7}$$

$\hat{h}_i$ is the one-electron Hamiltonian

$$\hat{h}_i = -\frac{1}{2}\Delta_i - \sum_K \frac{Z_K}{r_{iK}}, \tag{7.8}$$

and $r_{ij} = |\vec{r}_i - \vec{r}_j|$ is the interelectronic distance. The sums over i and j run over the electrons and the sums over K and L run over the nuclei in the molecule.

We write the molecular electronic wave function as

$$\Psi = \phi\psi_R = \exp(F)\psi_R = \phi^{-1}\psi_L = \exp(-F)\psi_L, \qquad F = \sum_{i<j} f_{ij}, \tag{7.9}$$

where f_{ij} is a symmetric two-electron function (geminal), which in the present work is chosen as a linear combination of *Gaussian-damped interelectronic distances*

$$f_{ij} = \sum_{m=1}^{M} c_m G_{ij}^m, \qquad G_{ij}^m = r_{ij}\exp(-\gamma_m r_{ij}^2). \tag{7.10}$$

The c_m and γ_m are adjustable parameters.

We multiply the molecular electronic Schrödinger equation $\hat{H}\Psi = E\Psi$ from the left by the operator $\exp(-F)$ to obtain

$$\exp(-F)\hat{H}\exp(F)\psi_R = E\psi_R, \tag{7.11}$$

which may be regarded as a Schrödinger equation with an effective, non-Hermitian *similarity-transformed Hamiltonian* (STH)

$$\hat{H}^F = \exp(-F)\hat{H}\exp(F), \tag{7.12}$$

which corresponds to the Hirschfelder Hamiltonian[2]

$$\hat{H}^F = \hat{H} + \phi^{-1}[\hat{H},\phi] = \hat{H} - \frac{1}{2}\phi^{-1}\sum_i \left\{(\Delta_i\phi) + 2(\vec{\nabla}_i\phi)\cdot\vec{\nabla}_i\right\}. \tag{7.13}$$

The nested-commutator expansion of $\hat{H}^F$ yields

$$\hat{H}^F = \hat{H} + [\hat{H},F] + \frac{1}{2}[[\hat{H},F],F]. \tag{7.14}$$

$[\hat{H},F]$ constitutes the two-electron operator

$$[\hat{H},F] = -\frac{1}{2}\sum_i\sum_{j\neq i}\left\{(\Delta_i f_{ij}) + 2(\vec{\nabla}_i f_{ij})\cdot\vec{\nabla}_i\right\}, \tag{7.15}$$

while the double commutator gives rise to the three-electron operator

$$\frac{1}{2}[[\hat{H},F],F] = -\frac{1}{2}\sum_i\sum_{j\neq i}\sum_{k\neq i}(\vec{\nabla}_i f_{ij})\cdot(\vec{\nabla}_i f_{ik}). \tag{7.16}$$

Since $[[[\hat{H},F],F],F] = 0$, there are no terms beyond the double commutator in the nested-commutator expansion.

The similarity-transformed Hamiltonian has right and left eigenfunctions ψ_R and ψ_L, respectively. In particular,

$$\hat{H}^F\psi_R = E\psi_R, \qquad \left(\hat{H}^F\right)^\dagger \psi_L = E\psi_L, \tag{7.17}$$

with

$$\left(\hat{H}^F\right)^\dagger = \exp(F)\hat{H}\exp(-F) = \hat{H}^F - 2[\hat{H}, F]. \tag{7.18}$$

Finally, the expectation value of an operator $\hat{O}$ is computed according to

$$\langle\hat{O}\rangle = \langle\Psi|\hat{O}|\Psi\rangle\langle\Psi|\Psi\rangle^{-1} = \langle\psi_L|\hat{O}^F|\psi_R\rangle\langle\psi_L|\psi_R\rangle^{-1}. \tag{7.19}$$

7.2.2 Two-electron systems

For a system with only two electrons, we obtain the following expression for the single commutator:

$$[\hat{H}, F] = \sum_{m=1}^{M} c_m[\hat{H}, G_{12}^m], \tag{7.20}$$

with

$$[\hat{H}, G_{12}^m] = -\frac{1}{2}(\Delta_1 G_{12}^m) - \frac{1}{2}(\Delta_2 G_{12}^m) - (\vec{\nabla}_1 G_{12}^m)\cdot\vec{\nabla}_1 - (\vec{\nabla}_2 G_{12}^m)\cdot\vec{\nabla}_2. \tag{7.21}$$

Noting that

$$\begin{aligned}
(\vec{\nabla}_1 G_{12}^m) &= \vec{r}_{12} r_{12}^{-1}\left(1 - 2\gamma_m r_{12}^2\right)\exp(-\gamma_m r_{12}^2), &(7.22)\\
(\Delta_1 G_{12}^m) &= r_{12}^{-1}\left(2 - 10\gamma_m r_{12}^2 + 4\gamma_m^2 r_{12}^4\right)\exp(-\gamma_m r_{12}^2), &(7.23)
\end{aligned}$$

we rewrite Eq. (7.21) as

$$\begin{aligned}
[\hat{H}, G_{12}^m] &= -r_{12}^{-1}\exp(-\gamma_m r_{12}^2)\left\{2 - 10\gamma_m r_{12}^2 + 4\gamma_m^2 r_{12}^4\right.\\
&+ \left.(1 - 2\gamma_m r_{12}^2)\,\vec{r}_{12}\cdot\left(\vec{\nabla}_1 - \vec{\nabla}_2\right)\right\}. &(7.24)
\end{aligned}$$

Similarly, for the double commutator, we obtain

$$\frac{1}{2}[[\hat{H}, F], F] = \frac{1}{2}\sum_{m=1}^{M}\sum_{m'=1}^{M} c_m c_{m'}[[\hat{H}, G_{12}^m], G_{12}^{m'}], \tag{7.25}$$

with

$$\begin{aligned}
\frac{1}{2}[[\hat{H}, G_{12}^m], G_{12}^{m'}] &= -\frac{1}{2}(\vec{\nabla}_1 G_{12}^m)\cdot(\vec{\nabla}_1 G_{12}^{m'}) - \frac{1}{2}(\vec{\nabla}_2 G_{12}^m)\cdot(\vec{\nabla}_2 G_{12}^{m'})\\
&= -\left(1 - 2\gamma_m r_{12}^2\right)\left(1 - 2\gamma_{m'} r_{12}^2\right)\exp\left\{-(\gamma_m + \gamma_{m'})r_{12}^2\right\}. &(7.26)
\end{aligned}$$

If we restrict the sum in Eq. (7.10) to only one term with $\gamma_1 = 0$, the commutators reduce to the expressions

$$[\hat{H}, r_{12}] = -\frac{2}{r_{12}} - \frac{\vec{r}_{12}}{r_{12}} \cdot \left(\vec{\nabla}_1 - \vec{\nabla}_2\right), \qquad \frac{1}{2}[[\hat{H}, r_{12}], r_{12}] = -1, \tag{7.27}$$

and the similarity-transformed Hamiltonian in this special case becomes

$$\hat{H}^F = V_{\text{nuc}} + \hat{h}_1 + \hat{h}_2 + (1 - 2c_1)\frac{1}{r_{12}} - c_1\frac{\vec{r}_{12}}{r_{12}} \cdot \left(\vec{\nabla}_1 - \vec{\nabla}_2\right) - c_1^2. \tag{7.28}$$

In Eq. (7.28), the Coulomb singularity in $(1 - 2c_1)/r_{12}$ vanishes when $c = 1/2$. Thus, for this value of c_1, a much improved convergence rate is expected for the CI expansion of $\hat{H}^F$ in comparison with $\hat{H}$.

7.2.3 Many-electron systems

It was shown that three-electron integrals are the most involved integrals to be computed for n-electron systems. Still, these integrals can be computationally quite demanding, especially in the multicenter case. Ten-no and co-workers [16–20] have derived methods to compute the three-electron integrals in Eq. (7.16) by means of resolution-of-identity approximations (closure approximations) to reduce the cost of the calculation.

These resolution-of-identity approximations should also be invoked in all of the formulae that occur with the correlation functions of the present work. All of the two-electron integrals are available to do so.

7.3 Computational details

The two-electron integrals required for the present study were implemented into the DALTON program [21]. This implementation is described in detail elsewhere [22].

The $19s16p14d12f10g8h6i4k$ Gaussian basis for He was derived from the $17s$ set of Huzinaga and Miguel[23, 24] in two steps. First, functions of angular symmetry ℓ were added whose exponents were obtained by multiplying the respective number of smallest exponents of the $17s$ set with the factor $(2\ell + 1)/3$. Second, two diffuse s functions were added with exponents 0.043 and 0.0215 a_0^{-2}.

The calculations on H_2 were carried out in the $5s4p$ subset of the aug-cc-pVQZ basis[24, 25].

Table 7.1: He atom ground-state energy, obtained from calculations with the similarity-transformed Hamiltonian of Eq. (7.28) with $c_1 = \frac{1}{2}$, in comparison with standard CI calculations.

Basis set[a]	$E(\hat{H}^F)/E_\mathrm{h}$	$\delta(\hat{H}^F)/\mu E_\mathrm{h}$[b]	$E(\hat{H})/E_\mathrm{h}$	$\delta(\hat{H})/\mu E_\mathrm{h}$[b]
$19s$	-3.01077236	-107048	-2.87902761	24697
$19s16p$	-2.90483130	-1107	-2.90051353	3211
$19s16p14d$	-2.90406141	-337	-2.90276212	963
$19s16p14d12f$	-2.90380589	-82	-2.90331421	410
$19s16p14d12f10g$	-2.90375143	-27	-2.90350963	215
$19s16p14d12f10g8h$	-2.90373520	-11	-2.90359460	130
$19s16p14d12f10g8h6i$	-2.90372933	-5	-2.90363464	90
$19s16p14d12f10g8h6i4k$	-2.90372745	-3	-2.90364706	77

[a] Subsets of the $19s16p14d12f10g8h6i4k$ basis.

[b] Error with respect to the exact value of E=-2.903724377 E_h from Ref. [26]. See also Ref. [27].

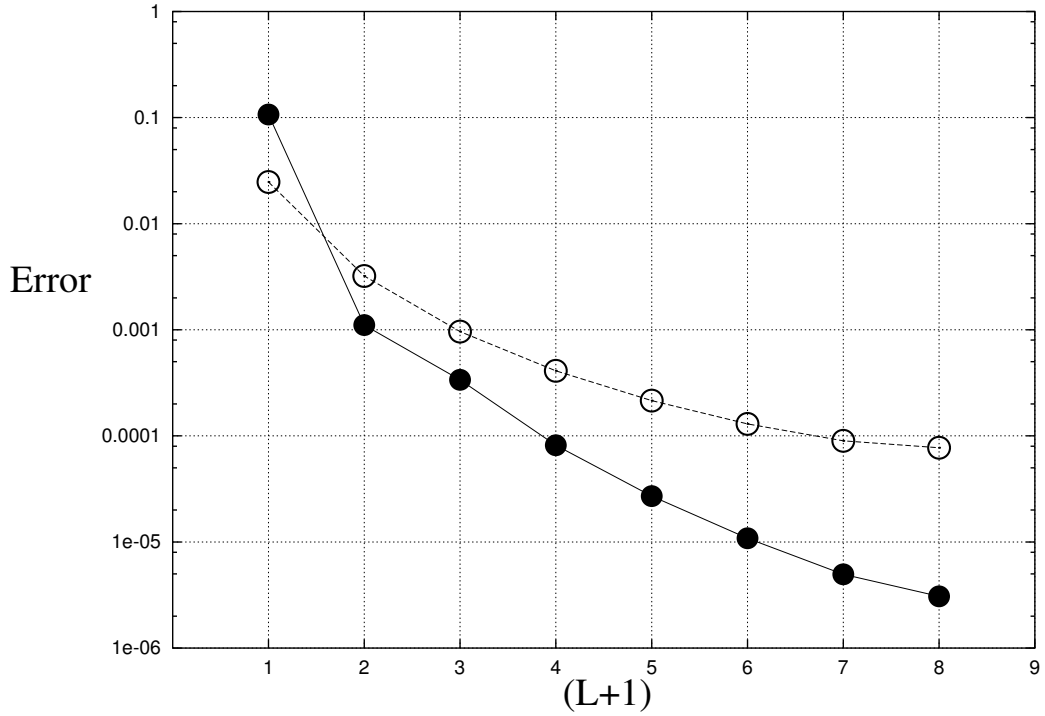

Figure 7.1: Absolute error (in E_h) in the He ground-state energy of the standard CI expansion (○) and of the similarity-transformed Hamiltonian of Eq. (7.28) with $c_1 = \frac{1}{2}$ (●) as a function of the basis set.

Table 7.2: He atom ground-state kinetic energy, potential energy, virial, and expectation values of r_{12}, obtained from standard CI calculations.

Basis set[a]	$\langle\hat{T}\rangle/E_\mathrm{h}$	$\langle V\rangle/E_\mathrm{h}$	$-\frac{1}{2}\langle V\rangle/\langle\hat{T}\rangle$	$\langle r_{12}\rangle/a_0$
$19s$	2.879027	-5.758055	1.000000	1.387999
$19s16p$	2.900513	-5.801026	1.000000	1.424184
$19s16p14d$	2.902761	-5.805523	1.000000	1.422838
$19s16p14d12f$	2.903313	-5.806627	1.000000	1.422413
$19s16p14d12f10g$	2.903508	-5.807017	1.000000	1.422254
$19s16p14d12f10g8h$	2.903595	-5.807189	1.000000	1.422182
$19s16p14d12f10g8h6i$	2.903623	-5.807257	1.000002	1.422149
$19s16p14d12f10g8h6i4k$	2.90,614	-5.807261	1.000006	1.422141
∞[b]	2.903724	-5.807449	1.000000	1.422070

[a] Cf. Table 7.1.

[b] From Ref. [28].

Table 7.3: He atom ground-state kinetic energy, potential energy, virial, and expectation values of r_{12}, obtained from calculations with the similarity-transformed Hamiltonian of Eq. (7.28) with $c_1 = \frac{1}{2}$.

Basis set[a]	$\langle\hat{T}\rangle/E_\mathrm{h}$	$\langle V\rangle/E_\mathrm{h}$	$-\frac{1}{2}\langle V\rangle/\langle\hat{T}\rangle$	$\langle r_{12}\rangle/a_0$
$19s$	2.747273	-5.758046	1.047956	1.386425
$19s16p$	2.902073	-5.806904	1.000475	1.416121
$19s16p14d$	2.901593	-5.805654	1.000425	1.421608
$19s16p14d12f$	2.902853	-5.806659	1.000164	1.421953
$19s16p14d12f10g$	2.903273	-5.807025	1.000082	1.422036
$19s16p14d12f10g8h$	2.903454	-5.807189	1.000048	1.422060
$19s16p14d12f10g8h6i$	2.903538	-5.807268	1.000033	1.422068
$19s16p14d12f10g8h6i4k$	2.903567	-5.807294	1.000028	1.422071
∞[b]	2.903724	-5.807449	1.000000	1.422070

[a] Cf. Table 7.1.

[b] From Ref. [28].

7.4 Results

Figure 7.1 as well as Tables 7.1 to 7.3 demonstrate that the STH method yields a more accurate total energy and interelectronic distance than standard CI calculations of the He atom ground-state. Furthermore, the error decreases much faster with the STH method than with standard CI when the number of basis functions is increased. More is gained by the STH method in a larger basis. When only s-type functions are used, the standard CI method appears to be superior in accuracy to the STH. This might be due to the choice of basis functions, which were optimized for standard CI calculations and not for the similarity-transformed Hamiltonian. However, although the total energy is very accurate, the individual STH expectation values for kinetic and potential energy are less accurate than their counterparts from standard CI calculations (Tables 7.2 and 7.3). Again, this might be due to the choice of basis set, which is nearly optimal for standard CI calculations. A better basis set for the STH calculations could perhaps be generated by scaling all basis-set exponents by a certain factor, but this has not yet been attempted.

When the quality of the calculation is tested as a function of γ, it is observed that the error is increased for intermediate values of γ (Table 7.4 and Figure 7.2). The reason for the deterioriation

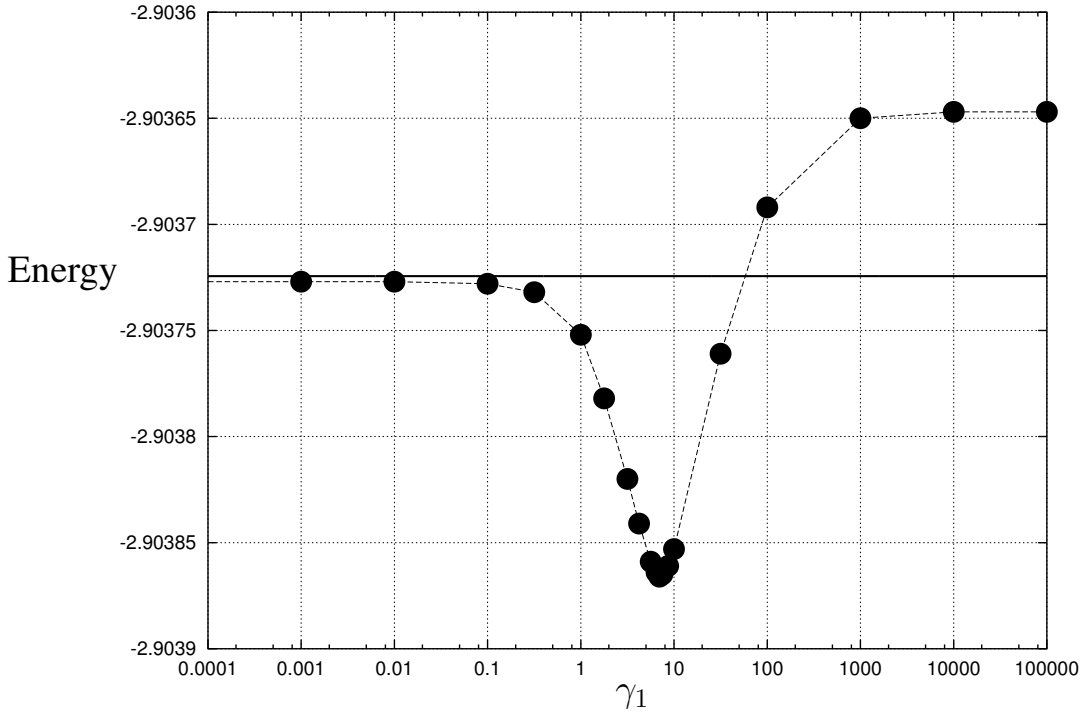

Figure 7.2: He atom ground-state energy obtained from calculations with the similarity-transformed Hamiltonian of Eq. (7.12) in the $19s16p14d12f10g8h6i4k$ basis with M=1 and $c_1 = \frac{1}{2}$, as a function of the damping parameter γ_1. The horizontal line indicates the exact energy.

is unknown. We conclude that γ should be kept small to describe short-range correlation effectively.

On the other hand, the calculations of the stretched H_2 molecule indicate that γ should be sufficiently large to maintain convergence in the calculation when the interelectronic distance is very long. Because of this controversy, it is impossible to make conclusive statements about the optimal value of parameter γ. The choice of γ obviously depends on the mutual distances between the electrons in the system. An STH calculation of a large n-electron molecule should perhaps be preceded by an inexpensive CI or even Hartree–Fock calculation in a small basis to estimate

Table 7.4: He atom ground-state energy obtained from calculations with the similarity-transformed Hamiltonian of Eq. (7.12) in the $19s16p14d12f10g8h6i4k$ basis with M=1 and $c_1 = \frac{1}{2}$.

$\log_{10}(\gamma_1)$	$-E/E_\mathrm{h}$
-∞	-2.903727
-3.00000	-2.903727
-2.00000	-2.903727
-1.00000	-2.903728
-0.50000	-2.903732
0.00000	-2.903752
0.25000	-2.903782
0.50000	-2.903820
0.62500	-2.903841
0.75000	-2.903859
0.81250	-2.903864
0.84375	-2.903866
0.87500	-2.903865
0.93750	-2.903861
1.00000	-2.903853
1.50000	-2.903761
2.00000	-2.903692
3.00000	-2.903650
4.00000	-2.903647
∞	-2.903647

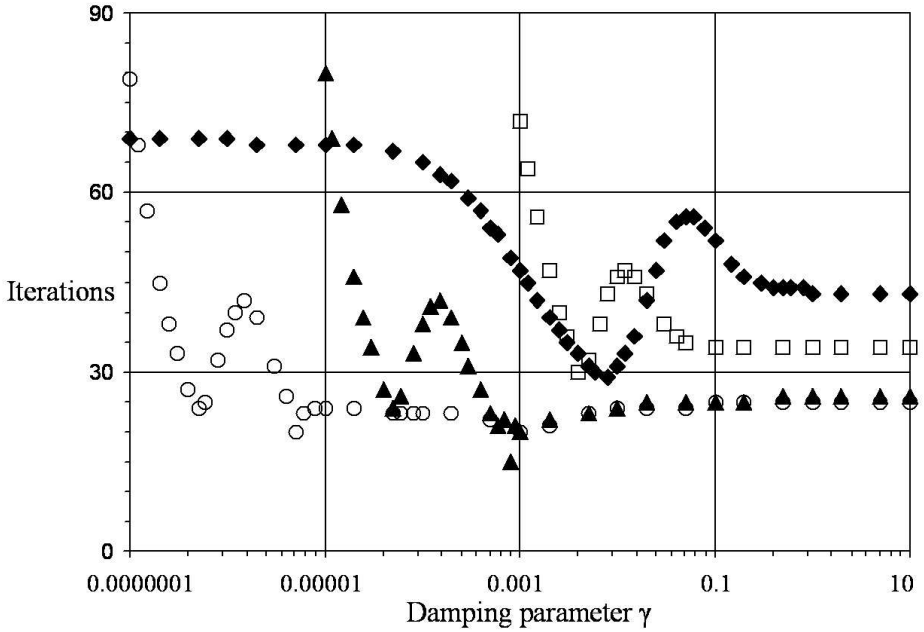

Figure 7.3: Number of iterations needed to solve the CI equations for the H_2 molecule as a function of the damping parameter γ. Results are shown for internuclear H–H distances of 5.0 (⧫), 10.0 (□), 100.0 (▲), and 1000.0 (○) a_0.

the average interelectronic distance $\langle r_{12} \rangle$. The damping parameters γ_m could perhaps be chosen accordingly.

The optimal value of γ seems to be a certain threshold value γ^{thr}, which is small but just large enough so that the calculation still converges. It is observed from Figure 7.3 that the threshold to convergence is $\gamma^{\mathrm{thr}} \propto \langle r_{12} \rangle$.

Finally, we note that Ten-no and co-workers [16–20] have developed a useful fitting procedure for obtaining the γ_m in the expansion Eq. (7.2) in terms of their correlation functions given in Eq. (7.5). it would therefore be interesting to see how the same procedure would perform with our correlation functions given in Eq. (7.3).

7.5 Conclusions

The newly developed STH method outshines the standard CI method in the description of the He atom. The error in the total energy is smaller and decreases much faster when the number of basis functions is increased. It has been shown that the STH method is also successful in calculating expectation values (*e.g.*, $\langle r_{12} \rangle$).

The STH method with the here presented correlation function is also capable of describing systems with large interelectronic distances, provided that the damping parameter γ is large enough. In future work, the method should be extended to many-electron systems using closure approximations in order to apply this and similar techniques to general molecules.

Acknowledgments

It is a pleasure to dedicate this paper to Dr. Petr Čársky, Dr. Ivan Hubač, and Dr. Miroslav Urban on the occasion of their 60^{th} birthday. The research of W.K. has been made possible by a fellowship of the Royal Netherlands Academy of Arts and Sciences. We gratefully acknowledge partial support from COST Chemistry Action D9 (Working Group 13/98) and a generous grant of computing time from National Computing Facilities (NCF) Foundation.

References

[1] T. Kato, Commun. Pure Appl. Math. **10**, 151 (1957).

[2] J. O. Hirschfelder, J. Chem. Phys. **39**, 3145 (1963).

[3] K. Jankowski, Acta Phys. Pol. **XXXII**, 421 (1967).

[4] K. Jankowski, Acta Phys. Pol. A **37**, 669 (1970).

[5] S. F. Boys and N. C. Handy, Proc. Roy. Soc. (London) **309**, 209 (1969).

[6] S. F. Boys and N. C. Handy, Proc. Roy. Soc. (London) **310**, 43 (1969).

[7] S. F. Boys and N. C. Handy, Proc. Roy. Soc. (London) **310**, 63 (1969).

[8] S. F. Boys and N. C. Handy, Proc. Roy. Soc. (London) **311**, 309 (1969).

[9] N. C. Handy, J. Phys. Chem. **51**, 3205 (1969).

[10] N. C. Handy, Mol. Phys. **21**, 817 (1971).

[11] N. C. Handy, Mol. Phys. **23**, 1 (1972).

[12] N. C. Handy, Mol. Phys. **26**, 169 (1973).

[13] W. Klopper, *Habil. Thesis*, Swiss Federal Institute of Technology, Zürich, (1996).

[14] W. Klopper, *In: The Encyclopedia of Computational Chemistry, Vol.4, pp. 2351–2375*, P. v. R. Schleyer, N. L. Allinger, T. Clark, J. Gasteiger, P. A. Kollman, H. F. Schaefer III, and P. R. Schreiner (Eds.), John Wiley & Sons, Ltd., Chichester, New York, (1998).

[15] M. Nooijen and R. J. Bartlett, J. Chem. Phys. **109**, 8232 (1998).

[16] S. Ten-no, Chem. Phys. Lett. **330**, 169 (2000).

[17] S. Ten-no, Chem. Phys. Lett. **330**, 175 (2000).

[18] O. Hino, Y. Tanimura, and S. Ten-no, J. Chem. Phys. **115**, 7865 (2001).

[19] O. Hino, Y. Tanimura, and S. Ten-no, Chem. Phys. Lett. **353**, 317 (2002).

[20] S. Ten-no and O. Hino, Int. J. Mol. Sci. **3**, 459 (2002).

[21] T. Helgaker, H. J. Aa. Jensen, P. Jørgensen, J. Olsen, K. Ruud, H. Ågren, T. Andersen, K. L. Bak, V. Bakken, O. Christiansen, E. K. Dalskov, T. Enevoldsen, B. Fernandez, H. Heiberg, H. Hettema, D. Jonsson, S. Kirpekar, R. Kobayashi, H. Koch, K. V. Mikkelsen, P. Norman, M. J. Packer, T. Saue, S. P. A. Sauer, P. R. Taylor, and O. Vahtras, *Dalton, a molecular electronic structure program*, Release 1.1.

[22] C. C. M. Samson, W. Klopper, and T. Helgaker, Comput. Phys. Commun. **149**, 1 (2002).

[23] S. Huzinaga and B. Miguel, Chem. Phys. Lett. **175**, 289 (1990).

[24] Basis sets were obtained from the Extensible Computational Chemistry Environment Basis Set Database, Version 2/20/02, as developed and distributed by the Molecular Science Computing Facility, Environmental and Molecular Sciences Laboratory which is a part of the Pacific Northwest Laboratory, P.O. Box 999, Richland, Washington 99352, USA, and funded by the U.S. Department of Energy. The Pacific Northwest Laboratory is a multiprogram laboratory operated by Battelle Memorial Institute for the U.S. Department of Energy under Contract No. DE-AC06-76RLO 1830.

[25] D. E. Woon and T. H. Dunning, Jr., J. Chem. Phys. **100**, 2975 (1994).

[26] K. Frankowski and C. L. Pekeris, Phys. Rev. **146**, 46 (1966).

[27] G. W. F. Drake, M. M. Cassar, and R. A. Nistor, Phys. Rev. A **65**, 054501 (2002).

[28] C. L. Pekeris, Phys. Rev. **115**, 1216 (1959).

8

Benchmarking ethylene and ethane: Second-order Møller–Plesset pair energies for localized molecular orbitals

Abstract

The second-order Møller–Plesset (MP2) correlation energies of the valence shells of C_2H_4 and C_2H_6 (with fixed nuclear coordinates) are computed as accurately as technically feasible today. The pair energies for singlet and triplet pairs are reported for localized molecular orbitals. An accuracy of the order of 0.01 mE_h is achieved for all of the individual pair energies. The best estimates of the total valence-shell MP2 correlation energies of C_2H_4 and C_2H_6 in the chosen geometries amount to -373.6$\pm$0.1 mE_h and -410.0$\pm$0.1 mE_h, respectively. In the aug-cc-pVQZ, aug-cc-pV5Z and aug-cc-pV6Z basis sets, 96.2%, 98.0% and 98.8% of the these values are recovered, respectively. The percentages are improved to 99.8% by means of spin-adapted two-point extrapolations from the aug-cc-pVQZ and aug-cc-pV5Z results. An extrapolation based on the aug-cc-pV5Z and aug-cc-pV6Z correlation energies yields 99.9%.

C. C. M. Samson and W. Klopper, Mol. Phys. (accepted for publication).

8.1 Introduction

Almost 30 years ago, Handy published an eye-opening review article [1] on explicitly-correlated wave functions, discussing not only the early and famous works by Hylleraas on the He atom [2] and by James and Coolidge [3] and Kołos and co-workers on the H_2 molecule [4, 5], but also his own works with Boys on the transcorrelated method [6–13]. The idea of that latter method is to solve the eigenvalue problem of a similarity-transformed Hamiltonian

$$\hat{H}_C = e^{-C} \hat{H} e^{C} \tag{8.1}$$

while choosing the correlation factor

$$C = \sum_{\mu<\nu} f(\mathbf{r}_\mu, \mathbf{r}_\nu) \tag{8.2}$$

in such a manner that the interelectronic Coulomb singularities in $\hat{H}$ are removed [14–16]. In Eq. (8.2), the sum runs over the electrons in the system. When the eigenfunction of $\hat{H}_C$ is expanded in a finite basis of (antisymmetrized) products of one-electron functions, and when this basis of one-electron functions is increased systematically towards a complete one-electron basis, convergence to the exact eigenvalue can be expected to be much faster than for the eigenfunction of the original Hamiltonian $\hat{H}$, because the expansion for $\hat{H}_C$ does not suffer from the difficulties that are encountered when products of one-electron functions are used in an attempt to describe the Coulomb holes in $\hat{H}$ for short interelectronic distances.

Unlike the standard electronic Hamiltonian, which only contains one- and two-electron operators, the similarity-transformed Hamiltonian Eq. (8.1) also contains three-electron terms—assuming that the correlation factor in Eq. (8.2) is chosen as a sum of (symmetric) two-electron functions. Thus, because three-electron integrals occur, correlated calculations in a given basis with the similarity-transformed Hamiltonian can be expected to be much more complicated than those in the same basis with the standard electronic Hamiltonian. Nevertheless, the transcorrelated calculation could still be less time-consuming than the standard calculation if the basis set could be kept much smaller than the large basis set that is needed to achieve high accuracy in that standard calculation. In any case, the transcorrelated method got somewhat forgotten in the late 1970s.

In the last few years, however, there has been a renewed and vivid interest in the transcorrelated method of Boys and Handy [17–23]. But even today, applications of the transcorrelated approach have thus far been restricted to systems not larger than, for example, the ten-electron systems Ne, HF, H_2O, NH_3, and CH_4 [21, 22]. In view of the complexity of the transcorrelated calculations due to the occurrence of three-electron integrals, it is quite remarkable that Handy was able to carry out transcorrelated calculations of similar systems (Ne, LiH, and H_2O) already in the early 1970s (although admittedly not with the same accuracy that is achieved today) [11–13].

The evaluation of three-electron integrals seems to have become a stumbling block in calculations that try to account for the correlation cusp by including terms into the wave function that depend explicitly on the distances $r_{\mu\nu} = |\mathbf{r}_\mu - \mathbf{r}_\nu|$ between the electrons μ and ν. Recent review articles [24–26] provide a comprehensive overview of the electronic systems that have been treated either with many-body perturbation theory and coupled-cluster methods using Gaussian geminals (GGs) [25] or with full configuration-interaction (FCI) calculations using explicitly-correlated Gaussians (ECGs) [26]. Three-electron integrals already occur at the level of second-order Møller-Plesset (MP2) theory with GGs, and the corresponding applications have been restricted to systems of the size of Be, LiH, He_2, Ne, and H_2O, to name a few. Coupled-cluster calculations with GGs even involve four-electron integrals (unless only the factorizable terms are retained and the so-called super-weak-orthogonality-plus-projection approximation is invoked), and applications are scarce (Be, Li^-, LiH, Ne). FCI calculations of a molecule or atom with n electrons in a basis of ECGs involve n-electron integrals over n-electron Gaussians. The results of such calculations have been impressive indeed (today, they represent the most accurate calculations of systems such as Be and H_2), but correlations of more than four electrons seem practically impossible and have not yet been reported.

At this point, one may wonder if explicitly-correlated calculations can be carried out at all on molecules such as the title molecules (ethylene and ethane) or larger. Such molecules seem out of reach for the explicitly-correlated methods just discussed. However, the R12 methods as developed by Kutzelnigg and co-workers [27–31] are well capable of calculating highly accurate correlation energies for these molecules. Because an approximate resolution-of-identity (*i.e.*, closure relation) is inserted into the many-electron integrals that occur in the theory, the complexity of the practical R12 methods is limited to the evaluation of two-electron integrals. Owing to this limited complexity, the computation time of an R12 calculation is of the order of that of a standard electron-correlation calculation in the same one-electron basis, in particular when we consider highly correlated methods such as the coupled-cluster [32, 33] and multireference configuration interaction (MRCI) approaches [34, 35]. It is the purpose of the present article to calculate the MP2 pair energies for ethylene and ethane as accurately as technically possible using the MP2-R12 method [27–31], which has recently been extended to work with localized molecular orbitals (LMOs). The MP2-R12 method as it is used in the present work (but with canonical orbitals) has also been implemented by Bearpark and Handy [36, 37] and, more recently, by Valeev and Schaefer [38–43]. Applications have thus far included systems as large as the benzene dimer [42].

Our benchmark study of C_2H_4 and C_2H_6 was motivated by similar work of Polly and co-workers [44], who have developed an explicitly-correlated MP2 program that uses GGs to expand the linear $r_{\mu\nu}$ terms in the spirit of Ref. [45]. Their program evaluates the three-electron integrals over GGs utilizing computer codes written by Persson and Taylor [46] and by Dahle and Tay-

lor [47]. Furthermore, Polly and co-workers have enabled their program to work with LMOs with the long-term goal to use GGs in the framework of the local-correlation methods of Schütz and Werner [48, 49]. Thus, to allow for future comparisons with their results, we provide benchmark MP2 pair energies for LMOs. We expect that the treatment of two-electron integrals over the operator $r_{\mu\nu}$ will not be much different from the treatment of integrals over the electronic repulsion operator $r_{\mu\nu}^{-1}$ when LMOs are used in conjunction with (projected) atomic orbitals [(P)AOs]. In MP2-R12 theory, the integrals occur as integrals over the functions $(ip|jq)$, where i and j denote LMOs and p and q AOs or PAOs. The integrals will be negligible for both operators $r_{\mu\nu}$ and $r_{\mu\nu}^{-1}$ when the overlap between the functions i and p or between j and q vanishes. However, integrals over the operator $r_{\mu\nu}$ are large when the distance between the LMOs i and j is large (with p in the proximity of i and q in the proximity of j). Concerning this aspect of MP2-R12 theory, it may be advantageous to use correlation factors of the type $r_{\mu\nu}\exp(-\gamma r_{\mu\nu}^2)$ instead of the linear $r_{\mu\nu}$-term [50].

One of the main differences between the explicitly-correlated MP2 program utilizing GGs and our program using terms that are linear in $r_{\mu\nu}$ is that the former evaluates the three-electron integrals exactly while ours does not. As already mentioned, these three-electron integrals form a real obstacle for calculations on molecules larger than, say, H_2O. It should also be mentioned, however, that this obstacle might vanish when density-fitting techniques are introduced [51, 52] into the GG methods, or that it might occur when the R12 methods are augmented with exact one-center three-electron integrals [53, 54]. Of course, what really matters is the accuracy that is achieved within a given unit of computer time. To be able to judge the accuracy of various techniques and approximations, benchmark calculations are needed, and such calculations for ethylene and ethane are reported below.

The present article is organized as follows: In the next section, we describe the computational methods, geometries, basis sets, extrapolation techniques, and programs used. In Section 8.3, we present the results for C_2H_4 and C_2H_6 including our best estimates for all of the MP2 pair energies for pairs of LMOs. Finally, the work is summarized in Section 8.4.

8.2 Computational Details

In this section, we describe the computational methods, the basis sets of Gaussian-type atomic orbitals (AO basis sets), and the fixed geometries of ethylene and ethane that were used in the present study. We have applied the MP2-R12/A and MP2-R12/B methods using very large AO basis sets (the largest basis contains more than 800 basis functions) both for the expansion of the correlated wave function and for the resolution-of-identity (RI) approximation of R12 theory. Recently, we have reported new R12 methods that utilize an auxiliary basis set for the RI approximation [55, 56].

This technique was introduced to allow for the expansion of the correlated wave function in a relatively small basis set. In the present study, however, we have chosen to use a single basis set as large as technically feasible to approach the limit of an effectively complete basis set as closely as possible.

The MP2-R12 approach will be described in the next subsection, both for the MP2-R12/A and MP2-R12/B models. The theory is presented in a spin-orbital formalism, following closely the notation of Ref. [57]. We use indices $i, j, k, l, \ldots$ for occupied spin orbitals, indices $a, b, c, d, \ldots$ for virtual spin orbitals, and indices $p, q, r, s, \ldots$ for arbitrary spin orbitals. Antisymmetrized pairs of spin-orbitals of the form

$$|ij\rangle = \tfrac{1}{\sqrt{2}}|\varphi_i(1)\varphi_j(2) - \varphi_j(1)\varphi_i(2)\rangle \tag{8.3}$$

are used to define antisymmetrized two-electron integrals over spin orbitals. Furthermore, we use the two-electron projection operator

$$\hat{Q}_{12} = (1 - \hat{P}_1)(1 - \hat{P}_2)\,, \tag{8.4}$$

where $\hat{P}_\mu$ is the projector onto the (finite) basis set of spin orbitals with respect to the (spin and spatial) coordinates of electron μ,

$$\hat{P}_\mu = \sum_p |\varphi_p(\mu)\rangle\langle\varphi_p(\mu)|\,. \tag{8.5}$$

In the following, we shall assume implicit summation over repeated indices.

8.2.1 MP2-R12/A and MP2-R12/B methods

In both standard approximations A and B, the MP2-R12 correlation energy can be expressed as

$$E^{(2)}_{\text{MP2-R12}} \;=\; \tfrac{1}{4}\text{Tr}(\mathbf{GT} + \mathbf{VC})\,. \tag{8.6}$$

In the case of the MP2-R12/B method, the amplitudes (collected in $\mathbf{T}$ and $\mathbf{C}$) satisfy the equations

$$\{\mathbf{f}_\text{v}, \mathbf{T}\} - \{\mathbf{T}, \mathbf{f}_\text{o}\} + \mathbf{G}^\dagger \;=\; \mathbf{0}\,, \tag{8.7}$$

$$(\mathbf{B} + \mathbf{Q} - \mathbf{P})\mathbf{C} + \frac{1}{2}\{\mathbf{f}_\text{o}, \mathbf{X}\}\,\mathbf{C} + \frac{1}{2}\{\mathbf{X}, \mathbf{f}_\text{o}\}\,\mathbf{C} - \mathbf{X}\,\{\mathbf{C}, \mathbf{f}_\text{o}\} + \mathbf{V}^\dagger \;=\; \mathbf{0}\,. \tag{8.8}$$

The rectangular matrix $\mathbf{G}^\dagger$ contains the Coulomb integrals $(\bar{G}^\dagger)^{ij}_{ab} = \bar{g}^{ij}_{ab} = \langle ab|r_{12}^{-1}|ij\rangle$ while the rectangular matrix $\mathbf{T}$ and the square matrix $\mathbf{C}$ contain the standard MP2 amplitudes t^{ij}_{ab} and the

R12 amplitudes c_{kl}^{ij}, respectively. Furthermore, the square matrices $\mathbf{X}$, $\mathbf{V}^\dagger$, $\mathbf{B}$, $\mathbf{Q}$, and $\mathbf{P}$ contain the integrals

$$\begin{aligned}
\bar{X}_{kl}^{ij} &= \langle kl|r_{12}\hat{Q}_{12}r_{12}|ij\rangle\,, && (8.9)\\
(\bar{V}^\dagger)_{kl}^{ij} &= \langle kl|r_{12}\hat{Q}_{12}r_{12}^{-1}|ij\rangle\,. && (8.10)\\
\bar{B}_{kl}^{ij} &= \frac{1}{2}\langle kl|r_{12}\hat{Q}_{12}[\hat{T}_{12},r_{12}]+[r_{12},\hat{T}_{12}]\hat{Q}_{12}r_{12}|ij\rangle\,, && (8.11)\\
\bar{Q}_{kl}^{ij} &= \frac{1}{2}\langle kl|r_{12}\hat{Q}_{12}r_{12}\hat{K}_{12}+\hat{K}_{12}r_{12}\hat{Q}_{12}r_{12}|ij\rangle\,, && (8.12)\\
\bar{P}_{kl}^{ij} &= \frac{1}{2}\langle kl|r_{12}\hat{Q}_{12}\hat{K}_{12}r_{12}+r_{12}\hat{K}_{12}\hat{Q}_{12}r_{12}|ij\rangle\,, && (8.13)
\end{aligned}$$

where $\hat{T}_{12}=\hat{t}_1+\hat{t}_2$ is the sum of the kinetic energy operators for electrons 1 and 2, and $\hat{K}_{12}=\hat{k}_1+\hat{k}_2$ the sum of the respective exchange operators.

In Eqs. (8.7) and (8.8), terms of the type $\{\mathbf{A},\mathbf{f}_\mathrm{o}\}$ or $\{\mathbf{f}_\mathrm{v},\mathbf{A}\}$ refer to 1-index transformations of the 4-index intermediate $\mathbf{A}$ with the occupied–occupied ($\mathbf{f}_\mathrm{o}$) or virtual–virtual ($\mathbf{f}_\mathrm{v}$) blocks of the Fock matrix,

$$\begin{aligned}
\{\mathbf{C},\mathbf{f}_\mathrm{o}\}_{kl}^{ij} &= c_{kl}^{oj}f_o^i+c_{kl}^{io}f_o^j\,, && (8.14)\\
\{\mathbf{T},\mathbf{f}_\mathrm{o}\}_{ab}^{ij} &= t_{ab}^{oj}f_o^i+t_{ab}^{io}f_o^j\,, && (8.15)\\
\{\mathbf{f}_\mathrm{v},\mathbf{T}\}_{ab}^{ij} &= f_a^c t_{cb}^{ij}+f_b^c t_{ac}^{ij}\,, && (8.16)\\
\{\mathbf{f}_\mathrm{o},\mathbf{X}\}_{kl}^{ij} &= f_k^o\bar{X}_{ol}^{ij}+f_l^o\bar{X}_{ko}^{ij}\,, && (8.17)\\
\{\mathbf{X},\mathbf{f}_\mathrm{o}\}_{kl}^{ij} &= \bar{X}_{kl}^{oj}f_o^i+\bar{X}_{kl}^{io}f_o^j\,, && (8.18)
\end{aligned}$$

with

$$\mathbf{f}=\begin{bmatrix}\mathbf{f}_\mathrm{o} & 0\\ 0 & \mathbf{f}_\mathrm{v}\end{bmatrix}=\mathbf{f}^\mathrm{D}+\mathbf{f}^\mathrm{O}=\begin{bmatrix}\mathbf{f}_\mathrm{o}^\mathrm{D} & 0\\ 0 & \mathbf{f}_\mathrm{v}^\mathrm{D}\end{bmatrix}+\begin{bmatrix}\mathbf{f}_\mathrm{o}^\mathrm{O} & 0\\ 0 & \mathbf{f}_\mathrm{v}^\mathrm{O}\end{bmatrix}\,. \qquad (8.19)$$

If we use canonical Hartree–Fock orbitals, then the Fock matrix is diagonal ($f_k^l=\delta_k^l\varepsilon_k$), and the amplitude equations, Eqs. (8.7) and (8.8), reduce to the simple form

$$\begin{aligned}
(\varepsilon_a+\varepsilon_b-\varepsilon_i-\varepsilon_j)t_{ab}^{ij}+\bar{g}_{ab}^{ij} &= 0\,, && (8.20)\\
\{\bar{B}_{mn}^{kl}+\bar{Q}_{mn}^{kl}-\bar{P}_{mn}^{kl}+\frac{1}{2}(\epsilon_m+\epsilon_n+\epsilon_k+\epsilon_l-2\epsilon_i-2\epsilon_j)\bar{X}_{mn}^{kl}\}c_{kl}^{ij}+(\bar{V}^\dagger)_{mn}^{ij} &= 0\,. && (8.21)
\end{aligned}$$

Eq. (8.20) corresponds to the standard expression for MP2 amplitudes while solving Eq. (8.21) yields the R12 amplitudes of MP2-R12 theory.

In the present study, however, we do not wish to use canonical Hartree–Fock orbitals, but rather localized molecular (spin) orbitals. Then, we must solve Eqs. (8.7) and (8.8) in an iterative manner. This is accomplished by decomposing the Fock matrix in Eq. (8.19) as well as its

occupied–occupied and virtual–virtual blocks into diagonal and off-diagonal matrices, which are characterized by the superscripts D and O, respectively. Using these diagonal and off-diagonal matrices, Eq. (8.7) is solved iteratively in the following manner:

$$\left\{\mathbf{f}_{\mathrm{v}}^{\mathrm{D}}, \mathbf{T}^{(N+1)}\right\} - \left\{\mathbf{T}^{(N+1)}, \mathbf{f}_{\mathrm{o}}^{\mathrm{D}}\right\} = -\mathbf{G}^{T} - \left\{\mathbf{f}_{\mathrm{v}}^{\mathrm{O}}, \mathbf{T}^{(N)}\right\} + \left\{\mathbf{T}^{(N)}, \mathbf{f}_{\mathrm{o}}^{\mathrm{O}}\right\} , \tag{8.22}$$

where $\mathbf{T}^{(N)}$ contains the amplitudes in iteration number N. Eq. (8.22) represents the commonly used iterative procedure that is utilized in the local-MP2 approach. In the same spirit, the R12 amplitudes in the matrix $\mathbf{C}$ are obtained from the following iterative scheme:

$$\begin{aligned}(\mathbf{B}+\mathbf{Q}-\mathbf{P})\mathbf{C}^{(N+1)} + \tfrac{1}{2}\left\{\mathbf{f}_{\mathrm{o}}^{\mathrm{D}}, \mathbf{X}\right\}\mathbf{C}^{(N+1)} + \tfrac{1}{2}\left\{\mathbf{X}, \mathbf{f}_{\mathrm{o}}^{\mathrm{D}}\right\}\mathbf{C}^{(N+1)} - \mathbf{X}\left\{\mathbf{C}^{(N+1)}, \mathbf{f}_{\mathrm{o}}^{\mathrm{D}}\right\} \\ = -\mathbf{V}^{\dagger} - \tfrac{1}{2}\left\{\mathbf{f}_{\mathrm{o}}^{\mathrm{O}}, \mathbf{X}\right\}\mathbf{C}^{(N)} - \tfrac{1}{2}\left\{\mathbf{X}, \mathbf{f}_{\mathrm{o}}^{\mathrm{O}}\right\}\mathbf{C}^{(N)} + \mathbf{X}\left\{\mathbf{C}^{(N)}, \mathbf{f}_{\mathrm{o}}^{\mathrm{O}}\right\} .\end{aligned} \tag{8.23}$$

If in MP2-R12 theory all matrix elements are taken into account, then the MP2-R12/B model is obtained, as outlined above. It is possible, however, to construct a much simpler method, denoted MP2-R12/A, by assuming that all contributions in Eq. (8.7)—and similarly in Eq. (8.23)—due to the matrices $\mathbf{X}$, $\mathbf{P}$, and $\mathbf{Q}$ can be neglected. Then, concerning the R12 contribution to the correlation energy in this method, it remains to solve

$$\mathbf{BC} = -\mathbf{V}^{\dagger} , \tag{8.24}$$

which does not require an iterative procedure, neither with canonical nor with localized molecular orbitals.

The correlation energies of both models MP2-R12/A and MP2-R12/B are invariant with respect to unitary transformations among the occupied (spin) orbitals [29]. Such transformations can be represented by an unitary matrix $\mathbf{U}$ that transforms the matrices $\mathbf{V}$ and $\mathbf{C}$ into

$$\tilde{\mathbf{V}} = \mathbf{U}^{\dagger}\mathbf{V}\mathbf{U} , \tag{8.25}$$

$$\tilde{\mathbf{C}} = \mathbf{U}^{\dagger}\mathbf{C}\mathbf{U} . \tag{8.26}$$

The R12 contribution to the MP2-R12 correlation energy is orbital-invariant, since

$$\tfrac{1}{4}\mathrm{Tr}(\tilde{\mathbf{V}}\tilde{\mathbf{C}}) = \tfrac{1}{4}\mathrm{Tr}(\mathbf{V}\mathbf{C}) . \tag{8.27}$$

8.2.2 Geometries

The geometries of C_2H_4 and C_2H_6 were provided to us by Polly [44] and were kept fixed throughout our study. Since we report benchmark results for these molecules, we give the geometries in full detail in Table 8.1.

Table 8.1: Coordinates (in a_0) of symmetry-unique atoms in C_2H_4 and C_2H_6.

Molecule	Atom	x	y	z
C_2H_4[a]	C	1.2713109500	0.0000000000	0.0000000000
	H	2.3482176200	1.7665270500	0.0000000000
C_2H_6[b]	C	1.4443977326	-0.0000160016	0.0000000000
	H	2.1995627792	-0.9699303417	1.6799781560
	H	2.1995542194	1.9398637239	0.0000000000

[a] Other atoms are generated by reflections in the xz- and yz-planes.

[b] Other atoms are generated by rotation about the z-axis and reflection in the xy-plane.

8.2.3 Basis sets

The standard MP2 calculations were performed in the correlation-consistent basis sets cc-pVXZ as well as in the augmented correlation-consistent basis sets aug-cc-pVXZ (X = D, T, Q, 5, 6) of Dunning and co-workers [58–60], with corresponding cardinal numbers X = 2, ..., 6. On C_2H_6, the aug-cc-pV6Z basis comprises 1,140 contracted basis functions.

The MP2-R12 calculations were carried out in subsets of the uncontracted basis sets $19s14p8d6f4g3h2i$ for C and $9s6p4d3f2g$ for H. This full basis is taken from Ref. [55] and is abbreviated as $spdfghi$. It comprises 820 functions on C_2H_4. Without i-functions on C and without g-functions on H, the basis set is denoted $spdfgh$ and contains 696 and 832 functions on C_2H_4 and C_2H_6, respectively. By deleting also the h- and f-functions on C and H, respectively, the $spdfg$ basis is obtained.

The overlap matrix eigenvalue threshold for numerical linear dependence was chosen as 10^{-6}. With this threshold, some orbitals were deleted in the calculations with the largest basis sets.

8.2.4 Extrapolation techniques

The MP2 correlation energies of the valence shell were decomposed into singlet (s=0) and triplet (s=1) correlation energies E^s_{MP2} as described in Ref. [61]. In standard MP2 calculations in correlation-consistent basis sets, it is then possible to estimate the values for the singlet and triplet correlation energies in the limit of an effectively complete basis from a two-point extrapolation formula [61, 62] that distinguishes between singlet and triplet pairs,

$$E^s_{\text{MP2}}(\infty) = \frac{X^{2s+3}E^s_{\text{MP2}}(X) - (X-1)^{2s+3}E^s_{\text{MP2}}(X-1)}{X^{2s+3} - (X-1)^{2s+3}}\,. \tag{8.28}$$

$E^s_{\rm MP2}(X-1)$ and $E^s_{\rm MP2}(X)$ are the standard MP2 singlet and triplet correlation energies that are obtained in the two correlation-consistent basis sets with consecutive cardinal numbers X-1 and X, respectively. $E^s_{\rm MP2}(\infty)$ is the estimated basis-set limit.

We refer to our extrapolation technique as spin-adapted two-point formula. The results will be characterized by putting the two basis sets that were used for the extrapolation between parentheses, for instance as aug-cc-pV(Q5)Z or aug-cc-pV(56)Z.

8.2.5 Programs and procedures

All calculations were carried out with a local version of the Dalton program [63]. In all of these calculations, only the valence orbitals of C_2H_4 and C_2H_6 were correlated (frozen-core approximation). The occupied orbitals in the valence space were localized by the Boys procedure using program parts of the GAMESS-UK package [64]. For C_2H_4, we have performed calculations in which the Boys procedure was applied to all of the valence orbitals, generating C–C banana bonds. However, we have also performed calculations on C_2H_4, in which only the valence orbitals within the molecular plane (σ-type orbitals) were localized, leaving the π-type orbital unchanged.

8.3 Results and discussion

In this section, we shall discuss the raw data, the best estimates, and the extrapolated data for the the valence-shell MP2 correlation energies of C_2H_4 and C_2H_6 and their respective pair energies for pairs of LMOs.

8.3.1 Raw data

The calculated valence-shell MP2 correlation energies of C_2H_4 and C_2H_6 are collected in Tables 8.2 and 8.3, respectively, where they have been decomposed into singlet and triplet contributions. The energies are reported for the standard MP2, MP2-R12/A, and MP2-R12/B methods, using standard basis sets or those designed for R12 calculations. The pair energies for pairs of Boys-localized molecular orbitals are then given in Tables 8.4, 8.5, and 8.6, for C_2H_4 with only in-plane localization, for C_2H_4 with so-called banana bonds, and for C_2H_6, respectively. These tables report the pair energies as calculated by the standard MP2, MP2-R12/A, and MP2-R12/B methods, in subsets of the large $spdfghi$ basis.

Table 8.2: Computed and extrapolated valence-shell second-order Møller–Plesset correlation energies (in mE_h) of C_2H_4.

Method	Basis[a]	Calculated			Extrapolated[b]		
		Singlet	Triplet	Total	Singlet	Triplet	Total
MP2	cc-pVDZ	-185.45	-90.80	-276.25			
	cc-pVTZ	-229.96	-106.57	-336.54	-248.70	-108.97	-357.67
	cc-pVQZ	-246.98	-110.14	-357.12	-259.40	-111.25	-370.65
	cc-pV5Z	-253.74	-111.14	-364.88	-260.83	-111.62	-372.46
	cc-pV6Z	-257.01	-111.46	-368.47	-261.51	-111.67	-373.18
	aug-cc-pVDZ	-191.80	-94.46	-286.26			
	aug-cc-pVTZ	-233.29	-107.66	-340.95	-250.75	-109.66	-360.41
	aug-cc-pVQZ	-248.77	-110.52	-359.30	-260.08	-111.41	-371.49
	aug-cc-pV5Z	-254.78	-111.28	-366.06	-261.09	-111.65	-372.74
	aug-cc-pV6Z	-257.63	-111.52	-369.15	-261.55	-111.68	-373.23
	$spdfg$	-251.79	-111.18	-362.97			
	$spdfgh$	-255.72	-111.47	-367.19			
	$spdfghi$	-257.30	-111.56	-368.85			
MP2-R12/A	$spdfg$	-262.24	-111.70	-373.94			
	$spdfgh$	-262.04	-111.70	-373.73			
	$spdfghi$	-261.99	-111.69	-373.68			
MP2-R12/B	$spdfg$	-261.47	-111.64	-373.11			
	$spdfgh$	-261.74	-111.68	-373.42			
	$spdfghi$	-261.81	-111.68	-373.50			
Best estimate[c]	$spdfg$	-261.93	-111.68	-373.61			
	$spdfgh$	-261.92	-111.69	-373.61			
	$spdfghi$	-261.92	-111.69	-373.61			

[a] $spdfghi$ means C:19s14p8d6f4g3h2i/H:9s6p4d3f2g; $spdfgh$ and $spdfg$ are subsets thereof.

[b] Two-point X^{-3} and X^{-5} extrapolations were applied to the singlet and triplet pairs, respectively [61].

[c] Obtained by adding 60% of the MP2-R12/A energy to 40% of the MP2-R12/B energy.

8.3.2 Best estimates

For C_2H_4, it appears that the MP2-R12/A energies increase monotonically and that the MP2-R12/B energies decrease monotonically when the basis set is enlarged from $spdfg$ to $spdfghi$ (Figure 8.1).

Table 8.3: Computed and extrapolated valence-shell second-order Møller–Plesset correlation energies (in mE_h) of C_2H_6.

Method	Basis[a]	Calculated			Extrapolated[b]		
		Singlet	Triplet	Total	Singlet	Triplet	Total
MP2	cc-pVDZ	-208.88	-93.96	-302.84			
	cc-pVTZ	-259.10	-111.30	-370.40	-280.24	-113.93	-394.18
	cc-pVQZ	-277.67	-114.96	-392.62	-291.22	-116.09	-407.31
	cc-pV5Z	-284.91	-115.94	-400.85	-292.52	-116.42	-408.94
	cc-pV6Z	-288.39	-116.26	-404.65	-293.16	-116.47	-409.63
	aug-cc-pVDZ	-216.13	-98.12	-314.25			
	aug-cc-pVTZ	-263.01	-112.50	-375.50	-282.74	-114.68	-397.42
	aug-cc-pVQZ	-279.50	-115.33	-394.83	-291.54	-116.21	-407.75
	aug-cc-pV5Z	-285.95	-116.08	-402.02	-292.71	-116.44	-409.15
	aug-cc-pV6Z	-288.99	-116.31	-405.30	-293.16	-116.47	-409.63
	$spdfg$	-281.83	-115.90	-397.74			
	$spdfgh$	-286.50	-116.24	-402.75			
MP2-R12/A	$spdfg$	-293.85	-116.49	-410.35			
	$spdfgh$	-293.62	-116.49	-410.12			
MP2-R12/B	$spdfg$	-292.96	-116.43	-409.39			
	$spdfgh$	-293.29	-116.47	-409.77			
Best estimate[c]	$spdfg$	-293.50	-116.47	-409.96			
	$spdfgh$	-293.49	-116.48	-409.98			

[a] $spdfghi$ means C:19s14p8d6f4g3h2i/H:9s6p4d3f2g; $spdfgh$ and $spdfg$ are subsets thereof.

[b] Two-point X^{-3} and X^{-5} extrapolations were applied to the singlet and triplet pairs, respectively [61].

[c] Obtained by adding 60% of the MP2-R12/A energy to 40% of the MP2-R12/B energy.

Now, assuming that the MP2-R12/A and MP2-R12/B results bracket the true basis-set limit, we can calculate a weighted average of the form

$$E^{(2)}_{\text{Best estimate}} = c\,E^{(2)}_{\text{MP2-R12/A}} + (1-c)\,E^{(2)}_{\text{MP2-R12/B}}\,. \tag{8.29}$$

The parameter c can be determined by requiring that inserting the energies of two different basis sets into Eq. (8.29) must yield the same value for $E^{(2)}_{\text{Best estimate}}$. This strategy yields c = 0.616 when applied to the results of the $spdfgh$ and $spdfghi$ basis sets. The basis-set pairs ($spdfg$,$spdfgh$)

Table 8.4: Valence-shell second-order pair energies (in mE_h) of C_2H_4. The orbital spaces transforming as a (σ) and a' (π) have been localized separately in C_s symmetry.

Pair	MP2			MP2-R12/A			MP2-R12/B		
	Singlet	Triplet	Total	Singlet	Triplet	Total	Singlet	Triplet	Total
				C:19s14p8d6f4g/H:9s6p4d					
σ^2_{CC}	-25.38		-25.38	-26.82		-26.82	-26.72		-26.72
σ^2_{CH}	-30.38		-30.38	-31.63		-31.63	-31.54		-31.54
π^2_{CC}	-27.32		-27.32	-27.89		-27.89	-27.85		-27.85
σ_{CC}-σ_{CH}	-4.53	-6.95	-11.47	-4.74	-6.99	-11.72	-4.72	-6.98	-11.70
σ_{CC}-π_{CC}	-18.45	-20.00	-38.45	-19.35	-20.09	-39.44	-19.27	-20.09	-39.36
σ_{CH}-π_{CC}	-7.07	-10.86	-17.93	-7.36	-10.90	-18.26	-7.33	-10.90	-18.23
σ_{CH}-σ'_{CH} (*geminal*)	-5.42	-8.18	-13.60	-5.65	-8.22	-13.87	-5.63	-8.21	-13.85
σ_{CH}-σ'_{CH} (*cis*)	-0.48	-0.93	-1.40	-0.49	-0.93	-1.42	-0.49	-0.93	-1.42
σ_{CH}-σ'_{CH} (*trans*)	-0.48	-0.87	-1.36	-0.50	-0.88	-1.38	-0.50	-0.87	-1.37
				C:19s14p8d6f4g3h/H:9s6p4d3f					
σ^2_{CC}	-25.87		-25.87	-26.79		-26.79	-26.74		-26.74
σ^2_{CH}	-30.87		-30.87	-31.60		-31.60	-31.57		-31.57
π^2_{CC}	-27.52		-27.52	-27.88		-27.88	-27.87		-27.87
σ_{CC}-σ_{CH}	-4.60	-6.97	-11.57	-4.74	-6.98	-11.72	-4.73	-6.98	-11.71
σ_{CC}-π_{CC}	-18.77	-20.05	-38.82	-19.33	-20.09	-39.42	-19.30	-20.09	-39.39
σ_{CH}-π_{CC}	-7.18	-10.88	-18.06	-7.35	-10.90	-18.26	-7.35	-10.90	-18.25
σ_{CH}-σ'_{CH} (*geminal*)	-5.51	-8.20	-13.71	-5.65	-8.22	-13.87	-5.64	-8.22	-13.86
σ_{CH}-σ'_{CH} (*cis*)	-0.48	-0.93	-1.41	-0.49	-0.93	-1.42	-0.49	-0.93	-1.42
σ_{CH}-σ'_{CH} (*trans*)	-0.49	-0.87	-1.37	-0.50	-0.88	-1.38	-0.50	-0.88	-1.38
				C:19s14p8d6f4g3h2i/H:9s6p4d3f2g					
σ^2_{CC}	-26.09		-26.09	-26.78		-26.78	-26.75		-26.75
σ^2_{CH}	-31.06		-31.06	-31.59		-31.59	-31.58		-31.58
π^2_{CC}	-27.60		-27.60	-27.88		-27.88	-27.87		-27.87
σ_{CC}-σ_{CH}	-4.64	-6.97	-11.61	-4.73	-6.98	-11.72	-4.73	-6.98	-11.71
σ_{CC}-π_{CC}	-18.91	-20.07	-38.98	-19.32	-20.09	-39.41	-19.30	-20.09	-39.39
σ_{CH}-π_{CC}	-7.22	-10.89	-18.11	-7.35	-10.90	-18.26	-7.35	-10.90	-18.25
σ_{CH}-σ'_{CH} (*geminal*)	-5.54	-8.21	-13.75	-5.65	-8.22	-13.87	-5.64	-8.22	-13.86
σ_{CH}-σ'_{CH} (*cis*)	-0.48	-0.93	-1.41	-0.49	-0.93	-1.42	-0.49	-0.93	-1.42
σ_{CH}-σ'_{CH} (*trans*)	-0.49	-0.87	-1.37	-0.50	-0.88	-1.38	-0.50	-0.88	-1.38

Table 8.5: Valence-shell second-order pair energies (in mE_h) of C_2H_4. The full valence space has been localized, thereby generating two C–C banana bonds (b_{CC}).

Pair	MP2			MP2-R12/A			MP2-R12/B		
	Singlet	Triplet	Total	Singlet	Triplet	Total	Singlet	Triplet	Total
				C:19s14p8d6f4g/H:9s6p4d					
b_{CC}^2	-27.42		-27.42	-28.54		-28.54	-28.46		-28.46
σ_{CH}^2	-30.43		-30.43	-31.68		-31.68	-31.59		-31.59
b_{CC}–b'_{CC}	-15.86	-19.05	-34.90	-16.53	-19.14	-35.66	-16.48	-19.13	-35.61
b_{CC}-σ_{CH}	-5.75	-8.89	-14.64	-6.00	-8.93	-14.93	-5.98	-8.93	-14.91
σ_{CH}-σ'_{CH} (*geminal*)	-5.59	-8.50	-14.09	-5.83	-8.54	-14.37	-5.81	-8.54	-14.35
σ_{CH}-σ'_{CH} (*cis*)	-0.52	-0.97	-1.48	-0.53	-0.97	-1.50	-0.53	-0.97	-1.50
σ_{CH}-σ'_{CH} (*trans*)	-0.57	-1.04	-1.61	-0.59	-1.05	-1.63	-0.59	-1.05	-1.63
				C:19s14p8d6f4g3h/H:9s6p4d3f					
b_{CC}^2	-27.81		-27.81	-28.52		-28.52	-28.48		-28.48
σ_{CH}^2	-30.92		-30.92	-31.65		-31.65	-31.62		-31.62
b_{CC}–b'_{CC}	-16.09	-19.09	-35.18	-16.51	-19.13	-35.65	-16.49	-19.13	-35.62
b_{CC}-σ_{CH}	-5.85	-8.91	-14.76	-6.00	-8.93	-14.93	-5.99	-8.93	-14.92
σ_{CH}-σ'_{CH} (*geminal*)	-5.68	-8.52	-14.20	-5.83	-8.54	-14.37	-5.82	-8.54	-14.36
σ_{CH}-σ'_{CH} (*cis*)	-0.52	-0.97	-1.49	-0.53	-0.97	-1.50	-0.53	-0.97	-1.50
σ_{CH}-σ'_{CH} (*trans*)	-0.58	-1.05	-1.62	-0.59	-1.05	-1.63	-0.59	-1.05	-1.63
				C:19s14p8d6f4g3h2i/H:9s6p4d3f2g					
b_{CC}^2	-27.98		-27.98	-28.51		-28.51	-28.49		-28.49
σ_{CH}^2	-31.11		-31.11	-31.64		-31.64	-31.63		-31.63
b_{CC}–b'_{CC}	-16.19	-19.11	-35.30	-16.51	-19.13	-35.64	-16.50	-19.13	-35.63
b_{CC}-σ_{CH}	-5.88	-8.92	-14.80	-6.00	-8.93	-14.93	-6.00	-8.93	-14.93
σ_{CH}-σ'_{CH} (*geminal*)	-5.71	-8.53	-14.25	-5.82	-8.54	-14.37	-5.82	-8.54	-14.36
σ_{CH}-σ'_{CH} (*cis*)	-0.52	-0.97	-1.49	-0.53	-0.97	-1.50	-0.53	-0.97	-1.50
σ_{CH}-σ'_{CH} (*trans*)	-0.58	-1.05	-1.62	-0.59	-1.05	-1.63	-0.59	-1.05	-1.63

Table 8.6: Valence-shell second-order pair energies (in mE_h) of C_2H_6.

Pair	MP2			MP2-R12/A			MP2-R12/B		
	Singlet	Triplet	Total	Singlet	Triplet	Total	Singlet	Triplet	Total
	C:19s14p8d6f4g/H:9s6p4d								
σ^2_{CC}	-27.82		-27.82	-29.19		-29.19	-29.09		-29.09
σ^2_{CH}	-30.19		-30.19	-31.42		-31.42	-31.33		-31.33
σ_{CC}-σ_{CH}	-5.54	-8.65	-14.19	-5.80	-8.69	-14.49	-5.78	-8.69	-14.46
σ_{CH}-σ'_{CH} (*geminal*)	-5.96	-9.36	-15.32	-6.23	-9.41	-15.64	-6.21	-9.40	-15.61
σ_{CH}-σ'_{CH} (*gauche*)	-0.39	-0.86	-1.25	-0.40	-0.87	-1.27	-0.40	-0.87	-1.26
σ_{CH}-σ'_{CH} (*anti*)	-0.51	-0.90	-1.41	-0.53	-0.90	-1.43	-0.53	-0.90	-1.43

and ($spdfg$,$spdfghi$) yield c = 0.601 and c = 0.604, respectively. Moreover, a similar value (c = 0.623) is found when we analyse the MP2-R12/A and MP2-R12/B energies of C_2H_6 in the $spdfg$ and $spdfgh$ basis sets. Since all of these values of c are close to 0.6, we decided to calculate our best estimates by adding 60% of the MP2-R12/A energy to 40% of the MP2-R12/B energy. These best estimates are given in Table 8.7. For the total valence-shell MP2 correlation energies, we thus obtain -373.6 mE_h and -410.0 mE_h, respectively, for the best estimates of C_2H_4 and C_2H_6. Since the three best estimates for C_2H_4 obtained from the energies of the basis sets $spdfg$, $spdfgh$ and $spdfghi$ mutually agree to within 3 μE_h, we are confident that our best estimates of the total valence-shell MP2 correlation energies of C_2H_4 and C_2H_6 are accurate to within 0.1 mE_h.

8.3.3 Extrapolated data

Having established the best estimates for the MP2 correlation energies of the two title molecules, we are in the position to investigate the effect of the spin-adapted two-point extrapolation technique. The extrapolated correlation energies are displayed in Tables 8.2 and 8.3 for C_2H_4 and C_2H_6, respectively, concerning extrapolations from both the cc-pVXZ and the aug-cc-pVXZ results. In particular for the aug-cc-pV(X–1,X)Z extrapolations, we find a smooth and monotonic convergence towards our best estimates (Figure 8.2).

Furthermore, the results collected in Tables 8.2 and 8.3 clearly show that the extrapolation of the triplet pairs must be performed on the basis of the formula X^{-5}. If for C_2H_4, for example, an X^{-3}-type extrapolation had been attempted from the aug-cc-pVQZ and aug-cc-pV5Z results for C_2H_4, a triplet energy of -112.08 mE_h would have resulted, whose magnitude is much too large.

Table 8.7: Best estimates of the valence-shell second-order pair energies (in mE_h) of C_2H_4 and C_2H_6 with localized molecular orbitals.

Pair	Singlet	Triplet	Total
		C_2H_4[a]	
σ^2_{CC}	-26.77		-26.77
σ^2_{CH}	-31.59		-31.59
π^2_{CC}	-27.88		-27.88
σ_{CC}-σ_{CH}	-4.73	-6.98	-11.72
σ_{CC}-π_{CC}	-19.31	-20.09	-39.40
σ_{CH}-π_{CC}	-7.35	-10.90	-18.26
σ_{CH}-σ'_{CH} (*geminal*)	-5.65	-8.22	-13.86
σ_{CH}-σ'_{CH} (*cis*)	-0.49	-0.93	-1.42
σ_{CH}-σ'_{CH} (*trans*)	-0.50	-0.88	-1.38
		C_2H_4 with banana bonds	
b^2_{CC}	-28.50		-28.50
σ^2_{CH}	-31.64		-31.64
b_{CC}–b'_{CC}	-16.50	-19.13	-35.64
b_{CC}-σ_{CH}	-6.00	-8.93	-14.93
σ_{CH}-σ'_{CH} (*geminal*)	-5.82	-8.54	-14.36
σ_{CH}-σ'_{CH} (*cis*)	-0.53	-0.97	-1.50
σ_{CH}-σ'_{CH} (*trans*)	-0.59	-1.05	-1.63
		C_2H_6	
σ^2_{CC}	-29.15		-29.15
σ^2_{CH}	-31.38		-31.38
σ_{CC}-σ_{CH}	-5.79	-8.69	-14.48
σ_{CH}-σ'_{CH} (*geminal*)	-6.22	-9.40	-15.62
σ_{CH}-σ'_{CH} (*gauche*)	-0.40	-0.87	-1.27
σ_{CH}-σ'_{CH} (*anti*)	-0.53	-0.90	-1.43

[a] With separately localized a (σ) and a' (π) orbital spaces.

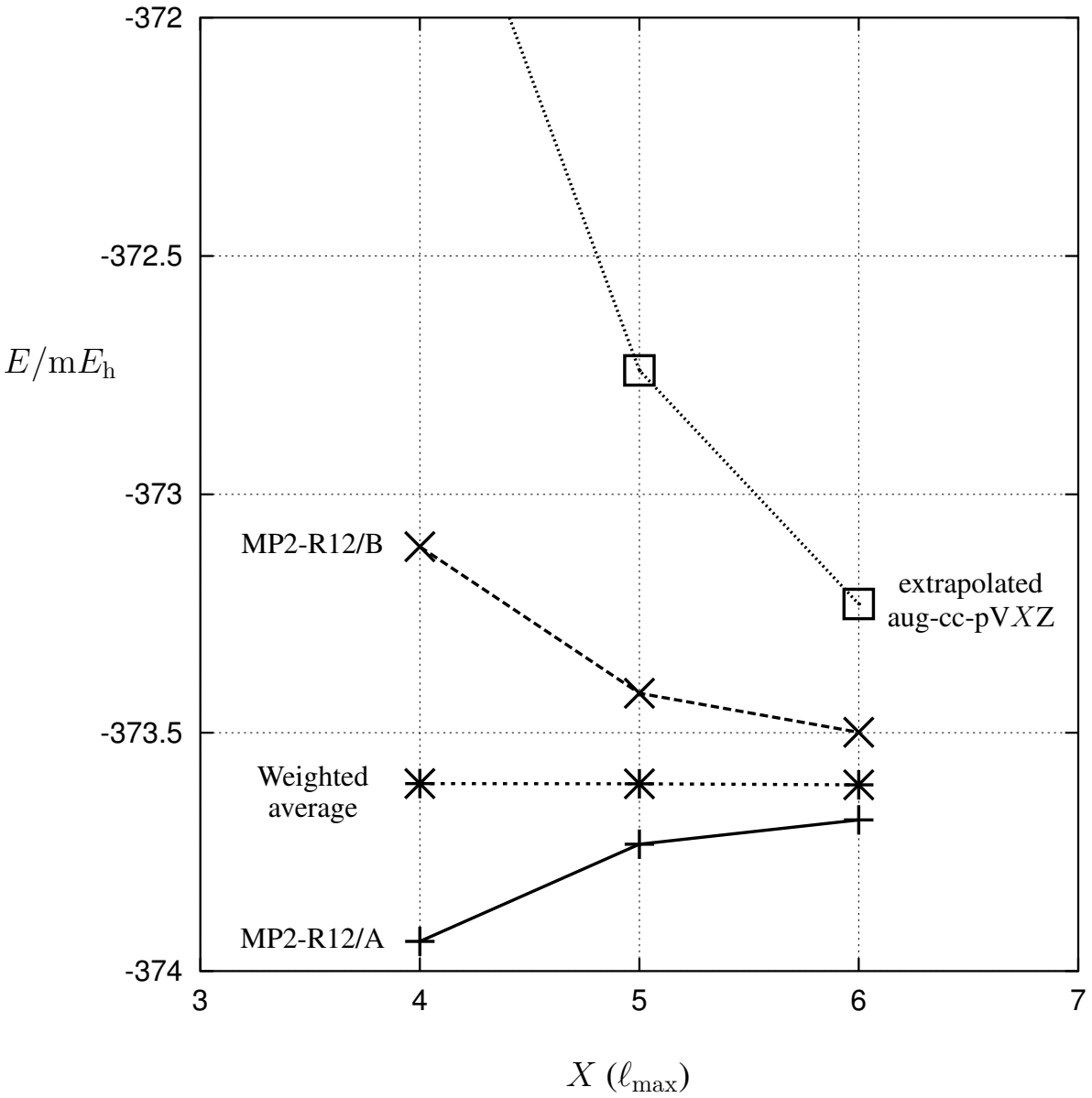

Figure 8.1: Second-order Møller-Plesset valence-shell correlation energy of C_2H_4 as function of the cardinal number X of the aug-cc-pVXZ basis sets, and as function of the maximum angular momentum quantum number ℓ_max of the basis used in the R12 calculations. Shown are the extrapolated aug-cc-pVXZ results ($\square$), the MP2-R12/A results ($+$), the MP2-R12/B results ($\times$), and the averaged MP2-R12 results ($*$).

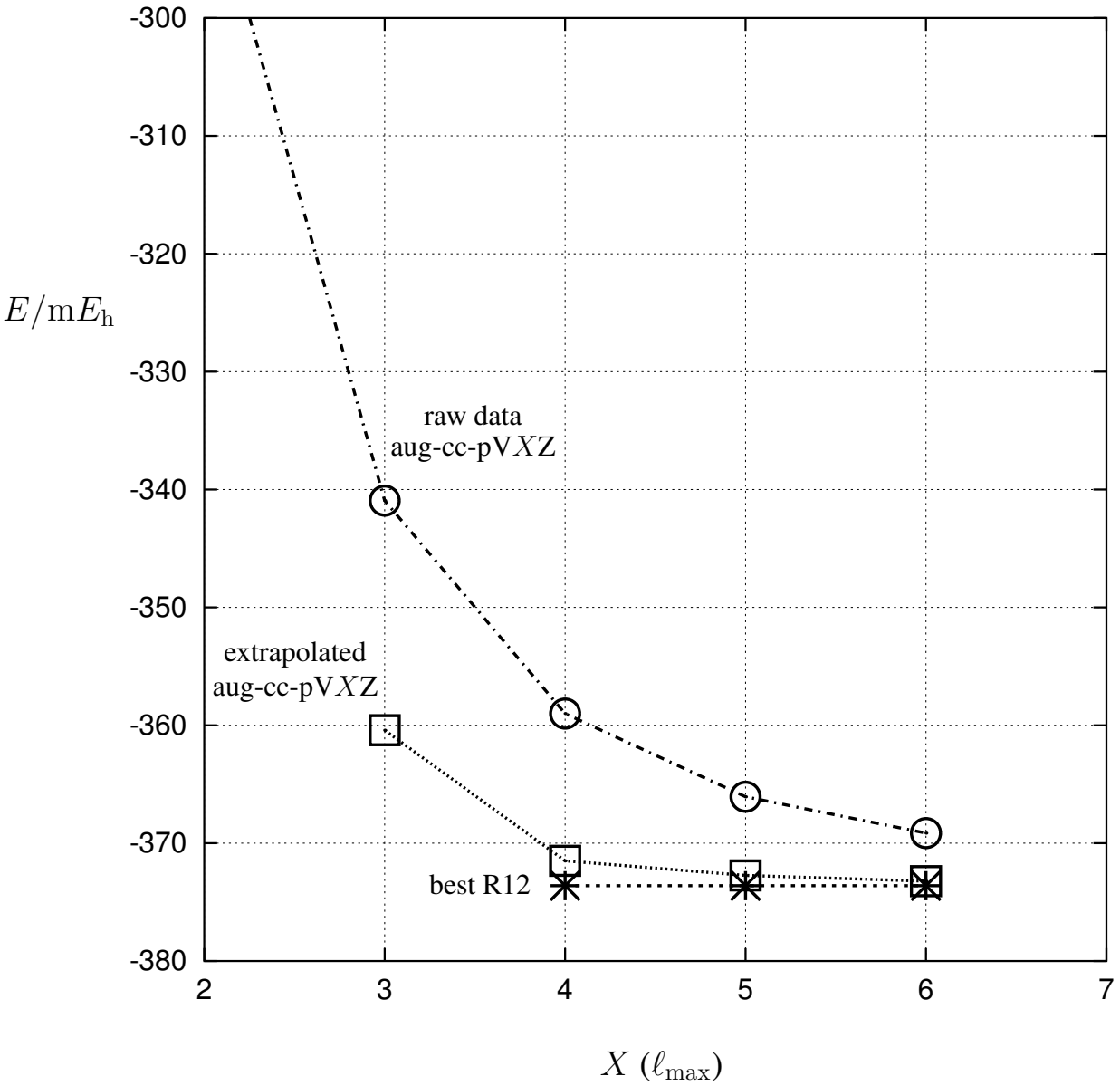

Figure 8.2: Second-order Møller-Plesset valence-shell correlation energy of C_2H_4 as function of the cardinal number X of the aug-cc-pVXZ basis sets, and as function of the maximum angular momentum quantum number ℓ_max of the basis used in the R12 calculations. Shown are the directly calculated aug-cc-pVXZ results (○), the extrapolated aug-cc-pVXZ results (□), and the averaged MP2-R12 results (∗).

A triplet energy of -111.85 mE_h would have resulted from the aug-cc-pV5Z and aug-cc-pV6Z results, still significantly below the limiting value of -111.68 mE_h. The X^{-5}-type extrapolation yields much better values (Table 8.2).

Our extrapolated energies are smaller in magnitude than the best estimates. Recently, Valeev and co-workers [40] proposed a slightly different extrapolation procedure, which differs from our scheme by replacing X by $X + \frac{1}{2}$. Their scheme yields accurate results indeed. For example, following the procedure of Valeev et al. [40], the extrapolated aug-cc-pV(TQ)Z, aug-cc-pV(Q5)Z and aug-cc-pV(56)Z valence MP2 energies for C_2H_4 amount to -374.20, -373.78 and -373.72 mE_h, respectively. For C_2H_6, the corresponding energies are -410.62, -410.26 and -410.15 mE_h. While our extrapolated energies are smaller, Valeev's extrapolated energies are larger in magnitude than the best estimates.

8.4 Conclusions

Using the R12 method as implemented in the Dalton program, we were able to determine the valence-shell MP2 correlation energies of ethylene and ethane (in the prescribed geometries of Table 8.1, which were kept fixed) accurate to within 0.1 mE_h. This corresponds to a relative accuracy of about 0.03%. Our best pair energies for pairs of LMOs are also believed to be accurate to within 0.03% (Table 8.7). In the aug-cc-pVQZ, aug-cc-pV5Z and aug-cc-pV6Z basis sets, 96.2%, 98.0% and 98.8% of our best estimates are recovered, respectively. These values are improved by means of spin-adapted two-point extrapolations to 99.8% and 99.9% for the aug-cc-pV(Q5)Z and aug-cc-pV(56)Z levels, respectively. The excellent agreement between our best R12 values and the extrapolated correlation energies gives us high confidence in the accuracy of the final results, which we regard as benchmark data for future work in the area of explicitly-correlated wave functions.

Acknowledgments

This research has been supported by the Deutsche Forschungsgemeinschaft through the Center for Functional Nanostructures (CFN, Project No. C2.3) and by the Fonds der Chemischen Industrie. We thank Dr. R. Polly of Stuttgart University for providing the geometries of ethylene and ethane for the purpose of benchmarking. We also thank Dr. J. H. van Lenthe of Utrecht University for allowing us to use parts of the GAMESS-UK program for the Boys localization procedure. All calculations were performed on the IBM pSeries 655 cluster of the Institut für Nanotechnologie (INT) of the Forschungszentrum Karlsruhe.

References

[1] N. C. Handy, *In: Computational Techniques in Quantum Chemistry and Molecular Physics, Vol. 15*, G. H. F. Diercksen, B. T. Sutcliffe, and A. Veillard (Eds.), NATO ASI Series C, D. Reidel Publishing Company, Dordrecht, (1975).

[2] E. A. Hylleraas, Z. Phys. **54**, 347 (1929).

[3] H. M. James and A. S. Coolidge, J. Chem. Phys. **1**, 825 (1933).

[4] W. Kołos and C. C. J. Roothaan, Rev. Mod. Phys. **32**, 219 (1960).

[5] W. Kołos and L. Wolniewicz, J. Chem. Phys. **43**, 2429 (1965).

[6] S. F. Boys and N. C. Handy, Proc. Roy. Soc. (London) **309**, 209 (1969).

[7] S. F. Boys and N. C. Handy, Proc. Roy. Soc. (London) **310**, 43 (1969).

[8] S. F. Boys and N. C. Handy, Proc. Roy. Soc. (London) **310**, 63 (1969).

[9] S. F. Boys and N. C. Handy, Proc. Roy. Soc. (London) **311**, 309 (1969).

[10] N. C. Handy, J. Phys. Chem. **51**, 3205 (1969).

[11] N. C. Handy, Mol. Phys. **21**, 817 (1971).

[12] N. C. Handy, Mol. Phys. **23**, 1 (1972).

[13] N. C. Handy, Mol. Phys. **26**, 169 (1973).

[14] J. O. Hirschfelder, J. Chem. Phys. **39**, 3145 (1963).

[15] K. Jankowski, Acta Phys. Pol. **XXXII**, 421 (1967).

[16] K. Jankowski, Acta Phys. Pol. A **37**, 669 (1970).

[17] M. Nooijen and R. J. Bartlett, J. Chem. Phys. **109**, 8232 (1998).

[18] S. Ten-no, Chem. Phys. Lett. **330**, 169 (2000).

[19] S. Ten-no, Chem. Phys. Lett. **330**, 175 (2000).

[20] O. Hino, Y. Tanimura, and S. Ten-no, J. Chem. Phys. **115**, 7865 (2001).

[21] O. Hino, Y. Tanimura, and S. Ten-no, Chem. Phys. Lett. **353**, 317 (2002).

[22] S. Ten-no and O. Hino, Int. J. Mol. Sci. **3**, 459 (2002).

[23] H. J. A. Zweistra, C. C. M. Samson, and W. Klopper, Collect. Czech. Chem. Commun. **68**, 374 (2003).

[24] W. Klopper, *In: The Encyclopedia of Computational Chemistry, Vol.4, pp. 2351–2375*, P. v. R. Schleyer, N. L. Allinger, T. Clark, J. Gasteiger, P. A. Kollman, H. F. Schaefer III, and P. R. Schreiner (Eds.), John Wiley & Sons, Ltd., Chichester, New York, (1998).

[25] R. Bukowski, B. Jeziorski, and K. Szalewicz, *In: Explicitly Correlated Wave Functions in Chemistry and Physics: Theory and Applications, Vol. 13, pp. 185–248*, J. Rychlewski (Ed.), Kluwer Academic Publishers, Dordrecht, (2003).

[26] J. Rychlewski and J. Komasa, *In: Explicitly Correlated Wave Functions in Chemistry and Physics: Theory and Applications, Vol. 13, pp. 91–147*, J. Rychlewski (Ed.), Kluwer Academic Publishers, Dordrecht, (2003).

[27] W. Klopper and W. Kutzelnigg, Chem. Phys. Lett. **134**, 17 (1987).

[28] W. Kutzelnigg and W. Klopper, J. Chem. Phys. **94**, 1985 (1991).

[29] W. Klopper, Chem. Phys. Lett. **186**, 583 (1991).

[30] W. Klopper and J. Almlöf, J. Chem. Phys. **99**, 5167 (1993).

[31] W. Klopper, R. Röhse, and W. Kutzelnigg, Chem. Phys. Lett. **178**, 455 (1991).

[32] J. Noga, W. Kutzelnigg, and W. Klopper, Chem. Phys. Lett. **199**, 497 (1992).

[33] J. Noga and W. Kutzelnigg, J. Chem. Phys. **101**, 7738 (1994).

[34] R. J. Gdanitz, Chem. Phys. Lett. **210**, 253 (1993).

[35] R. J. Gdanitz and R. Röhse, Int. J. Quantum Chem. **55**, 147 (1996).

[36] M. J. Bearpark, N. C. Handy, R. D. Amos, and P. E. Maslen, Theor. Chim. Acta **79**, 361 (1991).

[37] M. J. Bearpark and N. C. Handy, Theor. Chim. Acta **84**, 115 (1992).

[38] E. F. Valeev and H. F. Schaefer III, J. Chem. Phys. **113**, 3990 (2000).

[39] E. F. Valeev, W. D. Allen, H. F. Schaefer III, and A. G. Császár, J. Chem. Phys. **114**, 2875 (2001).

[40] E. F. Valeev, W. D. Allen, R. Hernandez, C. D. Sherrill, and H. F. Schaefer III, J. Chem. Phys. **118**, 8594 (2003).

[41] G. S. Tschumper, M. L. Leininger, B. C. Hoffman, E. F. Valeev, H. F. Schaefer III, and M. Quack, J. Chem. Phys. **116**, 690 (2002).

[42] M. O. Sinnokrot, E. F. Valeev, and C. D. Sherrill, J. Am. Chem. Soc. **124**, 10887 (2002).

[43] J. P. Kenny, W. D. Allen, and H. F. Schaefer III, J. Chem. Phys. **118**, 7353 (2003).

[44] R. Polly, *private communication*.

[45] B. J. Persson and P. R. Taylor, J. Chem. Phys. **105**, 5915 (1996).

[46] B. J. Persson and P. R. Taylor, Theor. Chim. Acta **97**, 240 (1997).

[47] P. Dahle and P. R. Taylor, Theor. Chim. Acta **105**, 401 (2001).

[48] M. Schütz, G. Hetzer, and H.-J. Werner, J. Chem. Phys. **111**, 5691 (1999).

[49] M. Schütz and H.-J. Werner, J. Chem. Phys. **114**, 661 (2001).

[50] C. C. M. Samson, W. Klopper, and T. Helgaker, Comput. Phys. Commun. **149**, 1 (2002).

[51] F. R. Manby, J. Chem. Phys. **119**, 4607 (2003).

[52] S. Ten-no and F. R. Manby, J. Chem. Phys. **119**, 5358 (2003).

[53] P. Wind, T. Helgaker, and W. Klopper, Theor. Chim. Acta **106**, 280 (2001).

[54] P. Wind, W. Klopper, and T. Helgaker, Theor. Chim. Acta **107**, 173 (2002).

[55] W. Klopper and C. C. M. Samson, J. Chem. Phys. **116**, 6397 (2002).

[56] W. Klopper, J. Chem. Phys. **120**, 10890 (2004).

[57] W. Klopper and J. Noga, *In: Explicitly Correlated Wave Functions in Chemistry and Physics: Theory and Applications, Vol. 13, pp. 149–183*, J. Rychlewski (Ed.), Kluwer Academic Publishers, Dordrecht, (2003).

[58] T. H. Dunning, Jr., J. Chem. Phys. **90**, 1007 (1989).

[59] R. A. Kendall, T. H. Dunning, Jr., and R. J. Harrison, J. Chem. Phys. **96**, 6796 (1992).

[60] Basis sets were obtained from the Extensible Computational Chemistry Environment Basis Set Database, Version 10/21/03, as developed and distributed by the Molecular Science Computing Facility, Environmental and Molecular Sciences Laboratory which is part of the Pacific Northwest Laboratory, P.O. Box 999, Richland, Washington 99352, USA, and funded by the U.S. Department of Energy. The Pacific Northwest Laboratory is a multi-program laboratory operated by Battelle Memorial Institute for the U.S. Department of Energy under contract DE-AC06-76RLO 1830. Contact David Feller or Karen Schuchardt for further information.

[61] W. Klopper, Mol. Phys. **99**, 481 (2001).

[62] T. Helgaker, W. Klopper, H. Koch, and J. Noga, J. Chem. Phys. **106**, 9639 (1997).

[63] T. Helgaker, H. J. Aa. Jensen, P. Jørgensen, J. Olsen, K. Ruud, H. Ågren, A. A. Auer, K. L. Bak, V. Bakken, O. Christiansen, S. Coriani, P. Dahle, E. K. Dalskov, T. Enevoldsen, B. Fernandez, C. Hättig, K. Hald, A. Halkier, H. Heiberg, H. Hettema, D. Jonsson, S. Kirpekar, R. Kobayashi, H. Koch, K. V. Mikkelsen, P. Norman, M. J. Packer, T. B. Pedersen, T. A.

Ruden, A. Sanchez, T. Saue, S. P. A. Sauer, B. Schimmelpfennig, K. O. Sylvester-Hvid, P. R. Taylor, and O. Vahtras, *Dalton, a molecular electronic structure program*, Release 1.2 (2001).

[64] GAMESS-UK is a package of ab initio programs written by M. F. Guest, J. H. van Lenthe, J. Kendrick, K. Schoffel, and P. Sherwood, with contributions from R. D. Amos, R. J. Buenker, H. J. J. van Dam, M. Dupuis, N. C. Handy, I. H. Hillier, P. J. Knowles, V. Bonačić-Koutecký, W. von Niessen, R. J. Harrison, A. P. Rendell, V. R. Saunders, A. J. Stone, D. J. Tozer, and A. H. de Vries., *The package is derived from the original GAMESS code due to M. Dupuis, D. Spangler and J. Wendoloski*, NRCC Software Catalog, Vol. 1, Program No. QG01 (1980).

9

Outlook on localized, Gaussian-damped R12 wave functions

R12 methods have proven their ability to provide highly accurate calculations on small to medium-sized molecules. The real challenge lies today in the enlargement of their application range. Combining R12 methods with algorithms in which computing requirements (time, memory as well as disk space) grow linearly with respect to the number of atoms in the system, is conceptually appealing to widen the application range [1, 2]. Since such algorithms are practically more expensive for small molecules than the conventional algorithms, the crossover point represents the size of a molecular system at which the linear-scaling-driven algorithm is more economical than the conventional algorithm, without any major loss of accuracy. The main question remains: is the cross-over point nowadays reachable for linear-scaling R12 methods? To provide some perspective on this issue we discuss in this chapter the results of preliminary work in which we tried to combine MP2-R12 concepts with local correlation concepts which are known to lead to linear-scaling behavior.

9.1 Local correlation scheme for MP2-R12 method

The traditional use of canonical orbitals is not adequate for benefiting from the short-range nature of chemical interactions. In 1983, Pulay proposed a promising local correlation framework [3] for molecular-orbital-based methods that has been proven particularly powerful thereafter when combined with direct integral evaluation and integral screening [4–8]. The occupied space is spanned by a set of localized molecular orbitals and the virtual space by a set of projected atomic orbitals which are by definition localized on the atoms and set orthogonal to the occupied space. The technique consists in a hierarchical treatment of different electron pairs based on the interorbital distance between two localized molecular orbitals and consequently according to their relative contributions to the total correlation energy. Werner and co-workers distinguish four types of electron pairs: the strong pairs (having at least one atom in common and accounting for about 95% of the total correlation energy), the weak pairs (interorbital distance less than 8 a_0), the distant pairs (interorbital distance between 8 and 15 a_0), and the very distant pairs (interorbital distance greater than 15 a_0). Only the number of very distant pairs, which give a negligible contribution to the total correlation energy (by a few μE_h), scales quadratically with size while the scaling of the three remaining pair-types is linear. Moreover the wave function expansion is truncated, so that excitations from occupied to virtual orbitals are restricted to a certain subspace, called domain. The domain corresponding to a given localized molecular orbital is composed of projected atomic orbitals located in its surroundings and the global domain associated with an electron pair is the simple union of the two respective domains. Hence the pair-domain size no longer increases but becomes constant with increasing molecular size [4–8].

R12 methods are combined here with this local correlation scheme at the MP2 level. The

adopted localization scheme has no crucial influence on the method possibilities (as long as it provides properly localized molecular orbitals) [9] and the Boys localization has been arbitrarily chosen here, which minimizes the expectation value of the squared distance between two electrons [10]. Our scheme varies slightly from the conventional domain selection. First the domain should not only contain projected atomic orbitals but also localized molecular orbitals (due to the insertion of the resolution-of-identity). Furthermore the Boughton-Pulay criterium [9] is not used to select the domain, since we need to investigate extra sets of integrals in addition to the integrals over the Coulomb operator r_{12}^{-1} that are solely required in conventional local MP2. For more flexibility, we define a threshold for the expectation value of the distance between the centers of charge of the studied localized molecular orbital and of each other molecular orbital. If this distance is larger than the threshold, the corresponding orbital is excluded from the domain. Using the notations defined in Section 2.1.1, the R12-integrals $\langle\bar{\Phi}_p(1)\bar{\Phi}_q(2)|\hat{\Omega}|\bar{\Phi}_i(1)\bar{\Phi}_j(2)\rangle$ (with $\hat{\Omega}$ a given operator) are computed only if $\bar{\Phi}_i\bar{\Phi}_j$ do not form a very distant pair and if $\bar{\Phi}_p$ and $\bar{\Phi}_q$ belong to the united domains of $\bar{\Phi}_i$ and $\bar{\Phi}_j$. The integrals are assumed to be zero otherwise and thus not explicitly computed nor stored. So far our analytical local MP2-R12 scheme based on the standard approximation has been implemented in a local version of the Dalton quantum chemistry program [11] in its most simple form, that is without auxiliary basis set (Chapter 5). Since the localized molecular orbitals do not necessarily have the same symmetry as the canonical molecular orbitals, the convenient use of symmetry has to be abandoned. The integrals are computed with the McMurchie-Davidson scheme [12].

If χ_a, χ_c, χ_b, and χ_d are Gaussian basis functions centered on A, B, C and D (as defined in Section 2.4.2) and f_{12} denotes the correlation factor (f_{12}=r_{12} for conventional R12 methods and f_{12}=$r_{12}\exp(-\gamma r_{12}^2)$ for Gaussian-damped R12 methods), one needs three types of atomic orbital integrals for linear R12 methods (Chapter 2):

$$I_1 = \langle\chi_a(1)\chi_c(2)|r_{12}^{-1}|\chi_b(1)\chi_d(2)\rangle\,, \tag{9.1}$$

$$I_2 = \langle\chi_a(1)\chi_c(2)|f_{12}|\chi_b(1)\chi_d(2)\rangle\,, \tag{9.2}$$

$$I_3 = \langle\chi_a(1)\chi_c(2)|[\hat{t}_1+\hat{t}_2, f_{12}]|\chi_b(1)\chi_d(2)\rangle\,. \tag{9.3}$$

and three extra sets of atomic-orbital integrals for Gaussian-damped R12 methods (Chapter 6):

$$I_4 = \langle\chi_a(1)\chi_c(2)|\frac{f_{12}}{r_{12}}|\chi_b(1)\chi_d(2)\rangle\,, \tag{9.4}$$

$$I_5 = \langle\chi_a(1)\chi_c(2)|f_{12}^2|\chi_b(1)\chi_d(2)\rangle\,, \tag{9.5}$$

$$I_6 = \langle\chi_a(1)\chi_c(2)|[[\hat{t}_1+\hat{t}_2, f_{12}], f_{12}]|\chi_b(1)\chi_d(2)\rangle\,. \tag{9.6}$$

The calculation of the atomic-orbital integrals is direct: the calculation of each batch of integrals is repeated for each set of electron pairs that strictly share the same domain. A priori this procedure

seems much more expensive than the sequential counterpart. Nevertheless, the efficiency of this method lies in the sparsity of the molecular-orbital coefficients matrix due to the local character of the molecular orbitals, which allows a screening during the calculation of the atomic-orbital integrals. Inside a domain, if all the molecular-orbital coefficients corresponding to a certain batch of atomic orbitals are smaller than a chosen threshold, the batch of integrals is skipped. Consequently, the smaller the domain can be, the cheaper is the calculation.

The main effect of R12 methods is meant to occur at short distances. So if by replacing the r_{12} term by a damped r_{12} term one can reduce the number of large integrals at long r_{12}, while keeping more or less the same correlation contribution at short r_{12} then this could yield a more efficient method by allowing smaller domain selection. This is what the Gaussian-damped R12 method, introduced in Chapter 6, attempts to do. The damping factor $\exp(-\gamma r_{12}^2)$ contains a new parameter γ which must be optimized, but one could hope that a single well-chosen value would work for most cases, so that no reoptimization is necessary for each case individually.

9.2 Integral study over s-type Gaussian basis functions

As an illustration, atomic-orbital integrals over s-type functions are studied here in detail for three specific operators: r_{12}^{-1} (integrals I_1 Eq. (9.1)), r_{12} and $r_{12}\exp(-\gamma r_{12}^2)$ (integrals I_2 Eq. (9.2)). The exponents p and q and the centers of charge P and Q are defined in Section 2.4.2. The variables α and R_{PQ}^2 are defined in Eq. (9.7).

$$\alpha \;=\; \frac{pq}{p+q} \quad \text{and} \quad R_{PQ}^2 = |\vec{P}-\vec{Q}|^2\,. \tag{9.7}$$

The prefactor M_{PQ} and normalization constant N_{PQ} read as in Eq. (9.8).

$$M_{PQ} = \exp(-\frac{ab}{p}R_{AB}^2)\,\exp(-\frac{cd}{q}R_{CD}^2) \quad \text{and} \quad N_{PQ} = \frac{2\,\pi^{\frac{5}{2}}}{pq\sqrt{p+q}}\,. \tag{9.8}$$

F_k denotes the Boys function (Eq. (9.9)) that can be readily calculated via recurrence relations [12].

$$F_k(x) = \int_0^1 \exp(-xt^2)t^{2k}dt. \tag{9.9}$$

The overlap integrals, conventional two-electron integrals, r_{12} integrals, and r_{12}-damped integrals

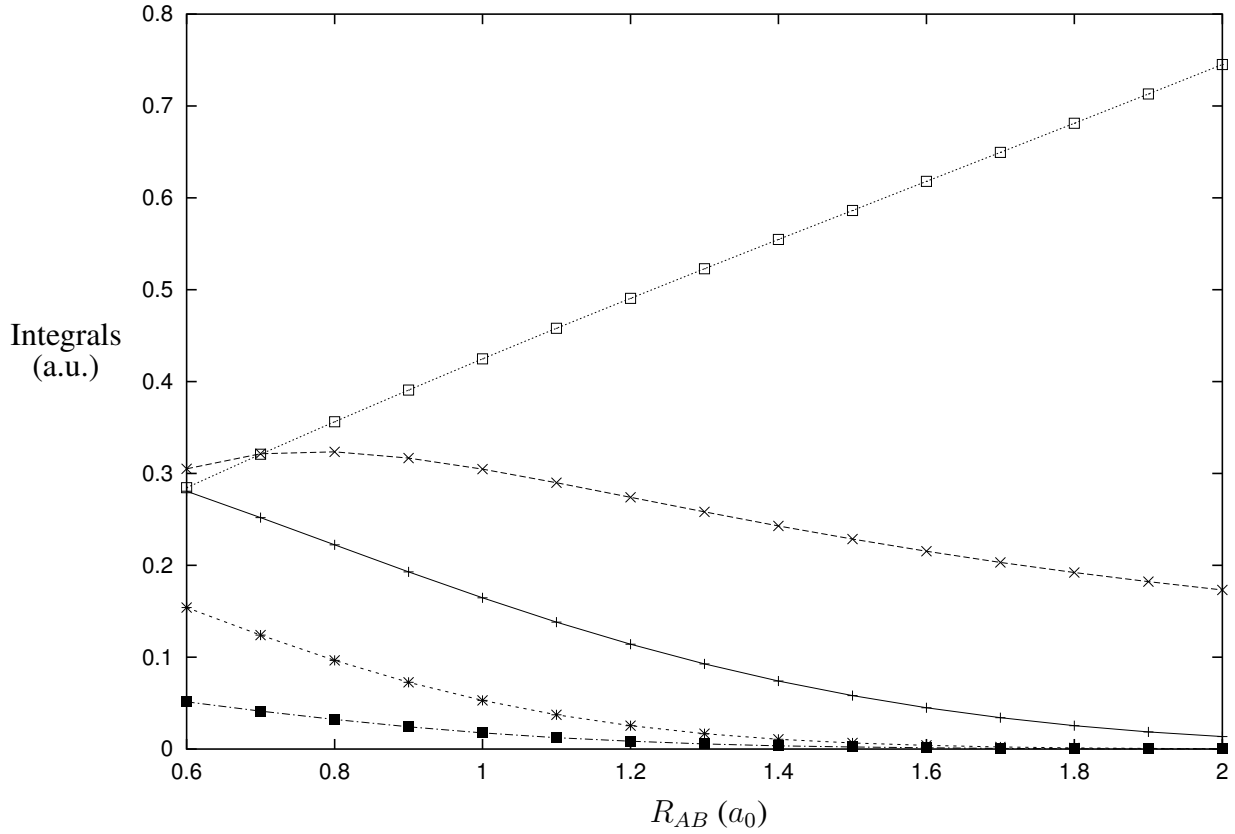

Figure 9.1: Integrals plotted versus the interorbital distance R_{AB} (in a_0) with χ_a and χ_b s-type atomic orbitals of exponents a=1 and b=5. The symbol $+$ corresponds to the overlap integral (Eq. (9.10)), the symbol $\times$ to $\langle\chi_a(1)\chi_b(2)|r_{12}^{-1}|\chi_a(1)\chi_b(2)\rangle$ (Eq. (9.11)), the symbol $*$ to $\langle\chi_a(1)\chi_a(2)|r_{12}^{-1}|\chi_b(1)\chi_b(2)\rangle$ (Eq. (9.11)), the symbol $\square$ to $\langle\chi_a(1)\chi_b(2)|r_{12}|\chi_a(1)\chi_b(2)\rangle$ (Eq. (9.12)), and the symbol $\blacksquare$ to $\langle\chi_a(1)\chi_a(2)|r_{12}|\chi_b(1)\chi_b(2)\rangle$ (Eq. (9.12)).

over s-type Gaussian basis functions are respectively:

$$\langle\chi_a(1)|\chi_b(1)\rangle = \big(\frac{\pi}{p}\big)^{\frac{3}{2}}\exp\big(-\frac{ab}{p}R_{AB}^2\big)\,, \tag{9.10}$$

$$\langle\chi_a(1)\chi_c(2)|\frac{1}{r_{12}}|\chi_b(1)\chi_d(2)\rangle = M_{PQ}\,N_{PQ}\,F_0(\alpha R_{PQ}^2)\,, \tag{9.11}$$

$$\begin{aligned}\langle\chi_a(1)\chi_c(2)|r_{12}|\chi_b(1)\chi_d(2)\rangle &= M_{PQ}\,N_{PQ}\,\Big(\frac{1}{\alpha}F_0(\alpha R_{PQ}^2)+\\ &\quad R_{PQ}^2\big[F_0(\alpha R_{PQ}^2)-F_1(\alpha R_{PQ}^2)\big]\Big)\,,\end{aligned} \tag{9.12}$$

$$\begin{aligned}\langle\chi_a(1)\chi_c(2)|r_{12}\exp(-\gamma r_{12}^2)|\chi_b(1)\chi_d(2)\rangle &= M_{PQ}\,N_{PQ}\,(\frac{\alpha}{\alpha+\gamma})^2\exp(-\gamma R_{PQ}^2)\\ &\quad\Big((R_{PQ}^2+\frac{1}{2\alpha})F_0(\alpha R_{PQ}^2)+\\ &\quad\frac{1}{2\alpha}\exp(-\alpha R_{PQ}^2)\Big)\,.\end{aligned} \tag{9.13}$$

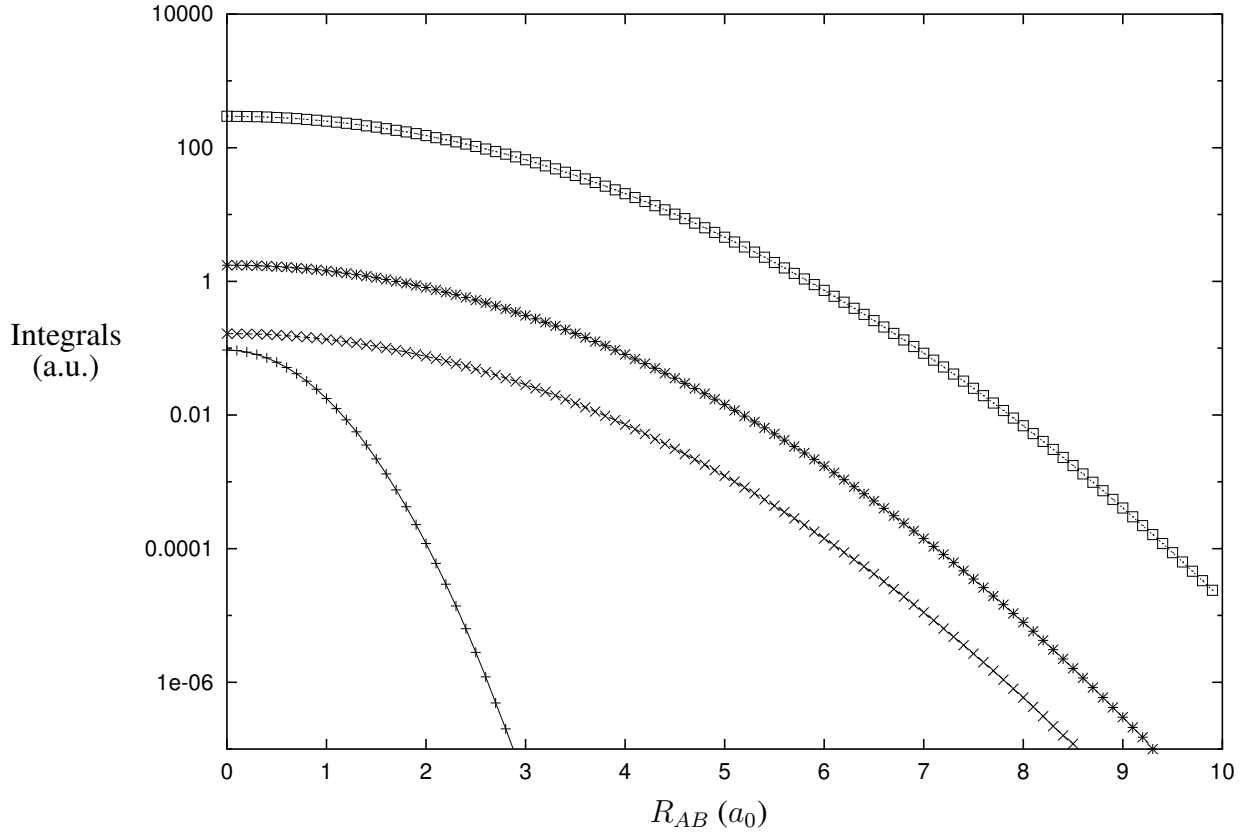

Figure 9.2: Integrals $\langle\chi_a(1)\chi_a(2)|r_{12}|\chi_b(1)\chi_b(2)\rangle$ plotted versus the interorbital distance R_{AB} (in a_0) with χ_a and χ_b s-type atomic orbitals of various exponents. The symbol $+$ corresponds to a=1 and b=5, the symbol $\times$ to a=0.1 and b=5, the symbol $*$ to a=0.1 and b=2.5, and the symbol $\Box$ to a=0.1 and b=0.5.

Figure 9.1 represents the overlap integral (Eq. (9.10)) and the two types of integrals of the form $\langle\chi_a(1)\chi_b(2)|\hat{\Omega}|\chi_a(1)\chi_b(2)\rangle$ and $\langle\chi_a(1)\chi_a(2)|\hat{\Omega}|\chi_b(1)\chi_b(2)\rangle$ (denoted here $aabb$-type integrals and $abab$-type integrals, respectively, by analogy to Mulliken notation) for $\hat{\Omega}$=r_{12}^{-1} (integrals I_1 (Eq. (9.1))) and r_{12} (integrals I_2 (Eq. (9.2))). The interorbital distance R_{AB} varies from 0.6 to 2 a_0 and the orbital exponents are arbitrarily chosen a=1 and b=5. It is observed that the $abab$-integrals for both operators vanish in a similar way as the overlap integral. This is due to the prefactor M_{PQ} resulting from the Gaussian product rule. The r_{12} $aabb$-integrals steadily increase since the influence of the r_{12} operator is not counterbalanced by any prefactor while the conventional $aabb$-integrals decrease steadily due to the nature of the Coulomb operator. A similar trend as for I_2 (Eq. (9.2)) would be observed for the integrals I_3 (Eq. (9.3)).

The integrals that are neglected via domain selections are of course of the type $abab$. Diffuse functions might create problems, since the prefactor M_{PQ} does not vanish as quickly in this case. As an illustration, the $abab$-integrals over r_{12} are plotted on Figure 9.2 for several pairs of exponents

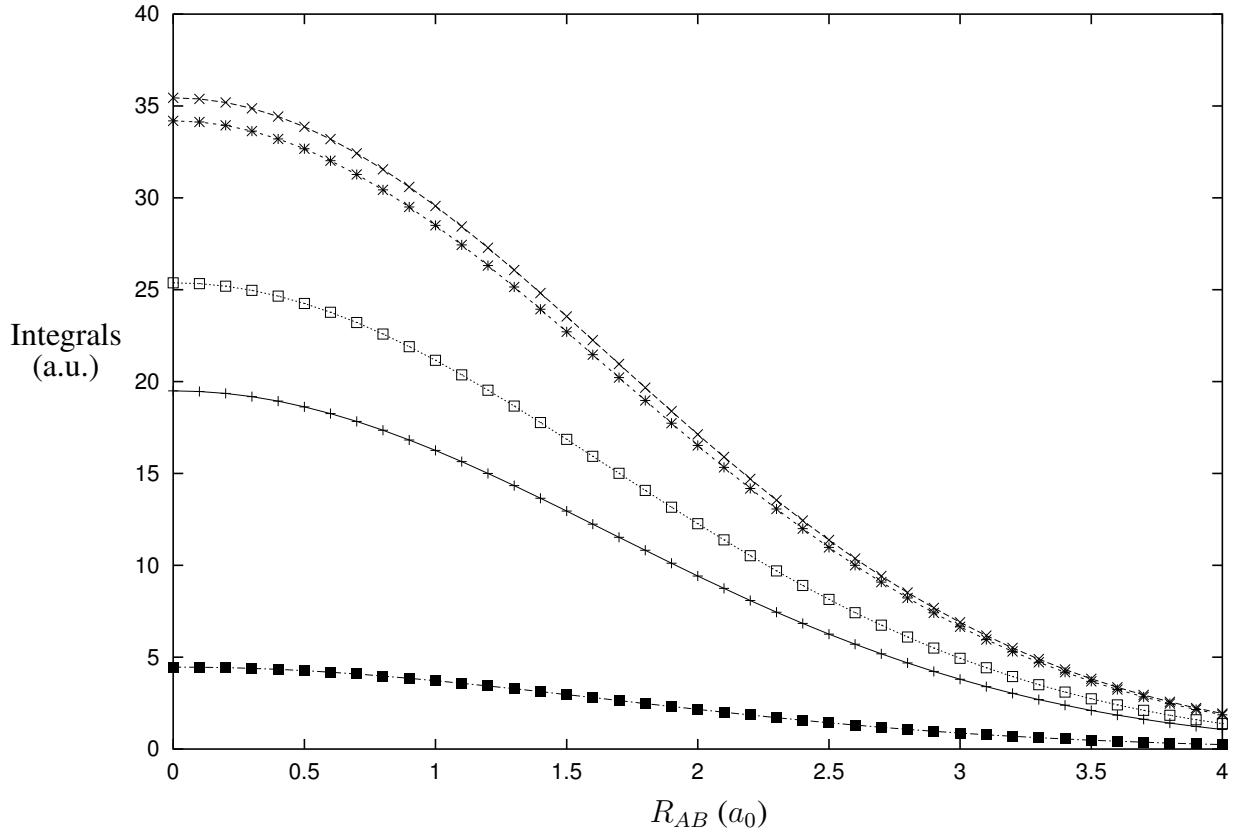

Figure 9.3: Integrals $\langle\chi_a(1)\chi_a(2)|\hat{\Omega}|\chi_b(1)\chi_b(2)\rangle$ plotted versus the interorbital distance R_{AB} (in a_0) with χ_a and χ_b s-type atomic orbitals of exponents a=0.1 and b=1. The symbol $+$ corresponds to $\hat{\Omega}$=r_{12}^{-1} (Eq. (9.11)), the symbol $\times$ to $\hat{\Omega}$=r_{12} (Eq. (9.12)), the symbol $*$ to $\hat{\Omega}$=$r_{12}\exp(-\gamma r_{12}^2)$ with γ=0.01 (Eq. (9.13)), the symbol □ to $\hat{\Omega}$=$r_{12}\exp(-\gamma r_{12}^2)$ with γ=0.1 (Eq. (9.13)), and the symbol ■ to $\hat{\Omega}$=$r_{12}\exp(-\gamma r_{12}^2)$ with γ=1 (Eq. (9.13)).

on a logarithmic scale. For exponents a=1 and b=5, the range of interorbital distance for which integrals are larger than 10^{-4} is less than about 2 a_0, while for a=0.1 and b=0.5, the range is as large as about 10 a_0. This bottleneck seems hard to break since diffuse functions are mandatory to give a good resolution of the identity. The damping has been introduced on this purpose, to cut off the superfluous long-range contribution of the R12 integrals while keeping the fundamental short-range behavior. On this basis, an expensive Gaussian exponent optimization of the parameter γ for each pair function $r_{12}\exp(-\gamma_{ij}\, r_{12}^2)\,\bar{\Phi}_i(1)\,\bar{\Phi}_j(2)$ can possibly be avoided since the short-range behavior is rather universal, that is insensitive to molecular rearragements and external fields.

In Figure 9.3, $abab$-integrals corresponding to operators $\hat{\Omega}$=r_{12}^{-1} and $\hat{\Omega}$=$r_{12}\exp(-\gamma r_{12}^2)$ are plotted for diffuse functions (a=0.1 and b=0.5) and for four fixed γ exponents, 0, 0.01, 0.1, and 1.0. The effect of the damping is clearly seen through the changes in the vanishing behavior of the integral with respect to R_{AB}. However the damping acts likewise on the $aabb$-integrals and should

imperatively not annul the crucial contribution of the R12 correction. Thus the parameter γ is bounded by two essential and conflicting requirements. It should be small enough to guarantee the total recovery of the R12 correction while large enough to erase as many unnecessary long-range integral contributions as possible. Series of calculations on small molecules in their ground state (CH_2 ($^1A_1$), H_2O, HF, N_2, F_2) have led to the conclusion that this damping can be set to 0.1 for covalent-dominated bonds.

9.3 Domain selection in the alkane series

The domain selection has been investigated for local MP2-R12 calculations on the alkane series up to butane. The number of molecular-orbital integrals smaller than the threshold 10^{-4} is first investigated in a s-function basis set taken from the TZV basis [13] for selected integrals of the type I_1 (Eq. (9.1)), I_2 (Eq. (9.2)) and I_3 (Eq. (9.3)). As expected, the number of small integrals steadily increases in the alkane series (Table 9.1). The Gaussian-damped R12 integrals over the operator $r_{12}\exp(-\gamma r_{12}^2)$ (with damping factor γ=0.1) present about the same behavior as the con-

Table 9.1: Percentage of molecular-orbital integrals $\langle\bar{\Phi}_p(1)\bar{\Phi}_q(2)|\hat{\Omega}|\bar{\Phi}_i(1)\bar{\Phi}_j(2)\rangle$ smaller than the threshold 10^{-4} for a series of alkanes C_kH_{2k+2} (k=1 to 4) for fixed frozen-core optimized geometries in the cc-pVTZ basis. The atomic basis set used is formed by the set of s basis functions of the TZV set [13]. γ is chosen equal to 0.1.

$\hat{\Omega}$=	r_{12}^{-1}	r_{12}	$r_{12}\exp(-\gamma r_{12}^2)$	$[T_1+T_2, r_{12}]$	$[T_1+T_2, r_{12}\exp(-\gamma r_{12}^2)]$
CH_4	0.42	0.83	0.42	1.53	1.53
C_2H_6	6.02	3.54	6.00	1.77	3.37
C_3H_8	16.10	7.86	12.81	3.47	6.02
C_4H_{10}	29.73	12.91	21.05	7.70	14.16

Table 9.2: Valence-shell MP2 correlation energy (in E_h) of butane in a large basis set ($11s6p3d2f$) / [$7s5p3d2f$] for carbon and ($5s2p$) / [$3s2p$] for hydrogen derived from the TZV basis series [13], at the fixed frozen-core optimized geometry in the cc-pVTZ basis. All results were obtained using local MP2 methods. The R12 results are given with approximation A and γ is chosen equal to 0.1 for the damped-R12 method.

Systems	MP2	MP2-R12	MP2-damped-R12
Full domain	-0.7223063	-0.7925746	-0.7920269
Domain 10 a_0	-0.7223063	-0.7857585	-0.7952894

ventional integrals over r_{12}^{-1}, while the percentage of small integrals over r_{12} is about two times less. Accordingly the R12-damped calculations are more appropriate for local MP2-R12. Nevertheless, the number of small integrals over the commutator operator remains a critical issue, even for Gaussian-damped R12 results. It means that the domain should definitely be selected larger for local MP2-R12 than for conventional local MP2 calculations. In Table 9.2, we verify this assumption on butane, computing the valence-shell MP2 correlation energy in a basis sufficiently large to provide a reasonable resolution-of-identity. For a very large domain selection of 10 a_0, which corresponds to excluding from the domain of the outermost pairs only the opposite outermost orbitals, the local MP2 energy is perfectly recovered with domain selection while the selected local MP2-R12 energies are both less accurate due to the long-range behavior of the extra sets of R12 integrals. It should however be noticed that the percentage of full-domain energy is better recovered with the Gaussian-damped R12 scheme than the linear scheme and that the Gaussian-damped R12 energy corresponding to a selected domain can be lower than the full domain energy due to the approximation made on the integrals. The problem certainly lies in the difficulty to adapt the domain selection for each type of integrals, even more for Gaussian-damped MP2-R12 where three extra types of integrals arise (Eqs. (9.4) to (9.6)).

9.4 Concluding remarks

The reasoning on the alkane series gives an impression of the problems encountered when combining R12 methods with the linear-scaling-driven local MP2 scheme. Considering that large basis sets with diffuse functions are mandatory for providing proper resolution-of-identity, the cross-over point of the local MP2-R12 method as presently developed is not accessible with the computer ressources available. First, the localized molecular orbitals present a significant contribution all over the space with large and diffuse basis sets and second the R12 integrals do not vanish as quickly as the conventional two-electron integrals with increasing interelectronic distances, which together cause the enlargement of the required domains. The introduction of an auxiliary basis set that solves the resolution-of-identity might partly open up this drawback (Chapter 5), specifically in the hybrid form that was recently proposed [14]. If p', q', ... denote molecular orbitals of the auxiliary basis, only integrals of the form $\langle\bar{\Phi}_{p'}(1)\bar{\Phi}_q(2)|\hat{\Omega}|\bar{\Phi}_i(1)\bar{\Phi}_j(2)\rangle$ are computed in the hybrid scheme, that is, integrals containing only one auxiliary molecular orbital. In such manner, two distinct thresholds could be defined to select the pair-domains. One for the molecular orbitals of the primary basis that would be similar to the conventional local MP2 method and a second one which would be larger for the molecular orbitals of the auxiliary basis. Moreover, more efficient integral evaluation techniques than the McMurchie-Davidson scheme can definitely help in decreasing the computational time (e.g. using the Obara-Saika scheme [15] or the density fitting procedure

[16, 17]). Combining these improvements, one can expect to approach the cross-over point of local MP2-R12 method in a few years.

References

[1] K. Morokuma, Phil. Trans. R. Soc. Lond. A **360**, 1149 (2002).

[2] S. Goedecker and G. E. Scuseria, Comp. Sci. Eng. **5**, 14 (2003).

[3] P. Pulay, Chem. Phys. Lett. **100**, 151 (1983).

[4] M. Schütz, G. Hetzer, and H.-J. Werner, J. Chem. Phys. **111**, 5691 (1999).

[5] G. Hetzer, M. Schütz, H. Stoll, and H.-J. Werner, J. Chem. Phys. **113**, 9443 (2000).

[6] M. Schütz and H.-J. Werner, J. Chem. Phys. **114**, 661 (2001).

[7] P. J. Knowles, M. Schütz, and H.-J. Werner, *In: Modern Methods and Algorithms of Quantum Chemistry, Vol. 3, pp. 97–179*, J. Grotendorst (Ed.), NIC series, Forschungszentrum Jülich, Germany, (2000).

[8] H.-J. Werner, F. R. Manby, and P. J. Knowles, J. Chem. Phys. **118**, 8149 (2003).

[9] J. W. Boughton and P. Pulay, J. Comput. Chem. **14**, 736 (1993).

[10] S. F. Boys, Proc. Roy. Soc. (London) **A258**, 402 (1960).

[11] T. Helgaker, H. J. Aa. Jensen, P. Jørgensen, J. Olsen, K. Ruud, H. Ågren, A. A. Auer, K. L. Bak, V. Bakken, O. Christiansen, S. Coriani, P. Dahle, E. K. Dalskov, T. Enevoldsen, B. Fernandez, C. Hättig, K. Hald, A. Halkier, H. Heiberg, H. Hettema, D. Jonsson, S. Kirpekar, R. Kobayashi, H. Koch, K. V. Mikkelsen, P. Norman, M. J. Packer, T. B. Pedersen, T. A. Ruden, A. Sanchez, T. Saue, S. P. A. Sauer, B. Schimmelpfennig, K. O. Sylvester-Hvid, P. R. Taylor, and O. Vahtras, *Dalton, a molecular electronic structure program*, Release 1.2 (2001).

[12] T. Helgaker, P. Jørgensen, and J. Olsen, *Molecular Electronic-Structure Theory*, John Wiley & Sons, Ltd., Chichester, New York, (2000).

[13] A. Schäfer, C. Huber, and R. Ahlrichs, J. Chem. Phys. **100**, 5829 (1994).

[14] W. Klopper, J. Chem. Phys. **120**, 10890 (2004).

[15] V. Weber and C. Daul, Comput. Phys. Commun. **158**, 1 (2004).

[16] F. R. Manby, J. Chem. Phys. **119**, 4607 (2003).

[17] S. Ten-no and F. R. Manby, J. Chem. Phys. **119**, 5358 (2003).

Summary

The accurate description of short-range electron correlation represents a fundamental challenge for state-of-the-art quantum chemical calculations. The hindrance that one has to face originates from an exceedingly slow convergence of dynamical correlation energy with increasing number of Gaussian basis functions. In this perspective, explicitly correlated wave functions and extrapolation techniques are two systematic ways to accelerate the basis-set convergence of molecular-orbital-based standard models. In this thesis, these two approaches are applied and refined to determine highly accurate ground-state properties for closed-shell molecular systems containing atoms of the first and second rows of the *Periodic Table of Elements*. The two correlation methods mainly used presently are second-order Møller-Plesset perturbation theory (MP2) and coupled-cluster theory including single and double excitations with a noniterative perturbative correction for connected triple excitations (CCSD(T)). The new extrapolation scheme is briefly described in the general introduction (Chapter 1) and is based on a distinct treatment of the triplet pair (X^{-5}) and singlet pair (X^{-3}) convergences, with X the cardinal number of a given correlation-consistent basis-set series. In parallel, explicitly correlated wave functions are utilized in this work in the framework of the so-called R12 methods that employ the bare interelectronic distance r_{12} as correlation factor (Chapter 2), in order to improve the conventional expansion of the wave function in Slater determinants. In passing, similarity-transformed-Hamiltonian techniques (introduced in Chapter 1) are also studied in one chapter. Chapters 3, 4 and 8 contain accurate applications to small to medium-sized molecular systems, while Chapters 5, 6, 7 and 9 are devoted to current method developments.

In Chapter 3 the equilibrium inversion barrier of ammonia, associated with the ν_2 umbrella mode, is extrapolated via the new extrapolation scheme to the basis-set limit of the CCSD(T) model in correlation-consistent series. The reference pyramidal (C_{3v}) and planar (D_{3h}) geometries are optimized at the fully-correlated CCSD(T)/cc-pCVQZ level. The valence-only CCSD(T)-R12 barrier computed in the [N/H]=[19s14p8d6f4g3h / 9s6p4d3f] basis is in excellent agreement with the best extrapolated data, respectively cc-pV(56)Z and aug-cc-pV(Q5)Z. A non-relativistic Born-Oppenheimer fully-correlated inversion barrier of +1767$\pm$12 cm^{-1} is so accurately obtained, by adding together +1613$\pm$3 cm^{-1}, +178$\pm$10 cm^{-1}, +40$\pm$2 cm^{-1}, and –64$\pm$4 cm^{-1} for respectively

Hartree-Fock, CCSD, perturbative triples (T), and core-valence contributions. Finally, accounting for relativistic effects (+20$\pm$2 cm^{-1}), Born-Oppenheimer diagonal correction (–10 cm^{-1}), and zero-point vibrational energy (+244$\pm$15 cm^{-1}) one finds an effective barrier of +2021$\pm$20 cm^{-1}.

The very low barrier to proton transfer in the $(H_2O)OH^-$ complex occurs between two equivalent equilibrum structures of C_1 symmetry that are interconnected through a transition structure $[HOHOH^-]‡$ of C_2 symmetry. We accurately determined it by performing CCSD(T)-R12 calculations and by applying the counterpoise approach using the three fragments OH^-, H^+, and OH^- to correct the basis set superposition error (Chapter 4), which should be taken care of in such a weakly bonded complex. All calculations are frozen-core. The R12 basis set comprises 389 basis functions, [O/H]=[15s9p7d5f / 9s7p5d], and the geometries of the equilibrium and transition structures are optimized at the MP2 level in the [O/H]=[aug-cc-pVQZ / aug-cc-pVTZ] basis. In this way, the best estimate of the barrier to proton exchange is 0.9$\pm$0.3 kJ mol^{-1}and the CCSD(T)-R12 electronic binding energy with respect to dissociation into H_2O and OH^- is estimated to 109$\pm$10 kJ mol^{-1}. Finally, a one-dimensional potential energy curve for the proton transfer between the two equivalent global minima is constructed at the CCSD(T)-R12 level by combining conventional CCSD(T) results with the R12-correction at the MP2 level. The lowest vibrational level corresponding to this proton motion is found to lie 5.2 kJ mol^{-1} above the global minimum, i.e. well above the barrier at the C2 geometry. Hence the barrier has little effect on the probability distribution of the hydrogen-bonding proton.

A new MP2-R12 approach is presented in Chapter 5 that uses an auxiliary basis set to resolve uniquely the resolution-of-identity. This makes it possible to employ standard Gaussian basis sets for R12 calculations. The R12 pair functions can be chosen orthogonal either to the full molecular orbital space (Ansatz **1**) or to the occupied space only (Ansatz **2**), which leads to different working equations contrarily to the genuine MP2-R12 approach. As a test case, MP2-R12 pair energies of the neon atom are computed by Ansatz **2** in the 20s14p11d9f7g5h orbital basis using the huge auxiliary basis 32s24p18d15f12g9h6i. The agreement with earlier calculations where all the three- and four-electron integrals are exactly calculated in the same orbital basis exhibits a maximum deviation of only 6 μE_h. Comparatively, the maximum deviation with accurate formerly extrapolated pair energies amounts only to 7 μE_h. More benchmark calculations are performed for a set of small molecules (CH_2, H_2O, NH_3, HF, N_2, CO, and F_2) at fixed geometries, optimized at the fully-correlated CCSD(T)/cc-pCVQZ level. The auxiliary basis sets are chosen very large: 19s14p8d6f4g3h2i for C, N, O, and F and 9s6p4d3f2g for H and correlation-consistent basis sets (aug)-cc-pVXZ ($2 \leq X \leq 6$) are taken as primary orbital bases. The basis set convergence is considerably speeded up. It is rather difficult to recover 98% of the valence shell MP2 correlation energy even in the largest basis, while it is reached already for X=4 in our new MP2-R12 scheme. In passing, it is observed that Ansatz **2** outperforms Ansatz **1** in most cases.

In Chapter 6 we develop an hybrid scheme for MP2-R12 calculations using a correlation factor of the form $r_{12}\exp(-\gamma r_{12}^2)$, a compromise between the linear and exponential correlation factors. Although the damping is not essential considering that linear R12 amplitudes already ensure a proper decay at large interelectronic distances, the aim is to cut off more rapidly unimportant large integrals for large r_{12}. This should be advantageous when combining R12 methods with linear-scaling-driven local-correlation techniques. Contrarily to Gaussian Geminal or explicitly correlated Gaussian methods, we want to avoid an expensive Gaussian exponent optimization. Here we only have to consider the two conditions that γ should be small enough to conserve the r_{12} benefit at small interelectronic distances and large enough to remove long-range integral contributions as early as possible. The evaluation of all two-electron integrals is achieved using the McMurchie-Davidson scheme and requires up to six-term recurrence relations involving Boys functions. None of the occurring five non-standard integrals requires much more computational effort than the usual two-electron integrals.

Chapter 7 is a pilot study of a new correlation function of the form $\left(\sum_{i<j} r_{ij}\exp(-\gamma r_{ij}^2)\right)$ introduced in the methodology of similarity-transformed Hamiltonians for configuration interaction (CI) calculations on two-electron systems. Calculations on the helium atom are performed in large Gaussian basis sets (subsets of the $19s16p14d12f10g8h6i4k$ basis) and calculations on the H_2 molecule in the subset $5s4p$ of the aug-cc-pVQZ basis. For a correlation function with coefficient c=$\frac{1}{2}$ and exponent γ=0, the basis-set convergences of the correlation energy and of the expectation value of the interelectronic distance are clearly superior to the conventional CI results. Furthermore, for c=$\frac{1}{2}$, the variation of the correlation energy with increasing damping exponents indicates that γ should be chosen below 0.1 to keep accurate results. Finally, the energy calculation versus the parameter γ on the H_2 molecule with different internuclear distances between 5.0 and 1000 a_0 indicates that for large internuclear distances, γ should be kept sufficiently large to maintain the convergence of the CI calculation. Because of this contradiction, it is difficult to make definite statements on an universal optimum value of γ.

The frozen-core MP2 pair correlation energies of ethylene and ethane are computed at given geometries for localized molecular orbitals (Chapter 8). The Boys procedure is applied to valence orbitals only and for ethylene, two cases are investigated: either all orbitals are localized generating C-C banana bonds or σ-type orbitals only are localized leaving the π-type orbitals unchanged. The Gaussian basis-set representation is enhanced through both the R12 method (in its genuine form) in subsets of the [C/H]=[$19s14p8d6f4g3h2i$ / $9s6p4d3f2g$] basis and through the new extrapolation scheme in the (aug)-cc-pVXZ series. Since the Fock matrix is not diagonal with localized molecular orbitals, the MP2-R12 amplitude equations have to be solved iteratively. The MP2-R12 energies for ethylene and ethane amount respectively to –373.6$\pm$0.1 mE_h and –410.0$\pm$0.1 mE_h and the aug-cc-pV(Q5)Z and aug-cc-pV(56)Z extrapolations agree to within 99.8% and 99.9%

with these values, respectively.

Finally, Chapter 9 gives an outlook on the use of localized, Gaussian-damped R12 wave functions in combination with linear-scaling-driven algorithms, in the aim to broaden the R12 application range. The goal is to devise a method in which unimportant long-range integrals vanish more rapidly, avoiding so the explicit computation or storage of zero integrals. In a formal form, the R12-integrals $\langle\bar{\Phi}_p(1)\bar{\Phi}_q(2)|\hat{\Omega}|\bar{\Phi}_i(1)\bar{\Phi}_j(2)\rangle$ (with $\hat{\Omega}$ a given operator, $\bar{\Phi}_p$, $\bar{\Phi}_q$ molecular spin orbitals, and $\bar{\Phi}_i$, $\bar{\Phi}_j$ occupied orbitals) are computed only if $\bar{\Phi}_i\bar{\Phi}_j$ do not form a very distant pair and if $\bar{\Phi}_p$ and $\bar{\Phi}_q$ belong to the union of the $\bar{\Phi}_i$ and $\bar{\Phi}_j$ domains. Calculations on the alkane series have led to the unfortunate conclusion that the domain associated with each occupied pair should be drastically enlarged compared to conventional MP2. First, one observes that the required non-standard integrals are much longer-range than the conventional two-electon integrals. Although the new Gaussian-damped R12 scheme improves slightly this behavior compared to the original linear R12 scheme, it is not sufficient to overcome enough the drawback. Second, the heavy prerequisite on the use of diffuse Gaussian basis functions to resolve the resolution-of-identity is responsible for the non-negligible contribution of the localized molecular orbitals all over the space. Thus, the cross-over point of the linear-scaling MP2-R12 method is not yet accessible and one should turn towards more efficient integral evaluation techniques together with parallelization of computer code to reduce substantially the computational time.

Samenvatting

Het geven van een nauwkeurige beschrijving van de correlatie tussen elektronen die zich op een korte afstand van elkaar bevinden, is een grote uitdaging voor huidige quantum chemische berekeningen. De hindernis die men tegenkomt, komt voort uit de uiterst trage convergentie van de dynamische correlatie energie met een toenemend aantal Gaussian basis functies. Vanuit dit gezichtspunt zijn expliciet gecorreleerde golffuncties en extrapolatie technieken twee systematische manieren om de basis set convergentie van standaard modellen, die gebaseerd zijn op molekulaire orbitaal theorie, te versnellen. In dit proefschrift worden deze twee benaderingen toegepast en verfijnd om zeer nauwkeurig de grondtoestand eigenschappen van molekulen, die atomen bevatten uit de eerste en tweede rijen van het periodiek systeem der elementen en volledig gevulde schillen hebben, vast te stellen. De twee methoden die in dit werk het meest gebruikt worden, zijn tweede orde Møller-Plesset storingstheorie (MP2) en coupled-cluster theorie waarbij enkele en dubbele excitaties meegenomen worden, en waarbij door middel van storingstheorie een correctie wordt berekend voor de gelinkte drievoudige excitaties (CCSD(T)). Het nieuwe extrapolatie schema wordt kort beschreven in de algemene introductie (Hoofdstuk 1) en is gebaseerd op een afzonderlijke behandeling van de triplet paar (X^{-5}) en singlet paar (X^{-3}) convergenties, waarbij X het cardinaalgetal van een gegeven correlatie-consistente basis set serie is. Tegelijkertijd worden expliciet gecorreleerde golffuncties gebruikt in dit werk in het kader van de zogenoemde R12 methoden die enkel de afstand tussen elektronen (r_{12}) gebruiken als correlatie factor (Hoofdstuk 2), om de conventionele expansie van de golffunctie in Slater determinanten te verbeteren. Ook worden gelijkvormigheids-getransformeerde Hamiltoniaan technieken (geïntroduceerd in Hoofdstuk 1) bestudeerd. Hoofdstukken 3, 4 en 8 bevatten nauwkeurige toepassingen op kleine tot middelgrote molekulen, terwijl Hoofdstukken 5, 6, 7 en 9 toegespitst zijn op methode ontwikkeling.

In Hoofdstuk 3 wordt beschreven hoe de inversiebarrière van ammoniak, welke geassocieerd wordt met de ν_2 paraplu vibratie, geëxtrapoleerd wordt via het nieuwe extrapolatie schema naar de basis set limiet van het CCSD(T) model in de correlatie-consistente serie. De referentie pyramidale (C_{3v}) en vlakke (D_{3h}) geometrieën worden geoptimaliseerd op het volledig gecorreleerde CCSD(T)/cc-pCVQZ niveau. De barrière, berekend met de CCSD(T)-R12 methode waarbij alleen de valentie elektronen gecorreleerd worden, in de [N/H]=[19s14p8d6f4g3h/9s6p4d3f] basis,

komt erg goed overeen met de beste geëxtrapoleerde data, van respectievelijk cc-pV(56)Z en aug-cc-pV(Q5)Z niveau. Een niet-relativistische Born-Oppenheimer volledig gecorreleerde inversie barrière van +1767 $\pm$ 12 cm^{-1} is zo nauwkeurig verkregen, door +1613 $\pm$3 cm^{-1}, +178 $\pm$ 10 cm^{-1}, +40 $\pm$ 2 cm^{-1}, en –64 $\pm$ 4 cm^{-1} te sommeren voor respectievelijk de Hartree-Fock, CCSD, tripel bijdragen verkregen met behulp van storingstheorie (T), en binnenschil-valentie bijdragen. Uiteindelijk, wanneer rekening gehouden wordt met relativistische effecten (+20 $\pm$ 2 cm^{-1}), Born-Oppenheimer diagonale correctie (–10 cm^{-1}), en nulpuntsvibrationele energie (+244 $\pm$ 15 cm^{-1}), wordt een effectieve barrière van +2021 $\pm$ 20 cm^{-1} gevonden.

De zeer lage barrière voor proton overdracht in het $(H_2O)OH^-$ complex vindt plaats tussen twee equivalente evenwichtsstrukturen met C_1 symmetrie welke met elkaar verbonden zijn door een overgangstoestand $[HOHOH^-]‡$ met C_2 symmetrie. We hebben deze nauwkeurig vastgesteld door het doen van CCSD(T)-R12 berekeningen waarbij ook gecorrigeerd wordt voor de basis set superpositie fout door het toepassen van de 'counterpoise' methode aan de drie fragmenten OH^-, H^+, en OH^- (Hoofdstuk 4). In zo'n zwak gebonden complex kan dit niet verwaarloosd worden. De binnenschil orbitalen worden niet gecorreleerd. The R12 basis set bestaat uit 389 basis functies, [O/H]=[15s9p7d5f/9s7p5d] en de geometrieën van de evenwichtsstruktuur en overgangstoestand worden geoptimaliseerd op het MP2 level in de [O/H]=[aug-cc-pVQZ/aug-cc-pVTZ] basis. Op deze manier wordt als beste schatting voor de barrière voor proton overdracht 0.9 $\pm$ 0.3 kJ mol^{-1} verkregen, en de CCSD(T)-R12 elektronische bindingsenergie voor dissociatie in H_2O en OH^- wordt geschat op 109 $\pm$ 10 kJ mol^{-1}. Tenslotte wordt een één dimensionale potentiële energie curve voor proton overdracht tussen de twee globale minima berekend op het CCSD(T)-R12 niveau door middel van de conventionele CCSD(T) resultaten te combineren met de R12 correctie berekend op MP2 niveau. Gevonden wordt dat het laagste vibrationele niveau dat correspondeert met deze beweging van het proton 5.2 kJ mol^{-1} boven het globale minimum ligt, dat wil zeggen ver boven de barrière van de C_2 geometrie. Dus de barrière heeft een klein effect op de waarschijnlijkheidsverdeling van het waterstofbrug gebonden proton.

Een nieuwe MP2-R12 benadering wordt gepresenteerd in Hoofdstuk 5. Deze maakt gebruik van een hulp basis set om eenduidig de resolutie van de eenheidsoperator uit te voeren. Dit maakt het mogelijk om standaard Gaussian basis sets te gebruiken voor R12 berekeningen. De R12 paar functies kunnen orthogonaal gekozen worden, óf op de volledige molekulaire orbitaal ruimte (Ansatz **1**), óf op alleen de bezette ruimte (Ansatz **2**), wat leidt tot verschillende vergelijkingen waarmee gewerkt wordt, in tegenstelling tot de oorspronkelijke MP2-R12 methode. Als test worden de MP2-R12 paar energieën van het neon atoom berekend in Ansatz **2** in de 20s14p11d9f7g5h orbitaal basis en wordt gebruik gemaakt van de bijzonder grote hulp basis 32s24p18d15f12g9h6i. De afwijking tussen eerdere berekeningen waarbij alle drie- en vier-elektron integralen exact werden berekend in dezelfde orbitaal basis en onze berekeningen is maximaal 6 μE_h. Ter vergelij-

king, de maximale afwijking met nauwkeurige geëxtrapoleerde paar energieën is slechts 7 μE_{h}. Meer benchmark berekeningen worden gedaan voor een serie kleine molekulen (CH_2, H_2O, NH_3, HF, N_2, CO en F_2) met een gefixeerde geometrie, geoptimaliseerd op het volledig gecorreleerde CCSD(T)/cc-pCVQZ niveau. De hulp basis sets worden erg groot gekozen: $19s14p8d6f4g3h2i$ voor C, N, O en F, en $9s6p4d3f2g$ voor H en correlatie consistente basis sets (aug-)cc-pVXZ ($2 \leqslant X \leqslant 6$) worden gebruikt voor de primaire orbitaal bases. De basis set convergentie is aanzienlijk versneld. Het is behoorlijk moeilijk om 98% van de valentie-schil MP2 correlatie energie te verkrijgen, zelfs in de grootste basis set, terwijl dat al behaald wordt voor X=4 met ons nieuwe MP2-R12 schema. Verder is ook waargenomen dat Ansatz **2** in bijna alle gevallen beter presteert dan Ansatz **1**.

In Hoofdstuk 6 ontwikkelen we een hybride schema voor MP2-R12 berekeningen waarbij een correlatie factor van het type $r_{12}\exp(-\gamma r_{12}^2)$, een compromis tussen de lineaire en exponentiële correlatie factoren, gebruikt wordt. Hoewel de demping niet noodzakelijk is omdat de lineaire R12 amplitudes al een goede afname verzekeren voor grote interelektronische afstanden, is het doel om sneller onbelangrijke, grote integralen voor grote r_{12} naar nul te laten naderen. Dit zou een voordeel zijn wanneer de R12 methoden gecombineerd worden met locale correlatie technieken, die lineair schalen. In tegenstelling tot Gaussian Geminal of expliciet gecorreleerde Gaussian methoden, willen wij een dure Gaussian exponent optimalisatie voorkomen. Hier hoeven we alleen rekening te houden met de twee voorwaarden dat γ klein genoeg moet zijn om het r_{12} voordeel te behouden voor kleine interelektron afstanden en groot genoeg moet zijn om lange-afstand integraalbijdragen zo vroeg mogelijk te verwijderen. De evaluatie van alle twee-elektron integralen is uitgevoerd met het McMurchie-Davidson schema en vereist tot aan zes-term recursieve relaties waarbij Boys functies zijn betrokken. Geen van de voorkomende vijf niet-standaard integralen vereist veel meer computationele inspanning dan de gewone twee-elektron integralen.

Hoofdstuk 7 is een proefonderzoek van een nieuwe correlatie functie met de vorm $(\sum_{i<j} r_{ij}\exp(-\gamma r_{ij}^2))$, geïntroduceerd in de methodologie van gelijkvormigheids-getransformeerde Hamiltonianen voor configuratie interactie (CI) berekeningen aan twee-elektron systemen. Berekeningen aan het helium atoom worden gedaan in grote Gaussian basis sets (deelverzamelingen van de $19s16p14d12f10g8h6i4k$ basis) en berekeningen aan het H_2 molekuul in de deelverzameling $5s4p$ van de aug-cc-pVQZ basis. Voor een correlatie functie met coefficient $c = \frac{1}{2}$ en exponent $\gamma = 0$ zijn de basis set convergenties van de correlatie energie en van de verwachtingswaarde voor de interelektron afstand duidelijk beter dan wat verkregen wordt met conventionele CI. Bovendien, voor $c = \frac{1}{2}$ geeft de variatie van de correlatie energie met toenemende dempings exponenten aan dat de parameter γ gekozen moet worden onder 0.1 om nauwkeurige resultaten te behouden. Uiteindelijk geeft de energie berekening als functie van de parameter γ voor het H_2 molekuul voor verschillende internucleaire afstanden tuusen 5.0 en 100 a_0 aan dat voor grote internucleaire

afstanden, γ voldoende groot gehouden moet worden om convergentie van de CI berekening te behouden. Vanwege deze tegenstelling is het moeilijk om sluitende conclusies te trekken over een universeel optimale waarde voor γ.

MP2 paar-correlatie energieën met bevroren binnenschil orbitalen worden voor etheen en ethaan berekend bij gefixeerde geometrieën met behulp van gelokaliseerde orbitalen (Hoofdstuk 8). De Boys procedure wordt toegepast voor alleen de valentie schillen en voor etheen worden twee gevallen onderzocht: óf alle orbitalen worden gelokaliseerd waarbij C-C banaanachtige bindingen worden gevormd, óf alleen de σ type orbitalen worden gelokaliseerd terwijl de π type orbitalen onveranderd blijven. De Gaussian basis set representatie wordt verbeterd door zowel de R12 methode (in zijn originele formulering) in deelverzamelingen van de [C/H]=[19s14p8d6f4g3h2i/ 9s6p4d3f2g] basis als door het nieuwe extrapolatie schema in de (aug-)cc-pVXZ serie. Omdat de Fock matrix niet diagonaal is met gelokaliseerde orbitalen, moeten de MP2-R12 amplitude vergelijkingen iteratief opgelost worden. De MP2-R12 energieën voor etheen en ethaan bedragen respectievelijk –373.6 $\pm$ 0.1 m$E_{\rm h}$ en –410.0 $\pm$ 0.1 m$E_{\rm h}$ en de aug-cc-pV(Q5)Z en aug-cc-pV(56)Z extrapolaties komen met deze waarden overeen voor respectievelijk 99.8 $\%$ en 99.9 $\%$.

Tenslotte wordt in Hoofdstuk 9 een toekomstvisie gegeven op het gebruik van gelokaliseerde, Gaussian-gedempte R12 golffuncties in combinatie met lineair-schalende algoritmen, met als doel het toepassingsgebied voor R12 te vergroten. Het doel is om een methode te ontwikkelen waarin onbelangrijke lange-afstand integralen sneller naar nul naderen, om op die manier de expliciete berekening of het opslaan van integralen die bijna nul zijn te voorkomen. In een formele vorm worden de R12 integralen $\langle\bar{\Phi}_p(1)\bar{\Phi}_q(2)|\hat{\Omega}|\bar{\Phi}_i(1)\bar{\Phi}_j(2)\rangle$ (waarin $\hat{\Omega}$ een bepaalde operator is, $\bar{\Phi}_p$, $\bar{\Phi}_q$ molekulaire spin-orbitalen en $\bar{\Phi}_i$, $\bar{\Phi}_j$ bezette orbitalen zijn) alleen berekend als $\bar{\Phi}_i\bar{\Phi}_j$ niet een erg verre-afstands paar is, en als $\bar{\Phi}_p$ en $\bar{\Phi}_q$ behoren tot de vereniging van de $\bar{\Phi}_i$ en $\bar{\Phi}_j$ domeinen. Berekeningen aan de alkaan reeks hebben geleid tot de onfortuinlijke conclusie dat de domeinen geassocieerd met ieder bezet paar aanzienlijk vergroot moet worden in vergelijking met conventionele MP2. Ten eerste, men observeert dat de vereiste niet-standaard integralen een veel groter afstandsbereik hebben dan conventionele twee-elektron integralen. Hoewel het nieuwe Gaussian gedempte R12 schema dit gedrag een beetje verbetert in vergelijking met het originele lineaire R12 schema, is het toch nog niet voldoende om over dit nadeel heen te komen. Ten tweede, de noodzaak om diffuse Gaussian basis functies te gebruiken om de resolutie van de eenheidsoperator uit te voeren is verantwoordelijk voor de niet-verwaarloosbare bijdrage van de gelokaliseerde orbitalen over de gehele ruimte. Dus het punt waarop de lineair-schalende MP2-R12 methode voordeliger wordt kan nog niet bereikt worden en men zou zich moeten richten op efficiëntere integraal evaluatie technieken samen met parallelisatie van het computer programma om de computer tijd drastisch te verminderen.

Zusammenfassung

Die genaue Beschreibung kurzreichweitiger Elektronenkorrelation stellt eine fundamentale Herausforderung für derzeitige quantenchemische Rechnungen dar. Das Hindernis, das es zu überwinden gilt, rührt von der äußerst langsamen Konvergenz der dynamischen Korrelationsenergie mit zunehmender Anzahl an Gauß-Funktionen her. Aus dieser Sicht sind explizit korrelierte Wellenfunktionen und Extrapolationstechniken zwei systematische Wege, die Basissatzkonvergenz der gewöhnlichen Molekülorbitalmodelle zu beschleunigen. In dieser Arbeit werden diese beiden Ansätze angewandt und verfeinert, um hochgenaue Grundzustandseigenschaften für geschlossenschalige molekulare Systeme zu bestimmen, die Atome der ersten und zweiten Reihe des Periodensystems enthalten. Die beiden Korrelationsmethoden, die zur Zeit hauptsächlich verwendet werden, sind Møller-Plesset-Störungstheorie zweiter Ordnung (MP2) und Coupled-Cluster-Theorie, Einfach- und Doppelanregungen eingeschlossen, wobei miteinander gekoppelte Dreifachanregungen störungstheoretisch berücksichtigt werden (CCSD(T)). Das neue Extrapolationsschema wird in der allgemeinen Einführung (Kapitel 1) kurz beschrieben und basiert auf einer eingehenden Behandlung der Konvergenz der Triplett- (X^{-5}) und Singulett- (X^{-3}) Paarenergien, wobei X die Kardinalzahl einer gegebenen korrelationskonsistenten Basissatzreihe ist. Parallel dazu werden in dieser Arbeit im Rahmen der sogenannten R12-Methoden korrelierte Wellenfunktionen behandelt, in denen der bloße interelektronische Abstand r_{12} als Korrelationsfaktor verwendet wird, um die konventionelle Entwicklung der Wellenfunktion in Slaterdeterminanten zu verbessern. Nebenbei werden Techniken bezüglich des änlichkeitstransformierten Hamiltonoperators (eingeführt in Kapitel 1) in einem eigenen Kapitel behandelt. Kapitel 3 ,4 und Kapitel 8 enthalten Anwendungen zu kleinen bis mittelgroßen molekularen Systemen, während Kapitel 5, 6, 7 und 9 aktuellen Methodenentwicklungen gewidmet sind.

In Kapitel 3 wird die Inversionsbarriere von Ammoniak im Gleichgewicht, verbunden mit der ν_2-Schwingungsmode, in korrelationskonsistenten Basissatzreihen mittels des neuen Extrapolationsschemas zum Basissatzlimit des CCSD(T)-Modells hin extrapoliert. Die pyramidalen (C_{3v}) und planaren (D_{3h}) Referenzgeometrien werden auf vollständig korreliertem CCSD(T)/cc-pCVQZ Niveau optimiert. Des Weiteren ist die CCSD(T)-R12 Barriere, die in der [N/H]= [19s14p8d6f4g-3h / 9s6p4d3f]-Valenzbasis berechnet wurde, in ausgezeichneter Übereinstimmung mit den extra-

polierten Daten, das heißt, den Ergebnissen in den Basissätzen cc-pV(56)Z und aug-cc-pV(Q5)Z. Man erhält so eine nicht-relativistische, vollständig korrelierte Born-Oppenheimer-Inversionsbarriere von +1767$\pm$12 cm^{-1}, die sich zusammensetzt aus +1613$\pm$3 cm^{-1}, +178$\pm$10 cm^{-1}, +40$\pm$2 cm^{-1}, und –64$\pm$4 cm^{-1} für jeweils Hartree-Fock, CCSD, störungstheoretisch berücksichtigte Dreifachanregungen (T) und Rumpf-Valenz-Beiträgen. Berücksichtigt man schließlich relativistische Effekte (+20$\pm$2 cm^{-1}), die Born-Oppenheimer-Diagonalkorrektur (–10 cm^{-1}) und die Nullpunktsschwingungsenergie (+244$\pm$15 cm^{-1}), so erhält man eine effektive Barriere von +2021$\pm$20 cm^{-1}.

Die sehr geringe Barriere bezüglich des Protonentransfers im (H_2O)OH^--Komplex tritt zwischen zwei äquivalenten Gleichgewichtsstrukturen von C_1-Symmetrie auf, die durch eine Übergangsstruktur [$HOHOH^-$]‡ von C_2-Symmetrie miteinander gekoppelt sind. Wir haben sie durch eine CCSD(T)-R12-Rechnung und durch Counterpoise-Methode bestimmt, bei dem die drei Fragmente OH^-, H^+, und OH^- verwendet werden, um den Basissatzsuperpositionsfehler zu vermeiden (Kapitel 4), auf den in solch schwach gebunden Komplexen Acht gegeben werden sollte. Alle Rechnungen werden bei eingefrorenen Rumpforbitalen durchgeführt. Der R12-Basissatz umfasst 389 Basisfunktionen [O/H]=[15s9p7d5f / 9s7p5d], die Geometrien der Gleichgewichts- und Übergangsstrukturen werden auf MP2-Niveau in einer [O/H]=[aug-cc-pVQZ / aug-cc-pVTZ]-Basis optimiert. Auf diese Art und Weise beläuft sich die beste Schätzung der Barriere für den Protonentransfer auf 0.9$\pm$0.3 kJ mol^{-1}. Die mittels CCSD(T)-R12 berechnete elektronische Bindungsenergie in Bezug auf den Zerfall in H_2O und OH^- kann man mit 109$\pm$10 kJ mol^{-1}abschätzen. Schließlich wurde eine eindimensionale Potentialkurve für den Protonentransfer zwischen den zwei äquivalenten globalen Minima auf CCSD(T)-R12-Niveau berechnet, indem konventionelle CCSD(T) Ergebnisse mit den R12-Korrekturen auf MP2-Niveau kombiniert wurden. Das niedrigste Schwingungsniveau, das mit dieser Protonenbewegung korrespondiert, lag 5.2 kJ mol^{-1} über dem globalen Minimum, das heißt, ein gutes Stück über der Barriere in der C_2 Geometrie. Damit hat die Barriere eine geringe Auswirkung auf die Wahrscheinlichkeitsverteilung des Wasserstoffbrückenprotons.

Ein neuer MP2-R12 Ansatz, bei dem eine Auxiliarbasis eingesetzt wird, um die Vollständigkeitsrelation darzustellen, wird in Kapitel 5 vorgestellt. Dieser ermöglicht es, Standardbasissätze bestehend aus Gauß -Funktionen für R12-Rechnungen zu verwenden. Die R12-Paarfunktionen können entweder orthogonal zum gesamten Molekülorbitalraum (Ansatz 1) oder nur zum besetzten Raum (Ansatz 2) gewählt werden, was, anders als im ursprünglichen MP2-R12-Ansatz, zu verschiedenen Gleichungen führt. Als Testfall wurden MP2-R12 Paarenergien des Neon-Atoms mit Ansatz 2 in einer 20s14p11d9f7g5h-Orbitalbasis und einer 32s24p18d15f12g9h6i-Auxiliarbasis berechnet. Die Übereinstimmung mit früheren Rechnungen, bei denen alle Drei- und Vierelektronenintegrale in derselben Orbitalbasis exakt berechnet wurden, zeigt eine maximale Abweichung

von $6\,\mu E_\mathrm{h}$. Im Vergleich dazu beläuft sich die maximale Abweichung zu genauen, zu einem früheren Zeitpunkt extrapolierten Paarenergien, auf nur $7\,\mu E_\mathrm{h}$. Weitere Validierungsrechnungen werden für einen Satz von kleinen Molekülen (CH_2, H_2O, NH_3, HF, N_2, CO und F_2) bei festen Geometrien, optimiert auf vollständig-korreliertem CCSD(T)/cc-pCVQZ-Niveau, durchgeführt. Die Auxiliarbasissätze werden sehr groß gewählt: $19s14p8d6f4g3h2i$ für C, N, O und F und $9s6p4d3f2g$ für H. Korrelationskonsistente Basissätze (aug)-cc-pVXZ ($2 \leq X \leq 6$) werden als primäre Orbitalbasis verwendet. Die Basissatzkonvergenz wird erheblich beschleunigt. Es ist ziemlich schwierig, 98% der MP2-Valenzkorrelationsenergie abzudecken, während das schon für X=4 in unserem neuen MP2-R12-Modell erreicht wird. Nebenbei wird beobachtet, dass Ansatz 2 Ansatz 1 meistens übertrifft.

In Kapitel 6 entwickeln wir ein Hybrid-Schema für MP2-R12-Rechnungen, indem wir einen Korrelationsfaktor der Form $r_{12}\exp(-\gamma r_{12}^2)$ verwenden, einen Kompromiss zwischen dem linearen und dem exponentiellen Korrelationsfaktor. Ziel ist es, störend große Integrale für große r_{12} abzuschneiden, obwohl die Dämpfung nicht essentiell ist, wenn man beachtet, dass die linearen R12-Amplituden schon einen angemessenen Abfall bei großen interelektronischen Abständen sicher stellen. Das sollte vorteilhaft sein, wenn man R12-Methoden mit lokal korrelierten Methoden kombiniert, die eine lineare Skalierung zum Ziel haben. Im Gegensatz zu Methoden, die Gauß'sche Geminale oder explizit korrelierte Gauß-Funktionen verwenden, wollen wir eine teure Optimierung des Exponenten der Gauß-Funktionen vermeiden. Hier müssen wir nur die beiden Bedingungen beachten, dass γ klein genug sein sollte, um den r_{12}-Nutzen bei kleinen interelektronischen Abständen zu bewahren und groß genug, um langreichweitige Integralbeiträge so bald wie möglich abzuschneiden. Die Auswertung aller Zweielektronenintegrale erhält man durch das McMurchie-Davidson-Modell. Dieses erfordert Rekursionsbeziehungen mit bis zu sechs Termen, die Boys-Funktionen enthalten. Keines der auftretenden fünf Nichtstandardintegrale erfordert viel mehr Rechenaufwand als die üblichen Zweielektronenintegrale.

Kapitel 7 ist eine Pilotstudie einer neuen Korrelationsfunktion der Form $\left(\sum_{i<j} r_{ij}\exp(-\gamma r_{ij}^2)\right)$, die in die Methodik ähnlichkeitstransformierter Hamilton-Operatoren für Konfigurationswechselwirkungsrechnungen (CI) Rechnungen an Zweielektronensystemen eingeführt wurde. Es wurden Rechnungen am He-Atom in großen Basissätzen, in denen Gauß-Funktionen verwendet werden (Untermengen des $19s16p14d12f10g8h6i4k$-Basissatzes) und Rechnungen am H_2-Molekül im einem 5s4p-Basissatz, der eine Untermenge des aug-cc-pVQZ-Basissatzes darstellt. Für eine Korrelationsfunktion mit dem Koeffizienten c=$\frac{1}{2}$ und dem Exponenten γ=0 sind die Basissatzkonvergenzen der Korrelationsenergie und des Erwartungswertes des interelektronischen Abstandes den konventionellen CI-Ergebnissen deutlich überlegen. Des Weiteren zeigt für c=$\frac{1}{2}$ die Variation der Korrelationsenergie mit steigendem Dämpfungs-Exponenten, dass γ, will man gleichwertige Ergebnisse erzielen, kleiner als 0.1 gewählt werden sollte. Schließlich zeigt die Energieberechnung

versus den Parameter γ am H_2-Molekül bei verschiedenen internuklearen Abständen zwischen 5.0 und 1000 a_0, dass für große internukleare Abstände γ genügend groß gehalten werden sollte, um die Konvergenzeigenschaften der CI-Rechnung zu erhalten. Auf Grund dieses Widerspruchs ist es schwierig, endgültige Aussagen über einen allgemeingültigen optimalen Wert von γ zu treffen.

Die MP2-Paarkorrelationsenergien von Ethylen und Ethan bei eingefrorenen Rumpforbitalen werden bei festen Geometrien für lokalisierte Molekülorbitale berechnet (Kapitel 8). Das Boys-Verfahren wird nur auf Valenzorbitale angewendet. Für Ethylen werden zwei Fälle untersucht: Entweder werden alle Orbitale lokalisiert, so dass C-C-Bananenbindungen erzeugt werden, oder es werden nur σ-artige Bindungen lokalisiert, π-artige Orbitale bleiben unberücksichtigt. Die Basissatzdarstellung unter Verwendung von Gauß-Funktionen wird durch beides weiter entwickelt: die R12-Methode (in ihrer ursprünglichen Form) in Untermengen des [C/H]=[19s14p8d6f4g3h2i / 9s6p4d3f2g]-Basissatzes und durch das neue Extrapolationsschema in der (aug)-cc-pVXZ-Basissatzreihe. Da die Fock-Matrix mit lokalisierten Molekülorbitalen nicht diagonal ist, müssen die MP2-R12-Gleichungen iterativ gelöst werden. Die MP2-R12-Gesamtenergien für Ethylen und Ethan belaufen sich auf jeweils –373.6$\pm$0.1 mE_h und –410.0$\pm$0.1 mE_h und die Extrapolationen in einem aug-cc-pV(Q5)Z bzw. aug-cc-pV(56)Z-Basissatz stimmen zu je 99.8% und 99.9% mit diesen Werten überein.

Schließlich gibt Kapitel 9 einen Ausblick auf die Verwendung von lokalisierten, mit Gauß-Funktionen gedämpften R12-Wellenfunktionen in Kombination mit Algorithmen, die durch eine lineare Skalierung motiviert sind, mit dem Zweck den Anwendungsbereich der R12-Methoden zu erweitern. Ziel ist es, eine Methode zu erarbeiten, in der unwichtige, langreichweitige Integrale schneller verschwinden, so dass die explizite Berechnung und Speicherung von nullwertigen Integralen vermieden wird. In einer formelleren Ausdrucksweise werden die R12-Integrale $\langle\bar{\Phi}_p(1)\bar{\Phi}_q(2)|\hat{\Omega}|\bar{\Phi}_i(1)\bar{\Phi}_j(2)\rangle$ (mit $\hat{\Omega}$ einem gegebenen Operator , Φ_p, $\bar{\Phi}_q$ Spinmolekülorbitale und Φ_i, $\bar{\Phi}_j$ besetzte Orbitale) nur dann berechnet, wenn $\bar{\Phi}_i\bar{\Phi}_j$ nicht ein sehr entferntes Paar bilden und wenn $\bar{\Phi}_p$ und $\bar{\Phi}_q$ zu der Vereinigung der $\bar{\Phi}_i$ und $\bar{\Phi}_j$-Domänen gehören. Rechnungen an Alkan-Ketten haben zu dem unerfreulichen Schluss geführt, dass die Domäne, die mit jedem einzelnen besetzten Paar verbunden ist, im Vergleich zu konventionellen MP2 drastisch vergrößert werden sollte. Erstens beobachtet man, dass die erforderlichen Nichtstandardintegrale viel langreichweitiger sind als die konventionellen Zweielektronenintegrale. Obwohl die neue, mittels Gauß-Funktionen gedämpfte R12-Methode dieses Verhalten im Vergleich zu dem ursprünglichen linearen R12-Modell leicht verbessert, ist es nicht ausreichend, um diesen Nachteil auszugleichen. Zweitens ist die wichtige Voraussetzung, diffuse Gauß-Funktionen zu verwenden, um die Vollständigkeitsrelation darstellen zu können, für den nicht vernachlässigbaren Beitrag der lokalisierten Molekülorbitale über den gesamten Raum verantwortlich. Das heißt, dass der Kreuzungspunkt der linear skalierenden R12-Methode noch nicht erreicht werden kann und man sich effizien-

teren Methoden zur Integralberechnung zusammen mit einer Parallelisierung des Computer-Codes zuwenden sollte, um die Rechenzeit wesentlich zu verkürzen.

Résumé

La description correcte de la corrélation électronique à courte distance est un défi fondamental pour la chimie théorique. L'énergie de corrélation dynamique obtenue avec les méthodes classiques de la chimie quantique converge très lentement avec la taille de la base de fonctions gaussiennes. Dans ce cadre, les méthodes explicitement corrélées et les techniques d'extrapolation sont deux moyens systématiques d'accélérer la convergence des modèles standards basés sur une description de la fonction d'onde comme produit d'orbitales moléculaires. Dans cette thèse, ces deux méthodes sont améliorées et utilisées de manière à déterminer les propriétés de molécules dans leur état fondamental et à couches fermées contenant des éléments de la première et deuxième lignes du tableau périodique des éléments. Les deux principales méthodes de corrélation utilisées ici sont: la théorie de la perturbation de Møller-Plesset au deuxième ordre (MP2) et la théorie du *coupled-cluster* comprenant les excitations simples et doubles avec une correction perturbative et non itérative des excitations triples connectées (CCSD(T)). D'une part, la méthode d'extrapolation employée dans ce travail, qui est brièvement décrite dans l'introduction générale (Chapitre 1), est basée sur le fait que la variation d'énergie de paires singulets et triplets est respectivement proportionnelle à X^{-3} et X^{-5}, X représentant la taille d'une base de type *correlation-consistent*. D'autre part, les fonctions d'onde explicitement corrélées utilisées dans cette thèse appartiennent à la famille des méthodes dites R12. Le principe de telles méthodes est d'introduire un facteur de corrélation dans l'expression de la fonction d'onde, qui est en l'occurrence égal à la simple distance entre deux électrons r_{12}. Cette procédure améliore ainsi la description conventionnelle de la fonction d'onde à l'aide des déterminants de Slater. Dans un chapitre, les techniques basées sur la transformation similaire de l'hamiltonien (introduites au Chapitre 1) sont aussi étudiées. Les chapitres 3, 4 et 8 contiennent des applications de haute précision sur des systèmes moléculaires de tailles petites à moyennes. Enfin, les chapitres 5, 6, 7 et 9 sont dédiés aux développements actuels de la méthode R12.

Au Chapitre 3, la barrière d'inversion de l'ammoniac, associée au mode spectroscopique ν_2 (communément appelé mode parapluie), est extrapolée à l'aide du nouveau type d'extrapolation dans une série de bases de type *correlation-consistent*. Ceci est fait afin d'obtenir la limite de la base du modèle CCSD(T). Les géométries de référence, pyramidale (C_{3v}) et plane (D_{3h}), sont

chacune optimisées dans la base cc-pCVQZ au niveau CCSD(T) en corrélant tous les électrons y compris ceux de coeur. La barrière est calculée avec exactitude en corrélant seulement les électrons de valence par la méthode CCSD(T)-R12 dans la base [N/H]=[19s14p8d6f4g3h / 9s6p4d3f]. Ce résultat concorde parfaitement avec ceux obtenus par extrapolation dans les bases cc-pV(56)Z et aug-cc-pV(Q5). Lorsque tous les électrons sont corrélés, la barrière d'inversion est estimée à +1767$\pm$12 cm^{-1} dans l'approximation de Born-Oppenheimer non relativiste. Plus en détail, la contribution de Hartree-Fock est égale à +1613$\pm$3 cm^{-1}, celle de CCSD à +178$\pm$10 cm^{-1}, celle des triplets (T) par perturbation à +40$\pm$2 cm^{-1} et la corrélation entre les électrons de coeur et de valence à –64$\pm$4 cm^{-1}. Enfin, lorsque les effets relativistes sont pris en considération (+20$\pm$2 cm^{-1}), ainsi que la correction diagonale de Born-Oppenheimer (–10 cm^{-1}) et l'énergie de point zéro (+244$\pm$15), la barrière effective est évaluée à +2021$\pm$20 cm^{-1}.

Dans le complexe $(H_2O)OH^{-1}$, la barrière d'activation de la réaction de transfert de proton entre deux structures d'équilibre équivalentes de symétrie (C_1) connectées entre elles par une structure de transition [HOHOH$^-$]‡ de symétrie (C_2) est peu élevée. Cette barrière est calculée avec une grande précision en utilisant la méthode CCSD(T)-R12 et en corrigeant l'erreur de superposition de la base grâce à la méthode de 'counterpoise' (Châpitre 4). Cette erreur n'est pas à négliger pour ce type de faibles interactions et les trois fragments utilisés ici pour la correction de 'counterpoise' sont OH$^-$, H$^+$ et OH$^-$. Tous les calculs sont effectués sans corréler les électrons de coeur. La base pour les calculs R12 comprend 389 fonctions [O/H]=[15s9p7d5f / 9s7p5d] et les géométries des structures d'équilibre et de transition sont optimalisées avec la méthode MP2 dans la base [O/H]=[aug-cc-pVQZ / aug-cc-pVTZ]. La meilleure estimation de la barrière au transfert du proton est ainsi obtenue (0.9$\pm$0.3 kJ mol^{-1}) et l'énergie électronique de liaison qui correspond à la dissociation du complexe en deux fragments, H_2O et OH$^-$, est évaluée à 109.10 kJ mol^{-1}. Pour finir, la courbe d'énergie potentielle à une dimension qui décrit le transfert protonique entre les deux minima globaux est construite au niveau CCSD(T)-R12 en combinant les résultats CCSD(T) avec la correction R12 obtenue au niveau MP2. Le niveau vibrationel le plus bas est évalué à 5.2 kJ mol^{-1} au-dessus du minimum global, c'est-à-dire largement au-dessus de la barrière. Cette barrière a donc peu d'effet sur la probabilité de distribution du proton qui forme la liaison hydrogène.

Une nouvelle manière d'aborder la méthode MP2-R12 est décrite au Chapitre 5. Elle consiste à utiliser une base auxiliaire pour résoudre exclusivement la résolution de l'identité, ce qui rend ainsi possible l'usage de bases standards de fonctions gaussiennes pour les calculs R12. Les paires de fonctions R12 peuvent être choisies, soit orthogonales à l'espace des orbitales moléculaires dans son ensemble (Ansatz **1**), soit seulement à l'espace des orbitales moléculaires occupées (Ansatz **2**). Ce choix conduit à des équations différentes contrairement à la méthode MP2-R12 d'origine. Afin de tester cette nouvelle méthode, les énergies de paires de l'atome de néon sont calculées avec

l'Ansatz **2** dans la base $20s14p11d9f7g5h$, prise comme base primaire, et avec la grande base $32s24p18d15f12g9h6i$ comme base auxiliaire. L'écart type maximal avec des résultats antérieurs où toutes les intégrales à trois et quatre électrons sont calculées exactement est de 6 μE_{h}. Quant on compare ces mêmes résultats a des énergies de paires extrapolées avec précision, l'écart type maximal est aussi très petit, de l'ordre de 7 μE_{h}. D'autres études sont faites sur un ensemble de petites molécules (CH_2, H_2O, NH_3, HF, N_2, CO et F_2) dont les géométries sont obtenues par optimisation dans la base cc-pCVQZ au niveau CCSD(T) en corrélant y compris les électrons de coeur. Les bases auxiliaires sont choisies très grandes ($19s14p8d6f4g3h2i$ pour C, N, O et F et $9s6p4d3f2g$ pour H) et les bases de type *correlation-consistent* sont prises comme bases primaires pour les orbitales. La convergence de la base est ainsi considérablement accélérée. Il est très difficile de recouvrer 98% de la corrélation électronique de valence avec la méthode MP2 conventionnelle, tandis que nous sommes en mesure d'atteindre ces 98% déjà pour la base X=4 avec la nouvelle méthode MP2-R12. Une dernière remarque à ce sujet: l'Ansatz **2** est meilleur que l'Ansatz **1** dans la plupart des cas.

Au Chapitre 6 une méthode hybride pour la théorie MP2-R12 est présentée. Elle emploie un facteur de corrélation de la forme $r_{12}\exp(-\gamma r_{12}^2)$, compromis entre les facteurs de corrélation linéaire et exponentiel. Bien que l'atténuation du facteur linéaire ne semble pas indispensable attendu que les amplitudes de la méthode R12 linéaire assurent déjà le comportement approprié pour de grandes distances entre électrons, elle est néanmoins utile pour accélérer la décroissance des intégrales requises pour de longues distances r_{12}. De cette façon il semble plus aisé de combiner la théorie R12 avec les techniques de corrélation locale qui visent à atteindre une croissance du coût de calcul strictement proportionnelle à la taille du système étudié. Contrairement à la famille des méthodes explicitement corrélées qui utilisent des facteurs exponentiels, nous voulons éviter une optimisation de l'exposant de la fonction gaussienne qui s'avèrerait trop chère. De fait, nous nous plions aux deux seules conditions que d'une part γ doit être assez petit pour conserver le bénéfice de la méthode quand r_{12} est courte et que d'autre part γ doit être assez grand afin de couper le plus tôt possible les larges contributions des intégrales quand r_{12} est grande. La procédure de McMurchie-Davidson est utilisée pour évaluer toutes les intégrales à deux électrons, ce qui conduit à résoudre des relations de récurrence allant jusqu'à six termes et contenant des fonctions dites de Boys. Aucune des cinq sortes d'intégrales supplémentaires ne demande beaucoup plus de temps de calcul que les intégrales conventionnelles à deux électrons.

Le Chapitre 7 contient une étude pilote (pour des systèmes à deux électrons) qui consiste à introduire une nouvelle fonction de corrélation de la forme $\left(\sum_{i<j} r_{ij}\exp(-\gamma r_{ij}^2)\right)$ en association avec une transformation similaire de l'hamiltonien dans le domaine des calculs d'interaction de configurations (CI). Des tests sont effectués sur l'atome d'hélium dans de grandes bases (sous-ensembles de la base $19s16p14d12f10g8h6i4k$) et la molécule de dihydrogène est étudiée dans le

sous-ensemble $5s4p$ de la base aug-cc-pVQZ. Lorsque le coefficient et l'exposant de la fonction de corrélation sont égaux à c=$\frac{1}{2}$ et γ=0 respectivement, la convergence de la base pour l'énergie de corrélation comme pour la valeur moyenne de r_{12} est nettement meilleure que pour les résultats CI conventionnels. De plus, lorsque c=$\frac{1}{2}$, les variations de l'énergie de corrélation avec l'exposant démontrent que γ doit rester au-dessous de 0.1 pour sauvegarder la précision. Pour finir, en étudiant les variations de l'énergie en fonction de γ pour H_2 et à différentes distances entre les noyaux, on observe que γ doit être gardé suffisamment large afin d'assurer la convergence du calcul CI. En raison de cette contradiction, il est ici difficile de faire la moindre conclusion définitive quant à une valeur universelle du paramètre γ.

L'énergie de corrélation des paires de valence est calculée pour les molécules d'éthylène et d'éthane à géométries fixes et en localisant les orbitales moléculaires (Chapitre 8). La procédure de Boys est utilisée pour localiser les orbitales de valence seulement et deux cas de figures sont examinés spécialement pour l'éthylène: soit toutes les orbitales sont localisées, ce qui génère un type de liaisons dites "de bananes", ou bien seulement les orbitales de type σ sont localisées laissant ainsi les orbitales π telles qu'elles. La représentation de la fonction d'onde à l'aide de sous-ensembles de la base de fonctions gaussiennes [C/H]=[$19s14p8d6f4g3h2i$ / $9s6p4d3f2g$] est améliorée, d'une part en utilisant la méthode R12 dans sa forme originelle, mais aussi en appliquant les techniques d'extrapolation dans la série de bases (aug)-cc-pVXZ. Comme la matrice de Fock n'est pas diagonale dans la base des orbitales moléculaires localisées, les amplitudes correspondant aux termes de R12 doivent être déterminées de manière itérative. Les énergies MP2-R12 pour l'éthylène et l'éthane sont respectivement de –373.6$\pm$0.1 mE_h et –410.0$\pm$0.1 mE_h. Les résultats extrapolés correspondant aux bases aug-cc-pV(Q5)Z et aug-cc-pV(56)Z sont en accord avec ces valeurs de 99.8% et 99.9% respectivement.

Pour finir, le Chapitre 9 donne une perspective d'avenir sur l'utilité des nouveaux développements concernant les fonctions d'ondes explicitement corrélées qui ont pour but de rendre les méthodes R12 plus abordables: localisation des orbitales moléculaires, atténuation du facteur linéaire de corrélation par une fonction gaussienne décroissante, introduction de techniques qui visent à restreindre le coût de calcul. Le but ultime est de créer une méthode qui permettrait d'annuler les intégrales requises plus rapidement pour de longues distances entre électrons. De cette manière ces intégrales négligeables ne sont ni calculées, ni stockées. En résumé, les intégrales R12 $\langle\bar{\Phi}_p(1)\bar{\Phi}_q(2)|\hat{\Omega}|\bar{\Phi}_i(1)\bar{\Phi}_j(2)\rangle$ (avec $\hat{\Omega}$ un opérateur donné, $\bar{\Phi}_p$, $\bar{\Phi}_q$ des orbitales moléculaires de spin et $\bar{\Phi}_i$, $\bar{\Phi}_j$ des orbitales occupées) sont calculées seulement si $\bar{\Phi}_i\bar{\Phi}_j$ ne forme pas une paire très distante et si $\bar{\Phi}_p$ et $\bar{\Phi}_q$ appartiennent a l'union des domaines de $\bar{\Phi}_i$ et $\bar{\Phi}_j$. Une étude sur la série des alcanes a conduit à la conclusion malheureuse que le domaine associé à chaque paire d'orbitales occupées doit être largement plus étendu que celui correspondant à un calcul MP2 conventionnel. Premièrement, on remarque que les intégrales R12 présentent une contribution beaucoup

plus large pour de grandes distances entre électrons comparées aux intégrales standards à deux électrons. Bien que l'atténuation du facteur linéaire apportée par la fonction gaussienne améliore légèrement ce problème, ce n'est cependant pas suffisant pour le faire disparaître efficacement. Deuxièmement, la lourde contrainte due à l'utilisation de fonctions diffuses pour vérifier convenablement la résolution de l'identité conduit les orbitales moléculaires à présenter des contributions conséquentes sur tout l'espace. Ainsi, le moment où cet algorithme est moins cher en terme de ressources d'ordinateur que l'algorithme MP2-R12 originel n'est pas encore atteint. Pour cela, il serait important de diminuer de façon conséquente le coût de calcul des intégrales grâce à des algorithmes plus efficaces ainsi qu'à la parallélisation du programme.

List of publications

1. W. Klopper, C. C. M. Samson, G. Tarczay and A. G. Császár, Equilibrium inversion barrier of NH_3 from extrapolated coupled-cluster pair energies, Journal of Computational Chemistry, Vol. **22**, No. 13, pp. 1306–1314 (2001).
   Reproduced with permission from John Wiley & Sons, Ltd.

2. C. C. M. Samson and W. Klopper, *Ab initio* calculation of proton barrier and binding energy of the $(H_2O)OH^-$ complex, Journal of Molecular Structure (Theochem), Vol. **586**, pp. 201–208 (2002).
   Reproduced with permission from Elsevier.

3. W. Klopper and C. C. M. Samson, Explicitly correlated second-order Møller-Plesset methods with auxiliary basis sets, Journal of Chemical Physics, Vol. **116**, No. 15, pp. 6397–6410 (2002).
   Reproduced with permission from the American Institute of Physics.

4. C. C. M. Samson, W. Klopper and T. Helgaker, Computation of two-electron Gaussian integrals for wave functions including the correlation factor $r_{12}\exp(-\gamma r_{12}^2)$, Computer Physics Communications, Vol. **149**, No. 1, pp. 1–10 (2002).
   Reproduced with permission from Elsevier.

5. H. J. A. Zweistra, C. C. M. Samson and W. Klopper, Similarity-transformed Hamiltonians by means of Gaussian-damped interelectronic distances, Collection of Czechoslovak Chemical Communications, Vol. **68**, pp. 374–386 (2003).
   Reproduced with permission from to the Institute of Organic Chemistry and Biochemistry of Prague.

6. C. C. M. Samson and W. Klopper, Benchmarking ethylene and ethane: Second-order Møller-Plesset pair energies for localized molecular orbitals, Molecular Physics, (*accepted for publication*).
   Reproduced with permission from Taylor & Francis.

Acknowledgments

First of all, I want to thank Prof. Dr. Wim Klopper for helping me patiently to find my way in the arduous world of explicitly correlated wave functions. You were always available and open for discussions and it was a great pleasure to work with you during all these years. Thank you also for the logistic support during my successive movings. I am also grateful to Prof. Dr. Frans van Duijneveldt who gave me the opportunity to carry out my Ph.D. project in Utrecht. I've learned a lot from your great concern in precision and clear explanations, and your advises have been very important to me. Furthermore I would like to thank Prof. Dr. Trygve Helgaker who taught me a lot about the ERI part of the Dalton program. I've never seen anybody debugging with such a contagious enthusiasm. I am also thankful to Prof. Dr. Reinhart Ahlrichs who made me feel comfortable in Karlsruhe from the very beginning.

I warmly acknowledge all my colleagues. It was so enriching to work with you all. In Utrecht, I would like to thank: Asger, Affen for your so precious help when I first arrived, Fokke, Henk and Henk, Henri, Jeanne, Jeroen, Joop and Paul for many relevant comments on my research, Joost, Petar, Remco for the Samenvatting as well as for picking me up in the storm at Arnhem train station, and Walter for having introduced me to your amazing daughter. I would like also to thank the people of the theoretical chemistry group of Oslo, with a special thank to Mark for his so British sense of humor. In Karlsuhre, I want to thank: as a whole, the people of the theoretical chemistry group working at the Forschungszentrum and those part of Prof. Ahlrichs group, as well as Andreas to have answered immediately present, Barbara, Cristian, Elena for the Zusammenfassung as well as for your daily smiles, Heike and her 'Ordnung muss sein!', and Jorge for reminding me the southern life. Furthermore I want to thank Alexia, Paola, Daniel, Filipp, Marco and Matthias for many good times in your company. I have of course also a thought for all the secretaries who eased my pain concerning administrative matters, namely Eli, Chantal, Susan, and Tine in Utrecht and Frau Legeland and Frau Kühn in Karlsruhe.

The backstage presence of all my friends has also been important for the accomplishment of this work. Many thanks to: Yuki and Ken my two dearest Japanese friends, Sean you've widened so much my musical horizons, Cyril et son incommensurable joie de vivre, Vincent, Philippe, Alex, ainsi que toute la clique des français expatriés à Utrecht, Juliette the ballerina, Florence toujours là

avec ton énergie débordante, Michel voor de verhuizing and Iris het slimme meisje.

Et puis, il y a aussi les amis de longue date: Olivier pour de folles soirées toulousaines, Aurélie aux grands yeux bleus, Caroline ma Noun, Murielle pour tant de discussions passionnantes, Manu et Mandy et leur petit Romain, Stéphane et Loic pour mes plus beaux souvenirs de fac, David pour ton soutien inaltérable et Yannick un grand merci, entre autre pour la relecture du résumé. Il y a aussi Sandra, ma Keuchine de toujours, l'essence de mon moteur. Ton rire plein de lucidité m'a tant aidé à traverser les épreuves mais a aussi éclairé de si beaux moments.

Jonas, it was so important for me to feel your constant support, specially when the only sight that I had from the world was this yellow curtain. What we have done was not easy but we finally managed. Thank you for being such a crazy dreamer.

Evidemment, je profite aussi de cette page pour remercier ma famille ainsi que toutes ses 'pièces rapportées' pour avoir été présentes (et même par-delà les océans) pendant toutes ces années. Et plus particulièrement, je remercie mon père lunaire pour m'avoir appris à rire de la vie ainsi que pour son soutien constant dans toutes mes entreprises, même les plus ambitieuses (ou saugrenues) et ma mère solaire pour m'avoir montré que les horizons d'une femme s'étendaient bien au-delà des murs d'une prison, aussi dorée soit-elle.

Finally, I also want to thank Emma, Anne and Rémi for making the world a bit more beautiful.

Karlsruhe, August 17th 2004

Curriculum Vitae

Claire Samson was born on the 9th of July 1976 in Aire sur Adour, France. She obtained her secondary school diploma in 1994 at the school Louis Barthou in Pau, France. She studied thereafter Physical Chemistry at the University Paul Sabatier, Toulouse, France. During her studies, she took part in an exchange program at the University of Virginia in Charlottesville, USA, carrying out a one-year research project in the Inorganic Chemistry Laboratory of Prof. Dr. Cassandra Fraser. In April 2000, she obtained her University Diploma and started her Ph.D. project in the Theoretical Chemistry Group of the Debye Institute, at the University of Utrecht under the supervision of Prof. Dr. Frans van Duijneveldt and Prof. Dr. Wim Klopper. She moved from the Netherlands to Germany in December 2002 where she worked further on her research project at the Technical University of Karlsruhe.